# APPLICATION OF TERAHERTZ CHARACTERIZATION METHODS FOR BUILDING AND CONSTRUCTION MATERIALS

Andreja Abina

**Doctoral Dissertation**
**Jožef Stefan International Postgraduate School**
**Ljubljana, Slovenia, May 2015**

**Evaluation Board**:

*Prof. Dr. Zvonko Trontelj, Chairman, Institute of Mathematics, Physics and Mechanics, Jadranska cesta 19, SI-1000 Ljubljana, Slovenia, and Jožef Stefan International Postgraduate School, Jamova cesta 39, SI-1000 Ljubljana, Slovenia*

*Prof. Dr. Anton Jeglič, Member, Jožef Stefan International Postgraduate School, Jamova cesta 39, SI-1000 Ljubljana, Slovenia, and Faculty of Electrical Engineering, University of Ljubljana, Tržaška cesta 25, SI-1000 Ljubljana, Slovenia*

*Prof. Dr. Gintaras Valušis, Member, Center for Physical Sciences and Technology, LT-01108 Vilnius, Lithuania*

MEDNARODNA PODIPLOMSKA ŠOLA JOŽEFA STEFANA
JOŽEF STEFAN INTERNATIONAL POSTGRADUATE SCHOOL




Andreja Abina

# APPLICATION OF TERAHERTZ CHARACTERIZATION METHODS FOR BUILDING AND CONSTRUCTION MATERIALS

**Doctoral Dissertation**

# UPORABA TERAHERČNIH KARAKTERIZACIJSKIH METOD PRI ANALIZI GRADBENIH IN KONSTRUKCIJSKIH MATERIALOV

**Doktorska disertacija**

*Supervisor*: Prof. Dr. Aleksander Zidanšek

Ljubljana, Slovenia, May 2015

To my lovely daughter Klara and my life traveller Marko.
You have given me the best days of my life.

*Research is to see what everybody else has seen,*
*and to think what nobody else has thought.*

Albert Szent-Györgyi

# Index

**Abstract** ..... **IX**

**Povzetek** ..... **XI**

**Abbreviations** ..... **XIII**

**Symbols** ..... **XV**

**1 Introduction** ..... **1**
1.1 Motivation ..... 1
1.2 Hypotheses and aims ..... 3
1.3 Original contributions ..... 5
1.4 Approbation of the scientific work ..... 5
1.5 Outline of the Dissertation ..... 6

**2 Terahertz Spectroscopy** ..... **9**
2.1 The terahertz range of the electromagnetic spectrum ..... 9
2.2 Fundamental principles of terahertz radiation ..... 11
2.2.1 Basic physical fundamental of THz generation and detection ..... 11
2.2.2 Photoconductive generation and detection ..... 12
2.2.3 Optical rectification and electrooptic sampling ..... 13
2.3 Terahertz time-domain spectroscopy ..... 15
2.3.1 System geometry ..... 15
2.4 Terahertz pulsed imaging ..... 16
2.5 Material interaction with terahertz radiation ..... 18
2.6 Terahertz wave interaction with gases, liquids and solids ..... 21
2.6.1 Gases ..... 21
2.6.2 Liquids ..... 21
2.6.3 Solids ..... 22
2.7 Data analysis ..... 24
2.7.1 Pre-processing methods ..... 24
2.7.2 Interpretation of terahertz waveform and terahertz spectrum ..... 25
2.8 Imaging analysis ..... 28
2.8.1 Time-domain imaging ..... 28
2.8.2 THz spectral imaging ..... 28

**3 Experimental Equipment and Methods** ..... **31**
3.1 Time-domain terahertz spectrometer in transmission configuration ..... 31
3.1.1 System elements and system operation ..... 31
3.1.2 Spectrometer operating characteristics ..... 33

3.2 Experimental procedure and sample preparation ..... 34
3.2.1 Powders ..... 34
3.2.2 Foams ..... 35
3.2.3 Microencapsulated particles ..... 35
3.3 Pre-processing techniques ..... 35
3.4 Post-processing techniques ..... 36
3.5 Reference methods ..... 36
3.5.1 Microscopy ..... 37
3.5.2 FTIR spectroscopy ..... 37

**4 Characterization of Construction and Building Materials by THz Spectrometer and Imager ..... 39**
4.1 Scientific article 1: Applications of terahertz spectroscopy in the field of construction and building materials ..... 39
4.2 Scientific article 2: Structural analysis of insulating polymer foams with terahertz spectroscopy and imaging ..... 67
4.3 Scientific article 3: Qualitative and quantitative analysis of calcium-based microfillers using terahertz spectroscopy and imaging ..... 79
4.4 Scientific article 4: Structural characterization of thermal building insulation materials using terahertz spectroscopy and terahertz pulsed imaging ..... 101

**5 Discussion ..... 117**
5.1 Future challenges ..... 119

**6 Conclusions ..... 121**

**7 Acknowledgements ..... 123**

**8 References ..... 125**

**Index of Figures ..... 131**

**Index of Tables ..... 133**

**Index of Algorithms ..... 135**

**Appendix A: THz measurement flow ..... 137**

**Appendix B: Matlab functions for data pre-processing ..... 139**

**Appendix C: Personal biography ..... 141**

**Appendix D: List of all publications in the period from 2009 in COBISS ..... 143**

# Abstract

Any construction and building material has specific physicochemical and mechanical properties to ensure safety, strength and durability of civil building structures. To correctly analyse and estimate these properties, non-destructive testing (NDT) methods are widely applied. Although several different types of NDT methods are used nowadays to analyse construction and building materials, there is an increasing demand for new systems with greater reliability, sensibility, in-situ operation as well as simple and fast execution. The capabilities and possible applications of one such method, known as terahertz (THz) spectroscopy and imaging, are discussed in the thesis.

In the last few years, the rapid development of novel THz sources and detectors has opened possibilities of creating spectroscopic and imaging systems, allowing in situ measurements and almost real-time analysis of different materials in the THz range which was until recently almost unexplored. Several advantages of THz systems over other NDT technologies have attracted interest in industry, thus the applications where this spectroscopy has shown a potential are increasing over the last two decades. Currently, the major research is devoted to the applications in pharmaceutical industry, security, medicine, and materials characterization, whereas the construction and building industry lags behind them. The last finding was confirmed with the first systematic review on related work made in the frame of this thesis. During the review, we observed that THz waves when they pass through different materials produce unique signal and spectral responses that can be applied for analysis of chemical composition, water content, porosity, material thickness, density, material aging, and others. In addition, supplementary imaging THz system configuration is capable to visualize hidden internal and surface defects, inclusions, and manufacturing imperfections. These approaches are partially used also in the construction industry, where THz spectroscopy and imaging can be a valuable substitute or complement to other NDT techniques.

The main goal of the thesis was to verify the capabilities of THz spectroscopy and imaging in the field of construction and building materials with the execution of some laboratory studies. Based on the prepared review, we selected five different types of materials, including powder, granular, fibrous, cellular, and microencapsulated materials. Most of them were investigated by THz radiation for the first time. When THz waves pass through these materials, they produce unique signal and spectral responses that were applied to both, the qualitative and quantitative structural analysis of material. Since the majority of the worldwide laboratories uses THz systems based on photoconductive antennas (PHCAs) and inorganic electrooptic (EO) crystals for materials characterization, we focused on the other type of THz system, comprising organic EO crystals. We believe that the selected THz spectroscopic and imaging system has shown applicable potential and some advantages over other THz systems and thus opens some new opportunities in the field of materials characterization.

In the thesis, the selected THz spectrometer was first applied for structural analysis of thermal insulating polymer foams. By calculating the THz spectroscopic constants we analysed certain material characteristics such as foam density and infrared radiation absorption. Moreover, the THz imaging was applied to analyse and visualize the beads

structure of polymer foams considering bead size, shape, air gaps and interconnections as well as defects, impurities and prebuilt inclusions. We also suggested a novel procedure of THz imaging analysis in a combination with image processing methods and particle analysis. In the second case, the same THz methods were applied for qualitative and quantitative analysis of calcium-based microfillers. Its concentration in polymer matrix, granulation, chemical treatment and the presence in binary-mixtures were studied by the analysis of peak absorbance amplitude, peak frequency position, and the appearance of characteristic spectral features. For the investigation of fibrous materials, we selected an aerogel composite, where different fibre orientations were recognized in THz spectra and amplitude images. The last testing material was microencapsulated phase change material, for which the phase transition from liquid to solid and vice versa was analysed with THz spectroscopy. To summarize, the results presented in the thesis indicated that the selected spectroscopic method can be applied for the analysis of construction materials, considering their chemical composition, density, temperature dependence, fibres orientation, infrared absorption, additive presence, particle granulation, and concentration in mixtures. In addition, supplementary imaging mode visualized hidden internal and surface defects, inclusions, manufacturing imperfections, inhomogeneous structure, layers, and fibres in a submillimetre resolution scale. Hence, the THz based research could contribute to processing companies with the optimisation of their products and production processes in order to improve the mechanical and physicochemical material properties.

The present status of THz capabilities in construction and building applications is in its early infancy, limited almost only to laboratory testing. Current THz technology will probably remain one of many NDT tools that will be applied in combination with other techniques, until radical progress will be achieved in the field of new high-speed, high resolution and high-power THz systems. Until then, the research of construction and building materials by using existent THz techniques should be enhanced and brought to such a level that when adequate technology will be at hand it could be easily transferred to a commercial use.

# Povzetek

Posamezni konstrukcijski in gradbeni materiali so okarakterizirani s specifičnimi fizikalno-kemijskimi in mehanskimi lastnostmi, ki zagotavljajo obstoječim zgradbam trdnost, zanesljivost in dolgotrajnost. Za pravilno analizo in ovrednotenje teh lastnosti se danes uporabljajo neporušne metode preizkušanja. Industrija, nacionalni uradi ter mednarodne institucije kljub številnim različnim obstoječim neporušnim metodam zahtevajo neprestan razvoj novih naprav, ki zagotavljajo večjo zanesljivost in občutljivost na eni strani ter hitro in enostavno delovanje v realnem okolju na drugi strani. V okviru disertacije smo preučili zmožnosti ene od takšnih metod, znane kot teraherčna (THz) spektroskopija in slikanje, ter demonstrirali primere aplikativnih raziskav na področju gradbeništva.

Hiter napredek na področju THz izvorov in detektorjev v zadnjih nekaj letih je omogočil razvoj inovativnih spektroskopskih in slikovnih sistemov, ki dopuščajo »in-situ« meritve in analizo različnih materialov v skoraj realnem času v THz frekvenčnem območju, ki je bilo dolgo časa znanosti in raziskovanju nedostopno. Nekatere prednosti THz sistemov pred ostalimi neporušnimi tehnikami so sprožile zanimanje v industriji, kjer so se zlasti v zadnjih dveh desetletjih aplikacije omenjene tehnologije izrazito povečale. Danes je razvoj še vedno večinoma usmerjen na področje farmacije, varnosti, medicine in karakterizacije materialov, medtem ko drugi sektorji, med njimi tudi gradbeništvo, močno zaostajajo, kar se tiče izkoriščanja aplikativnega potenciala, ki ga kaže THz tehnologija. Do te ugotovitve smo prišli v disertaciji z izvedbo sistematičnega pregleda literature, kjer se omenja uporaba THz tehnologije za analizo materialov, po katerih se pogosto posega tudi v gradbeništvu. Pri pregledu literature smo ugotovili, da sorodni materiali, kadar so obsevani s THz valovanjem, producirajo svojevrstne signalne in spektralne odzive, na osnovi katerih se lahko izvede analiza o kemijski sestavi snovi, določi vsebnost vode, poroznost, debelina materiala in njegova gostota ter analizira staranje materiala. Dopolnilna slikovna konfiguracija THz sistema je dodatno sposobna zaznavanja in vizualizacije skritih napak znotraj in na površini materiala, zaznavanja raznih vključkov in proizvodnih nepravilnosti. Ti analizni pristopi so deloma uporabljeni tudi za namene karakterizacije konstrukcijskih in gradbenih materialov, kjer lahko THz spektroskopija in slikanje predstavljata pomembno nadomestno ali dopolnilno neporušno orodje že obstoječim metodam.

Glavni cilj doktorske disertacije je preveriti zmožnosti THz spektroskopije in slikanja pri analizi gradbenih in konstrukcijskih materialov z izvedbo nekaterih laboratorijskih raziskav. Na podlagi izvedenega sistematičnega pregleda literature smo izbrali pet različnih tipov materialov, in sicer praškovne, zrnaste, fibriozne, celularne in mikrokapsulirane materiale. Večina izmed izbranih materialov je bila prvič preiskovana z uporabo THz valovanja. Na osnovi signalnih in spektralnih odzivov materialov na THz valovanje smo izvedli tako njihovo kvalitativno kot tudi kvantitativno strukturno analizo. Čeprav večina laboratorijev po svetu uporablja THz sisteme, osnovane na fotokonduktivnih antenah in anorganskih elektrooptičnih kristalih, smo naše raziskave izvedli s sistemom, kjer je THz valovanje generirano in detektirano z organskimi elektrooptičnimi kristali. Glede na dobljene rezultate verjamemo, da je izbran spektroskopski THz sistem pokazal dovolj velik potencial in nekatere prednosti pred ostalimi sistemi ter tako ponudil nove priložnosti na področju analize materialov.

Z izbranim THz sistemom smo najprej izvedli strukturno analizo toplotno izolativnih polimernih pen. Izračuni spektroskopskih konstant so bili uporabljeni za analizo določenih materialnih karakteristik, kot so gostota pene in absorpcija infrardečega sevanja. V nadaljevanju smo uporabili THz slikanje za analizo strukture zrn polimernih pen, njihove velikosti, oblike, medsebojne povezave in vmesnih praznin ter vizualizacijo napak, nečistoč in umetno vgrajenih vključkov. V sklopu te študije smo predlagali nov postopek analize THz slik z uporabo metod slikovnega procesiranja in analize delcev. V drugi študiji smo iste THz metode uporabili za kvalitativno in kvantitativno analizo na kalciju baziranih mikropolnil. Osredotočili smo se na določanje koncentracije mikropolnil v polimerni matrici, preučevali smo vpliv granulacije in kemijskih agentov na THz spektre ter zaznavali prisotnost posameznih mikropolnil v binarnih zmeseh. Te parametre smo določili z analizo amplitude absorpcijskega vrha, z analizo frekvenčne pozicije vrhov in s pojavom spektralnih značilk. Poleg celularne strukture polimernih pen smo preučevali tudi vlaknasto strukturo aerogelnega kompozita, kjer smo se osredotočili predvsem na vpliv orientacije vlaken na THz spekter in amplitudno THz sliko. Nenazadnje smo na THz spektru določevali fazni prehod iz tekočega v trdno stanje ter obratno na primeru mikrokapsuliranih fazno spremenljivih materialov. Če povzamemo vse rezultate, do katerih smo prišli v okviru raziskav te disertacije, ugotavljamo, da je izbrana spektroskopska metoda lahko uporabljena za analizo konstrukcijskih in gradbenih materialov, in sicer za določanje njihove kemijske sestave, gostote, temperaturne odvisnosti, orientacije vlaken, absorpcije infrardečega sevanja, prisotnosti aditivov, granulacije in koncentracije posameznih komponent v zmeseh. Dodatna možnost THz slikanja omogoči vizualizacijo skritih napak na površini in znotraj materiala, zaznavanje vključkov, nepravilnosti med proizvodnjo, nehomogene strukture, plastovite zgradbe in orientacije vlaken na submilimetrski skali. Iz tega lahko predpostavimo, da je omenjena tehnologija primerna za uporabo v gradbeni industriji, predvsem pri optimizaciji produktov in produkcijskih procesov, kjer lahko bistveno prispeva k izboljšanju mehanskih in fizikalno-kemijskih lastnosti materialov.

Trenutne zmožnosti uporabe THz sistemov za namene karakterizacije konstrukcijskih in gradbenih materialov so še v povojih in so večinoma omejene na laboratorijske raziskave. Obstoječi THz sistemi bodo najverjetneje ostali samo eno od mnogih orodij za neporušno preizkušanje, ki bodo še vedno ponudili najbolj zanesljive rezultate v kombinaciji z drugimi metodami. Takšno stanje se bo le stežka izboljšalo vse do tedaj, ko bo dosežen radikalen napredek na področju visokozmogljivih THz sistemov z izboljšano hitrostjo zajemanja podatkov in večjo občutljivostjo. Do takrat pa je potrebno na področju gradbenih in konstrukcijskih materialov obstoječe raziskave s THz metodo pripeljati do te faze, da bo možen hiter prenos na trg, ko bo na voljo ustrezna nova tehnologija.

# Abbreviations

| | | |
|---|---|---|
| 2D | = | two-dimensional |
| 3D | = | three-dimensional |
| ANN | = | artificial neural network |
| BLC | = | baseline correction |
| BS | = | beam splitter |
| $Ca(OH)_2$ | = | calcium hydroxide |
| $CaCO_3$ | = | calcium carbonate, calcite |
| CaO | = | calcium oxide |
| $CH_3CN$ | = | acetonitrile |
| CO | = | carbon monoxide |
| CPM | = | characteristic peak method |
| CT | = | computed tomography |
| CW | = | continuous wave |
| DAST | = | 4-N,N-dimethylamino-4'-N'-methyl-stilbazolium tosylate |
| DCDHF | = | dicyanodihydrofurane |
| DFT | = | density functional theory |
| DL | = | delay line |
| DSTMS | = | 4-N,N-dimethylamino-4′-N′-methyl-stilbazolium 2,4,6-trimethylbenzenesulfonate |
| EM | = | electromagnetic |
| EO | = | electrooptic |
| EPS | = | expanded polystyrene |
| FIR | = | far infrared |
| fs | = | femtosecond |
| FT | = | Fourier transform |
| FTIR | = | Fourier transform infrared |
| GaAs | = | gallium arsenide |
| GHz | = | gigahertz |
| $H_2S$ | = | hydrogen sulphide |
| HCl | = | hydrogen chloride |
| HCN | = | hydrogen cyanide |
| HDPE | = | high-density polyethylene |
| InP | = | indium phosphide |
| IR | = | infrared |
| LAPC | = | EO polymer based on Lemke |
| $LiNbO_3$ | = | lithium niobate |
| $LiTaO_3$ | = | lithium tantalate |
| LT-GaAs | = | low-temperature grown gallium arsenide |
| MLR | = | multiple linear regression |
| $N_2$ | = | nitrogen gas |
| $N_2O$ | = | nitrogen oxide |
| NDT | = | non-destructive testing |
| $NH_3$ | = | ammonia |

| | | |
|---|---|---|
| NIR | = | near infrared |
| PCA | = | principal component analysis |
| PCM | = | phase change material |
| PCR | = | principal component regression |
| PE | = | polyethylene |
| PHCA | = | photoconductive antenna |
| PLS | = | partial least square |
| PM | = | parabolic mirror |
| ps | = | picosecond |
| PTFE | = | polytetrafluoroethylene |
| S | = | lenses |
| SCI | = | Science Citation Index |
| SEM | = | scanning electron microscopy |
| SNR | = | signal-to-noise ratio |
| THz | = | terahertz |
| THZ-TDS | = | terahertz time-domain spectroscopy |
| TPI | = | terahertz pulsed imaging |
| TPX | = | polymethylpentene |
| VIP | = | vacuum insulated panel |
| XPS | = | extruded polystyrene |
| ZnTe | = | zinc telluride |

# Symbols

| | | |
|---|---|---|
| $[I]$ | = | image matrix |
| $\Delta k$ | = | frequency-dependent phase change per unit length |
| $\Delta t$ | = | time delay |
| $\Delta v$ | = | bandwidth |
| $\mu$ | = | magnetic permeability |
| $A$ | = | absorbance |
| $\mathbf{B}$ | = | magnetic field |
| $C$ | = | concentration |
| $c$ | = | vacuum velocity |
| $\mathbf{D}$ | = | electric field strength |
| $d$ | = | thickness (also $l$) |
| $E$ | = | amplitude of the electric field |
| $\mathbf{E}$ | = | electric field vector |
| $e$ | = | elementary charge |
| $\mathbf{H}$ | = | magnetic field strength |
| $I$ | = | intensity of EM radiation |
| $J$ | = | photocurrent |
| $\mathbf{J_f}$ | = | free electric current density |
| $k$ | = | complex propagation constant |
| $k_0$ | = | nonresonant wave vector |
| $\mathbf{M}$ | = | magnetization |
| $m$ | = | mobility of electron |
| $N$ | = | density of photocarriers |
| $n$ | = | refractive index |
| $\mathbf{P}$ | = | polarization |
| $P$ | = | spatial pattern, spatial distribution |
| $r$ | = | fraction of the reflected THz radiation |
| $R$ | = | reflectivity |
| $R_C$ | = | recognition coefficient |
| $S$ | = | absorbance spectra |
| $t$ | = | amplitude transmission |
| $T$ | = | transmittance, intensity transmission |
| $t_{ref}$ | = | reference pulse |
| $t_{sam}$ | = | sample pulse |
| $z$ | = | direction $z$ |
| $Z$ | = | number of scattering centres per unit volume |
| $\alpha$ | = | absorption coefficient |
| $\varepsilon$ | = | electric permittivity, extinction coefficient |
| $\varepsilon_0$ | = | permittivity of free space |
| $\lambda$ | = | wavelength |
| $\mu_0$ | = | permeability of free space |
| $v$ | = | frequency |

| | | |
|---|---|---|
| $\rho_f$ | = | free charge density |
| $\sigma$ | = | surface conductivity |
| $\sigma_s$ | = | scattering cross section, average particle size |
| $\tau$ | = | duration of an optical pulse |
| $\tau_c$ | = | carrier lifetime |
| $\phi_{ref}$ | = | phase of the reference |
| $\phi_{sam}$ | = | phase of the sample |
| $\chi^{(2)}$ | = | susceptibility |

# 1 Introduction

## 1.1 Motivation

The national and international standards and regulations dictate that any construction and building material should have specific physicochemical and mechanical properties to ensure safety, strength and durability of historic and modern civil building structures. To correctly analyse and assess these properties, non-destructive testing (NDT) methods are widely applied. Several different types of NDT methods, i.e. acoustic, ultrasonic, thermal, radiological, microscopic, and electromagnetic methods, are available nowadays and only the adequate combination of them significantly contributes to the reliable assessment of material properties. Therefore, it is obvious that novel testing methods should be continuously developed and improved in accordance to the national and international regulations as well as industrial requirements.

Recently, the development of non-destructive and contactless sensing methods based on electronic or optoelectronic components brings new analysing tools, appropriate for qualitative and quantitative materials investigation in the terahertz (THz) part of the electromagnetic (EM) spectrum, corresponding to the wavelengths between microwaves and near infrared (NIR) waves. For a long time, material properties in a frequency range between 0.3 THz and 10 THz were almost unexplored, mainly due to the lack of powerful and user-friendly THz sources and detectors [1,2]. The only technique used in far infrared (FIR) region was the Fourier transform infrared (FTIR) spectroscopy. Over the past fifteen years, a novel analytical tool known as a THz spectrometer has been developed and introduced in laboratories worldwide. Advances in the field have encouraged new research in various disciplines, including physics, chemistry, pharmacy, materials science, medicine, archaeology, and biology [3-7]. There are only few studies in the field of THz technology that are focusing on the exploration of construction materials for building structures [8-11]. Hence, a small number of reports in the literature shows that the construction and building industry lags behind other sectors in THz applications. However, one prediction for the future is that THz systems will make a breakthrough in the construction market by the year 2022 [12], but before that some technical and methodological improvements (e.g. higher acquisition rate and scanning speed, improved power performance, lower environmental conditions dependence, higher sensitivity to lower substance concentration) are needed. In addition, the improved reliability of THz measurements and the creation of uniform extensive database for a better interpretation of spectroscopic data is also necessary. In the next ten years, it is expected that the THz systems will become more achievable and less costly, especially due to the investments of telecommunications market in that field. Also the regulations will force industry to use non-contact and non-invasive methods to monitor their products before, during and after processing.

Based on systematic review, we found some published studies on materials that are also applied in the construction sector: detecting voids and heat damage in foams used in aircraft and polystyrene foam [13-15], various plastics analysis [10,16], detecting adhesive bonds between foam pieces [8], detecting the porosity and defects of ceramics [9,17], wood analysis [9,10,18,19], paint thickness and composition determination [20], imaging of defects in wood-plastic composites [21] and glass-fiber composites [22,23], spectral

analysis of different glasses [24,25], monitoring concrete and cement hydration [26-29], as well as some spectral analysis of stones, clay and asbestos [11,30,31] in THz frequency region. All of these studies were made by continuous wave THz system or pulse THz systems using photoconductive antennas (PHCAs) or ZnTe electrooptic (EO) crystals. Considering these studies, we can conclude that the initial potential of THz spectroscopy and imaging has been introduced for a few applications in the construction and building research, but it is obvious that much remains to be investigated in this area. When planning future research of materials by novel testing methods, the trends in the construction and building industry should be considered [32-36]. The focus should be given to the energy-efficient insulations and sustainable, eco-efficient, and recycling construction materials. Considering the results obtained in the above-mentioned literature, we can presume that THz spectroscopy and imaging can be applied to probe most of the insulation material characteristics ensuring low thermal conductivity and thermal transmittance [33,37]. In addition, THz imaging can be applied to visualize undesired hidden defects (e.g., cracks, water intrusion) in building envelopes made of modern materials, for instance vacuum insulation panels or aerogel composites. Moreover, the energy-efficiency, sustainability and eco-efficiency of construction and building materials are highly related to nanotechnology research. The incorporation of nanosized additives in existing construction materials enhance the mechanical properties and material durability as well as reduce their environmental impact [35]. THz radiation can probe the effects that these nanoparticles may cause on materials, including bacterial and fungal growth, water-repellent surfaces, and aging resistance. On the other hand, THz spectroscopy can be applied for characterization of hazardous and toxic substances that may remain in construction materials after exposure to extreme environmental conditions or natural catastrophes [38], and thus contribute to reuse and recycling of construction and building materials.

Currently, different NDT methods [29,37] are used to analyse construction materials, among which the most used are visual methods by means of microscopy and digital camera, ultrasound methods and acoustic imaging through detecting changes in acoustic attenuation and acoustic signature, as well as IR thermography, where the variation in temperature is recorded as a consequence of heat diffusion and cooling at the material surface. Other methods, involving ionizing radiation, are X-ray computed tomography (CT) and neutron tomography. X-ray computed microtomography [39] allows three-dimensional (3D) imaging but it can be time-consuming and costly, whereas neutron tomography [40] which enables description of the complex internal structure of materials is usually provided by a large instrument, not allowing in-situ measurements. Nowadays, FTIR and Raman spectroscopic techniques [5,41,42] have also become useful, non-destructive and easy to use techniques to study the structure of building and construction materials as well as to evaluate the processes that occur on materials due to their exposure to different environmental conditions. Without doubt, the THz spectroscopy as one of the IR spectroscopic techniques has not been really used in the qualitative and quantitative analysis of these materials. Thus, structural studies of these materials and sensing of compounds within it should be taken into consideration in this and future research with the THz techniques.

The main advantage of THz spectroscopy over other spectroscopic techniques such as FTIR spectroscopy is its high signal-to-noise ratio (SNR) below the frequency of 3 THz [43], allowing simultaneous transmission and reflection studies [44] of materials with relatively high absorption coefficients, and its operation at room temperature without the need of cryogenic system [45]. Above the frequency of 5 THz the FTIR spectroscopy is preferred to use due to the higher SNR at high frequencies where it also gives broader spectrum. In comparison to the existing NDT methods, THz technology offers numerous other advantages such as non-contact measurements, which can be performed on the

surface or in the bulk of material. In addition, THz waves are safe to use on humans and materials under investigation. Several advantages of THz systems over other technologies [6,16,46,47] have attracted interest in industry [12,48] and led to the development of compact, relatively inexpensive, and even portable THz systems [49], which are now commercially available on different markets. Almost all studies are performed with THz systems using PHCAs, inorganic EO crystals or continuous wave (CW) sources. The applications of THz system based on organic EO crystals are rare and the research studies are almost absent in literature. Thus, the verification of the application performance of this type of THz system is required for future system development and its optimization.

The THz detection is coherent, where both the amplitude and phase information are measured simultaneously, allowing the extraction of the complex dielectric constant of the material without the need of Kramers-Kronig relations [50]. In fact, the interactions between THz radiation and material give the information related to the dielectric properties of materials, from which important physical, mechanical and chemical properties can be extracted. When THz waves pass through materials, they produce unique transmission and absorption spectra that can be applied for analysis of construction and building material properties [9,33,37,42]. In addition, the supplementary amplitude and spectroscopic imaging modality of THz spectrometer can visualize hidden internal and surface defects, inclusions, and manufacturing imperfections. These specific characteristics can make THz spectroscopy and imaging a valuable complement or even substitute to other sensing techniques using ultrasound, microwaves, IR or X-ray radiation in the field of construction and building materials [37].

## 1.2 Hypotheses and aims

The most important issue in construction and building industry regarding the assessment of quality of construction materials is still the successful application of novel testing methods for in situ tests on sites or on the construction structures in use. Terahertz spectroscopy is one such novel analytical non-destructive tool that has already showed a great potential in other industrial sectors. Therefore, the main aim of this doctoral dissertation is to introduce and to spread the use of analytical tool based on THz radiation in the field of construction and building materials. For realization of the THz system application performance, it is necessary to verify its capabilities in the field of construction materials analysis and to perform laboratory testing that presents a base for practical use in industry. This aim originates from the statement that any study intended to explore the feasibility of application of a particular technology should be based on the relationship between three aspects: technology, experimental setup, and application [51] as shown in Figure 1.1.

The doctoral dissertation presents results of the experimental and analytical studies carried out at the Jožef Stefan International Postgraduate School in order to effectively demonstrate the case studies of THz sensing for construction and building materials characterization. In the frame of this approach, the objectives of the research are:

- to make a systematic overview of related work on construction materials and materials used in other fields that can also be applied as construction and building materials;
- to perform qualitative and quantitative THz spectroscopic and imaging analysis on different types of construction and building materials, including foams, composites, microfillers, and microencapsulated materials;
- to adapt the existing or to develop novel data processing procedures to generate appropriate THz spectra and THz images necessary for construction and building material analysis;

- to evaluate the THz analytical tool as a testing method for assessment of construction and building materials regarding the key advantages and limitations of the applied technology

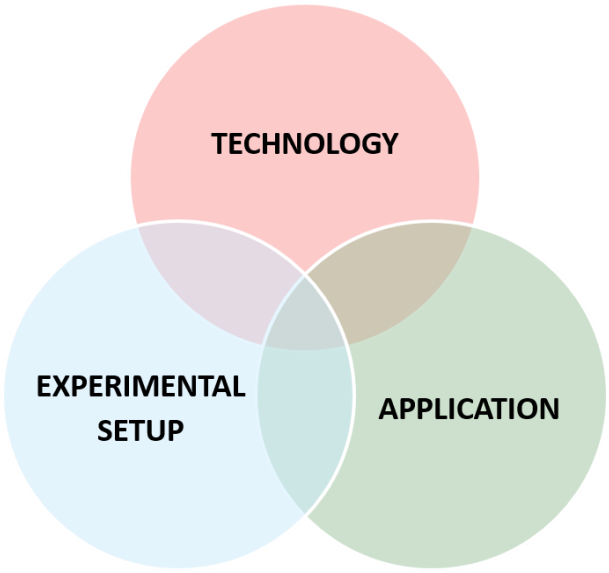


Figure 1.1: *The relationship between three aspects that should be considered when new technology is applied [51].*

The work presented in the thesis is based on the following hypotheses and approaches:

1. THz spectroscopy has a potential for characterization of different construction and building materials.
   - Since several construction and building materials are also widely used in other fields, where THz spectroscopy has already shown a great potential, a systematic overview of related work can be performed.
   - The calculations of spectroscopic constants and THz images based on existing and novel developed procedures can give both, the information about the macrostructure of investigated construction material and its composition.
2. THz spectroscopy and imaging can be applied as a testing method for assessment of construction materials during manufacturing process.
   - Assessment of construction material properties such as defects, impurities, porosity, changes in structure, particle size, thickness, particle distribution, honeycombing, chemical composition, etc.
3. THz spectroscopy and imaging can be applied as a testing method for assessment of construction materials during exposure to environmental conditions.
   - Assessment of construction material properties such as defects, humidity, external inclusions, temperature resistance, etc.
4. THz spectroscopy and imaging can be used in a combination with other sensing methods to improve the accuracy of assessment of construction materials.
   - Microscopy (scanning electron microscopy, confocal microscopy, optical microscopy) to comparatively analyse macrostructural properties and localized microstructural properties;
   - FTIR spectroscopy to verify characteristic spectral responses of construction and building materials in the IR frequency range.

## 1.3 Original contributions

Although THz technology has been widely used in various research fields and industry in the last two decades, the applications of this technology in construction and building field lag behind other sectors. To our knowledge, this dissertation provides the first systematic overview of current applications of THz technology in that field and submits novel applications based on results achieved during the research work. The practical and scientific novelty of the research performed in this thesis is summarized as:

1. THz spectra of some construction and building materials included in this dissertation, i.e. organic phase change material, aerogel composite, calcium oxide, calcium hydroxide, Bakelite foam, neoprene foam, micromass, plastazote, graphite-enhanced polystyrene foam, are reported for the first time. Thus, we contribute to the worldwide databases on THz spectroscopy.
2. Since the majority of the worldwide laboratories use THz systems based on PHCAs and inorganic EO crystals for materials characterization, we focused on the other type of THz system which uses organic EO crystals. We demonstrated that the selected THz-TDS and imaging system has shown applicable potential and some advantages over other THz systems and thus, open new opportunities in the field of materials characterization.
3. Macrostructure of polymer foams (voids, beads, defects, inclusions, internal structures, interconnections, density) was characterized with a submillimetre-scale resolution by using THz-TDS and TPI.
4. The novel procedure of THz imaging analysis in combination with the statistical analysis of data was proposed, enabling the visualization of some structural properties that were not easy detected by existing THz imaging methods by now.
5. The correlation between thermal conductance and THz absorption coefficient of polymer foams was introduced.
6. A special procedure how to discriminate between various granulations and chemical treatments of particles by using find spectral peak function and by analysing the spectral peak frequency position was proposed.
7. It was demonstrated that THz spectroscopy and imaging presents a valuable substitute or complement to other sensing techniques, i.e. FTIR and microscopy, and could contribute to the analysis and production process of construction materials in order to optimise their structure and functionality.

The results achieved during this research work were presented on national and international conferences and published in international journals with respected impact factor. Furthermore, we are confident that the results of the proposed dissertation will add value to the existing knowledge in both fields, THz technology and materials characterization, especially due to the predictions for the future which state that THz systems will make a breakthrough in the construction market by the year 2022. Additionally, the THz based research could enable processing companies to optimise their products and production processes in order to improve the mechanical and physicochemical material properties, which could also contribute to global efforts for energy and environmental conservation.

## 1.4 Approbation of the scientific work

The research was carried out in the period from 2009 to 2015. The obtained results are summarized in 4 publications, among which two were already published in SCI journals, one is accepted for publication and the last one is under review as a submitted manuscript.

1. Abina A, Puc U, Jeglič A, Zidanšek A. Structural analysis of insulating polymer foams with terahertz spectroscopy and imaging. *Polymer Testing*. 2013;32(4):739-747.
2. Abina A, Puc U, Jeglič A, Zidanšek A. Applications of terahertz spectroscopy in the field of construction and building materials. *Applied Spectroscopy Reviews*. 2015;50(4):279-303.
3. Abina A, Puc U, Jeglič A, Prah J, Venckevičius R, Kašalynas I, Valušis G, Zidanšek A. Qualitative and quantitative analysis of calcium-based microfillers using terahertz spectroscopy and imaging. *Talanta*. Manuscript number: TAL-D-15-00639R1 (accepted).
4. Abina A, Puc U, Jeglič A, Zidanšek A. Structural characterization of thermal building insulation materials using terahertz spectroscopy and terahertz pulsed imaging. *NDT & E International*. Manuscript number: NDTEINT-D-15-00148 (under review).

The results were also presented in the following international scientific conferences:

1. Abina A, Puc U, Jeglič A, Zidanšek A. Terahertz spectroscopy and imaging of foamed polymers. International THz Conference; 9-10 September 2013; Villach, Austria.
2. Abina A, Puc U, Heath DJ, Puc U, Zidanšek A. Spectroscopic THz imaging using organic DSTMS (4-N,N-dimethylamino-4'-N'-methyl-stilbazolium 2,4,6-trimethylbenzesulfonate) crystals. 4th Jožef Stefan International Postgraduate School Students Conference; 25 May, 2012; Ljubljana, Slovenia.
3. Abina A, Puc U, Jeglič A, Zidanšek A. Metode pri teraherčnem pulznem slikanju = Methods for terahertz pulse imaging. Paper presented at: 10th Symposia of Physicists at the University of Maribor; 8-10 December, 2011; Maribor, Slovenia.
4. Abina A, Puc U, Jeglič A, Zidanšek A. Applications of terahertz spectroscopy and imaging for building materials characterization. MIDEM 2015 51st International Conference Microelectronics, Devices and Materials, September 23-25, 2015, Bled, Slovenia (submitted).

Other publications related to the THz materials characterization, where I attended as a co-author can be found in Appendix D.

## 1.5 Outline of the Dissertation

The dissertation begins with the introductory chapter. Firstly, a motivation for work is given, from which aims and hypotheses are derived. Then original contributions and approbation of the scientific work are provided.

In the second chapter the theoretical background addressing THz spectroscopy is introduced. The first section explains the fundamentals of THz spectroscopy, beginning with the principle of THz generation and detection, and followed by the description of system configurations in transmission and reflection geometry. The next three subsections describe the THz imaging possibilities and the interactions between matter and THz radiation as well as the spectroscopic and imaging analysis techniques essential to describe the wave-matter interactions.

The third chapter is dedicated to the experimental preparations and the measurement execution procedure, including the description of selected THz time-domain spectroscopy (THz-TDS) and THz pulsed imaging (TPI), sample preparation procedure and measurement procedure with data acquisition and data analysis. Additionally, the reference methods used to validate the selected THz methods are listed and shortly described.

In the next chapter, the original research studies with results are provided as publications associated with this doctoral dissertation. The first publication is a systematic review of current applications of THz spectroscopy in the field of construction and building materials, along with the key advantages and drawbacks of technology and recommendations for future use. The next publication provides macroscopic structural analysis of insulating polymer foams with THz spectroscopy and imaging. The same THz methods are applied in the third study, where calcium-based microfillers were qualitatively and quantitatively analysed, considering its concentration in polymer matrix, granulation, chemical treatment and binary-mixtures. In the fourth publication, the THz-TDS and TPI are used to analyse the structure of various types of thermal building insulation materials, including polymer foams, aerogel composite, and microencapsulated phase change material (PCM).

The last two chapters highlight the main findings of the doctoral dissertation and discuss the future challenges of THz investigations in the field of construction and building materials.

# 2 Terahertz Spectroscopy

## 2.1 The terahertz range of the electromagnetic spectrum

In this section a brief introduction to THz technology is given, dealing with the answers to questions like:

- what is THz technology,
- when actually the research in this field started, and
- why the technology is so promising for material characterization?

In physics, THz radiation is also known as a submillimetre radiation, THz waves or T-rays, which occupy frequencies in the part of the EM spectrum that was relatively unexplored until recently, mainly due to the lack of powerful and user-friendly THz sources and detectors [51]. Therefore, this part of the EM spectrum is usually known as THz gap (Figure 2.1), corresponding to the wavelengths between microwaves and NIR waves. Some scientists range this gap between frequencies of 0.1 THz and 10 THz [3], the others between the high frequency edge of the millimetre wave band, i.e. 0.3 THz, and the low frequency edge of the FIR light band, i.e. 3 THz [6].

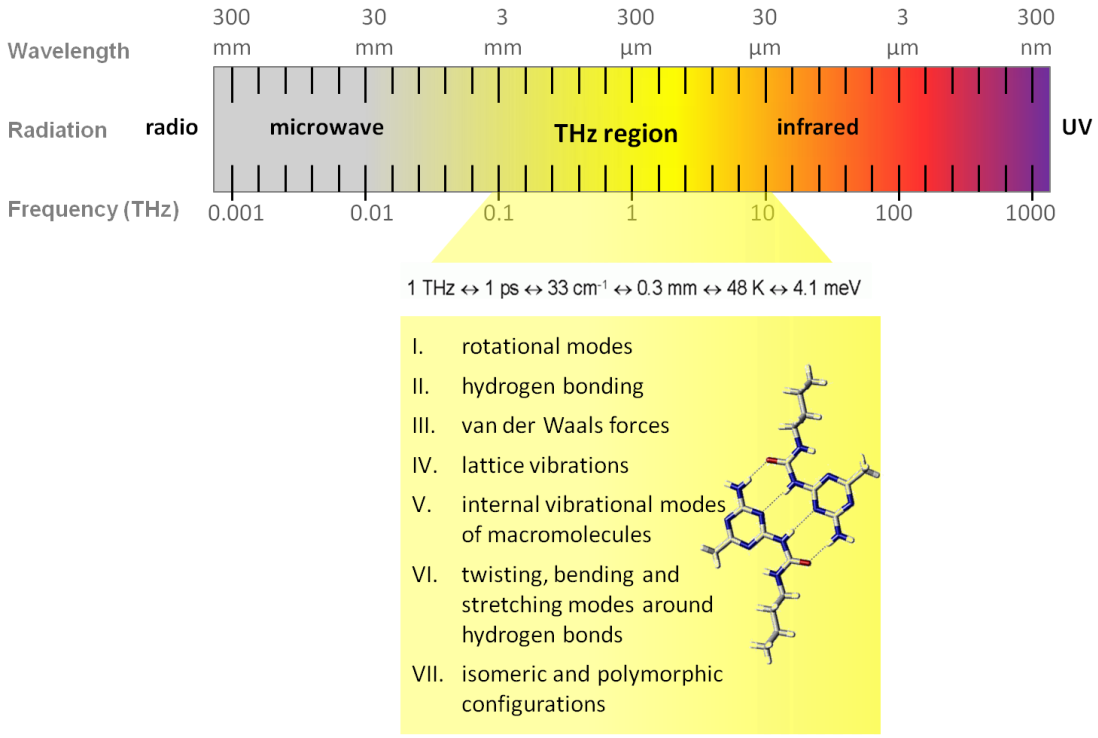


Figure 2.1: *The THz gap of the electromagnetic spectrum and the interactions between THz waves and molecules that THz technology is able to probe.*

At the end of the 80s of last century, the THz technology became interesting for physicists and other researchers. In 1988 the first demonstration of free-space THz

transmitters and detectors was performed by Smith, Auston and Nuss [52]. They successfully demonstrated that photoconducting dipole antennas are capable of generating and coherently detecting extremely short EM pulses in order of subpicoseconds. The described technique showed a significant potential for the spectroscopic measurements of materials such as dielectrics, semiconductors, superconductors, liquids, gases, and others in FIR region. Just a few years later, the same research team was also one of the first who performed imaging with the optoelectronic THz-TDS [53]. First demonstrations were done for package inspection, chemical content mapping, and food inspection. Since then, the articles focused on THz spectroscopy and imaging, published in SCI journals drastically increased (Figure 2.2). The major research work was dedicated to the development of novel THz sources and detectors, whereas the spectroscopic analysing and imaging methods had lagged behind. In the last few years, the rapid development of novel THz sources and detectors has opened additional possibilities of creating innovative spectroscopic and imaging systems, allowing in situ measurements and real-time analysis of different materials. Advances in the field have encouraged new research in various disciplines, including chemistry, pharmacy, physics, materials science, medicine, security, archaeology, and biology [3-7,54,55]. With certainty, we can state that at this time we almost reach the peak in publications, but there are still a lot of challenges and barriers regarding the THz spectroscopy and imaging which have to be resolved in the near future, especially if we want to diminish the gap between laboratory experiments and industrial use under real conditions.

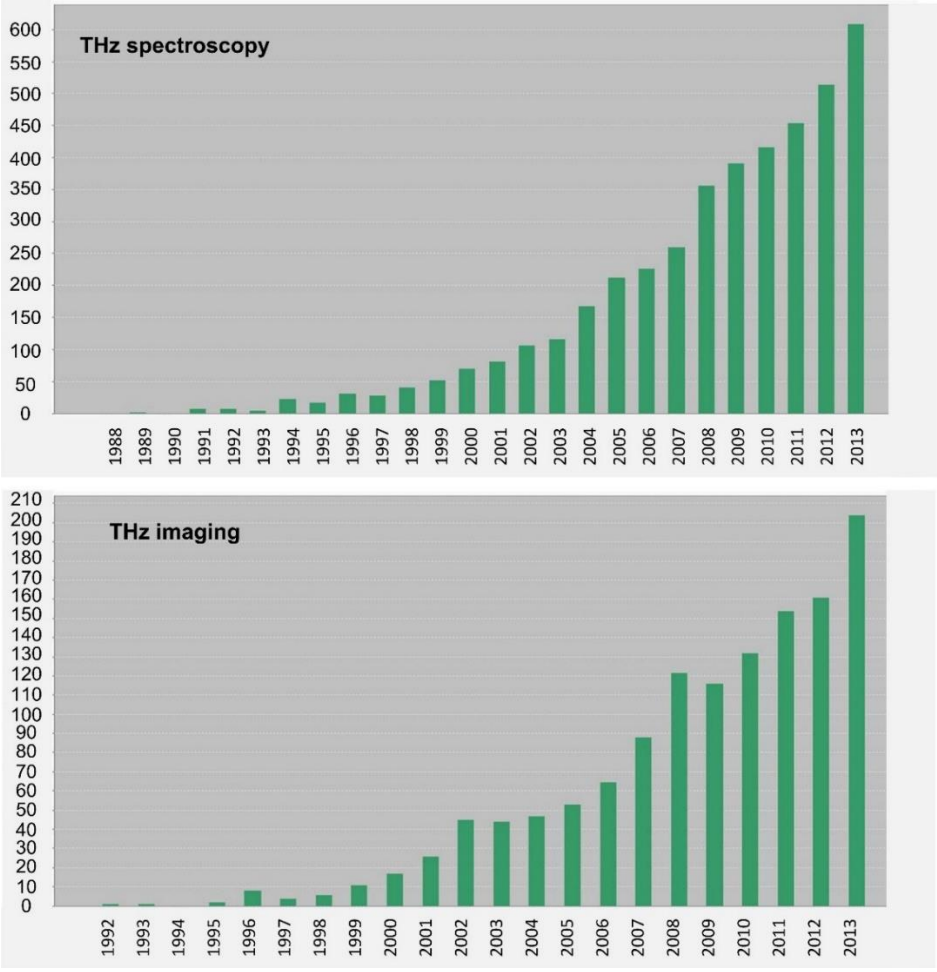


Figure 2.2: *Growth of SCI publications for keywords THz spectroscopy and THz imaging for the period 1988-2013 and 1992-2013, respectively*. Adopted from Web of Science Citation, Report made in April 2014.

The most promising aspect of this technology is that THz radiation is very sensitive to interactions between molecules and as such shows some interesting characteristics of materials. Here not only rotational energy levels as in case of microwaves but also vibrational transitions and various intermolecular bonds such as hydrogen bonds and van der Waals forces are important [3]. Furthermore, THz waves can also probe lattice vibrations, isomeric and polymorphic configurations [56], and thus allow differentiating between various chemical compounds [46] and even different variations of the same solid-state crystals [57]. These properties are specific to the molecule and thus, enable characteristic spectral features in the THz frequency range.

Several advantages of THz system over other technologies—for example, X-ray tomography, gamma rays, IR imaging and millimetre-wave imaging [6,16,46,47]—have attracted interest in industry and led to the development of compact, relatively inexpensive, and even portable THz systems, which are now commercially available on different markets. Certainly, the most value characteristic of THz waves for industry is its non-ionizing and non-destructive nature. Moreover, THz waves can penetrate barriers made of dielectric or non-conducting materials, e.g. plastics, ceramics, paper, cardboard, wood, natural and synthetic fabrics. Currently, THz waves can be hardly replaced by other waves, for instance X-rays which lead to photoionization in biological tissues; millimetre-waves which do not provide sufficient spatial resolution; or visible and IR waves which are more dependent from Mie scattering and cannot see through the barriers [58].

## 2.2 Fundamental principles of terahertz radiation

There have been several analytical tools, based on THz radiation, developed since its first mention in the literature almost 30 years ago. In general, THz systems can be divided into pulsed systems, known as THz-TDS, and CW systems. THz-TDS is the most commonly used technique when both amplitude and phase information are required. On the other hand, CW systems, where the duration of the pulse is infinite, are usually selected to measure only the intensity data at a fixed single frequency. Due to the coherent detection, the THz pulsed technique is more widely used for material inspection because measuring the phase at a single THz frequency is very hard or non-existent for current THz CW configurations [59]. However, CW systems also have some advantages, they offer higher average power in comparison to pulsed systems, the obtained spectra are less affected by water vapour absorption lines and they can be more easily settled up to small and portable devices [51]. The work in this thesis is based on THz pulsed system, thus the following subsections are dedicated to this approach.

### 2.2.1 Basic physical fundamental of THz generation and detection

The THz part of the EM spectrum was almost unexplored until recently, mainly due to the lack of appropriate emitters capable to send out THz signals and efficient sensors to detect and record generated THz radiation. The technological development in the last 30 years brings several efficient THz emitters and detectors that have a great potential for THz spectroscopic systems. The THz system performance and capability depend on the characteristics of the particular THz emitter and detector. However, there are two most common mechanisms for the generation and detection of pulsed THz beams: resonant photon-induced conductivity changes in semiconductors or PHCAs, and non-resonant optical rectification with electrooptic sampling in EO crystals. Also the system with the combination of PHCA as an emitter and the EO crystal as a detector was introduced [60]. Although the physical mechanisms of EO crystals and PHCAs differ considerably, both tend to high-bandwidth pulses, high SNR, and high generated power in the THz beam,

which all significantly contribute to the high-quality THz spectrum necessary for material analysis. Usually, an average generated THz power is in the nW to μW range, whereas the average power of the femtosecond (fs) optical source is in the range of mW to W [51]. In the next two subsections, a brief explanation of both physical mechanisms is provided.

### 2.2.2 Photoconductive generation and detection

The photoconductive antennas are widely used for pulsed THz generation as well as THz detection. The mechanism is based on the conductivity changes in a semiconductor, which are induced with ultrafast laser pulses, e.g. Ti:sapphire laser with 800 nm wavelength. PHCAs usually have a form of dipole structure, i.e. two metal electrodes typically made of gold and separated by 5-30 μm, with a gap between electrodes at the centre of antenna (Figure 2.3). Other possible forms are spiral [61] and bow-tie antennas [62]. The most widely used semiconductor substrate material on which electrodes are coated is low-temperature grown gallium arsenide (LT-GaAs) due to its high mobility that ensures a larger THz bandwidth. The thickness of the semiconductor substrate in a form of thin film is assumed to be much less than the THz wavelength. Usually, the gap between the electrodes is in the range of few μm.

In the generation mode, a dc voltage is applied across the electrodes. The gap has the role of a photoconductive switch that is turned on when it is illuminated with the fs laser pulses. The illumination of the gap with a laser pulse creates photocarriers, which are then accelerated by an electric field and produce a transient photocurrent *J(t)* expressed by equation [51]:

$$J(t) = N(t)emE_b \tag{2.1}$$

where $N$ is the density of photocarriers, $e$ is the elementary charge, $m$ is the mobility of electron, and $E_b$ is the bias electric field amplitude. Thus, the reservoir of electric energy stored in the gap is opened and released in the form of freely propagating sub-picosecond transient or THz wave, where the THz electric field amplitude, $E_{THz}$, is in the Hertzian dipole approximation proportional to the time derivative of photocurrent [63],

$$E_{THz}(t) \propto \frac{\partial J(t)}{\partial t} \tag{2.2}$$

The detection mode principle based on PHCAs is almost the same as the generation mode, the main difference is that the dc-bias is replaced with an ampere meter connected with a lock-in amplifier. When the THz pulse is incident upon the detector PHCA, it induces a time varying voltage across the active region, i.e. gap, of the PHCA. In the presence of laser excitation, a photocurrent through the antenna is generated, with the amplitude proportional to the amplitude of the incident THz wave, $E_{THz}$. The photocurrent in the antenna induced by the incoming THz pulse is detected by a lock-in amplifier. The photocurrent in the detector is given by:

$$J(\tau) = \frac{1}{T}\int_0^T E_{THz}(t)\sigma(t-\tau_c)dt \tag{2.3}$$

where $\sigma$ is the surface conductivity in the photoconductive gap and $\tau_c$ is the carrier lifetime of the substrate, which is typically much shorter than the THz pulse duration and thus, the antenna acts as a photoconductive sampling gate. The THz waveform is obtained by measuring the average photocurrent versus time delay between THz pulse and the gating optical pulse. From the measured THz waveform one can extract the information about the

amplitude and the phase of the incident THz field by using a Fourier analysis. PHCAs are typically capable of relatively large average THz powers up to 50 mW and bandwidths up to 5 THz [64]. The bandwidth of THz signals is actually limited by the antenna's frequency response, the carrier lifetime, and resistivity of the PHCA material [65]. The basic mechanism of this type of THz wave generation and detection is shown in Figure 2.3.

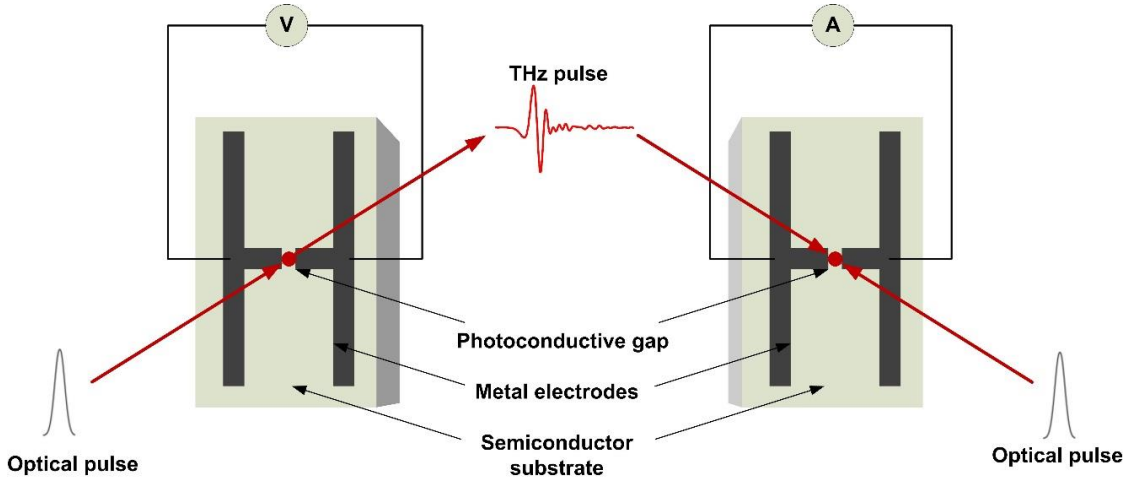


Figure 2.3: *THz generation and detection by PHCA emitter (left) and PHCA detector (right) illuminated by a femtosecond laser pulse.*

### 2.2.3 Optical rectification and electrooptic sampling

Another widely used principle of THz wave generation is an optical rectification based on second-order optical nonlinearity with the main advantage of achieving a broader spectral bandwidth and a lower emission power in comparison to PHCAs. The major difference from PHCAs is that the radiation here is generated only by the short fs pulse of EM radiation that contains a broad bandwidth of frequency components that are mixed inside the EO crystal. In general, materials with a large second-order optical nonlinear coefficient and a low absorption for both optical and THz waves are good candidates for THz source and detectors. Most commonly used nonlinear crystal for EO sampling at wavelengths around 800 nm is ZnTe due to its physical durability and great phase-matching properties. Some other crystals, including dielectric crystals ($LiTaO_3$, $LiNbO_3$, etc.), semiconductors (InP, GaAs, etc.), organic EO polymers (LAPC, DCDHF, etc.), and organic crystals (DAST, DSTMS, etc.), have also shown appropriate performance for THz wave generation and EO sampling.

When fs laser pulse interacts with EO material with a second-order nonlinearity, a transient polarization occurs that leads to the radiation of an EM wave, whose polarization depends on the crystal orientation and the incident pump beam polarization. (Figure 2.4). Hence, the emitted THz field, $\mathbf{E}_{THz}$, can be expressed as [66]:

$$\mathbf{E}_{THz}(t) \propto \frac{\partial^2 \mathbf{P}(t)}{\partial^2 t} \tag{2.4}$$

where $\mathbf{P}(t)$ is the polarization and can be expressed as [67]:

$$\mathbf{P}(t) \propto \chi^{(2)} \mathbf{E}_{opt}(t)^2 \tag{2.5}$$

The polarization can be expanded into a power series of the electric field, where the second term is related with the optical rectification. The induced THz electric field is thus

proportional to the square of the incident optical power of the time series of optical pump pulse, $\mathbf{E}_{opt}$, and the second-order optical nonlinear coefficient or susceptibility, $\chi^{(2)}$. The shape of the THz temporal waveform and the frequency distribution of the generated THz wave is highly dependent on parameters of crystals, such as crystal orientation, thickness, absorption, dispersion, diffraction, and saturation. The thinner EO crystals ensure broader frequency response but on the other hand the interaction distance is shorter, resulting in reduced sensitivity. The bandwidth of coherent THz spectroscopy depends not only on EO crystal parameters but also on the phase-matching conditions and laser pulse duration. The last one can be expressed by equation:

$$\Delta\nu = \frac{1}{\tau} \tag{2.6}$$

where $\tau$ is the duration of an optical pulse in fs. Today, lasers pulse duration below 10 fs exists, thus a bandwidth of THz spectroscopy can be significantly expanded up to 100 THz. The phase matching is the most important parameter and requires conservation of energy and momentum in the nonlinear process to satisfy the condition that all three waves involved in the process are kept in phase. In only this way, the generated THz field will continually increase along the entire depth of the nonlinear crystal.

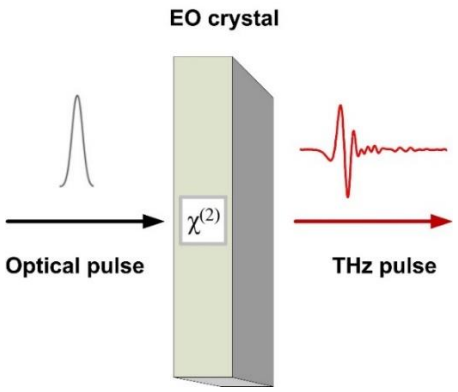


Figure 2.4: *THz pulse generation through a second order nonlinear process.*

The reciprocal process of optical rectification is an electrooptic sampling. Based on this principle the THz field is measured by modulating a probe laser beam inside an EO crystal, where the THz field changes the birefringence of the EO crystal which causes the differences in refractive index. The incoming probe beam is phase-modulated by this refractive index change. The phase change is converted to an intensity change by an analyser, also known as a polarization beam splitter. Thus, from the refractive index change, one can calculate a phase delay. The phase delay of the probe laser beam can be measured in two most commonly used methods [51]:

- Balanced measurement, where a quarter-wave-plate is used to bias the polarization of the probe beam, either in the front or after the EO crystal. An analyser splits the polarization in two components, and the difference between them is measured by using a pair of balanced photo detectors. In case that no THz field is applied, both components have the same intensity and the detector gives no signal, whereas the THz field appears, the polarization of the probe beam is changed and the detector can measure a signal.
- Cross measurement does not use quarter-wave-plate. The analyser is set before the EO crystal. When THz field is applied, the probe beam polarization is modified which causes the probe beam to leak through the analyser. Thus, the signal is detected.

## 2.3 Terahertz time-domain spectroscopy

In general, the pulsed THz spectroscopy system is based on a pump and a probe beam concept as schematically presented in Figure 2.5. The system with such an arrangement of components is called a THz time-domain spectroscopy. The measurements are performed by using an external fs source, usually a laser pulse with wavelengths around 780 nm or 1560 nm. The initial fs laser beam is split on a beam splitter (BS) into two beams: the pump beam (1) for generating and the probe beam (2) for detecting the THz waves. In the first case (Figure 2.5 A), the pump beam, still an optical pulse, is focused through the system of lenses (S) and mirrors to the semiconductor PHCA or EO emitter crystal that are responsible for THz wave (3) generation through the photoconductivity mechanism or optical rectification, respectively. The mechanisms are explained in section 2.2. The test material is placed in the middle of the THz beam path. The THz beam is guided by parabolic mirrors (PM) through the sample to the THz detector. The probe beam is appropriately delayed in time relative to the THz wave using an optical delay line (DL). A delay stage can be also applied to the pump beam [68] instead of the probe beam path (Figure 2.5 B) since its function is that the THz pulse can be traced as a function of time by controlling the delay between the two pulses. Thus, a complete THz time-domain waveform can be acquired. The probe beam is also transmitted through the detector, where it is split into polarization components inside the analyser, and detected by a photodiode in conjunction with a lock-in amplifier. This type of THz detection is known as a coherent homodyne detection [69].

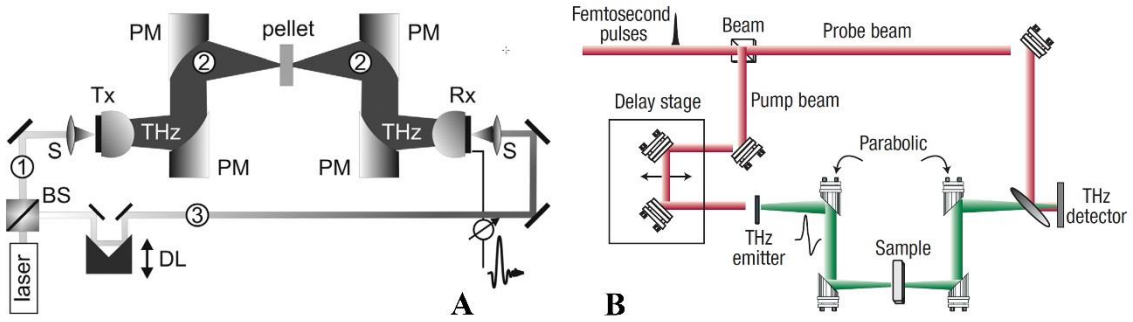


Figure 2.5: *Schematic presentation of a typical transmission-mode THz time-domain spectrometer.* Reprinted from [69] and [68].

### 2.3.1 System geometry

Depending on the inspection needs, THz-TDS can be designed either in a transmission or in a reflection mode (Figure 2.6), each described by specific performance characteristics. However, some systems also combine both modes in a single system setup [44]. The coherent detection of the transmitted or reflected THz radiation can be achieved through a few different approaches, which in the end all give very similar signals containing the amplitude and the phase information of the electric field, necessary for the spectroscopic analysis of materials.

Terahertz transmission configuration is applied when someone wants to measure the intensity of a THz pulse after it had propagated through the samples, which are transparent in the THz region and are quite thin. The mechanism of transmission geometry is presented in the previous section. The transmission measurements can be used for the determination of the direct refractive index and the dielectric constant of a sample. Because a method is phase-sensitive, both real and imaginary part of the dielectric constant of the material can

be studied without carrying out the Kramers-Kronig relations. For measuring a THz transmission spectrum, a reference spectrum is required. This is usually achieved by measuring the THz signal when the sample is removed from the THz beam. Moreover, this configuration mode is used for quantitative analysis of samples, for instance for thickness measurements and concentration determination according to Beer-Lambert relationship explained in section 2.5.

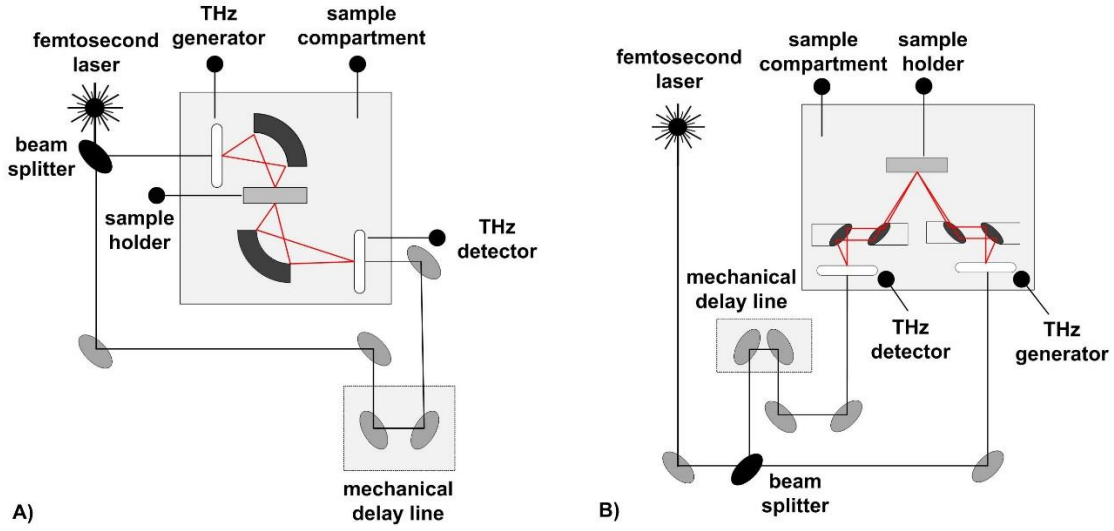


Figure 2.6: *Schematics of THz spectroscopy in transmission (A) and reflection (B) configuration.*

When the investigated samples are thick and less transparent in THz region, then a more appropriate method is reflection THz spectroscopy. The THz experiments performed in a reflection mode also provide a train of optical laser pulses that are split into a pump beam and a probe beam. A THz beam, generated from a pump beam that is guided through the THz emitter, is focused on the surface of the sample under investigation. The THz beam is incident upon the air/sample interface at a certain angle to normal incidence, usually 30° or 45°. The reflected THz pulses are then recolimmated using PMs and focused onto the THz detector. The rest of the procedure for THz beam detection and recording is the same as in case of THz transmission configuration. The difference from transmission mode is also in measuring the reference spectrum. In this case, a metal surface is usually selected as a reference material. However, it is more difficult to extract the spectroscopic constant, e.g. complex refractive index, by measuring the spectrum in a reflection mode. The reflection geometry is the most realistic approach for practical applications in industry.

## 2.4 Terahertz pulsed imaging

THz pulsed imaging is actually an extension of the THz-TDS that enables a 2D or 3D visualization of the inner structures of material samples with a submillimetre spatial resolution. TPI technique uses either nonlinear optics or a photoconductivity mechanism for generating and detecting THz pulses. Its setup can be performed in a transmission or in a reflection geometry. For THz imaging the most important parameter of a system is the time needed for the THz waveform acquisition, which is limited by the scan rate of the optical DL. Typically, a THz image is obtained by using motorized scanning stage to raster the object under investigation. The data for image formation is acquired in a manner one pixel at a time. In general, TPI data set contains three dimensions, two in space (2D) and the third one in time (1D). Thus, the THz image acquisition is usually a time consuming

process. Noteworthy is the fact that a shorter scan range limits the spectral resolution and the range of depths to which THz pulse can penetrate [70]. First limit is important for multispectral imaging, whereas the second one affects the time-of-flight imaging.

After a complete data set of THz time-domain waveforms acquisition, a THz image can be generated. In the literature at least three different 2D THz imaging techniques can be found, each suitable for different applications. These techniques can be divided into two groups as shown in Figure 2.7: time-domain imaging and frequency-domain imaging, including multispectral imaging and spatial distribution map. Typically, by using different set of data for image formation, different information about the material can be obtained and visualized. The obtained time-domain THz image does not contain any spectroscopic information; thus, this type of imaging is suitable only for the detection purposes. Since different chemical compounds show specific spectral features in THz frequency band, imaging in the frequency domain contains important information about each individual substance and enables identification as well as classification [71,72].

The false-colour time-domain THz image is constructed based on key parameters—for example, maximum amplitude or peak-to-peak amplitude—which are obtained from the each THz time-domain waveform. Once using the transient time of the THz pulse through the sample, thickness variations within the sample can be visualized because the thicker regions delay the THz beam. The spectroscopic imaging is performed using Fourier transform of the time-domain waveform to obtain the spectral frequency dimension, allowing imaging at different frequencies. By changing the frequency emitted by THz emitter within a certain spectral range, multispectral images can be obtained [3,73]. By upgrading this technique with a component spatial pattern analysis method, the enhanced THz images can be obtained from frequency-domain images recorded at different THz frequencies, indicating the separation of the spatial distribution patterns of individual substance within the heterogeneous samples [71,74]. All three imaging methods are in detail explained in section 2.8.

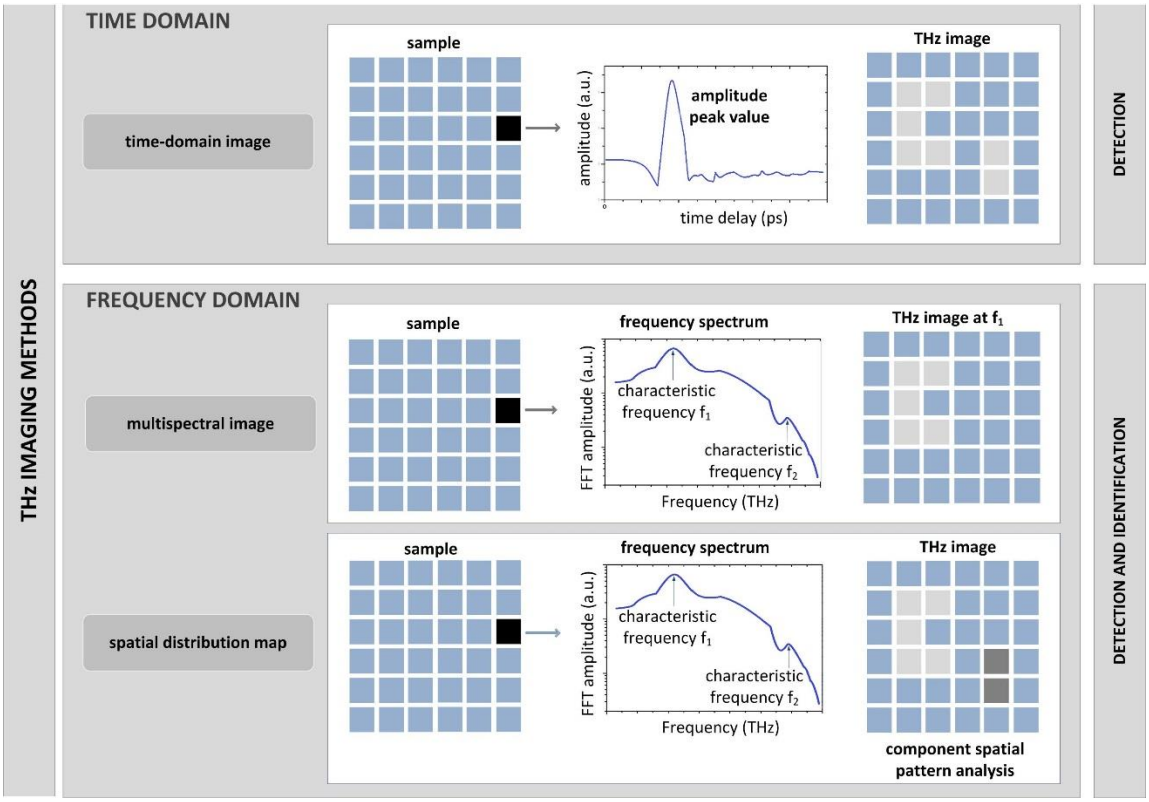


Figure 2.7: *THz imaging methods in time-domain and frequency domain.*

During the last decade, the THz imaging has garnered a lot of attention in the development of novel spectroscopic imaging techniques not only in 2D but also in 3D. For instance, a 3D imaging method based on time of flight approach is capable to estimate the depth information of the internal dielectric profiles of the material during the time that is required to travel over a certain distance [75]. Using this concept a 3D imaging was extended to THz tomography, which is similar to X-ray imaging. Other imaging methods involving THz radiation are near-field THz imaging, THz chemical microscope, THz emission imaging, and CW THz imaging. Because the focus of this dissertation is not on other imaging methods, they are not discussed in details.

## 2.5 Material interaction with terahertz radiation

Since one of the major applications of THz spectroscopy is material characterization, it is important to understand an interaction between EM radiation and material under investigation. Understanding this aspect is necessary for the interpretation of obtained THz spectrum. According to Maxwell equations 2.7-2.10, the EM waves can interact with the matter in the following ways: absorption, transmission, reflection, refraction, emission, and scattering (Figure 2.8). The macroscopic form of Maxwell's equations is given as:

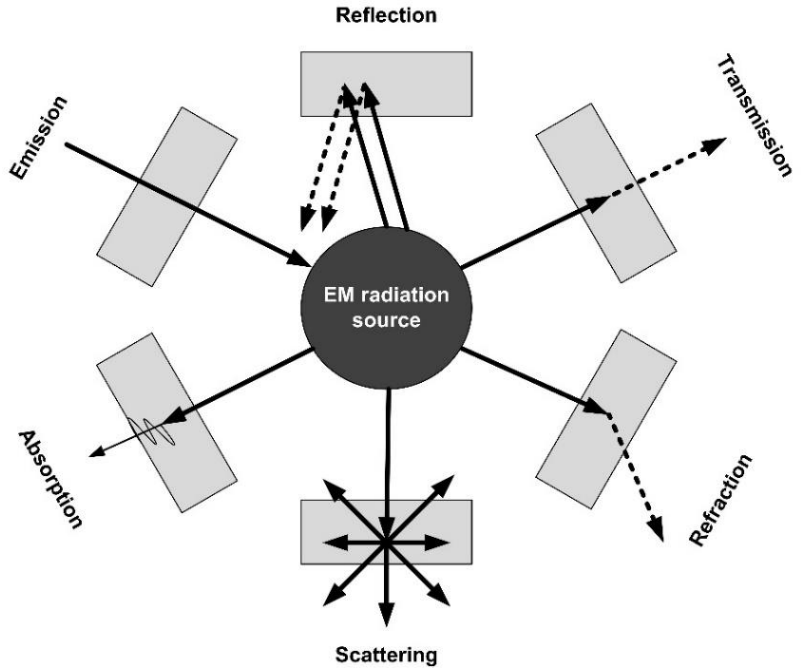


Figure 2.8: *Possible interactions between electromagnetic waves and material.*

$$\nabla \bullet \mathbf{D} = \rho_f \tag{2.7}$$

$$\nabla \bullet \mathbf{B} = 0 \tag{2.8}$$

$$\nabla \times \mathbf{E} = -\frac{\partial \mathbf{B}}{\partial t} \tag{2.9}$$

$$\nabla \times \mathbf{H} = \mathbf{J}_f + \frac{\partial \mathbf{D}}{\partial t} \tag{2.10}$$

where $\rho_f$ is the free charge density and $\mathbf{J}_f$ is the free current density. The electric displacement **D** and magnetic field strength **H** are related to the electric fields **E** and the magnetic field **B** by equations:

$$\mathbf{D} = \varepsilon_0 \mathbf{E} + \mathbf{P} \tag{2.11}$$

$$\mathbf{H} = \frac{1}{\mu_0}\mathbf{B} - \mathbf{M} \tag{2.12}$$

where $\varepsilon_0$ and $\mu_0$ are the permittivity and the permeability of free space, respectively. The polarization **P** and the magnetization **M** are related to the macroscopic properties of the matter. If the media is isotropic and linear, the equations 2.11 and 2.12 can be written as $\mathbf{D} = \varepsilon\mathbf{E}$ and $\mathbf{H} = \frac{1}{\mu}\mathbf{B}$, where $\varepsilon$ and $\mu$ are the electric permittivity and the magnetic permeability, respectively.

In general, THz radiation is strongly reflected from materials with a high permittivity and a high refractive index, e.g. metals. For such materials, we can say that they are opaque to THz waves. Actually, the refraction occurs when the EM radiation is incident on a boundary of two materials with different refractive indices, $n_1$ and $n_2$. If we neglected the scattering effect on THz wave attenuation, then the reflectivity *R* and transmittance *T* of the material can be determined by using Fresnel equations [76]:

$$R = \frac{|E_R|^2}{|E_0|^2} \propto \frac{I_R}{I_0} \tag{2.13}$$

$$T = \frac{n_2|E_T|^2}{n_1|E_0|^2} \propto \frac{I_T}{I_0} \tag{2.14}$$

where $n_1$ and $n_2$ are the refractive indices of the materials, whereas $E_0$, $E_R$ and $E_T$ are the incident field amplitude, reflection field amplitude, and transmitted field amplitude, respectively. In case of THz-TDS, where the measurements are coherent, we measure the THz electric field, $\mathbf{E}_{THz}(t)$, and not the intensity, $|\mathbf{E}_{THz}(t)|^2$ that is measured in standard FTIR spectroscopy. An intensity measurement $|\mathbf{E}|^2 \propto I$ does not contain the entire phase information. The broadband THz pulse, $E(z,\nu)_{in}$ propagating in the *z* direction through the material involves the information about the amplitude and the phase of EM waves according to equation [77,78].

$$E(z,\nu)_{out} = E(0,\nu)_{in} e^{ik_0 z} e^{i\Delta k(\nu) z} e^{-\alpha(\nu) z/2} = E(0,\nu)_{in} e^{ik(\nu) l} \tag{2.15}$$

where *l* is the thickness of the material (also in *z* direction) that THz pulse propagates through, and *k* is the complex propagation constant, containing the real part related to the propagation in free space, and the imaginary part corresponding to the material absorption. The complex propagation constant is used to describe the interaction of the electric field with the material in frequency domain by the equation [78]:

$$k(\nu) = k_0 + \Delta k(\nu) + i\frac{\alpha(\nu)}{2} \tag{2.16}$$

where the term $k_0 = \nu\left(\frac{n}{c}\right)$ is the nonresonant wave vector in the sample and *n* is the refractive index outside the material resonances, the term $\Delta k$ is describing the frequency-dependent phase change per unit length, and $\alpha(\nu)$ is the absorption coefficient of the material. Hence, the refractive index can be directly determined through measuring the relative phases of the incident and transmitted EM waves. The amplitude transmission, *t*, obtained by THz measurements, where the spectral amplitude of a sample is divided by that of a reference material, contains both the amplitude and phase information, and can be

derived as [77]:

$$t(\nu) = \frac{E(z,\nu)_{sam}}{E(z,\nu)_{ref}} = e^{-\alpha(\nu)l/2} e^{i[k_0 + \Delta k(\nu)]l} \tag{2.17}$$

the intensity transmission, *T*, is therefore expressed as:

$$T(\nu) = |t|^2 = \frac{I(\nu)_{sam}}{I(\nu)_{ref}} = e^{-\alpha(\nu)l} \tag{2.18}$$

The absorption is actually the energy of incident EM radiation that is transferred to the electrons of material when THz beam propagates through the material. This occurs when the frequency of EM radiation is resonant with the transition of vibration states of the nuclei within the material. The absorption is determined with the material structure and its thickness since the penetration depth of THz waves within the material is limited with the continuous energy loss exponential to the depth of material. If the scattering effect is neglected, then the absorption *A* is described by the Beer-Lambert law [79], given by equation:

$$A(\nu) = -\log_{10} \frac{I_T(\nu)}{I_0(\nu)} = \varepsilon(\nu) C l = \alpha(\nu) l = -\log_{10} T(\nu) \tag{2.19}$$

where $I_0$ and $I_T$ are the intensity of incident EM radiation and the intensity of the EM radiation transmitted through the medium. Moreover, in chemistry the absorption is proportional to the concentration of the compound in the solution, *C*, the thickness of the material, *l*, and the specific extinction coefficient of the absorbing material, *ε*. The product of the concentration and the specific extinction coefficient is also known as the absorption coefficient of the material, *α*. The absorption is also equal to the negative log of the transmission of EM radiation.

Even though the absorption of the material is low, the attenuation of EM waves can be high due to the scattering effect that occurs on structures within the material. This effect decreases the attenuation and increases the absorption coefficient, but it does not affect the index of refraction. Considering the scattering effect, the attenuation of EM wave intensity can be expressed as:

$$A = Z \sigma_S l \tag{2.20}$$

where *Z* is the number of scattering centres per unit volume and $\sigma_s$ is the scattering cross section. The product of these two terms corresponds to Beer's law, $\alpha = Z\sigma_S$. Scattering can either be elastic or inelastic. Two elastic scatterings are known, Rayleigh and Mie scattering. In the first case, the wavelength $\lambda$ of the incident EM radiation is much greater than the average particle size $\sigma_S$ in the material, $\sigma_S \ll \lambda$, also expressed with $\sigma_S \propto \frac{1}{\lambda^4}$. This means that smaller wavelengths are scattered more strongly. In the second case, the wavelength of the EM radiation is in the comparable size as the particles, $\sigma_S \approx \lambda$. In general, THz waves have longer wavelengths in comparison to visible and near IR waves, thus they are more affected by Mie scattering, when dealing with inhomogeneities with tens of microns in size. The Mie scattering is especially expressed when the wavelength of THz waves is on the same order as structural features in materials (thin layer, surface roughness, grain, particles, bubbles, etc.). Thus, the thickness of the layers should be below 100 μm and the size of particles in order of few 10's of microns. For solids, the scattering losses lead to complications in the quantitative analysis [80]. Usually, more than one interaction

occurs at the same time. Low absorption and low scattering are two key parameters of THz radiation that are known with common word “loss”. For non-homogeneous samples measured with the THz system in transmission configuration, the incident radiation can be redirected due to the non-uniformities in the mixture. Thus, the detector placed beyond the sample can miss the scattered radiation.

## 2.6 Terahertz wave interaction with gases, liquids and solids

Most chemical compounds, especially organic solids, exhibit very strong, highly specific frequency-dependent absorption and dispersion in the THz frequency range between 0.3 THz and 5 THz (Figure 2.9). The reason for these characteristics are rotational and vibrational transitions that express not only the properties of the molecule but also the surrounding environment, e.g. hydrogen bonding, bond water, crystal clustering. Usually, the THz features are modified when a substance changes aggregate states from gas to liquid to solid.

### 2.6.1 Gases

THz waves have the ability to strongly interact with the rotational transitions that exist in a gas phase of substances. The measurements of gas samples require long interaction length, i.e. long DL, to get appropriate absorption and high resolution. The gas is measured within the cell with transparent window, in order to avoid the absorption lines of water vapour. Additionally, the information about the cell length and pressure is needed due to the pressure-dependent spectral linewidths [77], which are also dependent on the system resolution. The THz spectra of gases exhibit narrow lines with few distortions and errors. Usually, the polar water molecules absorb fraction of the THz intensity, which is expressed as a reduced peak amplitude in the time-domain waveform and as a cut out of the particular frequencies in a frequency domain [77]. The water absorption lines can be removed numerically after measurements. An even better way to avoid this effect is to preform measurements in a dry air or nitrogen atmosphere. The linewidths are far narrower than the spectral resolution of the measurements [81]. From measured THz data, the absorption coefficient and the dispersive phase can be independently derived from the time-domain waveform by FT. Even without the FT, the rotational constants used to provide a rapid gas identification can be determined from the periodic recurrences in the time-domain waveform Several toxic gases, e.g. HCN, CO, $H_2S$, $NH_3$, HCl, $CH_3CN$, and $N_2O$, exhibit rotational spectra in THz band [35]. Besides identification also quantitative analysis of gases is possible. When knowing the absorption coefficient and the absorption length within the cell, it is easy to determine the concentration of gas in the ppm range [77]. Thus, THz-TDS allows both single species identification and quantitative analysis of gas mixtures.

### 2.6.2 Liquids

In comparison to gases, the absorption spectra of liquids do not exhibit narrowband spectral features. The THz spectra of liquids are used to show a general attenuation over the THz band. The polar liquids such as water strongly absorb the EM radiation in THz frequency range due to its sensitivity to permanent and induced dipoles inside the liquids caused by the formation of hydrogen bonds between water molecules. For most liquids the THz absorption coefficient decreases as the dipole moment decreases. If the samples contain a high concentration of water, thin cells are required due to high water absorption in THz frequency range. Non-polar liquids show a weak absorption in THz region [77].

The dipoles can also be induced in non-polar liquids. Hoffmann et al. [82] described that the THz wave interacts with the non-polar liquids in the same way as a fs laser pulse. The molecules in liquid are aligned by the THz field, causing optical anisotropy, also known as Kerr effect related with the third-order nonlinear optical properties.

The reorientation of dipoles in liquids on a picosecond (ps) time scale is essential for both chemical reactions and biological functions. As expected, water and aqueous solutions are the most widely studied liquids, mainly for biological and medicine applications, where the major limitation presents the low penetration depth of THz waves within the tissue. THz-TDS spectroscopy was successfully applied to the analysis of ionic liquids and ionic liquid-water mixtures [34]. THz spectroscopy called attenuated total reflection turns out to be very useful for identification of ingredients in solution [83], and also to determine their concentration with high accuracy, e.g. concentration of alcohol in beverages [84]. On the other hand, the high water absorption also has an advantage that allows THz spectroscopy to be used as moisture detection. Some experiments already showed the exponential decay of the THz transmission as a function of moisture content in powder samples.

### 2.6.3 Solids

The spectra of solids show some characteristic spectral features due to the low-frequency phonon modes existing in a long range order of the environment of molecules. These absorption lines are not sharp as in case of gas samples. These characteristic spectral features allow applications related to the recognition and analysing of pharmaceuticals, illicit drugs and explosives based on a priori created databases and multispectral data analysis.

When measuring solids, internal reflections within the material may occur. This means that when the wavelength is comparable to the size of the material under investigation, multiple reflections occur that can be noticed in a time-domain waveform. This effect is called “etalon effect” [77] which causes the appearance of periodic structures in the THz spectra. The same effect can be observed in case when the measurements are performed for samples in a pellet form due to the reflections of the THz wave at the back surface of the sample. If the investigated sample is relatively thick with high absorption, the problem is solved with the cut off of the data in the time domain before the first echo occurs.

Solid samples with a weight of a few milligrams are often mixed with a reference material (HDPE or PTFE powder), which are inactive in the THz region and guarantee a homogeneous sample with fewer scattering losses [77]. However, the spectral distortions can be observed in THz spectra, especially in the case of granulated materials, due to the scattering and refractive-index mismatch between the investigated substance particles and their surrounding medium [85]. The prepared mixture, usually containing up to 30 wt% of an investigated substance, is pressed into the thin pellets with a thickness between 1-3 mm. For very small quantities of substance, in submilligram order, a THz waveguide technique is used [77].

The absorption peaks of solid drugs can be linked with the states of crystallinity and the chirality of molecules. Thus, a polymorphism of the same molecule can be investigated by THz-TDS, which is especially important for pharmaceutical applications. The polycrystalline solids exhibit extensive intermolecular as well as intramolecular vibrations in this frequency range owing to the hydrogen-bonded networks. These vibrations can be observed in the THz spectra, but for the correct assignments of the spectral features the molecular modelling based on the density functional theory (DFT) calculations are often applied [57,85]. Usually, DFT is performed on molecular monomer or dimer or molecular clusters to verify the origin of the vibrational modes, i.e. non-localized or collective (phonon-like) nature. The THz measurements with the cryogenic option also showed

temperature-dependent low-frequency vibrational spectra characteristics, where it was found that vibrational modes shift to higher intensities and frequencies as the temperature is reduced [86].

Amorphous solids such as glasses and polymers respond to THz radiation in a different way than crystalline solids due to the lack of a long-range order. Hence, no spectral features can be found in THz spectrum. In the pharmaceutical industry, this approach is especially important to distinguish between amorphous and crystalline state of drugs. The molecular arrangement in the amorphous solid features a crystal-like short-range order with regions of different density [87]. TDS-THz can reveal the optical and dielectric properties, e.g. absorption and refractive index, of amorphous materials in THz frequency range. Their absorption is related with the disorder in the material and phonon process. For amorphous solids it is expected the same as for liquids that the absorption increases with the increasing frequency [11]. In comparison to crystalline solids, where the intermolecular vibrations found in THz range are related with the lattice modes, for amorphous solids, e.g. polymers, the inter- and intramolecular vibrations in this region are typically very broad due to the complexity in the structure and the diversity in the morphology [88]. Furthermore, THz-TDS is also suitable to monitor the glass transition in polymers, which is the core feature of the amorphous phase. The glass transition is determined by observing the refraction index that changes if the amorphous solid is exposed to low temperatures due to the reduced segmental motions of macromolecules in amorphous phase [88,89]. Usually oscillations are observed at low frequencies due to the secondary reflection signals in thin samples. It is also possible to characterize amorphous materials regarding the contribution of the short range order in the amorphous state between neighbouring molecules to the THz spectra, but only at higher wavenumbers [56]. Thus, systems with wider bandwidth are extremely important for the spectral characterization of amorphous solids.

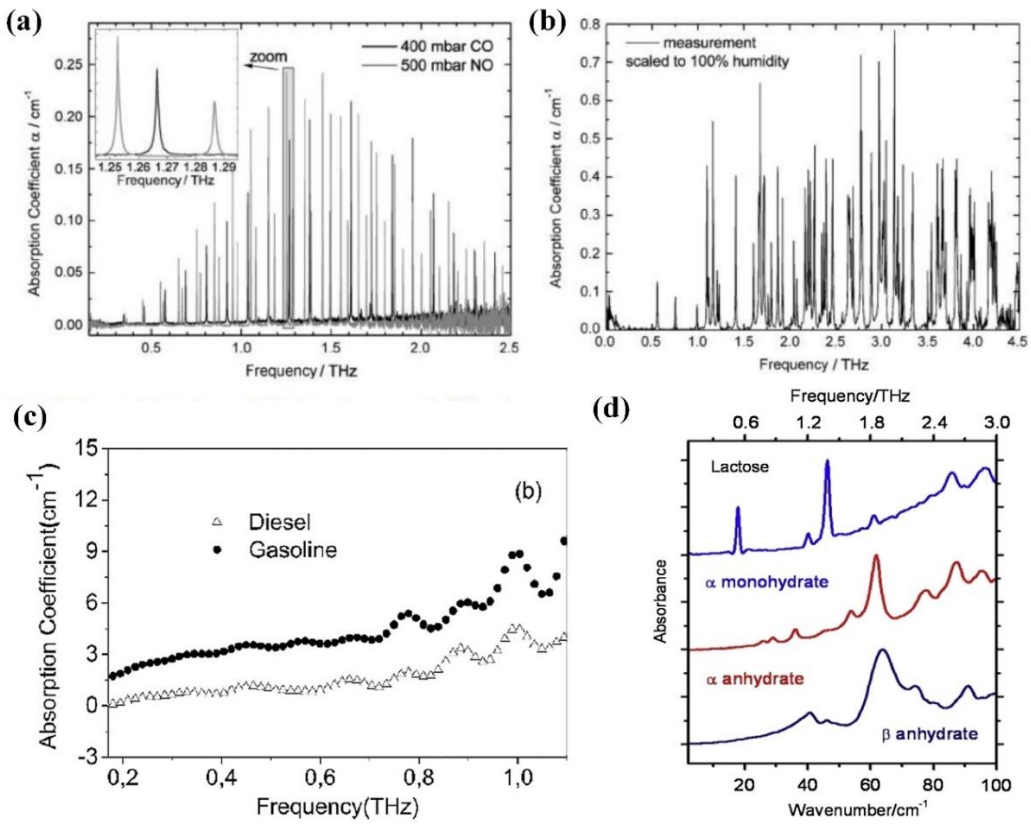


Figure 2.9: *Measured absorption coefficient for gases (a), water vapour (b), non-polar liquid (c), and solids (d) samples.* Reprinted from [77], [6] and [90].

## 2.7 Data analysis

Before any spectroscopic measurement one should define some issues regarding:

- the investigated material samples;
- THz system components and geometry;
- obtained THz waveform;
- used pre-processing methods, and
- post-processing methods.

Sample forms (e.g., gas, liquid, solid) discussed in section 2.6 are related with the frequency resolution and the bandwidth due to the scattering on particles and inhomogeneities. The chemical composition of samples affects the absorption and SNR, whereas the material optical properties are associated with the Fresnel losses and delays. Two basic system geometries are described in section 2.3. The last three issues are explained in this section.

### 2.7.1 Pre-processing methods

The pre-processing methods are necessary for the extraction of value information from waveforms that are the result from the interaction between THz wave and the investigated material and not the consequence of the THz system operation. However, in THz waveform one or more signals may occur due to the multiple reflection of the THz wave within the investigated material or the optical components of the system. This effect is often present in inhomogeneous samples where two regions with different properties are within the focus of the THz beam and contribute to the measured signal. Thus, double features can be observed that overlap in both time and frequency domain [91]. Currently, there is no unique procedure of data pre-processing that one should perform before THz data analysis. The selection of the appropriate methods depends upon the state of the material (e.g., gas, liquid, solid, amorphous) as well as the selected THz system configuration. Wu et al. [92] even reported that the samples in a dry pellet form give the best results without the pre-processing methods. Usually, prior to the Fourier transform of the THz waveform, the signals are enhanced by the apodization functions to eliminate undesirable effects and baseline correction.

The apodization functions are carried out in time-domain in order to reduce the oscillations in spectrum that occur due to the difference between the Fourier transform for which the signals are infinite and the experimental data where the signals are finite. Sampling windows affect frequency resolution and spectral leakage. Hence, when using the apodization one has to be careful since it can also lead to distortion or even loss of the spectral information. The apodization is also known as windowing functions with different multiplication patterns that enhance different parts of the THz waveform. The multiplication of the waveform *E(t)* with the sampling window *w(t)* is actually the convolution between the Fourier transform of the waveform and the Fourier transform of the window described by equation [58]:

$$F[E(t) \bullet w(t)] = F[E(t)] * F[w(t)] = E(\nu) * w(\nu) \tag{2.21}$$

The most common used windowing functions in THz spectroscopy are [91,93]:

- Rectangular window corresponds to the case where no apodization is carried out and is used to cut off the signal before the main peak and after the main peak;
- Hamming window is a symmetric function centered at the absolute maximum and truncated at the borders. It is used to eliminate the effects of spectral leakage in case when high frequency resolution is acquired;

- Blackman-Harris leaves the peak amplitude of the THz waveform unchanged and alter its tails;
- Mertz asymmetric triangular window is used to minimize sidelobe levels in the spectrum; and
- Nuttall window is used to supress the information before the main pulse. It assumes the maximal amplitude as a desire information and neglects (filtered away) any other pulses that occur in the time-domain waveform, which are considered as undesired information. This function is selected depending on the width of the reference pulse [91].

The zero-padding method provides additional interpolated points within a measured spectral range. These points do not contain any additional chemical information and do not enhance the spectral resolution. The main aim of the method is to smooth the spectral features of the measured points. Although the apodization functions smooth the spectral features, also additional smoothing can be applied in order to smooth spectral values below the noise floor and at the same time to preserve the characteristic spectral peaks. Usually, before that the filtering is applied, e.g. moving average, least square fitting with polynomial, wavelet shrinkage or Savitzky-Golay filter, which is most used in chemometrics due to fast calculability and its capacity to preserve peaks [91]. Another issue is a baseline that covers the entire spectrum and arises from the sample preparation, sample properties (e.g. grain size), environmental conditions (humidity, temperature) and system performance. The baseline does not contain only artefacts but also valuable information regarding the investigated sample. In fact, a baseline is a low frequency signal that should be separated from the absorption spectra. By using baseline correction (BLC) the background variation in the data is removed, usually with the simple method for drawing a linear fit across the spectra such that the intercept and slope is zero [94]. Other commonly used processing methods include normalization or scaling and differentiation (estimation first and second derivative).

Nowadays, more advanced methods are applied to THz signal treatment such as artificial neural network (ANN), a mathematical method used for solving problems related with nonlinearities in the calibration, e.g. analyte concentration [85]. The detailed explanations of these methods are beyond the scope of this thesis and are not given herein. However, for experiments it is important that one uses consistent pre-processing procedure across all samples in an experiment to ensure data comparability. Another important issue is to repeat measurements several times in several different points to determine error bar for the measurement.

### 2.7.2 Interpretation of terahertz waveform and terahertz spectrum

The spectroscopic analysis provides information about the properties of the sample. The analysis can be performed on waveforms in time domain and spectra in frequency domain. The specific parameters that can be observed in the THz waveform and THz spectrum are shown in Figure 2.10.

A specific parameter of THz waveform is its temporal shift that can be used for sample thickness determination. This temporal shift in ps occurs when a sample is inserted within the THz beam path. The time delay, $\Delta t$, between the reference pulse, $t_{ref}$, and sample pulse, $t_{sam}$, is proportional to the sample thickness, $l$, and is given by equation [77]:

$$\Delta t = t_{sam} - t_{ref} = \frac{(n-1)}{c} l \tag{2.22}$$

where $c$ is the vacuum velocity and $n$ is the refractive index of the sample in the THz

range. The refractive index is determined by measuring a sample of known thickness or by checking literature values. In such a way a thickness of a few micrometres can be resolved with a system in transmission mode. An example for propagation of THz wave through plastic layers of various thickness is shown in Figure 2.11 (A) where the evaluation of the time delay of the pulse maximum of the THz waveforms is given. Moreover, in Figure 2.11 (B) one can notice a linear fit of the measured delay values versus layer thickness. This parameter is usually applied for the non-destructive evaluation of porous materials, e.g. plastics, ceramics, and foams, based on THz imaging in transmission mode. Besides thickness, also material impurities, inhomogeneities, inclusions, and other defects can be detected. In reflection mode by the evaluation of the delay time a depth profile of the sample with the interface between two or more media with refractive index $n_1$ and $n_2$ can be resolved according to Fresnel's law where a fraction of the reflected THz radiation is given by $r = (n_1 - n_2)/(n_1 + n_2)$. This method is known as time of flight and is used for 3D tomography.

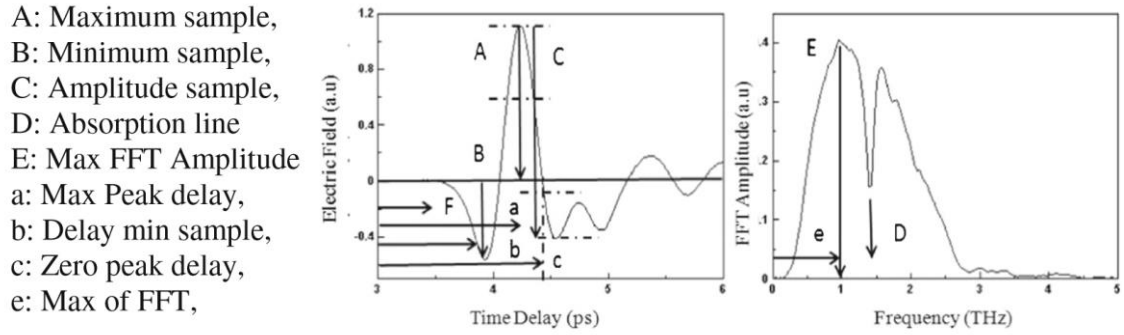


Figure 2.10: *The specific parameters of THz waveform (left) and THz spectrum (right).* Reprinted from [95].

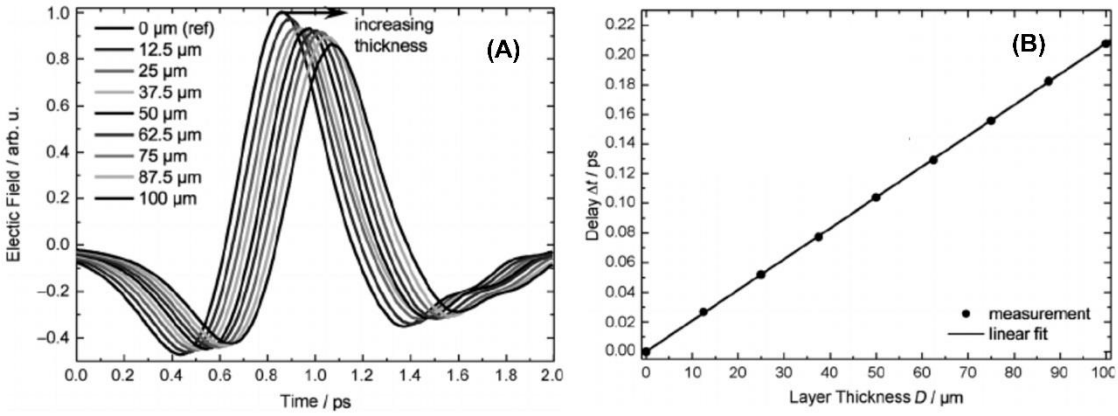


Figure 2.11: *THz waveforms measured after propagation through the plastic layers with various thickness (A) and a linear fit of the measured pulse delay versus plastic sample thickness (B).* Reprinted from [77].

In spectroscopy, the analysis of data in frequency domain is needed for identification and quantification purposes. For identification and recognition usually a simple comparison between two or more THz spectra is performed to study their similarities and differences. To get the THz spectrum in frequency domain, a Fourier transform (FT) of a time-domain signal is performed according to the equation:

$$\mathbf{E}_{THz}(\nu) = \int_{-\infty}^{+\infty} \mathbf{E}_{THz}(t) e^{-i\nu t} dt \tag{2.23}$$

Since FT provides information about the amplitude and phase of the THz wave, the detection is considered to be a coherent measurement. Thus, it is possible to determine the real and imaginary part of the dielectric constant by measuring the optical constants such as refractive index, *n*, and absorption coefficient, $\alpha$, of the material in THz frequency range. These two optical constants can be calculated in transmission mode as [58]:

$$n(\nu) = 1 + \frac{c\left[\phi_{sam}(\nu) - \phi_{ref}(\nu)\right]}{2\pi\nu l_{sam}} \tag{2.24}$$

$$\alpha(\nu) = -\frac{1}{l_{sam}} \ln\left[\frac{E_{sam}(\nu)}{E_{ref}(\nu)\frac{2\sqrt{n(\nu)}}{n(\nu)+1}}\right] \tag{2.25}$$

where $l_{sam}$ is the sample thickness, $\nu$ is the frequency, *c* is the speed of light, $\phi_{sam}$ and $E_{sam}$ are the phase and electric filed amplitude of the sample, and $\phi_{ref}$ and $E_{ref}$ are the phase and electric field amplitude of the reference. The location and the amplitude of the absorption peaks is molecule-dependent, thus each molecule exhibits a characteristic fingerprint in THz range that can be used for its identification.

In frequency domain there are a few relations that we need to describe. The first one links a frequency resolution to the window length, which are inversely proportional. For solids, the scan lengths around 10 ps are usually enough to achieve a resolution around 100 GHz [58]. The second relation connects bandwidth with sampling frequency. The bandwidth is defined by the Nyquist-Shannon sampling theorem, which determines that the sampling should be at least twice the bandwidth. For THz-TDS a typical bandwidth is 5 THz which requires a sampling frequency of 10 THz or a sampling interval of 100 fs [58]. The third relation is dedicated to noise level that can be reduced by averaging which on the other hand requires longer time to complete the measurement.

The use of chemometrics that is well established in other fields of spectroscopy, was not well explored in THz range for qualitative analysis. Probably the most common used chemometric method in THz spectroscopy and imaging is principal component analysis (PCA) which is explained in section 2.8. For quantitative analysis, several chemometric methods have already been applied in THz data analysis [92]. The univariate calibration curve is often used to present the THz signal characteristic (e.g., maximum amplitude, absorption peak value, etc.) versus the varying parameter, e.g. substance concentration. This method is also known as characteristic peak method (CPM) [92]. In this method the quality of calibration is evaluated by a linear least squares regression [85]. When more spectral features appear in the THz spectrum, the preferred method is multivariate data analysis [92]. In this method multivariate calibration methods are used to correlate the THz spectra of mixture with the substance concentration. These methods are multiple linear regression (MLR), principal component regression (PCR) and partial least square (PLS) regression. In case of no correlation between variables a multi-linear regression (MLR) is applied. This method can be used to simultaneously explain the absorption of two or more compounds in mixtures in the absence of distinct peaks attributed to single components [85,96]. All methods showed some advantages and limitations that have to be taken into consideration, especially when mixtures contain both crystalline and amorphous forms (e.g. pharmaceutical tablets). However, the CPM can be used in case of amorphous material for estimating component concentration, whereas for crystalline materials multivariate data analysis is preferred. The CPM involves two steps: identifying a characteristic peak for a particular constituent and correlating the integrated absorbance of that characteristic peak with the substance concentration [87]. For each characteristic peak, the peak intensities are

plotted against concentration values of that particular component. A linear regression model is then used to correlate the characteristic peak absorbance value with the component concentration value for respective components. In most cases, linear relationships can be found.

As mentioned in section 2.7.1 the numerical simulations are usually applied for modelling THz spectra by using commercial software (e.g. Gaussian) enabling DFT calculations. The DFT results are used for understanding and assignment of spectral features in THz spectra obtained by experimental measurements. This approach is especially useful in case of polycrystalline samples and polymorphs to understand the origin of the vibrational modes.

## 2.8 Imaging analysis

The acquired THz data can be further used for image formation. THz imaging is usually applied for non-destructive evaluation of materials. THz images recorded in time-domain can reveal structures with the resolution in the order of sub-mm. If pulsed THz-TDS is applied, the spectral imaging can be performed where each recorded waveform contains spectral information that could be used to characterize and identify the investigated material. Thus, not only structural but also chemical information can be extracted. For imaging applications, the frequency and acquisition rate have a major role. The spatial resolution depends on frequency, e.g. at the frequency of 1 THz the wavelength is 300 μm, whereas the acquisition rate is determined by the scan rate of the optical DL and the motorized scanning stage that is usually used to raster scanning of the object.

### 2.8.1 Time-domain imaging

The image data in time-domain are acquired one pixel at a time by raster scanning an object through the focus of the THz beam or by moving the emitter and the detector across a sample. The data set consists of time-domain waveforms recorded in each pixel, containing the amplitude and phase of the transmitted THz pulse. A 2D false-colour image can be created using different portions of the data that carry various information of the sample. The grey scale of the image can be determined by different parameters of time-domain waveform (some depicted in Figure 2.10), e.g. the maximum amplitude, peak-to-peak amplitude, phase of the pulse, and time delay of the THz pulse through the sample. These images are known as B-scans or time of flight analysis [58] when formed by using reflection geometry of the THz system. This mode is commonly used to measure layer thickness or to detect defects or structures within the sample. This simple imaging technique cannot allow distinction between the chemicals.

### 2.8.2 THz spectral imaging

In the spectral mode of operation the complete waveform is recorded in each pixel. Each recorded waveform is then transformed to frequency domain by using numerical FT and an image can be obtained at each frequency of the spectrum. Since many chemical substances show characteristic spectral features at different frequencies, false-colour image can visualize the chemical discrimination between different substances (Figure 2.12). For this case, a recognition coefficient, $R_C$, proportional to the height of a spectral feature with respect to its baseline can be determined by equation [97]:

$$R_C = \alpha(\nu_2) - \frac{1}{2}\left[\alpha(\nu_1) + \alpha(\nu_3)\right] \tag{2.26}$$

where $\alpha$ is the absorption coefficient. If more spectral features are present in the absorption spectrum, then $R_C$ may be taken as the sum of several peak heights.

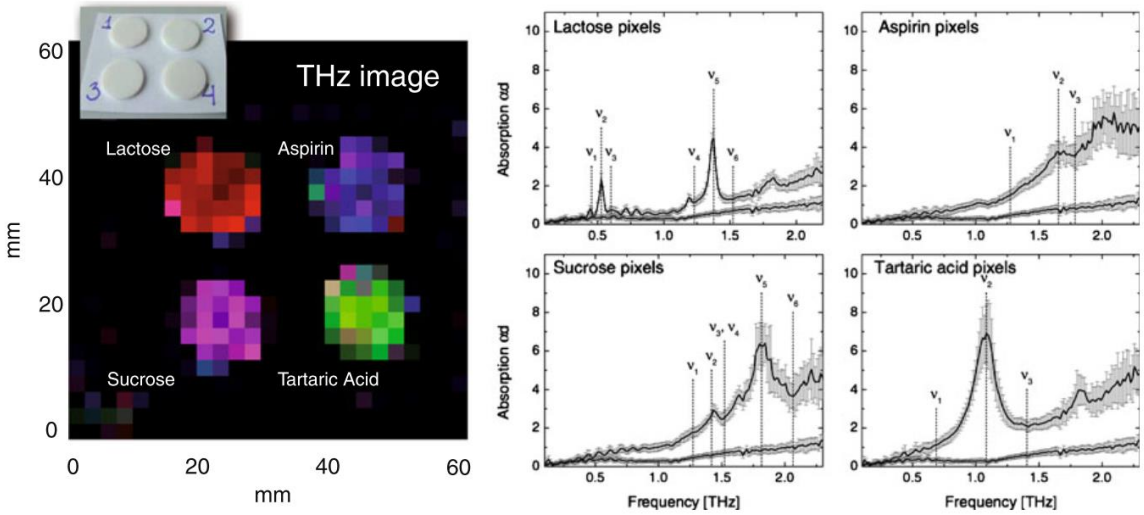


Figure 2.12: *Terahertz spectral image of four samples containing different substances.* The colours in the left image represent a measure for the presence of specific spectral feature, which is characteristic for a certain sample. Reprinted from [3,97].

Chemometrics method PCA which was already mentioned in the previous section is also widely used for spectral image analysis. By using this statistical method one can extract the principal spectral features of an unknown sample from the multispectral THz images which has a special value for detection and identification in real time applications. In this method, a series of measured THz spectra are simultaneously compared through measuring the covariance [85]. Thus, the dimensionality of the measured data set is reduced by transforming it to a new set of variables known as the principal components that summarize the features of the data. In general, the intensity of THz image keeps attenuated by absorption linearly due to the variation in concentration or thickness of the samples. Therefore, the image $I(x,y,v)$ observed at each of the frequency $v$ is expressed as a linear combination of absorbance spectra $S(v)$ and spatial pattern $P(x,y)$ that gives a matrix equation for PCA:

$$[I]=[S][P] \tag{2.27}$$

There are two possible contexts in THz spectroscopic analysis where PCA can be applied. First is to extract the similarity of the spectral features for all pixels of THz images, whereas the second is to extract the common spatial features of a set of THz images [98]. The first one is also known as component pattern analysis (Figure 2.13).

The first context where PCA is used shows spatial distribution of individual chemical substance in the sample [46,71,73]. For this method a 3D data set is needed, where two axes present vertical and horizontal spatial dimensions, and the third axis describes the spectral frequency dimension. First 3D data set is compressed to a 2D matrix $I_{N\times L}$, which has $N$ recorded images whose row vectors represent each $L$-pixel image taken at an individual frequency. Assuming that the sample has $M$ substances, each having known absorption spectrum with $N$ frequency components, then a matrix of $S_{N\times M}$ can be created. Since $[I]$ and $[S]$ are measured directly, the spatial distribution of individual substance in the sample, i.e. component pattern analysis, can be resolved by using a least-squares method which as a result gives the matrix $[P]$ expressed with equation [71]:

$$[P_{MxL}] = ([S_{NxM}]^t [S_{NxM}])^{-1} [S_{NxM}]^t [I_{NxL}] \quad (2.28)$$

where $P_{ij}$ is the probability of the occurrence of the *i*th substance at the *j*th pixel given in a matrix form and *t* is the matrix transpose operation. [*P*] is also called the spatial distribution of the samples. The matrix [*S*] is formed by extraction of the measured absorption spectra of each substance *M* at *N* frequencies, whereas [*I*] is a matrix of the observed image generated by a transmission scanning of the sample, where row vectors represent the spatial pattern of each drug with *L* pixels. This method is particularly useful for investigating heterogeneous mixture and inhomogeneous samples.

By second context of PCA use, it is possible to determine how many principal components in total account the most variance in the data. This information tells us how far the initial data can be reduced without the loss of important information. Since this procedure applies multivariate calibration method it uses mean data, where the average spectrum of all the spectra in the data set is calculated and then subtracted from each spectrum [99]. The method is especially useful in cases where large data size is a big issue. Since this method is out of the focus for this dissertation, its procedure is described elsewhere [98].

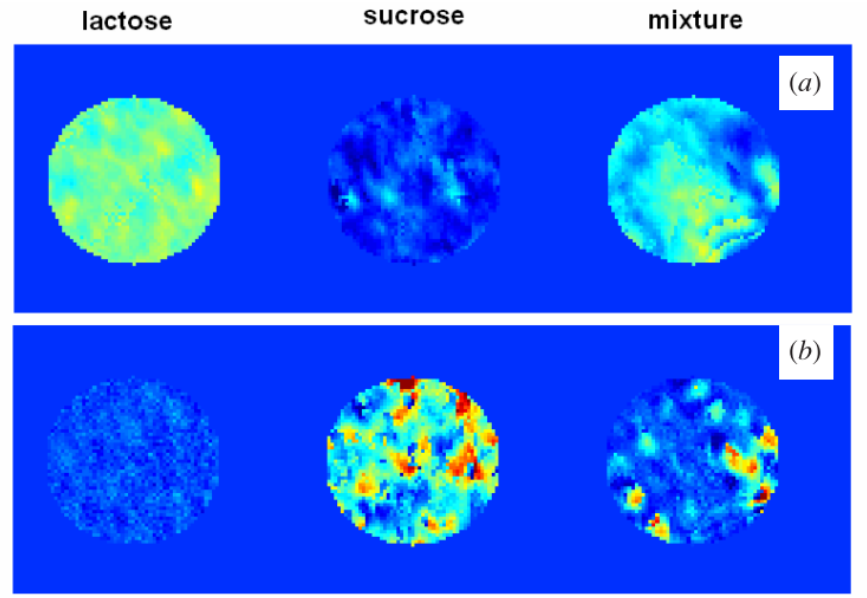


Figure 2.13: *THz image showing the spatial distributions of two substances, lactose (a), and sucrose (b).* Reprinted from [71].

.

# 3 Experimental Equipment and Methods

This chapter discusses the experimental equipment and procedures used to collect and present the data within this dissertation. The THz instrument configuration and its operating characteristics are described first, followed by the experimental procedures and sample preparation. Although the THz system setup may vary from one case to another, the basic procedure of measurements is common to all of them. Any additional measurement steps and deviation from this procedure are discussed within the relevant publication. The following subsections in this chapter describe the data pre-processing and post-processing, including image processing, spectroscopic data analysis, image analysis and standard computation techniques, done in our experiments. In the last subsection the reference macroscopic and spectroscopic methods for structural characterization of construction and building materials are presented.

## 3.1 Time-domain terahertz spectrometer in transmission configuration

### 3.1.1 System elements and system operation

THz spectroscopic and imaging measurements were performed by TeraIMAGE obtained from Rainbow Photonics AG. The system operation is controlled by an in-house modified software developed within Labview programming environment. The THz system is based on organic EO crystals, allowing measurements at THz frequencies not yet available with conventional THz antennas. A schematic drawing of the THz system for spectroscopy and imaging in transmission geometry is illustrated in Figure 3.1. The instrument includes optical, mechanical and electronic components for the generation and detection of THz radiation. The free space optical components (e.g. lenses, windows, beam splitters, sample holders, etc.) are preferably made of materials that exhibit excellent transparencies with relatively low reflectivity in the THz frequency range. Thus, the polymers such as polytetrafluoroethylene (PTFE), HDPE, polymethylpentene (TPX), and silicon are used rather than quartz. The TeraIMAGE system operates with an erbium doped fs fibre laser (T-Light, Menlo Systems) that emits IR radiation at a centre wavelength of 1560 nm with an average output power greater than 120 mW and a pulse duration less than 90 fs at a repetition rate of 100 MHz.

Before the measurements execution, all optical elements should be adjusted perfectly by changing the position of mirrors and lenses according to the system manual instructions. For optimum operation of the THz system the pump beam and the probe beam have to overlap at the position of the germanium slab which acts as a chopper to periodically block the THz beam. The THz detection is additionally optimized by adjusting the probe beam to the detector photodiode with respect to equally distributed power on the two monitoring channels. Thus, the highest possible dynamic range and the lowest noise level in the measurement is achieved.

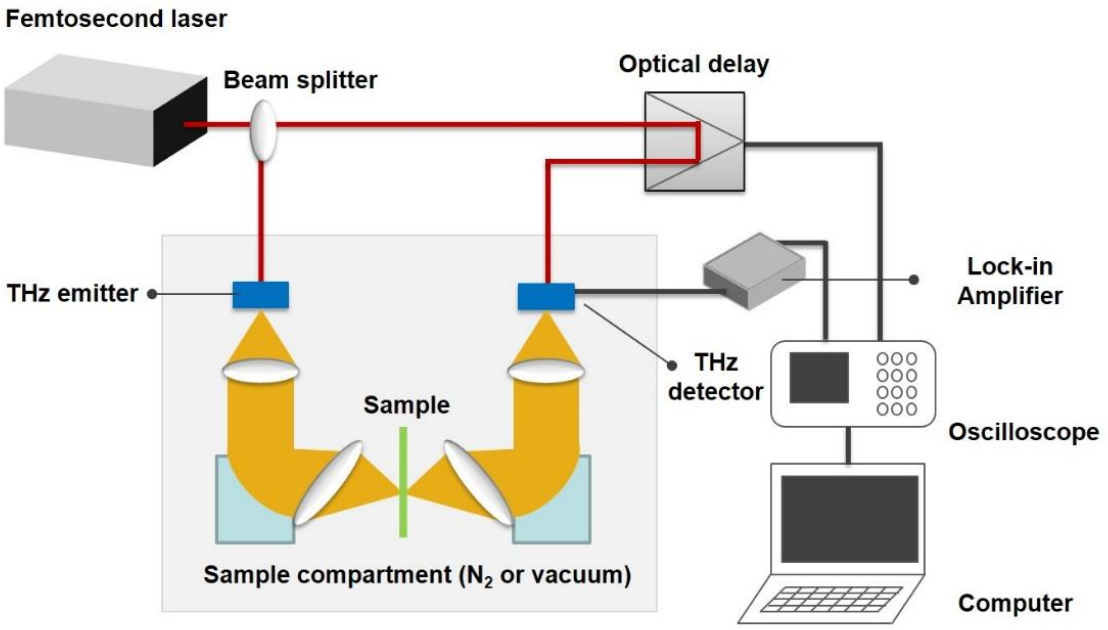


Figure 3.1: *Schematic illustration of a TeraIMAGE THz spectrometer in transmission mode.*

After the successful optics alignment, the measurement can be performed. First, the initial fs laser beam is split at a beam splitter into two parts: a pump and a probe beam. By aligning the beam splitter the incident THz and laser pulses enter the EO detector from the same side at the same point. The beam paths are indicated in Figure 3.2. The pump beam is delayed for a few ps with a DL and focused onto the THz generator, which is in our system an electrooptic DSTMS organic crystal [100]. The THz generator generates THz radiation through optical rectification. THz waves are focused through the sample onto the THz DSTMS detector crystal using the PMs. The PMs are used to either collimate or focus a parallel THz beam to a point. Usually four PMs are needed, two before the sample with the function of divergent to collimate the beam and collimated to focus on a sample, and two after the sample with the function of focused to collimated and finally collimated to focus. In our system only two PMs are used. The electric field of the THz pulse is measured by electrooptic sampling in the DSTMS crystal. By changing the time delay between the probe beam and the pump beam by means of an optical DL, the entire time profile of the THz waveform can be traced. Due to the small pulse energy of the laser, the relatively weak detected THz signal needs to be measured using lock-in amplification. This technique requires a modulation of the THz signal, which is achieved by mechanically chopping the THz beam. The signal is finally detected by a photodiode detector and the data are transferred to the computer for further signal processing. The experiments are conducted within the sample compartment purged with nitrogen gas ($N_2$) to avoid water vapour absorption lines. The THz measurements are recorded via a graphical user interface created with LabView software. All measurements are made in the time domain.

Moreover, the THz system allows performing TPI in two ways, as a monochromatic fast imaging without the need for spectroscopic information, and a broadband or multispectral imaging by using the FT of the time-domain waveform. The monochromatic image is constructed at a fixed maximum amplitude of the THz waveform. At each point on the sample, only the amplitude of the THz field is recorded in a matrix while scanning the sample across the THz beam. The next step is the

extraction of the amplitude peak value followed by the time-domain THz image reconstruction using the peak intensity at each pixel. In the case of multispectral imaging, the entire frequency spectrum is recorded in every single point of the sample. Such TPI measurement gives a 3D data set where two axes describe vertical and horizontal spatial dimensions and the third axis represents the spectral frequency dimension. In the measurements, the sample was placed across the THz beam at its focal spot, following by raster scanning in a plane perpendicular to the THz beam. The scanning area was limited to 50 mm x 50 mm.

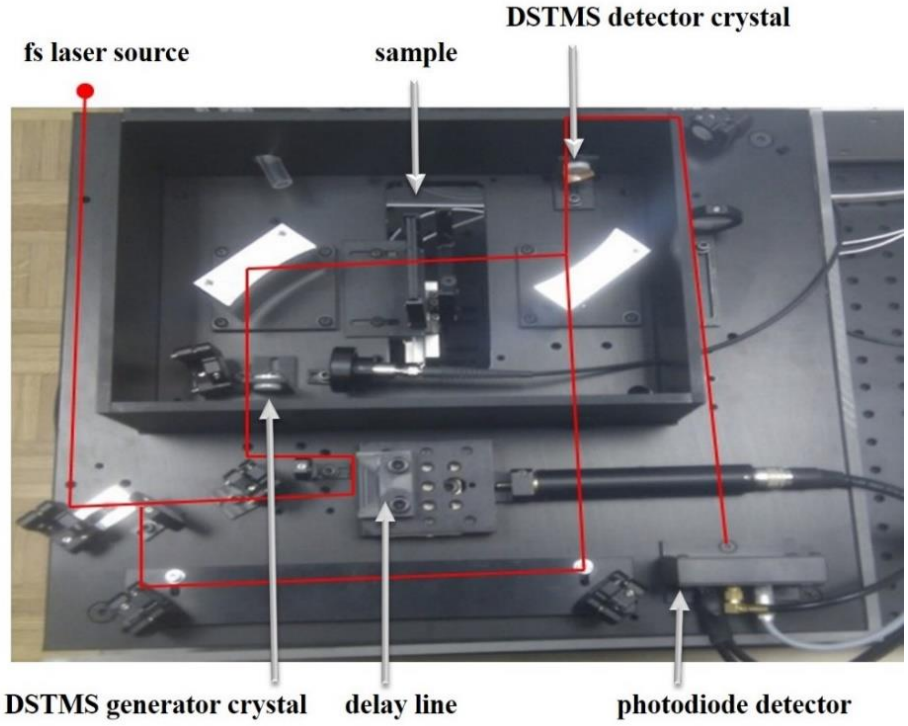


Figure 3.2: *Photograph of a selected THz-TDS system.*

### 3.1.2 Spectrometer operating characteristics

The selected THz spectroscopic system is characterized with the parameters summarized in Table 1. A key parameter of any THz-TDS system is a dynamic range which defines if a measurement can be undertaken or not. When comparing data between different measurement systems or between temporal periods of the same system special care must be given to the calibration of the following parameters: SNR, spectral range, and spectral resolution. The SNR is frequency dependent (Figure 3.4).

Table 1. *Characteristics of TeraIMAGE spectroscopic and imaging system.*

| General specifications | |
|---|---|
| Spectral range | 1 THz - 6 THz |
| Dynamic range | > 50 dB |
| Spectral resolution | 50 GHz |
| Scan range | up to 60 ps |
| Imaging resolution | > 50 μm |
| Maximum imaging scanning range | 50 x 50 $mm^2$ |

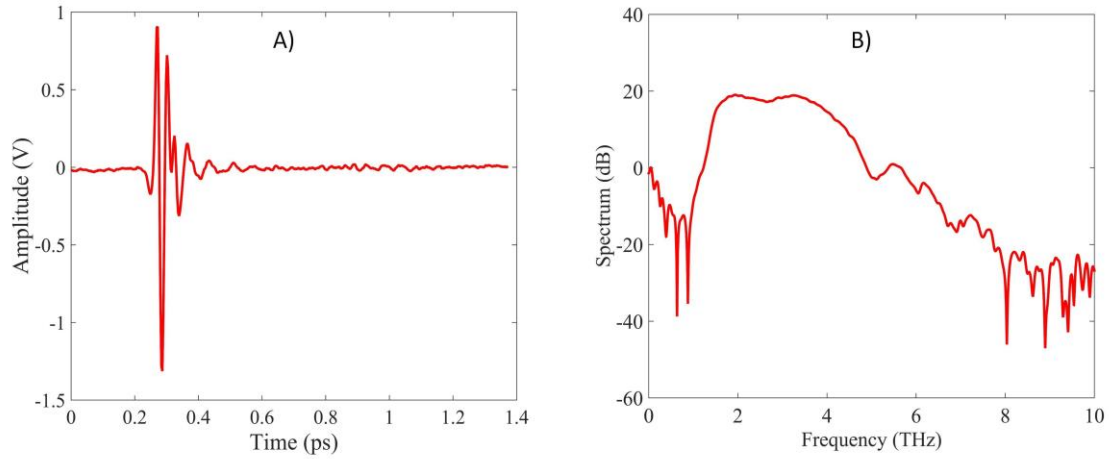


Figure 3.3: *Typical THz pulse waveform (a) and THz power spectrum (b) acquired with a TeraIMAGE spectrometer in a nitrogen atmosphere*.

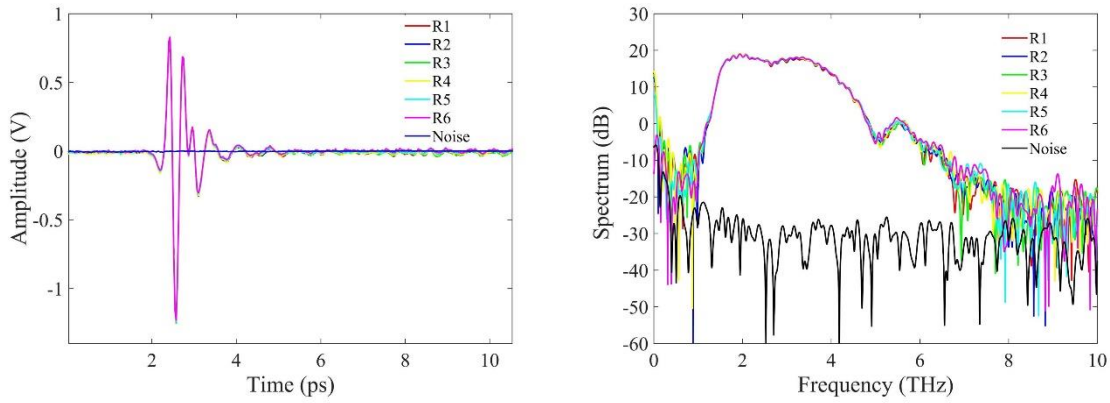


Figure 3.4: *THz reference signals and noise level (a) and THz power spectra with a noise floor (b) for six successive measurements in nitrogen atmosphere*.

## 3.2 Experimental procedure and sample preparation

For each experiment, several key parameters according to the constructed THz measurement flow (Appendix A) should be considered to properly prepare samples and to successfully perform an experiment. A detailed explanation of each experimental procedure is given in each individual study. In the next subsections only the instructions how to deal with different types of materials are shortly described.

### 3.2.1 Powders

For powder samples we used similar preparation procedure reported by others [6]. Before pellets making, the powder samples were dried in an oven at 65°C overnight to remove undesired moisture. Afterwards, the tablets were finely powdered in a mortar with pestle and then mixed with ultra-high molecular weight polyethylene PE powder at appropriate wt% according to the absorbance of the selected sample. PE powder is transparent to THz radiation and is therefore typically used as diluent materials. PE powder with the particle size between 53-75 µm was obtained from Sigma Aldrich. The particle size of both sample and PE diluent is preferably below 100 mm to minimize scattering. The mixture was

compressed into the pellets of thickness below 1 mm in a 13 mm die at the approximate pressure of 1500 kg/cm$^2$ for 2 min. Among other gases, atmospheric water vapour exhibits a very strong rotational spectrum in the THz range which can be observed in the THz spectra of solids as more intense and very narrow features [6]. Consequently, they can be easily distinguished from the spectral signatures of solid materials. However, to minimize the contribution of the water vapour to the sample spectrum, the sample compartment is purged with dry nitrogen throughout the measurements.

### 3.2.2 Foams

The foam samples were cut with a blade into slices with *x-y* dimensions according to the THz sample holder size. The slice thickness in mm for each sample investigated by THz spectrometer was measured at ten different positions and its average thickness was calculated. The thickness was usually below 3 mm. The THz spectra were recorded without any special sample modification and drying.

### 3.2.3 Microencapsulated particles

The powder of microencapsulated materials cannot be treated in the same way as polycrystalline powders due to the incorporation of organic core the structure of which can be distort during the exposure to high pressure. Therefore, the microencapsulated particles were measured without prior mixing with the PE powder. A weighed portion of PCM powder equivalent to 80 mg was gently pressed between two layers of scotch tape with hands into a disk shape within the hole of sample holder with a diameter of 12 mm and thickness below 1 mm. In that case, a scotch tape was selected as a reference material.

## 3.3 Pre-processing techniques

After THz measurements the recorded data were pre-processed with some techniques described in section 2.7.1. Next, we list the data pre-processing techniques applied to the raw THz data:

- baseline correction;
- Blackman-Harris apodization;
- zero-padding.

Algorithm 1: *Data pre-processing procedure.*

```
%%% 1. Baseline correction
bRef1=Ref1(:,2)-mean(Ref1(:,2));
bData1=Data1(:,2)-mean(Data1(:,2));

%%% 2. Blackman-Harris apodization
t0 = 2.5e-12;
dt = 13e-12;
REF1_1(:,1)=REF1(:,1);
REF1_1(:,2)=bREF1.*blha(REF1(:,1)-t0, dt, dt);
Data1_1(:,1)=Data1(:,1);
Data1_1(:,2)=bData1.*blha(Data1(:,1)-t0, dt, dt);

%%% 3. Zero-padding and the Fourier transform
zp = 1e5;
[fREF1,sREF1]=ampl2spec2(REF1_1, zp);
[fData1,sData1]=ampl2spec2(Data1_1, zp);
```

The Algorithm 1 written in Matlab programming environment is describing the procedure of data pre-processing for one measurement. For each sample a series of at least three measurements was performed prior to data pre-processing. The programming codes for the *blha* and *ampl2spec2* functions are included in Appendix B. After pre-processing the spectral power was plotted to determine the suitable THz frequency range and to check if the spectrum coincides with the THz system performance considering its SNR. The Matlab programming environment is used to process all time-domain data for the purpose of data analysis and graphical visualization.

## 3.4 Post-processing techniques

For THz data analysis, both the reference and the sample signals are measured. The reference signal is that of the test environment (e.g. nitrogen atmosphere, PE pellet, scotch tape, etc.) in which the sample is contained. The Fourier components of these two signals define the transmission function of the sample. Similarly to the transmittance *T*, other spectral properties of the sample such as absorbance *A* and absorption coefficient $\alpha$ were extracted by comparing the sample spectrum with the reference spectrum. The Algorithm 2 presents the procedure how these spectral properties were calculated.

Algorithm 2: *Data post-processing procedure.*

```
%%% 1. Calculate transmittance
T_Data1=abs(sData1./sREF1);

%%% 2. Calculate absorbance
A_Data1=-log(T_Data1.^2);

%%% 3. Calculate absorption coefficient
aData1==-log(T_Data1.^2)/d;
```

Moreover, the THz system was used to perform TPI in two ways as a monochromatic imaging and a broadband imaging by using the FT of the time-domain waveform. The monochromatic image is constructed at a fixed maximum amplitude of the THz waveform. At each point on the sample, the amplitude of the THz field is recorded in a matrix while scanning the sample across the THz beam. This matrix is then used for visualization and image processing (brightness, contrast, square root, cosine, median spatial filtering) in Matlab and Origin software. The THz amplitude image is reconstructed by using the peak intensity at each pixel. In the case of broadband imaging, the entire frequency spectrum is recorded in every single point of the sample. Such TPI measurement gives a 3D data set where two axes describe vertical and horizontal spatial dimensions and the third axis represents the spectral frequency dimension. The software for THz image recording is written in LabView programing environment. The multispectral THz images were used for component pattern analysis described in section 2.8. The programing code for this analysis was developed in Matlab in our laboratory. Other data analysis techniques are explained in each publication.

## 3.5 Reference methods

Different microscopy and FTIR spectroscopy were selected as a reference methods to study the structural and morphological properties of construction and building materials at micro- and macroscale. FTIR spectroscopy is usually applied as a non-destructive analytical technique, which enables identifying the chemical and partially physical structure of

substance, e.g. identification of functional groups in molecules. With the FTIR spectrometer and the microscope, the qualitative and to some extent quantitative analysis of unknown materials is possible. The selected reference methods are appropriate for the analysis of materials studied in this thesis.

### 3.5.1 Microscopy

- *Optical microscopy*. For powder particle size and shape verification we used optical microscopy (Nikon Eclipse E600) at 200x, 600x and 1000x magnification.

- *Scanning electron microscope* (SEM) enables imaging and microanalysis of the morphological and structural characteristics of materials, including crystals size, shape and modification. We used scanning electron microscope JEOL JSM-7600F which enables magnifications from 25 to 1.000.000 times. It can work with acceleration voltages from 0.1 to 30 kV. With SEM we also performed the microstructural analysis of polymer foams. The samples prepared for SEM imaging were sputtered with gold to ensure better morphological investigation.

- *Confocal optical microscope* (Zeiss Axio CSM 700) is an optical imaging technique used when increased optical resolution and contrast of a microscopic image are needed, particularly in thick samples. The difference from conventional optical microscopy is the presence of the confocal pinholes which allow that only light from the plane of focus reaches the detector. Thus, the light which is out of focus is removed from the image. Unlike samples for conventional microscopy, sample preparations for confocal microscopy do not need to be thin. The microscope acquires the image of the sample surface which can be presented in two ways: all-in-focus image and surface topography. From the topographic image one can perform particle analysis and analysis of the sample roughness and layer thickness. The microscope allows to produce 3D representations of the sample by measuring series of *x-y* images across different *z* positions by moving the object or by changing the plane of focus. This type of microscopy was used for the polymer foams characterization.

### 3.5.2 FTIR spectroscopy

The FTIR spectroscopy measurements were performed at Optoelectronics Department, Center for Physical Sciences and Technology, Vilnius. For powder pellets we used the same samples as for THz measurements. The measurements were performed in a spectral range of 20-500 $cm^{-1}$ (0.6 THz - 15 THz) at temperature of 300 K and vacuum environment using the resolution of 5 $cm^{-1}$. In some cases, the transmittance was measured in different sample area applying a 5 mm diameter pinhole.

# 4 Characterization of Construction and Building Materials by THz Spectrometer and Imager

## 4.1 Scientific article 1: Applications of terahertz spectroscopy in the field of construction and building materials

***Authors:*** Andreja Abina, Uroš Puc, Anton Jeglič, and Aleksander Zidanšek
***Publication:*** Applied Spectroscopy Reviews
***DOI:*** 10.1080/05704928.2014.965825
***Year:*** 2015 ***Volume:*** 50
***Issue:*** 4 ***Pages:*** 279-303
***Impact factor 2013:*** 3.109 ***Submitted date:*** 29 Aug 2014
***Accepted date:*** 11 Sep 2014 ***Published online:*** 30 Oct 2014
***Ranking:***

| Category name | Journal rank in category | Quartile in category |
|---|---|---|
| instruments & instrumentation | 4/57 | 1 |
| spectroscopy | 9/44 | 1 |

In this chapter, the paper entitled: "Applications of Terahertz Spectroscopy in the Field of Construction and Building Materials" by Andreja Abina, Uroš Puc, Anton Jeglič, and Aleksander Zidanšek is presented. The paper was published in Applied Spectroscopy Reviews, 2015.

This paper reviewed the use of THz spectroscopy in research and industry related to construction and building materials, along with the key advantages and limitations of THz technology. The use of THz spectroscopy in that field is usually excluded from reviews, which stress security, medicine, pharmacy, food, biology, and telecommunications.

In the last few years, the rapid development of novel THz sources and detectors has opened additional possibilities of creating innovative imaging and spectroscopic systems, allowing "in situ" measurements and real-time analysis of different materials. Several advantages of THz systems over other technologies have attracted interest in industry and led to the development of compact, relatively inexpensive, and even portable THz systems, which are now commercially available on different markets. However, the review showed that the construction and building industry lags behind other sectors in applications of THz system for the NDT characterization of physicochemical and mechanical properties of materials.

We considered the analysis of different construction and building materials, including plastics, foams, ceramics, wood, paint, composite, glass, concrete, stones, clay, and asbestos. When THz waves pass through these materials, they produce unique signal and spectral response that can be applied for the analysis of chemical composition, water content, porosity, material thickness, density, material aging, and others. In addition, supplementary imaging modalities can visualize hidden internal and surface defects, inclusions, and manufacturing imperfections. These specific characteristics can make THz

spectroscopy and imaging a valuable substitute or complement to other sensing techniques using ultrasound, microwaves, IR, or X-ray waves in the field of construction and building industry. Each of current used techniques has advantages and limitations that must be taken into account, especially when they are combined, in order to enhance the reliability of measured data. Therefore, in this review we critically presented the advantages and limitations of THz spectroscopy against other sensing methods used for characterization of construction materials. The paper also presented the THz systems and techniques that are currently available on the market or that are still under development. In conclusion, some recommendations for the future use of THz spectroscopy in the building and construction sector considering the current trends, focused on sustainability, energy-efficiency, eco-efficiency, and recycling, were provided. The paper concluded that the initial research and industrial requirements clearly show that THz spectroscopy has a promising potential for both researchers to understand the structure of material and engineers to manipulate the production process to enhance material properties and durability.

*Covering the objectives of this thesis:* Based on critical overview in this publication the hypothesis 1 of this thesis was confirmed by finding the examples of THz investigations of several construction and building materials that are also widely used in other fields. Thus, we concluded that THz spectroscopy has a potential for characterization of different construction and building materials.

*Applied Spectroscopy Reviews*, 50:279–303, 2015
Copyright © Taylor & Francis Group, LLC
ISSN: 0570-4928 print / 1520-569X online
DOI: 10.1080/05704928.2014.965825

Taylor & Francis
Taylor & Francis Group

# Applications of Terahertz Spectroscopy in the Field of Construction and Building Materials

ANDREJA ABINA,[1] UROŠ PUC,[1,2] ANTON JEGLIČ,[1,2] AND ALEKSANDER ZIDANŠEK[1,3,4]

[1]Jožef Stefan International Postgraduate School, Ljubljana, Slovenia
[2]Faculty of Electrical Engineering, University of Ljubljana, Ljubljana, Slovenia
[3]Department of Condensed Matter Physics, Jožef Stefan Institute, Ljubljana, Slovenia
[4]Faculty of Natural Sciences and Mathematics, University of Maribor, Maribor, Slovenia

Downloaded by [Jozef Stefan Institute] at 06:13 12 November 2014

**Abstract:** *In last two decades, rapid development in the field of terahertz (THz) technology has opened new possibilities for creating innovative imaging and sensing systems. Although the applications of THz technology in different sectors constantly increase, the construction industry lags behind them. The aim of this article is to review the current applications of THz spectroscopy in research and industry related to construction and building materials, along with the key drawbacks of technology and recommendations for future use. The review concludes that THz spectroscopy and imaging have promising potential and provide many opportunities for applications in construction and building materials characterization.*

**Keywords:** Building material, construction material, industrial applications, material characterization, terahertz imaging, terahertz spectroscopy

## Introduction

The terahertz (THz) part of the electromagnetic spectrum corresponding to the wavelengths between microwaves and near-infrared (IR) waves was relatively unexplored until recently, mainly due to the lack of powerful and user-friendly sources and detectors (1, 2). In the last few years, the rapid development of novel THz sources and detectors has opened additional possibilities of creating innovative imaging and sensing systems, allowing in situ measurements and real-time analysis of different materials. Advances in the field have encouraged new research in various disciplines, including chemistry, pharmacy, physics, materials science, medicine, archaeology, and biology (2–8). Several advantages of THz systems over other technologies—for example, X-ray tomography, gamma rays, IR imaging, and millimeter-wave imaging (6, 9–11)—have attracted interest in industry and led to

Address correspondence to Andreja Abina, Jožef Stefan International Postgraduate School, Jamova 39, SI-1000 Ljubljana, Slovenia. E-mail: andreja.abina@mps.si

Color versions of one or more of the figures in the article can be found online at www.tandfonline.com/laps.

the development of compact, relatively inexpensive, and even portable THz systems, which are now commercially available on different markets.

The evaluation and analysis of some specific physical and mechanical properties of construction and building materials, responsible for safety and durability of historic and modern civil structures, require nondestructive testing (NDT) methods. Several different types of NDT methods are now available and only the adequate combination of them significantly contributes to the reliable assessment of material properties. More recently, research in the field of THz technology is also focusing on the exploration of building materials. There are some research studies focused on detecting and analyzing material thicknesses and density (12–16), water absorption (17–19), optical constants (20–24), voids and delaminations (18, 22, 25), inclusions (22), mechanical defects (26, 27), material aging (11), weld joints and adhesion (12, 18, 28), as well as process control (29–31). A small number of literature references show that the construction and building industry lags behind other sectors in THz applications. However, one prediction for the future is that THz systems will make a breakthrough in the construction market by the year 2022 (32).

The aim of this article is to review the recent applications of THz spectroscopy in building- and construction-related research and industry, along with the key advantages and limitations of THz technology. In conclusion, some recommendations for the future use of THz spectroscopy in the building and construction sector considering the current trends are provided.

Downloaded by [Jozef Stefan Institute] at 06:13 12 November 2014

## Terahertz Systems and Techniques

Depending on the inspection needs, different configurations of a THz setup can be selected, each described by specific performance characteristics, which will not be discussed in detail in this article. However, herein a brief introduction to THz spectroscopic and imaging techniques will be given.

First, THz systems can be divided into pulsed systems, more commonly known as THz time-domain spectroscopy (THz TDS), and continuous wave (CW) systems. THz TDS is the most commonly used technique when both amplitude and phase information are required. On the other hand, CW systems are usually selected to measure only the intensity data at fixed frequency. Due to the coherent detection, the THz pulsed technique is more widely used for material inspection because measuring the phase at a single THz frequency is very hard or nonexistent for current THz CW techniques (26).

THz TDS can be designed either in transmission (Figure 1A) or reflection modes (Figure 1B). However, some systems also combine both modes in a single system setup (33). The coherent detection of the transmitted or reflected THz radiation can be achieved through a few different approaches, which in the end all give very similar signals containing the amplitude and phase information of the electric field, necessary for the spectroscopic analysis of materials.

The THz system performance and capability depend on the characteristics of the particular THz generator and detector. However, there are two key mechanisms for the generation and detection of THz radiation: optical rectification in electrooptic (EO) crystals (12, 22, 34) and photoconductivity in semiconductors or photoconductive antennas (PCAs) (20, 35, 36). Although the physical mechanisms of EOs and PCAs differ considerably, both tend to high-bandwidth pulses, high signal-to-noise ratios, and high generated power in the THz beam, which all significantly contribute to the high-quality THz spectrum necessary for material analysis.

Downloaded by [Jozef Stefan Institute] at 06:13 12 November 2014

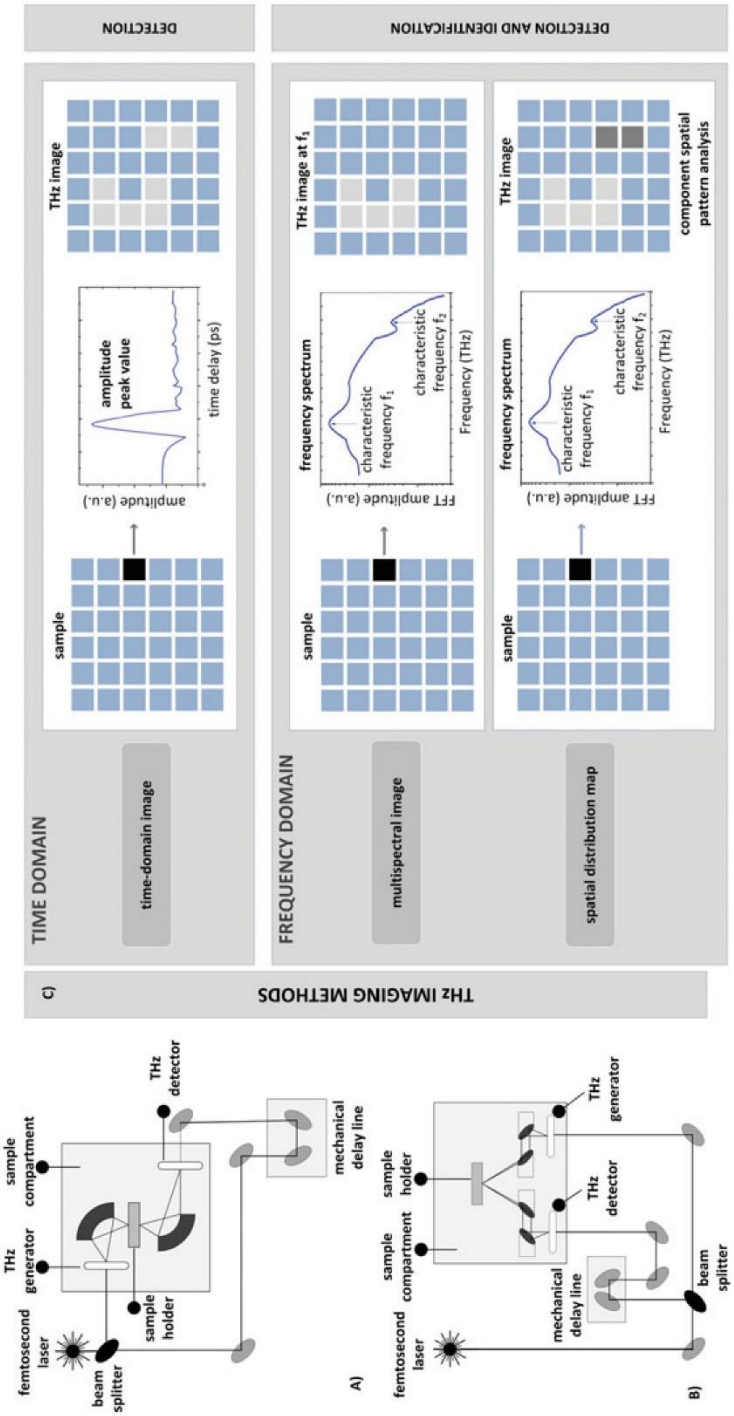


**Figure 1.** THz TDS system in transmission (A) and reflection (B) mode; two-dimensional THz imaging techniques (C).

In addition, THz TDS can comprehend supplementary imaging modality. In the literature at least three different two-dimensional (2D) THz imaging techniques can be found, each suitable for different applications. These techniques can be divided into two groups as shown in Figure 1C: the first one is in the time domain and the other two, multispectral imaging (37) and spatial distribution map (38, 39), are in the frequency domain. The obtained time-domain THz image does not contain any spectroscopic information; thus, this type of imaging is suitable only for detection purposes. On the contrary, imaging in the frequency domain contains important information about each individual substance and enables identification as well as classification (38, 40). The time-domain THz image is constructed based on key parameters—for example, maximum amplitude—which is obtained from the THz time-domain waveform, whereas multispectral imaging is performed using Fourier transform of the time-domain waveform to obtain the spectral frequency dimension, allowing imaging at different frequencies (2, 37). By upgrading this technique with a component spatial pattern analysis method, the enhanced THz images can be obtained, indicating the separation of the spatial patterns of individual substance within heterogeneous samples from multispectral THz images at different THz frequencies, as shown in the last row in Figure 1C (38, 39). However, the THz imaging has garnered a lot of attention to development of novel spectroscopic imaging techniques, not only in 2D but also in three dimensions (3D), during the last decade.

Downloaded by [Jozef Stefan Institute] at 06:13 12 November 2014

## Recent Applications of THz Spectroscopy in Construction and Building-Related Research and Industry

The use of THz spectroscopy in the construction and building industry is usually excluded from reviews, which stress security, medicine, pharmacy, food, biology, and telecommunications. Therefore, the following section introduces the THz analysis of different construction and building materials considering research and industrial applications (summarized in Table 1).

Currently, different NDT methods (14) are used to analyze construction and building materials, among which the most used are visual methods by means of microscopy and digital camera, ultrasound methods, and acoustic imaging through detecting changes in acoustic attenuation and acoustic signature, as well as IR thermography, where the variation in temperature is recorded as a consequence of heat diffusion and cooling at the material surface. Other methods, involving ionizing radiation, are X-ray computed tomography and neutron tomography. In comparison to the existing NDT methods, THz technology offers numerous advantages such as noncontact measurements, which can be performed at room temperature on the surface or in the bulk of material. In addition, THz waves are safe to use on humans and materials under investigation. All of these characteristics make THz spectroscopy and imaging a potential tool for NDT of construction and building materials.

### *Plastic and Foam Polymer Materials*

The use of plastic and foamed polymers is increasing globally in building and construction sectors, particularly due to material-specific properties such as light weight, high thermal and acoustic insulation properties, and high energy absorption capacity. Understanding the physical and mechanical properties of a material, either as a consequence of production processes or as a consequence of degradation, could significantly contribute to the optimization of the structure and composition of plastics and porous foams for a given application. Recently, many researchers reported that several polymer materials feature

Downloaded by [Jozef Stefan Institute] at 06:13 12 November 2014



**Table 1**
THz analysis of various properties of different construction and building materials

| Material group | Investigated material | Property | THz system (wave nature,[a] configuration,[b] THz detector[c]) | Reference |
|---|---|---|---|---|
| Polymer | Sprayed-on foam insulation | Voids, delamination | CW, THz TDS, R and T, Gunn diode, GaAs, ZnTe | (25, 27, 31, 46) |
| | Polymer pumice stone | Heat damage | THz TDS, T, PCA (GaAs) | (44) |
| | Polymer foam and slab | Density distribution, glue lines, adhesive bond | THz TDS, T, EO (ZnTe) | (12, 13) |
| | Bakelite foam, EPS foam, XPS foam, EPS foam with graphite particles | Spectral properties, macrostructure, distribution, filler content, density | THz TDS, T, EO (organic crystal DSTMS) | (22) |
| | PVC cable shield | Corrosion, water intrusion | THz TDS, T, R, NA[d] | (10, 45) |
| | Polymer materials (Bakelite, PP, PE, HDPE, PA, PMMA, PVC, PS, PC, Plexiglas, etc.) | Spectroscopic parameters, additives and fillers, coatings and pores, cracks, delamination, weld joints | THz TDS, T, PCA | (11, 20, 28) |
| | Polystyrene foam | Spectral properties, gas content, density distribution | THz TDS, T, NA | (15, 21) |
| Ceramics | Alumina ceramic | Porosity | THz TDS, T, EO (ZnTe) | (14) |
| | Ceramic tile | Defects, adhesion defects | CW, T and R, Schottky diode | (18, 46) |
| Wood | Beech wood | Density mapping | THz TDS, T, PCA | (49) |
| | Spruce, pine, oak, handboard, beech, etc. | Spectral properties | THz TDS, T, PCA | (20, 51) |
| | Balsa, paulownia, sugi, hinoki, etc. | Water content/distribution, density, defects | CW, T | (18) |
| | Linden, aspen | Knotted areas | THz TDS, T, PCA | (48) |

*(Continued on next page)*

Downloaded by [Jozef Stefan Institute] at 06:13 12 November 2014





**Table 1**
THz analysis of various properties of different construction and building materials *(Continued)*

| Material group | Investigated material | Property | THz system (wave nature,[a] configuration,[b] THz detector[c]) | Reference |
|---|---|---|---|---|
| Paint | Paint on aluminum substrate | Under paint corrosion, paint thickness | THz TDS, R | (57) |
| | Organic binding media | Chemical composition | THz TDS, T, EO (ZnTe) | (16) |
| | White enamel paint, acryl–melamine with pigments, black acryl paint | Thickness distribution, defects, chemical composition, drying process | THz TDS, R, EO (ZnTe) | (52, 56) |
| Composite | Wood plastic composite | Water distribution, water content | THz TDS, T, PCA | (19) |
| | Glass fiber composites | Mechanical damage, fiber content, fiber orientation | THz TDS, T and R, PCA | (60, 66) |
| | Carbon fiber–based materials | Heat damage, fiber orientation | CW, THz TDS, R, EO (ZnTe) | (25) |
| | Glass fiber composites | Burns, voids, delamination, cracks | THz TDS, T/R, EO (ZnTe) | (34, 58) |
| | Polyethylene composite | Delamination, punctures, bulges | THz TDS | (61) |
| Glass | Double-pane glass windows, typical window panes | Spectral parameters | THz TDS, T/R, PCA | (20, 68) |
| | Quartz, silica, Pyrex, BK7, $As_2S_3$ glass, etc. | Spectral parameters, chemical composition | THz TDS, T, EO (ZnTe) | (5, 65, 67) |

Downloaded by [Jozef Stefan Institute] at 06:13 12 November 2014



| | | | | |
|---|---|---|---|---|
| Concrete | Concrete, hydrated cement, concrete paste | Thermocol, air bubble, hydration process | CW, THz TDS, T | (70, 72) |
| | Portland cement with river sands | Water distribution, cracks | CW, T | (18) |
| | Cement paste and mortar | Chloride-induced corrosion | THz TDS, PCA | (35) |
| | Sand-lime brick, clay brick, gypsum | Spectral properties | THz TDS, T, PCA | (20) |
| | Concrete, cement, sand | Spectral properties | THz TDS | (51) |
| Stone | Marble, sandstone, limestone, tuff | Spectral properties, porosity, air gaps | THz TDS, T/R | (69) |
| | Marble, brown gem, red agate, etc. | Spectral properties | THz TDS | (51) |
| Clay | Beck-ceramique | Spectral properties, cracks, hidden objects | THz TDS, T and R, PCA | (36) |
| Asbestos | Pure asbestos, mixture with concrete | Spectral properties, fiber content | THz TDS | (51) |

[a]Continuous wave or pulsed THz TDS.
[b]Configuration in transmission (T) or reflection (R) mode.
[c]Photoconductive dipole antennas and electrooptic materials.
[d]Data not available.

EPS, expanded polystyrene; XPS, extruded polystyrene; PP, polypropylene; PE, polyethylene; HDPE, high-density polyethylene; PA, polyamide; PMMA, poly(methyl methacrylate); PVC, polyvinyl chloride; PS, polystyrene; PC, polycarbonate; BK7, borosilicate glass; CW, continuous wave; THz TDS, terahertz time-domain spectroscopy; R, reflection; T, transmission; GaAs, gallium arsenide; ZnTe, zinc telluride; $As_2S_3$, arsenic trisulfide; DSTMS, 4-N,N-dimethylamino-40-N0-methyl-stilbazolium 2,4,6-trimethylbenzenesulfonate; PCA, photoconductive antenna; EO, electrooptic; NA, not available.

very low absorption and refractive index in the THz region (11, 21). Thus, THz technology appears to be useful for characterizing dielectric material properties (23), superstructures (13), voids (22, 31, 41), inclusions (22, 42), defects (22, 25, 27), glass transition (43), and material aging processes (11). Moreover, the wavelength of THz radiation is comparable to foam cell size (14, 21) and additives or fillers (22, 23).

*Defects, Density, and Additives.* Most recently there has been an increasing interest in imaging of foam and porous materials. The THz attenuation of foam depends on the density of the foam and the dielectric properties of the polymer matrix. Hence, it follows that the difference in the THz response of the foam matrix and air-filled gaps can be visible in THz images. Based on this knowledge, THz technology has been used as a nondestructive tool for inspection of voids and delaminations within the lightweight polyurethane sprayed-on foam insulation (25, 27, 31). THz beams have also been used for detection of the heat-induced damage in porous polymer pumice stone (44) due to the changes in dielectric properties, which decrease when the material is exposed to high temperatures. In addition to defects, properties such as material density (13, 22) and IR radiation absorption on nanoadditives (22, 30) can be probed by THz waves. Increased material density reduces thermal conductivity as well as transmission due to scattering and absorption effects, which can also be seen in THz transmission spectra. Thus, THz radiation can be used to investigate the far IR light absorption through polymer insulation foam. Moreover, the experimental results have shown that polystyrene foam containing graphite particles has lower transmission in most of the THz frequency region in comparison to the sample without additives due to the reflection of IR waves by small IR absorbing particles (22). Additionally, it was reported that THz imaging can reveal the foam macrostructure like beads and their interconnections as well as inclusions, as shown in Figure 2 (22). Accordingly, THz technology can be applied as a complementary macroscopic imaging technique to optical or electron microscopy, which is usually selected to image foam structures at the microscopic level.

*Adhesion and Corrosion.* In the construction sector, polymer foam plates are often glued together to form a single unit. Detection of glue lines or adhesive bonds between two or more elements is possible by the THz imaging due to the higher density of the adhesive layer (12, 13). Furthermore, calculation of the complex refractive index as a function of frequency reveals the thickness of the adhesive layer. This procedure can be also applied to monitor the drying process of the glue joint or water intrusion because the water content within the adhesive joint is one of the crucial factors for deterioration of the blocks (12). Additionally, THz spectroscopy can diagnose corrosion growth under the opaque polymer layer covering the electrical power cables (45), induced by exposure to water (10), copper chloride, and copper carbonate (45).

### *Ceramics and Clay*

Due to its high durability against freeze–thaw processes, chemical attacks, mechanical wear, and higher temperature resistance, ceramics are an advanced construction material with versatile applications in civil engineering. Different studies have proved that THz waves are superior for the analysis of ceramics and enable insight into the structure of opaque ceramic materials.

*Porosity.* In order to achieve better controlled porosity of ceramics, NDT techniques are needed. Dodson et al. (14) used THz technology to find the connection between the structure

Downloaded by [Jozef Stefan Institute] at 06:13 12 November 2014

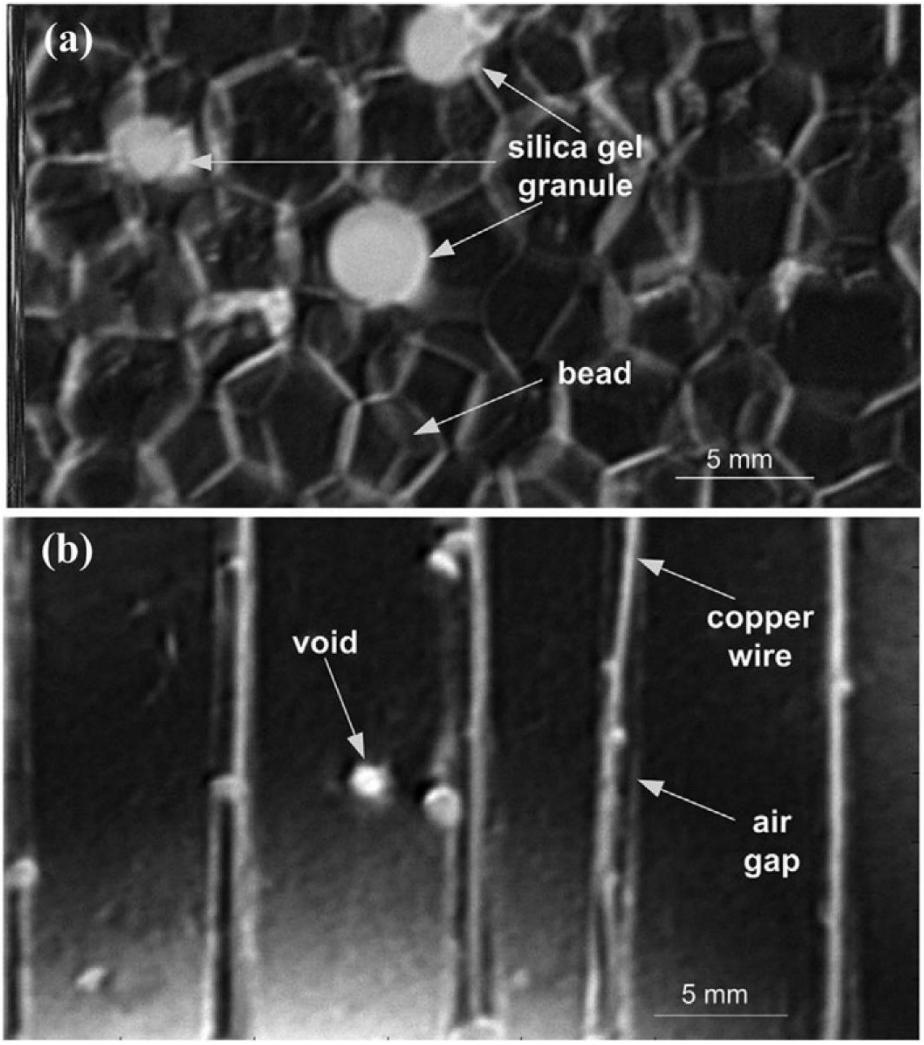


**Figure 2.** THz images of silica gel granules (a) and copper wires (b) within the polymer foam. © Elsevier. Reprinted from (22) with permission from Elsevier. Permission to reuse must be obtained from the rightsholder.

Downloaded by [Jozef Stefan Institute] at 06:13 12 November 2014

of porous alumina ceramics and optical properties at THz frequencies. In many applications this material is used for insulation purposes and has excellent durability over a long period of time. Based on the measurements of optical constants and the different formations of pore size and thickness it was demonstrated that ceramic samples with low porosity have an index of refraction near 1.2, whereas higher porosity ceramics have indices that vary across the THz frequency range (14).

*Defects and Structures Underneath.* THz imaging was used to observe the adhesion defects of ceramic tiles on a concrete wall. The results showed that defects can be easily evaluated by THz imaging instead of the traditional hammer strike method or thermography (18). In addition, Karpowicz et al. (46) investigated defects such as voids, debonding, manufacturing

artefacts, and density inhomogeneities in a molded ceramic tile composed of compressed silica fibers at 0.2 THz by a CW system.

### *Wood*

In the wood industry, THz waves may be considered as a promising tool for sensing and imaging applications, particularly due to the ability of THz radiation to probe the fiber structure of wood. Until now most work has been dedicated to detection of moisture and invisible defects (e.g., annular rings, knots, termite damage, and fungal decay) in wood timbers (17–19, 47–50), which are important parameters in the manufacture of wood products. Moreover, from an ecological point of view, the capability of THz waves to detect imperfections in the production processes can significantly contribute to cost savings and forest conservation.

*Wood Density and Defects.* The imperfections in timber and the internal fiber structure affect the strength of wood products. As reported by some authors (18, 49), density mapping in timber can be analyzed by THz spectroscopy in the frequency range between 0.1 and 2.5 THz where wood is quite transparent. Because the chemical composition of common woods is almost the same, including celluloses, hemicelluloses, and lignin, the absorption coefficient differences are due to the cell-wall volume ratios of different wood species (18). Thus, the absorption coefficients of different wood species are approximately in proportion to timber densities as shown in Figure 3C. In fact, hardwood species such as oak have higher THz attenuation and softwoods such as pine have lower THz attenuation (51). THz system has been used to distinguish between the surrounding ordinary wood and higher-absorption knotted areas (Figures 3A and 3B) (18, 48).

*Water Absorption.* In general, the low water level in timber can improve its mechanical strength, whereas excess of water in timber leads to degradation of the material (17). The experiments showed that the measured THz absorbance in wood varies linearly with the water content (Figure 3D), wherein the dry wood exhibit lower absorption than the damp wood (18). When evaluating the water absorption in materials one should consider both bound and free water content. Due to the fact that the vibrations of the bound water molecules are different from those of free water, THz waves can be applied to determine bound/free water content (19) according to refractive index and absorption coefficient calculations from the dielectric response. This approach is especially useful for wood–plastic composites, which are widely employed in construction applications. Within these materials water interacts with the host material, usually a polymer, and modifies the vibrations of the bound water relative to the free water, which results in a slightly different dielectric response that can be probed by THz radiation (17).

### *Paint*

In the construction industry, paints in the form of thin films or layers present an important component, with functions such as rust prevention, waterproofing, insulation, and heating/cooling regulation. To maintain these functions, evaluation and quality control of paint layers is required. One possible method for noncontact and nondestructive measurement is THz wave probing, which has already shown potential to measure the thickness of coatings and thin films (52, 53), evaluate multilayered paint (12, 52, 54), map thickness

Downloaded by [Jozef Stefan Institute] at 06:13 12 November 2014

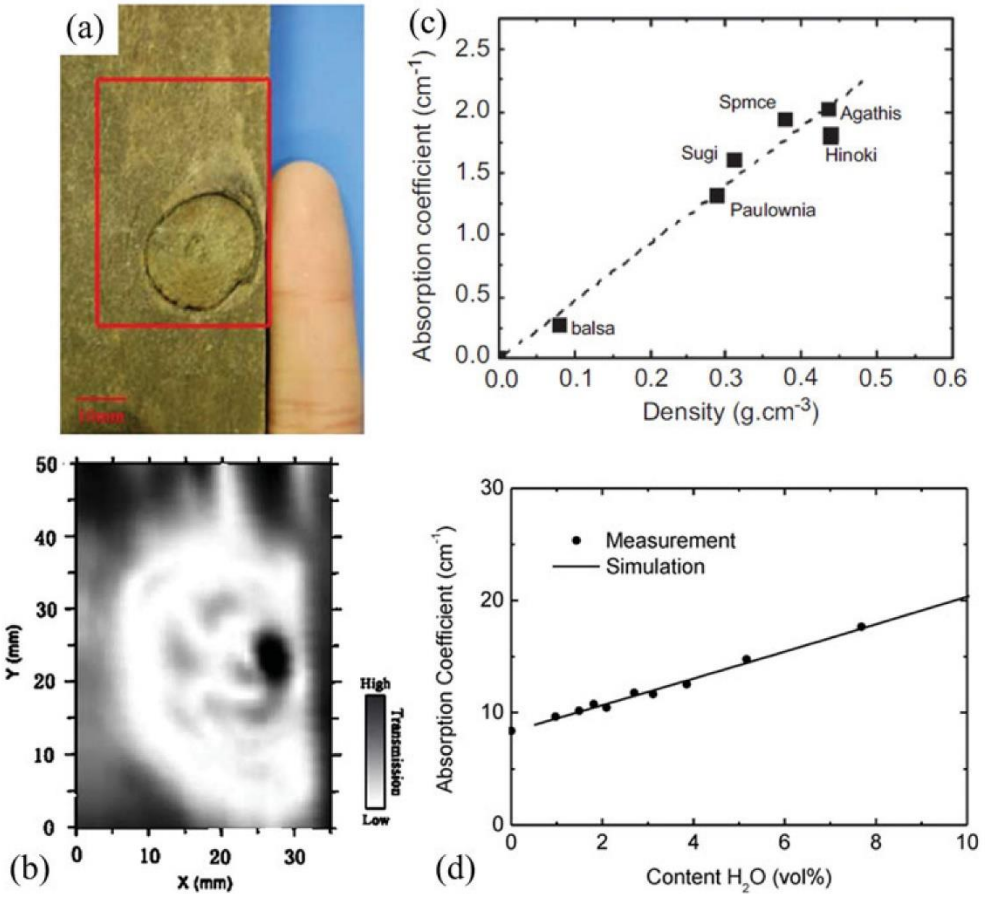


**Figure 3.** Photograph (a) and THz image (b) of the knotted wood sample and absorption coefficients of various wood samples (c). Reprinted from (18) with permission from Elsevier. Absorption coefficient obtained from THz measurements for wood plastic composite with increasing water content at 600 GHz (d).

© Elsevier. Reprinted from (19) with permission from Elsevier. Permission to reuse must be obtained from the rightsholder.

Downloaded by [Jozef Stefan Institute] at 06:13 12 November 2014

distribution (52), detect paint layer defects and inhomogeneities (48, 52), monitor wet-to-dry transformations (52), and determine chemical composition or concentration (16).

*Chemical Composition and Wet-to-Dry Transformation.* The analysis of paints is usually a complex process, in particular investigation of the composition and structure, because paints often contain solvents, pigments, and additives mixed with a binding medium. Several paint films were tested by (52) to show that the difference in THz refractive indices between different paints comes from various pigment components. Because the depth of the peak depends on the paint concentration and thickness variations (52, 55), quantitative analysis is achievable. Another advantage of THz radiation is its ability to monitor the drying process. THz radiation does not easily penetrate through polar liquids such as water or any other solvent with high permittivity. Accordingly, there is a high contrast in the THz image between wet and dry regions. Dry and wet areas of paint film showed an obvious

difference between the spectroscopic characteristics in the THz range due to the presence of volatilizable ingredients tha are added to the paint to enhance the drying process (56). In fact, the paint is dry when the solvent evaporates and consequently the paint layer shrinks. This process is visible as changes in the attenuation, delay, and distortion of the THz pulse echoes (17, 52).

*Thickness and Defects.* A THz paint meter for noncontact measurements of thickness of single-layer and multilayer paint films has been proposed (52, 56). The layer thickness determination is usually carried out by measuring the time delay between two echoes of the THz pulse, the first reflected from the paint surface and the second reflected from the paint–substrate boundary. In general, the areas of thick and thin paint can be identified by signal amplitude correlation in the THz image (57). Moreover, Yasui et al. (52) demonstrated that THz waves can perform mapping of the paint thickness distribution in both single- and multilayer films. In addition, THz imaging was applied for the detection of defects in paint films, such as separation of the paint from the substrate, which might be the result of corrosion or moisture (52, 58).

Downloaded by [Jozef Stefan Institute] at 06:13 12 November 2014

### *Composite Materials*

Composite materials have achieved a rapid development in recent years with an emphasis on optimizing the general properties, such as mechanical strength, light weight, increased safety, and reduced corrosion. Wide application of these materials in various sectors including the construction industry supersedes that of traditional materials like plastic, wood, ceramics, glass, and metals. Because the production of composite materials is a complex process, defects are introduced either during the manufacturing phase or later during the application period. Thus, nondestructive quality control to optimize the production process or detect defective parts is becoming more and more demanding. Recently, THz technology has shown great potential for inspection of various composites on the surface and inside, including in carbon-fiber composites (25, 59), wood plastic composites (19), glass-fiber composites (60), polyethylene fiber composites (61), and polymer nanocomposites (29, 62).

*Fiber Content and Orientation.* The mechanical properties of composites are highly dependent on fiber content and fiber orientation. The fibers usually form a grid structure within the host material and exhibit significantly higher permittivity than the host material; thus, THz waves can be used to probe the fiber content and orientation. Redo-Sanchez et al. (25) reported that carbon fibers have a polarization-dependent reflectivity in the THz frequency range, which is higher when the radiation's electric field is parallel to the grid and lower when it is perpendicular. In addition, Wietzke et al. (63) employed THz technology to identify the fiber orientation based on a novel proposed algorithm for extracting the actual fiber orientation at a specific spatial position. In addition, uniformly dispersed nanometer-sized fillers also enhance the mechanical, thermal, and insulating properties of conventional materials. Some experiments showed that THz spectroscopy can probe even these properties (22, 23).

*Defects.* Several published papers showed that THz radiation is suitable for the inspection of defects such as voids, delaminations, inclusions, and cracks within the composite materials, among which glass fiber- and carbon fiber–reinforced plastics are predominant (59, 64). Such defects usually occur when the material is exposed to undesirable environmental conditions; for example, water intrusion, high temperatures, or high pressure. When the

structure is distorted or damaged due to heat or mechanical stress, the local THz transmission or reflectivity is changed.

### *Glass*

Near- and far-IR absorption spectra of glasses in the frequency region between 0.3 and 300 THz have attracted many researchers during the past decades mainly due to the ability to provide insight into the glass structure and the relation to optical and mechanical properties of glass. Lately, several investigations of the absorption spectra and the refractive indices of glasses and glass-reinforced materials in the THz region have been reported (5, 60, 65–68).

*Structure.* Naftaly and Miles (5) reported that the THz absorption and refractive indices of silica and quartz samples are identical and relatively low, whereas those of silicate glass differ significantly mainly due to the ionic network modifiers, which increase the microscopic polarizability and cause much stronger absorption and higher refractive indices at THz frequencies. They also defined the relation between the fraction of alkali oxides used as ionic network modifiers in glass and the increasing THz refractive indices. Furthermore, the proportion of alkali oxides and absorption parameter are inversely related to the bonding strength in the glass and the glass melting temperature. Noteworthy is the fact that THz refractive indices of glasses are higher than in the visible range due to ionic polarizability. In addition, for silica the THz refractive index appears to be linearly related to the visible refractive index (5).

*Glass Fibers.* Glass fibers integrated into various host materials exhibit enhanced mechanical properties of conventionally used material such as light weight, corrosion resistance, and high tensile strength (60, 66). When the host material (e.g., polymer) is transparent for THz waves, the glass additives can be easily determined by THz spectroscopy and imaging due to the changes in dielectric properties. Therefore, any damage such as delamination, voids, or material inhomogeneity that disturb the distribution of refractive index can be observed. However, Jördens et al. (66) proposed a method for determining the preferential fiber orientation and the fraction of orientated glass fibers in a reinforced-polymer matrix using THz spectroscopy. Additionally, Chady et al. (60) used harmonic analysis of THz signals as a health monitoring technique for wind turbine blades made of glass-reinforced composites exposed to various environmental conditions.

### *Concrete, Brick, Sand, Cement, Stone*

The advantages of THz waves over conventional techniques (e.g., ground penetrating radar, IR thermography and spectroscopy, microscopy, ultrasonic, X-ray, and $\gamma$-ray) when applied to the study of internal concrete structure are associated with higher penetration capability, nondestructivity, and submillimeter resolution. Thus, THz technology can enhance the potention to inspect degradation and defects in building blocks, which frequently contribute to the collapse of buildings, bridges, dams, or road tunnels.

*Structure.* Xu and Zhang (51) investigated the attenuation coefficient of some widely used building materials such as concrete, sand, stone, and cement in the THz frequency range from 0.1 to 1.6 THz. The samples of concrete and sand showed almost similar attenuation coefficients, whereas the cement powder slightly differed from the others. In comparison with concrete, most stone samples have lower attenuation because the scattering of

Downloaded by [Jozef Stefan Institute] at 06:13 12 November 2014

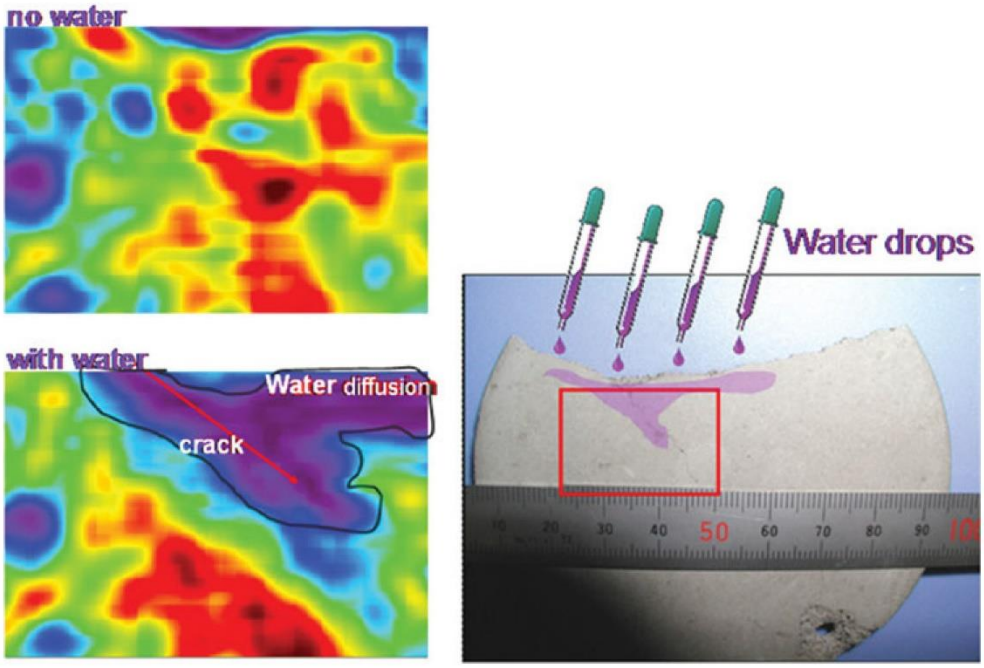


**Figure 4.** Sub-THz imaging of cracks in concrete with no water and with diffused water along the cracks to enhance the detection sensitivity of cracks.
© Elsevier. Reprinted from (18) with permission from Elsevier. Permission to reuse must be obtained from the rightsholder.

concrete is higher than that of most stones. Furthermore, Schwerdtfeger et al. (69) investigated different stone samples that can be found as construction material in buildings of cultural and historical importance. Different stones reflect different composition and porosity and therefore different dielectric properties according to the refractive index and absorption coefficient in THz frequency range. Piesiewicz et al. (20) presented frequency-dependent refractive index and absorption coefficients of different brick samples at frequencies between 0.1 and 1 THz. Gypsum samples showed a lower refractive index compared to the clay brick and sand-lime brick, which had almost the same values. Research studies have shown that THz radiation is promising for sensing and imaging purposes in cultural heritage conservation and restoration.

*Defects.* Concrete surfaces are often exposed to various environmental factors that may result in external defects or internal cracks over time. THz imaging was used for nondestructive evaluation of internal structure and defects (70) as well as for the successful inspection of degradation in concrete blocks (18). The experimental results showed that defects and water absorption areas inside the concrete become clearly visible on the basis of the characteristic features of THz waves. In fact, sub-THz imaging of cracks is enhanced when water diffuses through the concrete due to a high absorption coefficient of THz waves for water (Figure 4). Furthermore, chloride-induced corrosion within reinforced concrete (35) was investigated by measuring the frequency-dependent optical constants in the THz range. For instance, the absorption coefficient increases almost linearly with increasing chloride concentration; thus, THz waves are able to detect the chloride ion concentration

Downloaded by [Jozef Stefan Institute] at 06:13 12 November 2014

and penetration, which are responsible for cracks, delamination, and other defects in the concrete structure.

*Hydration and Contamination.* Based on THz spectra, Maruyama et al. (71) determined that the lower frequencies of 0.1 and 0.05 THz are more appropriate for evaluating the moisture content of hardened cement paste due to the nonsensitivity to chemically bounded water that occurs at higher frequencies. Moreover, Dash et al. (72) reported that THz spectroscopy is a promising tool to quantify the hydration process; that is, the time-dependent reaction of cement with water, which can significantly contribute to the improved understanding of the hydration kinetics of cement necessary to optimize the mechanical characteristics of concrete. Concerning the fact that THz sensing is able to detect the hazardous gases (24), another issue related to the contamination of concrete can be studied. However, concrete is a highly porous material, and gases or radioactive contaminants (e.g., radon) can often penetrate to a few centimeters below the surface due to the mass diffusion process. The identification and characterization of this contamination into porous concrete is extremely important because it determines whether or not a facility can be released for reuse. Current methods that operate in the IR spectrum are not able to detect gases within concrete walls but THz radiation can penetrate such obstacles (73).

Downloaded by [Jozef Stefan Institute] at 06:13 12 November 2014

### *Asbestos and Rock Wool*

Asbestos-containing materials were widely used in building construction after World War II. In general, asbestos is a common name for a group of naturally occurring minerals that form long thin fibers instead of crystals. However, the long-term exposure to airborne asbestos fibers is dangerous for humans and can cause asbestos-related diseases. Xu and Zhang (51) reported that THz TDS can be applied to analyze the presence of asbestos in building materials due to the higher attenuation coefficient that occurs in the samples with asbestos and its unique spectral absorption between 1.2 and 1.4 THz. Another possible use of THz imaging system is the detection of corrosion in pipes under thin insulation materials such as mineral wool without removing the covering material. The thin mineral wool is transparent enough to allow the identification of imperfections on the surface of metal pipes; for instance, dry or wet areas and rust spots (74).

## Limitations of Technology and Future Application Trends

### *Advantages and Limitations of THz Spectroscopy and Imaging*

Many applications in research and industry related to construction require nondestructive, contactless, and spatially resolved investigations. Several methods, covering different parts of the electromagnetic spectrum, have been proposed to satisfy this need, including THz waves, X-ray, IR waves, microwave radiation, and neutron radiation. Each of them has advantages and limitations that must be taken into account, especially when they are combined, in order to enhance the reliability of measured data. In this review we add two additional technologies, visual and ultrasound methods, which are also widely used in the construction and building industry. For instance, THz waves were combined with ultrasound to enhance the contrast and resolution of imaging applications (75) as well as with electron and confocal microscopy to understand the relation between the micro- and macrostructure of materials (22). In Figure 5 the advantages of THz waves (designated

Downloaded by [Jozef Stefan Institute] at 06:13 12 November 2014





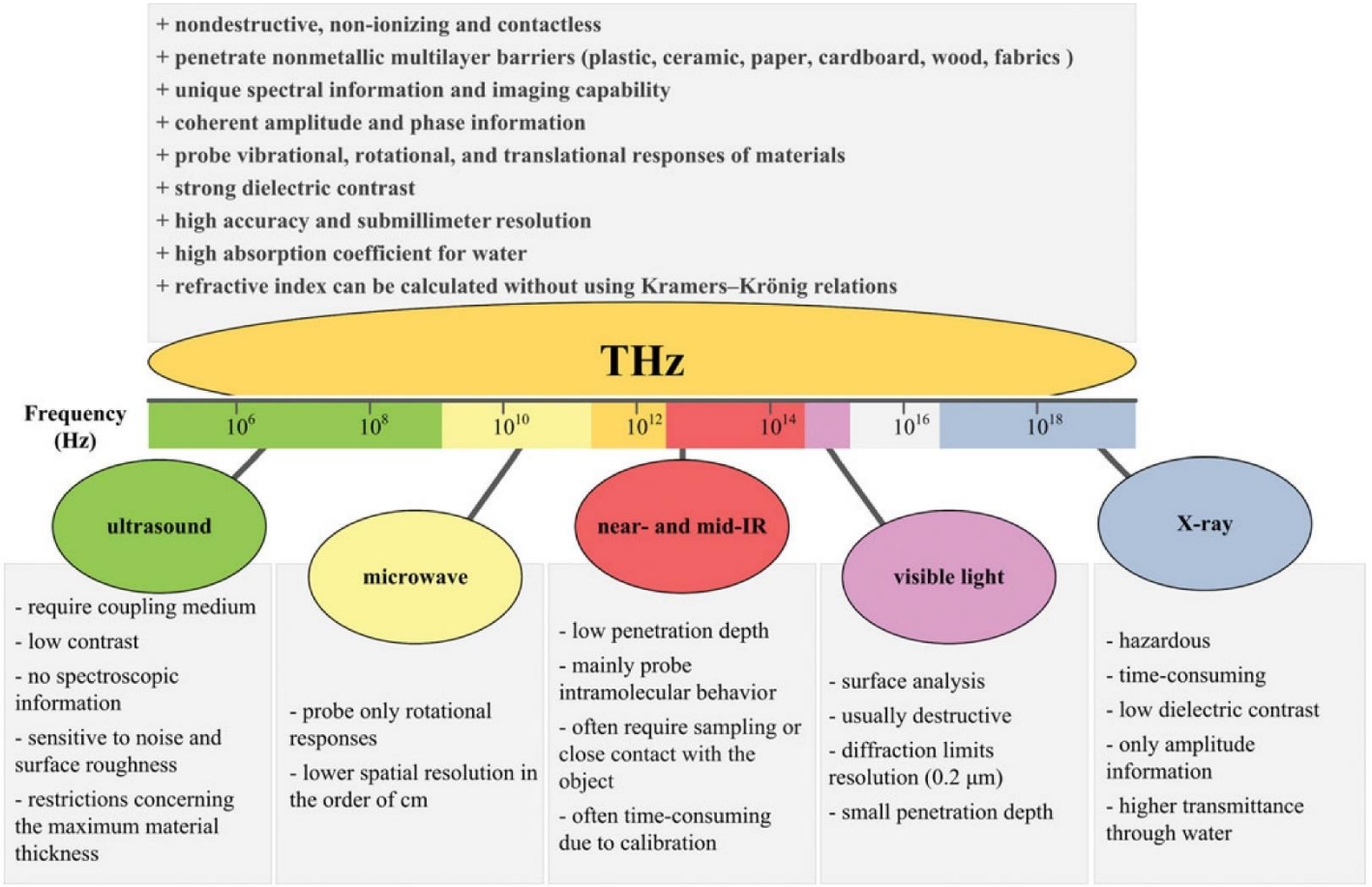


**Figure 5.** Advantages of THz waves (designated with a plus sign) against the limitations (designated with a minus sign) of other technologies.

with a plus sign) and the limitations (designated with a minus sign) of other technologies are summarized.

THz waves exhibit some drawbacks that have aroused great interest among researchers and manufacturers, especially to facilitate the current applications in industrial environments. We emphasize the most meaningful ones in the following subsections.

*Low-Cost, Compact, and Portable Devices.* Industrial applications require low-cost, easy-to-use, portable systems that are still compact and reliable. Modern fiber lasers and fiber-coupled detectors and emitters have enable the development of flexible, robust, and portable fiber-coupled THz TDS (62, 63), which can be easily implemented to online monitoring in industry. There already exist portable battery-powered handheld THz spectrometers that allow NDT to be performed in various environmental settings (76). Very recently, a THz spectroscopic system with cryogenic solution (77) reached the market. A majority of THz systems available on the market are still quite expensive and usually provided as a large instrument, not allowing in situ measurements in industry; thus, their application is more or less limited to laboratory research. Only by reducing the size, weight, and power requirements, as well as improving the performance of THz detectors and generators, either with all-fiber setup or any other integration approach, will the gap between the industrial and laboratory use be diminished.

*Higher Acquisition Rate and Scanning Speed.* The major limitation of THz systems in industrial environments is the low acquisition rate, especially in the THz TDS imaging configuration with a conventional mechanical delay line. Usually, higher resolution demands long-time measurements, which are not desirable in real-world applications where both speed and specificity are required. On the other hand, CW modalities are capable of faster data acquisition and higher output powers but do not provide any spectroscopic information. Recently, new designs of nearly alignment-free THz systems without any mechanical delay line were introduced: optical sampling by cavity tuning (78), asynhronous optical sampling (79), and electronically controlled optical sampling (80). The last has already been applied for the reflection 3D imaging of defects in composite materials (42). Hence, the majority of research work is focused on the development of high-speed, high-resolution, and high-power sources based on graphene, metamaterials, quantum cascade lasers, plasmonic photoconductive emitters, and THz detector arrays.

*Environmental Conditions.* The results obtained by THz measurements are highly dependent on humidity and temperature, which in industry are usually quite different from that found in laboratories. Water strongly absorbs THz radiation, whereas temperature variations affect collective vibrational, rotational, and torsional modes of molecular complexes and chains and consequently change the absorption bands (81). Hence, in the laboratory, the THz optics is set up in a compartment with a controllable atmosphere, usually vacuum or nitrogen. In addition, acoustic vibrations are often present in industry. Therefore, it is rather challenging to transfer a conventional THz TDS system using free space optical elements in a highly precise arrangement into a real production line. Instead a flexible all-fiber system enabling rapid changes between transmission and reflection configurations without the need for a mechanical delay line was introduced.

*Sample Condition.* Another issue when using THz technology for material characterization is sample preparation. Conventional laboratory transmission systems use samples in the form of a thin film, tablet, or solution (81, 82). Solid samples are often mixed with an

Downloaded by [Jozef Stefan Institute] at 06:13 12 November 2014

adequate quantity of reference material such as high-density polyethylene or Teflon to ensure an optimal absorption range and to prevent possible scattering effects between sample molecules. One of the challenges for THz TDS is the increase in sensitivity to enable the detection of small quantities of compounds in mixtures even at parts per million. Moreover, THz imaging is usually limited to small sample surfaces due to long-lasting measurements. In practice, different materials demand different THz system setups; that is, transmission or reflection geometry with ordinary imaging or tomography options. However, reflection mode is far more desirable than transmission mode because real samples are thicker and access from two sides is impossible. Herein another difficulty appears related to the sample surface roughness, which can significantly influence the measured THz spectra in a frequency-dependent way and consequently the reliable identification of individual substances. These distortions can be improved to a certain degree with corrective algorithms.

Downloaded by [Jozef Stefan Institute] at 06:13 12 November 2014

*Uniform Database.* Over the years of development and research in the field of THz technology, the creation of a uniform database was not prioritized. In the last decades, a few THz spectrum databases providing transmittance and absorbance data mainly for medicine-, bio-, and food-related materials were set up worldwide, which dispersed data across multiple places. This approach tends to be less practically useful for researchers and manufacturers; thus, the integration of existing THz spectra into one uniform extensive database is necessary to improve the reliability of THz measurements essential for better interpretation of spectroscopic data. The most promising web database was established by the National Institute of Information and Communication Technology and RIKEN (83). Most recently, a computer tool that provides all measured and reported THz absorption signatures for solids and liquids (e.g., colorant, pigments, bio-related materials, optics, semiconductors, polymers, liquid crystals, photonic crystals, metamaterials, and carbon nanotubes) in transmission and reflection, in the range from 100 GHz to 10 THz, was introduced (84). However, the major difficulty in creating a uniform database is the specificity of each individual THz system. Hence, noticeable differences can be found in published THz spectral features for the same material or chemical compound. Currently, this issue is resolved by providing the THz spectrum with additional information about sample preparation, measurement techniques (reflection, transmission), environmental conditions (temperature, humidity, nitrogen, or vacuum atmosphere), or even sample composition.

These drawbacks might be improved by using various statistical analysis techniques, neural networks, and decision trees, which are especially meaningful for samples that are not chemically pure; for example, building materials. Another possible solution to improve the reliability of THz results is to introduce THz standards for measurements, sample preparation, and system design.

## *Future Trends of THz Technology in Construction and Building Research and Industry*

Although the initial potential of THz spectroscopy and imaging has been introduced for a few applications in the construction and building industry, it is obvious that much remains to be investigated in this area. Herein, we will briefly expose some of the issues in correlation with trends (85–87) in the construction and building industry that should be considered in the future.

*Energy-Efficient Insulation Materials.* The main function of insulation is to ensure low thermal conductivity and thermal transmittance, which is highly dependent on the thickness

of a material and some other contributions detailed in Jelle (87). However, THz spectroscopy can be applied to probe most of these characteristics, including material thickness, gas and moisture content, IR transmittance, material density, and temperature dependence. High-power THz imaging can reveal the structure of conventional insulation materials regarding fiber or filler content as well as fiber orientation, which determine the physical and mechanical properties of final material and can be controlled during the technological process. Furthermore, because THz waves can probe gases, they can be applied to evaluate the presence of expansion gas (hydrofluorocarbons, $CO_2$ or $C_6H_{12}$) captured in the cells of traditional polymer foams (e.g., polyurethane, expanded and extruded polystyrene) after production.

Because energy consumption in the construction and building sector presents a significant part of the total energy use worldwide, new insulation materials have been introduced to improve the energy efficiency of buildings. In comparison to traditional building envelopes, novel insulation materials have an advantage to become thinner or to be formed in a multilayered structure, which is also suitable for THz sensing. At the moment the most promising high-performance thermal insulation material is aerogel (88), with very high porosity, which enables THz waves to easily penetrate through the material. Thus, a THz system can be used to control the production process of aerogels; for instance, the unreacted alkoxide groups in silica aerogel networks, the water content in pores during the drying process, and the distribution of larger pores within the material, which are not desirable for insulation purposes. THz TDS has been used to study silica aerogels regarding the adsorption process of the molecular vapors of water, ammonia, methyl chloride, and others (89). In addition, THz imaging can be applied to visualize hidden defects (e.g., cracks, water intrusion) in building envelopes made of modern vacuum insulation panels or gas insulation panels. These panels consist of an open porous core of fumed silica enveloped by several metallized polymer laminate layers where even a small puncture causes an increase in the thermal conductivity and enables water as well as air intrusion (87). Phase change materials (e.g., organic paraffin, non-paraffin, salt hydrate, or metallics) incorporated in the form of microcapsules or planar or cylindrical elements show great potential as insulation material (90). Their main function is to change phase from a solid state to a liquid when heated and vice versa when cooled. For most this change occurs in the temperature range between 18 and 32°C (85), which can be easily determined by THz spectrometry in combination with a cryogenic system.

*Sustainability, Eco-Efficiency, and Recycling of Construction Materials.* The construction industry worldwide consumes more raw materials than any other sector. It is expected that the construction industry will keep on growing and the crucial issue to which directives and regulations should be paid more attention is the eco-efficiency, sustainability, and recycling of materials (85, 91). With the exception of a few natural construction materials that are almost completely renewable and recyclable, all others are associated with a negative environmental impact. The reuse of construction materials is often limited due to the content of hazardous and toxic substances, which can be determined by THz technology, especially for detection of radioactive elements such as radon, toxic gases, or other dangerous compounds (e.g., dioxins, furans, heavy metals) that leak out of the materials when exposed to extreme environmental conditions.

Sustainability and eco-efficiency of construction materials are highly related to nanotech research (86). The incorporation of nanosized additives in existing construction materials like concrete and asphalt enhance the mechanical properties and material durability as well as reduce their environmental impact (91). Similarly, for thermal insulation

Downloaded by [Jozef Stefan Institute] at 06:13 12 November 2014

materials, the enhanced properties are achieved by making pores in the nano range (92). Usually, nano-$SiO_2$ is added to concrete (92) to reduce calcium leaching, which influences the degradation process of concrete and other cement-based materials due to increasing the porosity and consequently the permeability of water or other compounds (e.g., chloride, copper oxide). The calcium leaching process might be controlled by THz spectrometry with imaging modality. Another nanoparticle more often used in concrete, facade coatings, or paints is nano-$TiO_2$, which has a role of self-cleaning with regards to photocatalytic degradation of environmental pollutants (92), which can be detected by THz waves. In addition to gases, THz radiation can probe bacterial and fungal growth, water-repellent surfaces, and aging resistance.

## Conclusions

The article reviews the recent applications of THz spectroscopy in research and industry related to the construction and building sector. In addition, the key advantages and limitations of the present technology are outlined and a few new approaches for applications in the field of construction and building materials are introduced. Initial research and industrial requirements clearly show that THz spectroscopy has promising potential for both researchers to understand the structure of material and engineers to manipulate the production process to enhance material properties and durability. When THz waves pass through materials, they produce unique absorption spectra that can be applied for analysis of chemical composition, water content, porosity, material thickness, density, material aging, and others. In addition, supplementary imaging modalities can visualize hidden internal and surface defects, inclusions, and manufacturing imperfections. These specific characteristics make THz spectroscopy and imaging a valuable substitute or complement to other sensing techniques using ultrasound, microwaves, IR, or X-ray waves. Although the construction industry lags behind other industries in applications of THz technology and its innovative practices, there are many possibilities for further research. It is expected that the potential of THz spectroscopy for characterization of construction and building materials will improve significantly when radical progress is achieved in new high-speed, high-resolution, and high-power sources.

Downloaded by [Jozef Stefan Institute] at 06:13 12 November 2014

## Funding

The authors gratefully acknowledge financial support from the Slovenian Research Agency grants P2-0348-2338 and J2-4266.

## References

1. Scheller, M., Yarborough, J.M., Moloney, J.V., Fallahi, M., Koch, M., and Koch, S.W. (2010) Room temperature continuous wave milliwatt terahertz source. *Optic. Express*, 18 (26): 27112–27117.
2. Walther, M., Fischer, B., Ortner, A., Bitzer, A., Thoman, A., and Helm, H. (2010) Chemical sensing and imaging with pulsed terahertz radiation. *Anal. Bioanal. Chem.*, 397 (3): 1009–1017.
3. Yu, C., Fan, S., Sun, Y., and Pickwell-MacPherson, E. (2012) The potential of terahertz imaging for cancer diagnosis: a review of investigations to date. *Quant. Imaging Med Surg.*, 2 (1): 33–45.
4. Siegel, P.H. (2004) Terahertz technology in biology and medicine. *IEEE Trans. Microw. Theor. Tech.*, 52 (10): 2438–2447.
5. Naftaly, M. and Miles, R.E. (2007) Terahertz time-domain spectroscopy for material characterization. *Proc. IEEE*, 95 (8): 1658–1665.

6. Pawar, A.Y., Sonawane, D.D., Erande, K.B., and Derle, D.V. (2013) Terahertz technology and its applications. *Drug Invention Today*, 5 (2): 157–163.
7. Xie, L., Yao, Y., and Ying, Y. (2013) The application of terahertz spectroscopy to protein detection: a review. *Appl. Spectros. Rev.*, 49 (6): 448–461.
8. Qin, J., Ying, Y., and Xie, L. (2013) The detection of agricultural products and food using terahertz spectroscopy: a review. *Appl. Spectros. Rev.*, 48 (6): 439–457.: 103104-1103104-5
9. Lu, M., Shen, J., Li, N., Zhang, Y., Zhang, C., Liang, L., and Xu, X. (2006) Detection and identification of illicit drugs using terahertz imaging. *J. Appl. Phys.*, 100 (10): 103104-1–103104-5.
10. Fuse, N., Takahashi, T., Ohki, Y., Sato, R., Mizuno, M., and Fukunaga, K. (2011) Terahertz spectroscopy as a new tool for insulating material analysis and condition monitoring. *IEEE Electr. Insul. Mag.*, 27 (3): 26–35.
11. Pastorelli, G., Trafela, T., Taday, P., Portieri, A., Lowe, D., Fukunaga, K., and Strlič, M. (2012) Characterisation of historic plastics using terahertz time-domain spectroscopy and pulsed imaging. *Anal. Bioanal. Chem.*, 403 (5): 1405–1414.
12. Jansen, C., Wietzke, S., Wang, H.Y., Koch, M., and Zhao, G.Z. (2011) Terahertz spectroscopy on adhesive bonds. *Polymer Test*, 30 (1): 150–154.
13. Brahm, A., Schmidt, D., Riehemann, S., Notni, G., Wostmann, F.J., and Tunnermann, A. (2010) Non-destructive determination of the density distribution of polymer foam models with THz-pulses. *Proceedings of Infrared Millimeter and Terahertz Waves (IRMMW-THz)*, Rome, Italy, September 5–10.
14. Dodson, C., Spicer, J., Fitch, M., Schuster, P., and Osiander, R. (2005) Propagation of terahertz radiation in porous polymer and ceramic materials. *AIP Conference Proceedings*, 760 (1): 562–569.
15. Pradarutti, B., Riehemann, S., Notni, G., and Tünnermann, A. (2007) Terahertz imaging for styrofoam inspection. *Proceedings of Terahertz Physics, Devices, and Systems II*, Boston, MA, September 26.
16. Manceau, J.M., Nevin, A., Fotakis, C., and Tzortzakis, S. (2008) Terahertz time domain spectroscopy for the analysis of cultural heritage related materials. *Appl. Phys. B*, 90 (3–4): 365–368.
17. Federici, J. (2012) Review of moisture and liquid detection and mapping using terahertz imaging. *Journal of Infrared, Millimeter and Terahertz Waves*, 33 (2): 97–126.
18. Oyama, Y., Zhen, L., Tanabe, T., and Kagaya, M. (2009) Sub-terahertz imaging of defects in building blocks. *NDT & E International*, 42 (1): 28–33.
19. Jördens, C., Wietzke, S., Scheller, M., and Koch, M. (2010) Investigation of the water absorption in polyamide and wood plastic composite by terahertz time-domain spectroscopy. *Polymer Test.*, 29 (2): 209–215.
20. Piesiewicz, R., Jansen, C., Wietzke, S., Mittleman, D., Koch, M., and Kürner, T. (2007) Properties of building and plastic materials in the THz range. *Int J Infrared Millimet. Waves*, 28 (5): 363–371.
21. Zhao, G., Mors, M.T., Wenckebach, T., and Planken, P.C.M. (2002) Terahertz dielectric properties of polystyrene foam. *J. Opt. Soc. Am. B*, 19 (6): 1476–1479.
22. Abina, A., Puc, U., Jeglič, A., and Zidanšek, A. (2013) Structural analysis of insulating polymer foams with terahertz spectroscopy and imaging. *Polymer Test.*, 32 (4): 739–747.
23. Ohki, Y., Okada, M., Fuse, N., Iwai, K., Mizuno, M., and Fukunaga, K. (2008) Terahertz spectroscopy as a new analyzing tool for dielectric properties of various insulating materials. *Proceedings of Annual Report Conference on Electrical Insulation and Dielectric Phenomena*, Quebec, Canada, October 26–29.
24. Ikari, T. and Fukasawa, R. (2009) Terahertz characterization of construction materials for remote gas, sensing. *Proceedings of Infrared, Millimeter, and Terahertz Waves (IRMMW-THz)*, Busan, Korea, September 21–25.
25. Redo-Sanchez, A., Karpowicz, N., Xu, J., and Zhang, X.-C. (2006) Damage and defect inspection with terahertz waves. *The 4th International Workshop on Ultrasonic and Advanced Methods for Non-destructive Testing and Material Characterization*, Dartmouth, MA, June 19.


Downloaded by [Jozef Stefan Institute] at 06:13 12 November 2014

26. Rahani, E.K., Kundu, T., Wu, Z.R., and Xin, H. (2011) Mechanical damage detection in polymer tiles by THz radiation. *IEEE Sensor. J.*, 11 (8): 1720–1725.
27. Zhong, H., Xu, J.Z., Xie, X., Yuan, T., Reightler, R., Madaras, E., and Zhang, X.C. (2005) Nondestructive defect identification with terahertz time-of-flight tomography. *IEEE Sensor. J.*, 5 (2): 203–208.
28. Wietzke, S., Jordens, C., Krumbholz, N., Baudrit, B., Bastian, M., and Koch, M. (2007) Terahertz imaging: a new non-destructive technique for the quality control of plastic weld joints. *J. Eur. Opt. Soc.*, 2: 07013-1–07013-5.
29. Krumbholz, N., Hochrein, T., Vieweg, N., Hasek, T., Kretschmer, K., Bastian, M., Mikulics, M., and Koch, M. (2009) Monitoring polymeric compounding processes inline with THz time-domain spectroscopy. *Polymer Test*, 28 (1): 30–35.
30. Rutz, F., Koch, M., Khare, S., Moneke, M., Richter, H., and Ewert, U. (2006) Terahertz quality control of polymeric products. *Int. J. Infrared Millimet. Waves*, 27 (4): 547–556.
31. Winfree, W.P. and Madaras, E.I. (2005) Detection and characterization of flaws in sprayed on foam insulation with pulsed terahertz frequency electromagnetic waves. *Proceedings of 41st AIAA/ASME/SAE/ASEE Joint Propulsion Conference & Exhibit*, Tucson, AZ, July 10–13.
32. Robin, T. and Bouyé, C. (2014) THz technologies offer varied options for industry. *Industrial Photonics*, 1. Available at: http://www.photonics.com/Article.aspx?AID=56089
33. Brunner, F.D.J., Schneider, A., and Günter, P. (2009) A terahertz time-domain spectrometerfor simultaneous transmission and reflection measurements at normal incidence. *Optic. Express*, 17 (23): 20684–20693.
34. Stoik, C.D., Bohn, M.J., and Blackshire, J.L. (2008) Nondestructive evaluation of aircraft composites using transmissive terahertz time domain spectroscopy. *Optic. Express*, 16 (21): 17039–17051.
35. Tripathi, S.R., Ogura, H., Kawagoe, H., Inoue, H., Hasegawa, T., Takeya, K., and Kawase, K. (2012) Measurement of chloride ion concentration in concrete structures using terahertz time domain spectroscopy (THz-TDS). *Corros. Sci.*, 62: 5–10.
36. Labaune, J., Jackson, J.B., Fukunaga, K., White, J., d'Alessandro, L., Whyte, A., Menu, M., and Mourou, G. (2011) Investigation of terra cotta artefacts with terahertz. *Appl. Phys. A Mater. Sci. Process.*, 105 (1): 5–9.
37. Kawase, K., Ogawa, Y., Watanabe, Y., and Inoue, H. (2003) Non-destructive terahertz imaging of illicit drugs using spectral fingerprints. *Optic. Express*, 11 (20): 2549–2554.
38. Shen, Y.C., Taday, P.F., Newnham, D.A., and Pepper, M. (2005) Chemical mapping using reflection terahertz pulsed imaging. *Semicond. Sci. Tech.*, 20 (7): S254–S257.
39. Watanabe, Y., Kawase, K., Ikari, T., Ito, H., Ishikawa, Y., and Minamide, H. (2004) Component analysis of chemical mixtures using terahertz spectroscopic imaging. *Opt. Comm.*, 234 (1–6): 125–129.
40. Shen, Y.-C. (2011) Terahertz pulsed spectroscopy and imaging for pharmaceutical applications: a review. *Int. J. Pharm.*, 417 (1–2): 48–60.
41. Karpowicz, N., Zhong, H., Xu, J.Z., Lin, K.I., Hwang, J.S., and Zhang, X.C. (2005) Comparison between pulsed terahertz time-domain imaging and continuous wave terahertz imaging. *Semicond. Sci. Tech.*, 20 (7): S293–S299.
42. Jin, K.H., Kim, Y.-G., Cho, S.H., Ye, J.C., and Yee, D.-S. (2012) High-speed terahertz reflection three-dimensional imaging for nondestructive evaluation. *Optic. Express*, 20 (23): 25432–25440.
43. Wietzke, S., Jansen, C., Jung, T., Reuter, M., Baudrit, B., Bastian, M., Chatterjee, S., and Koch, M. (2009) Terahertz time-domain spectroscopy as a tool to monitor the glass transition in polymers. *Optic. Express*, 17 (21): 19006–19014.
44. Rahani, E.K., Kundu, T., Wu, Z.R., and Xin, H. (2011) Heat induced damage detection by terahertz (THz) radiation. *Journal of Infrared, Millimeter and Terahertz Waves*, 32 (6): 848–856.
45. Komatsu, M., Sato, R., Mizuno, M., Fukunaga, K., and Ohki, Y. (2012) Feasibility study on terahertz imaging of corrosion on a cable metal shield. *Jpn. J. Appl. Phys.*, 51 (12): 122405-01–122405-5.

Downloaded by [Jozef Stefan Institute] at 06:13 12 November 2014

46. Karpowicz, N., Zhong, H., Zhang, C., Lin, K.-I., Hwang, J.-S., Xu, J., and Zhang, X.C. (2005) Compact continuous-wave subterahertz system for inspection applications. *Appl. Phys. Lett.*, 86 (5): 054105-1–054105-3.
47. Reid, M. and Fedosejevs, R. (2006) Terahertz birefringence and attenuation properties of wood and paper. *Appl. Optic.*, 45 (12): 2766–2772.
48. Skryl, A.S., Jackson, J.B., Bakunov, M.I., Menu, M., and Mourou, G.A. (2014) Terahertz time-domain imaging of hidden defects in wooden artworks: application to a Russian icon painting. *Appl. Optic.*, 53 (6): 1033–1038.
49. Koch, M., Hunsche, S., Schumacher, P., Nuss, M.C., Feldmann, J., and Fromm, J. (1998) THz-imaging: a new method for density mapping of wood. *Wood Sci. Technol.*, 32 (6): 421–427.
50. Jackson, J.B., Mourou, M., Labaune, J., Whitaker, J.F., Duling, I.N., Williamson, S.L., Lavier, C., Menu, M., and Mourou, G.A. (2009) Terahertz pulse imaging for tree-ring analysis: a preliminary study for dendrochronology applications. *Meas. Sci. Technol.*, 20 (7): Article 075502.
51. Xu, G. and Zhang, X. (2000) *Real-Time Identification and Characterization of Asbestos and Concrete Materials with Radioactive Contamination*. U.S. Department of Energy, Environmental Management Science Program: Washington, DC.
52. Yasui, T., Yasuda, T., Sawanaka, K.-I., and Araki, T. (2005) Terahertz paintmeter for non-contact monitoring of thickness and drying progress in paint film. *Appl. Optic.*, 44 (32): 6849–6856.
53. Theuer, M., Beigang, R., and Grischkowsky, D. (2010) Highly sensitive terahertz measurement of layer thickness using a two-cylinder waveguide sensor. *Appl. Phys. Lett.*, 97 (7): 071106–071106-3.
54. Feige, V.K.S., Berta, M., Nix, S., Ellrich, F., Jonuscheit, J., and Beigang, R. (2012) Contact-free multilayer thickness determination of industrial coatings using THz measuring techniques. *tm-Tech. Mess.*, 79 (2): 87–94.
55. Abraham, E., Younus, A., Delagnes, J.C., and Mounaix, P. (2010) Non-invasive investigation of art paintings by terahertz imaging. *Appl. Phys. A Mater. Sci. Process.*, 100 (3): 585–590.
56. Yasuda, T., Iwata, T., Araki, T., and Yasui, T. (2007) Improvement of minimum paint film thickness for THz paint meters by multiple-regression analysis. *Appl. Optic.*, 46 (30): 7518–7526.
57. Anastasi, R.F. and Madaras, E.I. (2006) Terahertz NDE for under paint corrosion detection and evaluation. *AIP Conference Proceedings*, 820 (1): 515–522.
58. Stoik, C., Bohn, M., and Blackshire, J. (2010) Nondestructive evaluation of aircraft composites using reflective terahertz time domain spectroscopy. *NDT & E International*, 43 (2): 106–115.
59. Amenabar, I., Lopez, F., and Mendikute, A. (2013) In introductory review to THz non-destructive testing of composite mater. *Journal of Infrared, Millimeter and Terahertz Waves*, 34 (2): 152–169.
60. Chady, T., Lopato, P., and Szymanik, B. (2012) Terahertz and thermal testing of glass-fiber reinforced composites with impact damages. *J Sensor.*, 14: Article 954867.
61. Miedzinska, D., Niezgoda, T., Palka, N., Panowicz, R., Szustakowski, M., Oblocki, H., and Zyczkowski, M. (2011) Non-destructive terahertz investigations of polyethylene composite materials. *36th International Conference on Infrared, Millimeter and Terahertz Waves (IRMMW-THz)*. Houston, TX, October 2–7.
62. Ellrich, F., Weinland, T., Molter, D., Jonuscheit, J., and Beigang, R. (2011) Compact fiber-coupled terahertz spectroscopy system pumped at 800 nm wavelength. *Rev. Sci. Instrum.*, 82 (5): 053102-1–053102-7.
63. Wietzke, S., Jansen, C., Krumbholz, N., Peters, O., Vieweg, N., Jordens, C., Scheller, M., Romeike, D., Jung, T., Reuter, M., Chatterjee, S., Koch, M., Baudrit, B., Zentgraf, T., Hochrein, T., and Bastian, M. (2010) Terahertz spectroscopy: a powerful tool for the characterization of plastic materials. *Proceedings of 10th IEEE International Conference on Solid Dielectrics (ICSD)*, Potsdam, Germany, July 4–9.
64. Ospald, F., Zouaghi, W., Beigang, R., Matheis, C., Jonuscheit, J., Recur, B., Guillet, J.P., Mounaix, P., Vleugels, W., Bosom, P.V., González, L.V., López, I., Edo, R.M., Sternberg, Y., and Vandewal, M. (2013) Aeronautics composite material inspection with a terahertz time-domain spectroscopy system. *OPTICE*, 53 (3): 031208-1–031208-14.


Downloaded by [Jozef Stefan Institute] at 06:13 12 November 2014

65. Parrott, E.P.J., Zeitler, J.A., Gladden, L.F., Taraskin, S.N., and Elliott, S.R. (2009) Extracting accurate optical parameters from glasses using terahertz time-domain spectroscopy. *Journal of Non-Crystalline Solids*, 355 (37–42): 1824–1827.
66. Jördens, C., Scheller, M., Wietzke, S., Romeike, D., Jansen, C., Zentgraf, T., Wiesauer, K., Reisecker, V., and Koch, M. (2010) Terahertz spectroscopy to study the orientation of glass fibres in reinforced plastics. *Compos. Sci. Technol.*, 70 (3): 472–477.
67. Naftaly, M. and Miles, R.E. (2007) Terahertz time-domain spectroscopy of silicate glasses and the relationship to material properties. *J. Appl. Phys.*, 102 (4): 043517-1–043517-6.
68. Jansen, C., Piesiewicz, R., Mittleman, D., Kurner, T., and Koch, M. (2008) The impact of reflections from stratified building materials on the wave propagation in future indoor terahertz communication systems. *IEEE Trans. Antenn. Propag.*, 56 (5): 1413–1419.
69. Schwerdtfeger, M., Castro-Camus, E., Krügener, K., Viöl, W., and Koch, M. (2013) Beating the wavelength limit: three-dimensional imaging of buried subwavelength fractures in sculpture and construction materials by terahertz time-domain reflection spectroscopy. *Appl. Optic.*, 52 (3): 375–380.
70. Dash, J., Ray, S., Nallappan, K., Sasmal, S., and Pesala, B. (2013) Non-destructive inspection of internal defects in concrete using continuous wave 2D terahertz imaging system. *Proceedings of Infrared, Millimeter, and Terahertz Waves (IRMMW-THz)*, Mainz, Germany, September 1–6.
71. Maruyama, I., Kishi, N., and Kawase, K. (2010) Measurement of water content in hardened cement paste using terahertz radiation. *J Struct Constr Eng.*, 75 (652): 1073–1079.
72. Dash, J., Ray, S., Nallappan, K., Sasmal, S., and Pesala, B. (2014) Terahertz spectroscopy of concrete for evaluating the critical hydration level. *Proceedings of Terahertz, RF, Millimeter, and Submillimeter-Wave Technology and Applications VII*, San Francisco, CA, March 7.
73. Jotzu, G., Cooper, M., Parkinson, P., and Johnston, M.B. (2007–2009) Virtual terahertz spectrometer. Available at: https://www-thz.physics.ox.ac.uk/spectrometer/ (accessed April 2014)
74. Zomega Terahertz Corporation. (2012) The Terahertz Wave eBook. Available at: http://dl.z-thz.com/eBook/zomega_ebook_pdf_1206_sr.pdf (accessed April 2014).
75. Nguyen, A. (2010) Investigation of THz for possible use in medical ultrasound technique. *Proceedings of SPIE7650, Health Monitoring of Structural and Biological Systems*, San Diego, CA, April 9.
76. Redo-Sanchez, A., Laman, N., Schulkin, B., and Tongue, T. (2013) Compact, portable Terahertz systems for on-site inspection applications. *38th International Conference on Infrared, Millimeter, and Terahertz Waves (IRMMW-THz)*, Mainz, Germany, September 1–6.
77. Lake Shore Cryotronics. (2014) *8500 Series THz System for Materials Characterization.* Available at: http://www.lakeshore.com/Documents/8500_Series_THz_System.pdf (accessed May 6 2014).
78. Wilk, R., Hochrein, T., Koch, M., Mei, M., and Holzwarth, R. (2011) Terahertz spectrometer operation by laser repetition frequency tuning. *J. Opt. Soc. Am. B*, 28 (4): 592–595.
79. Kim, Y., Yee, D.S., Yi, M., and Ahn, J. (2010) High-speed high-resolution terahertz spectrometers. *J. Kor. Phys. Soc.*, 56 (1): 255–261.
80. Liu, J., Mbonye, M.K., Mendis, R., and Mittleman, D.M. (2010) Measurement of terahertz pulses using electronically controlled optical sampling (ECOPS). *Proceedings of Conference on Lasers and Electro-Optics 2010*, San Jose, CA, May 16–21.
81. Manceau, J.M., Nevin, A., Fotakis, C., and Tzortzakis, S. (2008) Terahertz time domain spectroscopy for the analysis of cultural heritage related materials. *Appl. Phys. B Laser. Optic.*, 90 (3–4): 365–368.
82. El Haddad, J., Bousquet, B., Canioni, L., and Mounaix, P. (2013) Review in terahertz spectral analysis. *TrAC-Trends Anal. Chem.*, 44: 98–105.
83. Notake, T., Endo, R., Fukunaga, K., Hosako, I., Otani, C., and Minamide, H. (2014) State-of-the-art database of terahertz spectroscopy based on modern web technology. *IEEE Trans. Terahertz Sci. Technol.*, 4 (1): 110–115.

Downloaded by [Jozef Stefan Institute] at 06:13 12 November 2014

84. Mathew, R.G., Middendorf, J.R., and Brown, E.R. (2011) Database of all THz signatures measured on solids and liquids in the range 100 GHz to 10 THz. *36th International Conference on Infrared, Millimeter and Terahertz Waves (IRMMW-THz)*, Houston, TX, October 2–7.
85. Pacheco-Torgal, F. (2014) Eco-efficient construction and building materials research under the EU Framework Programme Horizon 2020. *Constr. Build. Mater.*, 51: 151–162.
86. Pacheco-Torgal, F. and Jalali, S. (2011) Nanotechnology: advantages and drawbacks in the field of construction and building materials. *Constr. Build. Mater.*, 25 (2): 582–590.
87. Jelle, B.P. (2011) Traditional, state-of-the-art and future thermal building insulation materials and solutions—properties, requirements and possibilities. *Energy Build.*, 43 (10): 2549–2563.
88. Baetens, R., Jelle, B.P., and Gustavsen, A. (2011) Aerogel insulation for building applications: a state-of-the-art review. *Energy Build.*, 43 (4): 761–769.
89. Zhang, J. and Grischkowsky, D. (2004) Terahertz time-domain spectroscopy study of silica aerogels and adsorbed molecular vapors. *J. Phys. Chem. B*, 108 (48): 18590–18600.
90. Ling, T.C. and Poon, C.S. (2013) Use of phase change materials for thermal energy storage in concrete: an overview. *Constr. Build. Mater.*, 46: 55–62.
91. Pacheco-Torgal, F. and Labrincha, J.A. (2013) The future of construction materials research and the seventh UN Millennium Development Goal: a few insights. *Constr. Build. Mater.*, 40: 729–737.
92. Sanchez, F. and Sobolev, K. (2010) Nanotechnology in concrete—a review. *Constr. Build. Mater.*, 24 (11): 2060–2071.

Downloaded by [Jozef Stefan Institute] at 06:13 12 November 2014

## 4.2 Scientific article 2: Structural analysis of insulating polymer foams with terahertz spectroscopy and imaging

***Authors:*** Andreja Abina, Uroš Puc, Anton Jeglič, and Aleksander Zidanšek
***Publication:*** Polymer testing
***DOI:*** 10.1080/05704928.2014.965825
Y***ear:*** 2013 ***Volume:*** 32
***Issue:*** 4 ***Pages:*** 739-747
***Impact factor 2013:*** 1.816 ***Received date:*** 29 December 2012
***Accepted date:*** 5 March 2013 ***Published online:*** 14 March 2013
***Ranking:***

| Category name | Journal rank in category | Quartile in category |
|---|---|---|
| materials science, characterization & testing | 2/33 | 1 |
| polymer science | 35/82 | 2 |


In this chapter, the paper entitled: "Structural analysis of insulating polymer foams with terahertz spectroscopy and imaging" by Andreja Abina, Uroš Puc, Anton Jeglič, and Aleksander Zidanšek is presented. The paper was published in Polymer Testing, 2013.

This paper presented the use of THz spectroscopy and imaging for structural analysis of insulating polymer foams. We demonstrated that several polymer foams feature low absorption in the THz region which makes THz-TDS and TPI viable methods for characterizing their macrostructure with a submillimetre-scale resolution.

Many physical and mechanical properties of polymer foams are a direct consequence of their micro- and macrostructure. The macroscopic properties of beads and voids are highly dependent on the local microstructure which is characterized by the cell distribution, cell size and shape as well as the wall thickness. Among all parameters, the analysis of voids, inclusions, superstructures, defects and material thickness is very important for thermal insulation properties. Today, 2D and 3D investigation of the internal macro- and microstructure of polymer foams are usually analysed with optical microscopy or SEM. The alternative to microscopy is X-ray computed microtomography or neutron tomography. For chemical characterisation and identification, the routinely used techniques are FTIR and Raman spectroscopy. One solution suitable for both chemical and structural characterisation of polymer foams is THz spectroscopy.

Since the wavelength of THz radiation is comparable to cell size and additives in polymer foams [58], scattering can distort the propagation of the THz pulses through the material and a unique spectral response can be observed. Hence, we demonstrated that by measuring the difference between THz waveforms and by calculating the spectroscopic constants one can determine certain material characteristics such as cell density or IR radiation absorption. Moreover, the TPI method was applied to analyse and visualize the beads structure of polymer foams considering bead size, shape, air gaps and interconnections. The macrostructure characterized by the bead properties was additionally comparatively analysed taking into consideration the local microstructure examined by using SEM and confocal microscopy in combination with the statistical analysis of the data. In addition, we introduced a special algorithm to extract beads in two dimensions for understanding the bead size and its distribution within the foam. TPI was also used to image impurities and prebuilt inclusions within the polymer foams.

*Covering the objectives of this thesis:* This chapter addresses hypothesis 1, 2 and 4.

Polymer Testing 32 (2013) 739–747

Contents lists available at SciVerse ScienceDirect

Polymer Testing

journal homepage: www.elsevier.com/locate/polytest

Test method

# Structural analysis of insulating polymer foams with terahertz spectroscopy and imaging

Andreja Abina [a,*], Uroš Puc [a,b], Anton Jeglič [a,b], Aleksander Zidanšek [a,c,d]

[a] Jozef Stefan International Postgraduate School, Jamova 39, SI-1000 Ljubljana, Slovenia
[b] Faculty of Electrical Engineering, University of Ljubljana, Tržaška cesta 25, SI-1000 Ljubljana, Slovenia
[c] Department of Condensed Matter Physics, Jozef Stefan Institute, Jamova 39, SI-1000 Ljubljana, Slovenia
[d] Faculty of Natural Sciences and Mathematics, University of Maribor, Koroška cesta 160, SI-2000 Maribor, Slovenia

ARTICLE INFO

*Article history:*
Received 29 December 2012
Accepted 5 March 2013

*Keywords:*
Insulation material
Macrostructure
Polymer foam
Terahertz pulsed imaging
Terahertz time-domain spectroscopy

ABSTRACT

Structural analysis of polymer foams for insulation enables manufacturers and research facilities to optimise their products and production processes for applications such as building construction. Therefore, two- and three-dimensional investigation of the macro- and microstructure of these materials is important in order to characterize their physical and mechanical properties. In this paper, we present terahertz time-domain spectroscopy and pulsed imaging method to analyse the macroscopic structure of foamed polymers including analysis of voids, inclusions and bead distribution. By measuring the difference between the terahertz waveforms and by calculating the spectroscopic constants we analyse certain material characteristics such as foam density and infrared radiation absorption. Furthermore, we demonstrate that terahertz techniques have several advantages over other technologies, in particular as a non-ionizing alternative to X-ray tomography, and a complementary imaging method to optical or electron microscopy enabling chemical and structural characterization of foamed polymers.

© 2013 Elsevier Ltd. All rights reserved.

## 1. Introduction

Industrial production of foamed polymers is increasing globally due to their light weight, high thermal and acoustic insulation properties and high energy absorption capacity. These properties are crucial in applications such as building construction. In recent decades, only a few polymer foams for insulation based on new monomer building blocks have been successfully introduced to the market, mainly because of the relatively high cost of production. However, many modifications of the traditional polymer foams become possible due to new advances in material and technology development. For instance, nanotechnology allows the construction of nanocellular foams in which only one or no gas molecule can occupy individual pores, and thus enhance the thermal insulation properties by preventing the thermal conductivity of gas molecules [1]. Furthermore, the pore size can be reduced to below 100 nm using materials such as aerogel and xerogel [2]. The foam properties such as thermal insulation, structural reinforcement, flame retardant or thickness reduction can be improved with various inclusions including infrared attenuators [2,3], different fibres [4] and composites [5,6]. On the other hand, the environmental issues force industry to return to natural materials. Hence, sustainable and biodegradable polymers, e.g. starch foam [7], are becoming more attractive. In spite of the fact that high-tech polymer foams offer further potential for improvements, they have to compete with traditional materials and achieve lower production cost.

In general, polymer foams are produced by dispersing a gas within a liquid polymer matrix, which creates a characteristic structure of cells, walls and pores when the liquid matrix solidifies [8]. Many physical and mechanical

* Corresponding author. Tel.: +386 1 477 36 02; fax: +386 1 477 31 10.
*E-mail addresses:* andreja.abina@mps.si (A. Abina), aleksander.zidansek@ijs.si (A. Zidanšek).

0142-9418/$ – see front matter © 2013 Elsevier Ltd. All rights reserved.
http://dx.doi.org/10.1016/j.polymertesting.2013.03.004

**Table 1**
Properties of polymer foam insulation material samples including mechanical and thermal conductance data summarized from the manufacturer specifications.

| Material | Manufacturer | Brand name | Density ($kg/m^3$) | Thermal conductance (W/mK) | Slab thickness (mm) | Slice average thickness (mm) |
|---|---|---|---|---|---|---|
| Expanded polystyrene (EPS) | Weber | weber.therm family EPS-F | 16 | 0.040 | 29 | 3.80 |
| EPS with graphite | Weber | weber.therm clima 032 | 16 | 0.032 | 29 | 3.10 |
| EPS with graphite | Fragmat Tim | Fragmat Neo Super 100 (Neopor®) | 20 | 0.0312 | 40 | 2.97 |
| Extruded polystyrene (XPS) | Weber | weber.therm XPS | 30 | 0.034 | 29 | 3.46 |
| Expanded Bakelite | Weber | weber.therm plus ultra 022 | 40 | 0.024 | 30 | 2.45 |

properties of polymer foams are thus a direct consequence of their micro- and macrostructure. The macroscopic properties of beads and voids are highly dependent on the local microstructure which is characterized by the cell distribution, cell size and shape as well as the wall thickness. All mentioned parameters are the result of many processing conditions including temperature, pressure, humidity, impurities, chemical composition and cure time [9]. Nowadays, the control of industrial processes is restricted mainly to monitoring the pressure and temperature, while the effect of other factors is still relatively unknown. Among all parameters, the analysis of voids, inclusions, superstructures, defects and material thickness is very important for thermal insulation properties. The laboratory measurements of these values are important both to the manufacturers and the end-users. The available bibliographic data considering these parameters for polymer foams are often incomplete and out of date.

Today, two- (2D) and three-dimensional (3D) investigation of the internal macro- and microstructure of polymer foams is an important method of characterizing its properties and gaining some insight into the formation process [10,11]. The 2D structure of polymer foams (e.g. cell size distribution) is usually analysed with optical or scanning electron microscopy (SEM) [10]. The drawback of this approach is that only the sample surface can be analysed, unless the sample is cut to reveal the internal structures. The alternative to microscopy is X-ray computed microtomography [10,12] which allows 3D imaging but it can be time-consuming and costly. Another 3D imaging method which enables description of the complex internal structure of materials is neutron tomography [13] which is usually provided by a large instrument, not allowing in-situ measurements. Also, both X-rays and neutrons are ionizing radiation. For chemical characterisation and identification of polymer materials, the routinely used techniques are Fourier transform infrared [14] and Raman [15] spectroscopic methods. Hence, it follows that the polymer foam industry is not well supported with non-destructive and contactless analytical techniques. One solution suitable for this purpose could be terahertz (THz) technology which has a significant potential for both chemical and structural characterisation of polymers [16]. Since many polymers feature very low absorption in the THz region [17,18] and the wavelength of THz waves is in the order of submillimetre [19], the THz spectroscopy and imaging methods

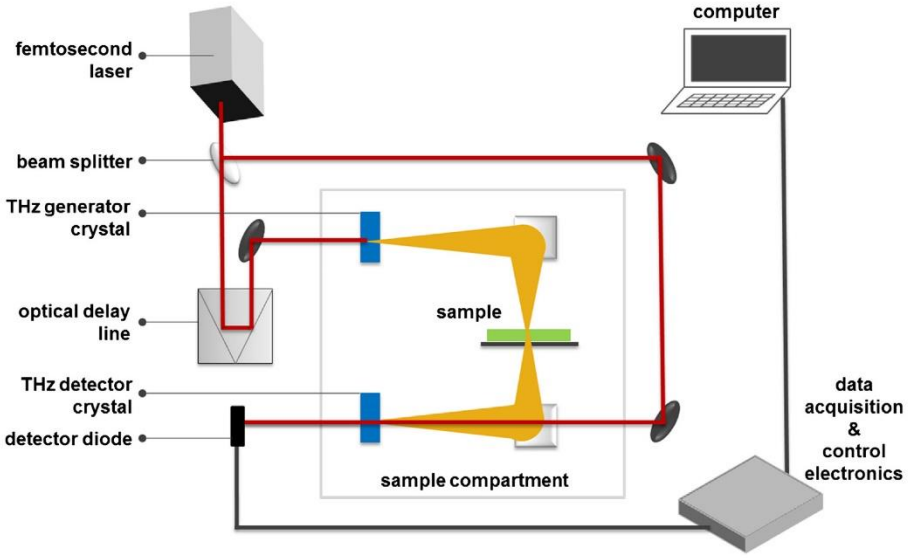


**Fig. 1.** A schematic drawing of the THz spectroscopy and imaging system in transmission geometry.

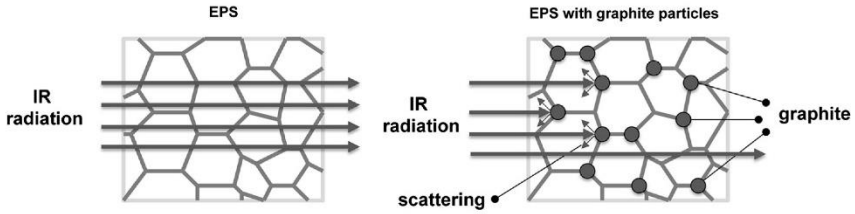


**Fig. 2.** IR radiation through EPS and EPS containing graphite particles as IR attenuators.

have been recently used for detecting and analysing material thicknesses [20], dielectric material properties [21], superstructures [22], voids [13,23], inclusions [24,25], defects [26,27], material ageing [17], weld joints [28] and process control [29]. THz technology has several advantages over other technologies, it can be non-ionizing alternative to X-ray tomography and a complementary imaging technique to optical or electron microscopy.

In this paper, we demonstrate that THz time-domain spectroscopy (TDS) and THz pulsed imaging (TPI) have the potential to analyse the macroscopic structure of insulation foamed polymers in a submillimetre-scale resolution. We introduce the procedure for extraction the spectroscopic constants of polymer foams from THz data. Moreover, the TPI method is applied to analyse and visualize the beads structure of polymer foams considering bead size, shape, air gaps and interconnections. The macrostructure characterized by the bead properties is additionally comparatively analysed taking in consideration the local microstructure examined by using SEM and confocal microscopy. Also, TPI is used to image impurities (e.g. voids) and prebuilt inclusions (e.g. silica gel granules and thin metal wires) within the polymer foams.

## 2. Experimental setup

### 2.1. Samples used and their preparation

Several commercially available polymer foam insulation samples were selected for TDS and TPI measurements. Table 1 presents an overview of the selected samples, including material type, manufacturer, brand name, sample slab thickness, density and thermal conductance. The mechanical and thermal conductance data of the foam materials are summarized from the manufacturer specifications. The selected samples were cut with a blade into slices with almost identical planar (x-y) dimensions of 50 mm by 30 mm according to the THz sample holder size. The slice thickness in mm for each sample investigated by THz imaging method was measured at ten different positions and its average thickness is also given in Table 1. After THz measurements each slice was divided into two parts: the small part was used for SEM and the rest for confocal microscopy. In addition, the small slices were dried in an oven at 60 °C for 1 h to remove remaining pentane to prevent foam deformation in the high vacuum of SEM. The samples prepared for SEM imaging were sputtered with gold to ensure better morphological investigation.

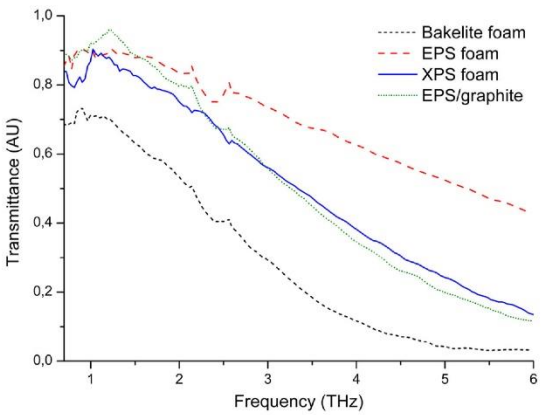


**Fig. 3.** THz-TDS transmission spectra of a variety of insulation polymer foams in the frequency range between 0.7 THz and 6.0 THz.

### 2.2. Terahertz system and methods of data processing

#### 2.2.1. THz spectrometer and imager

The samples were investigated by a TeralMAGE system by Rainbow Photonics AG [30] which enables THz spectroscopic and imaging measurements. A schematic drawing of the THz system for spectroscopy and imaging in transmission geometry is illustrated in Fig. 1. The THz system includes optical, mechanical and electronic components for the generation and the detection of THz waves. The erbium-doped femtosecond (fs) fibre laser (Menlo Systems) is

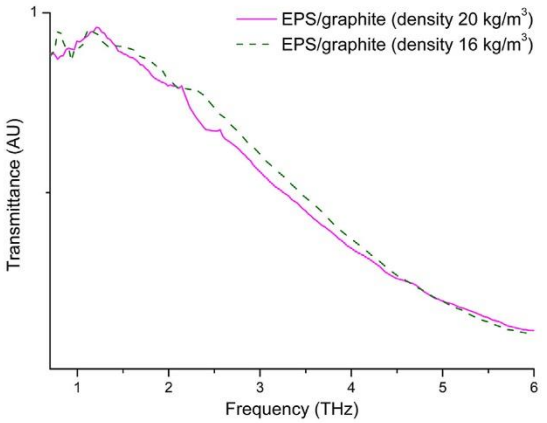


**Fig. 4.** THz-TDS transmission spectra for two EPS foams containing graphite particles with various densities in the frequency range between 0.7 THz and 6.0 THz.

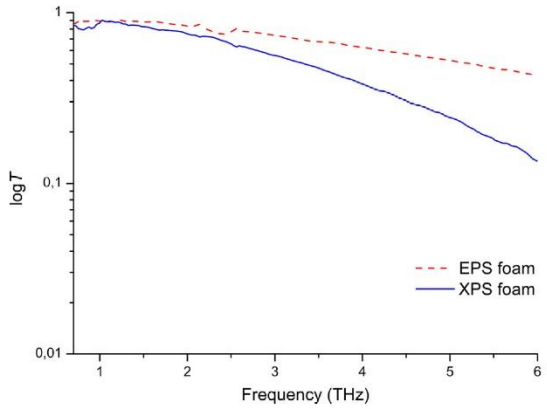


**Fig. 5.** THz transmittance in logarithmic scale for EPS and XPS foams both containing the polystyrene matrix but differ in voids volume.

operating at a centre wavelength of 1560 nm with an average output power greater than 150 mW and a pulse duration less than 90 fs at repetition rate of 100 MHz. First, the initial fs laser beam is split at a beam splitter into two parts: a pump and a probe beam. The pump beam is delayed for a few picoseconds (ps) and focused onto the THz generator, which is in our case an electrooptic DSTMS (4-N,N-dimethylamino-4′-N′-methyl-stilbazolium 2,4,6-trimethylbenzenesulfonate) organic crystal [31]. The THz generator generates THz radiation which is focused through the sample onto the THz DSTMS detector using the parabolic mirrors. By changing the time delay between the probe and the pump beams by means of an optical delay line, the entire time profile of the THz waveform can be traced. The signal is finally detected by a photodiode detector and the data are transferred to the computer for further signal processing. The experiments were conducted within the sample compartment purged with nitrogen gas to avoid water vapour absorption lines. This combination of system setup has a frequency response up to 6 THz.

*2.2.2. Spectroscopic and imaging data analysis methods*

The THz system we used ensures measurements of spectroscopic constants [32]. The method requires two measurements. First, a reference waveform $E_{ref}(t)$ without the sample is measured, followed by the measurement of a sample waveform $E_s(t)$. The Fourier transform of the temporal reference and sample waveforms gives spectral distribution of the THz pulse in the frequency domain, called the reference spectrum and the sample spectrum, respectively:

$$E_{ref}(\omega) = A_{ref}(\omega)\exp^{-i\varphi_{ref}(\omega)} \quad (1)$$

$$E_s(\omega) = A_s(\omega)\exp^{-i\varphi_s(\omega)} \quad (2)$$

where $\omega$ is the frequency of the THz wave, $A$ is the amplitude and $\varphi$ is the phase difference between the waveforms of the sample signal and the reference signal. The Fourier components of the two signals define the transmission function of the sample:

$$T(\omega) = E_s(\omega)/E_{ref}(\omega) \quad (3)$$

Similarly to the transmittance $T(\omega)$, other spectral properties of the sample can be extracted by comparing the sample spectrum with the reference spectrum:

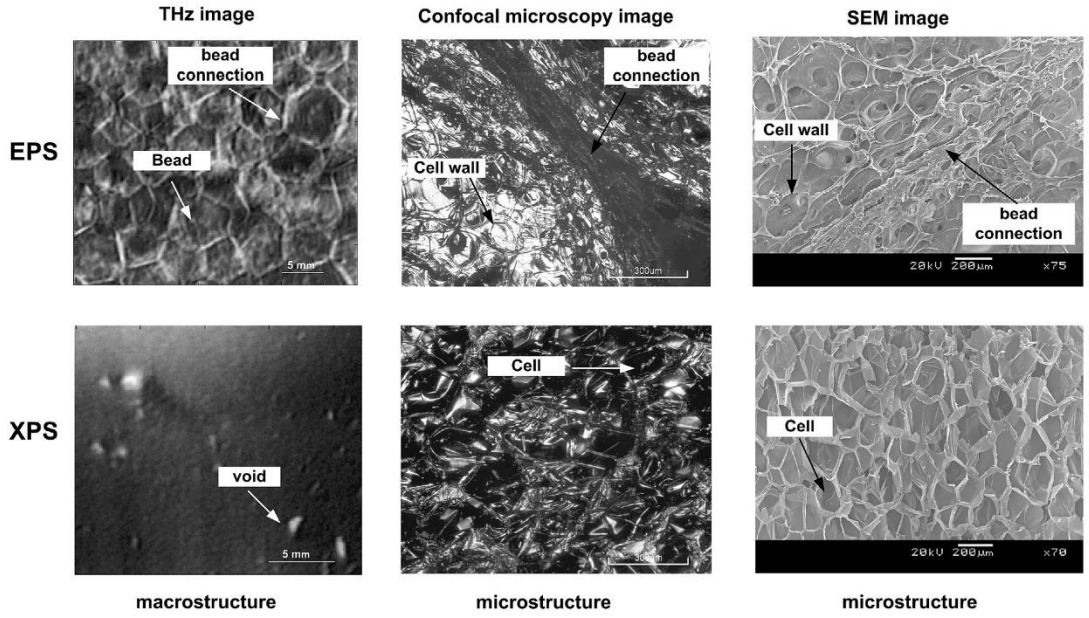


**Fig. 6.** Foam macro- and microstructure characterization by THz imaging, confocal microscopy and SEM imaging, an example for EPS (upper images) and XPS (lower images).

$$\alpha = (1/d)\ln(A_{ref}/A_s) \quad (4)$$

$$n = 1 + [\varphi_s(\omega) - \varphi_{ref}(\omega)]c/d\omega \quad (5)$$

where $\alpha$ is the absorption coefficient, $n$ is the refractive index, $d$ is the thickness of the sample and $c$ is the speed of light in vacuum.

Moreover, the THz system used allows performing TPI in two ways [33], as a monochromatic fast imaging without the need for spectroscopic information, and a broadband or multispectral imaging by using the Fourier transform of the time domain waveform. The monochromatic image is constructed at a fixed temporal delay, in our case at the maximum amplitude of the THz waveform. At each point on the sample, only the amplitude of the THz field is recorded in a matrix while scanning the sample across the THz beam. The next step is the extraction of the amplitude peak value followed by the time-domain THz image reconstruction using the peak intensity at each pixel. In the case of multispectral imaging, the entire frequency spectrum is recorded in every single point of the sample. This makes TPI favourable in comparison to common optical image or X-ray image where each pixel contains just the intensity of the beam. Such TPI measurement gives a 3D data set where two axes describe vertical and horizontal spatial dimensions and the third axis represents the spectral frequency dimension. In the experiment, the sample was placed across the THz beam at its focal spot, following by raster scanning in a plane perpendicular to the THz beam. The scanning area was limited to 50 mm × 30 mm.

## 3. Results and discussion

### 3.1. Spectroscopic constants of insulating polymer foams

The thermal properties of the polymer foams regarding the insulation behaviour are characterized by the thermal conductivity [3]:

$$\lambda = \lambda_s + \lambda_g + \lambda_r + \lambda_c \quad (6)$$

where $\lambda$ is the total thermal conductivity defined by $\lambda_s$, $\lambda_g$, $\lambda_r$, and $\lambda_c$, representing the contributions of the conduction in the solid phase (polymer matrix), conduction in the gas phase (blowing agent), radiation, and convection in the closed cells, respectively. Over the past few years, a series of new approaches have been proposed to improve the thermal insulation properties, such as incorporation of low amount of infrared (IR) attenuators (e.g. carbon black and graphite) and modification of the structure, particularly the cell size. Inorganic additives such as carbon black and graphite serve as attenuators to IR radiation by the means of reducing the thermal conductivity of foam [2]. The IR radiation through expanded polystyrene (EPS) foam is schematically shown in Fig. 2. It is known that the foam with larger cell size and greater cell wall thickness might be more efficient as regards the reduction of thermal conductivity than a foam with a higher number of cells but with a smaller cell wall thickness [3]. The cell size is related to both transmission and scattering of THz waves through the foam. For instance, smaller cell size increases the thermal conductivity and, as a consequence, the material becomes more transparent to IR radiation. On the other hand, IR attenuators reduce thermal conductivity as well as transmission due to scattering and absorption effects [2]. In the next paragraphs, it is explained how these properties can be verified and proved by THz transmission spectroscopy.

Since THz radiation occupies electromagnetic spectrum at the low frequency edge of the far IR light band, it could be used as a tool to investigate the IR absorption through the polymer insulation foams. Herein, THz transmission spectra of different polymer foams were first determined using THz-TDS. In Fig. 3 we present first systematic investigation of THz spectra of polymer foams where one can note that different polymer foams of the same thickness (z − 2 mm) exhibit different transmittance in the region 1.0-6.0 THz. Among the five samples the expanded Bakelite foam showed the lowest transmission in this frequency range whereas the EPS has extremely high transmission. The THz measurements of EPS foam in frequency region between 0.1-4.0 THz done by Zhao et al. [18] showed that

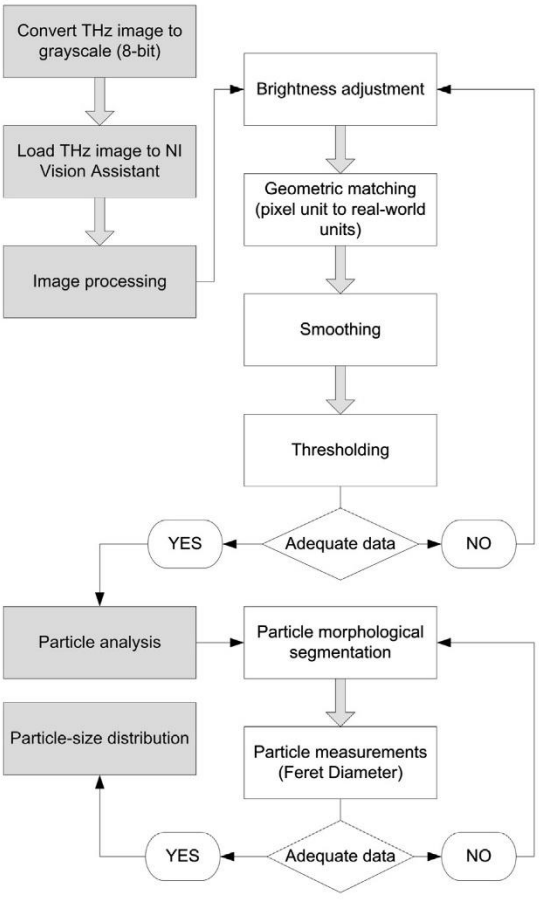


**Fig. 7.** Schematically presentation of the THz imaging based algorithm developed in NI Vision Assistant to visualize the beads or voids distribution within the polymer foam slice.

this material could be used as a filter to block near-IR radiation in THz systems or as a sample substrate for THz imaging. Both commercial samples of EPS foam containing graphite particles have lower transmission in comparison to EPS without additives in almost the whole restricted THz frequency region, except within the area between 1.0-1.6 THz where the transmission for EPS with graphite is higher than 90%. The IR radiation as a main contributor to the heat conductivity would be normally pass through EPS but, in case of graphite, the IR waves are reflected by these small IR absorber particles resulting in reduced transmittance. According to the THz spectra plotted in Fig. 4, one can also differentiate between two samples of graphite added EPS foams with various densities. The sample with density of 20 kg/m$^3$ exhibits lower transmittance in comparison with the sample of reduced density of 16 kg/m$^3$, particularly due to higher volume of polymer matrix or graphite particles within the first sample. The increased density reduces thermal conductivity referred to the manufacturer specifications as well as transmission data due to scattering and absorption effects.

In Fig. 5 it is seen that the increase of the transmission on a logarithmic scale for EPS and extruded polystyrene (XPS) is very slight between 0.7-2 THz. Above the frequency of 2 THz, greater difference is observable for EPS and XPS, both containing the polystyrene matrix but the manufacturing process differs. The XPS foam is manufactured with homogenous closed cells almost void-free, whereas the EPS foam is a two-level structure produced by sintering together the pre-expanded polystyrene beads made of small cells. Therefore, a complex structure of EPS foam contains unit cells of different size and shape, which are expected to form more voids within the foam structure. The air gaps between the cells allow air penetration, and thus reduce the material's resistance to heat flow. Consequently, the thermal conductivity increases and the material become more transparent to IR, which can be clearly seen comparing the THz spectra of EPS and XPS in Figs. 3 and 5.

Differences in transmission spectra of various polymer foams indicate that THz spectroscopy could be a significant tool to improve the understanding of the efficiency and behaviour of thermal insulation materials. Especially, the contributions of gas phase, open or closed cell structure and IR additives to the thermal conductivity can be explained.

### 3.2. Foam structure

Polymer foams have a skeletal structure composed of open or closed cells representing the basic unit of these materials. The cell is not a specific uniform unit. Usually, a wide range of different sized cells are presented in single foam. This complex microstructure determines the macrostructure and the characteristics of cellular foams. For the investigation of foam structure, we used two complementary methods: a pulsed THz imaging which can reveal foam structures like beads and their interconnections and microscopy methods to image cell structure.

The macrostructure of foam was analysed using a monochromatic fast imaging method. The transmission THz image of EPS as shown in Fig. 6 clearly indicates the structure of the foam, considering the beads and their intermediate connections. In the case of XPS, the beads are not present, thus the THz image shows only voids within the foam. The microstructure of polymer foams was analysed with 2D imaging using SEM and confocal microscopy. Based on THz and microscopy images, we determined two categories of features for quantitative description of the foam structure. Local feature characteristics for each individual cell such as cell diameter and distribution of cell size were determined by SEM, whereas the global features such as bead size and distribution were characterized by THz

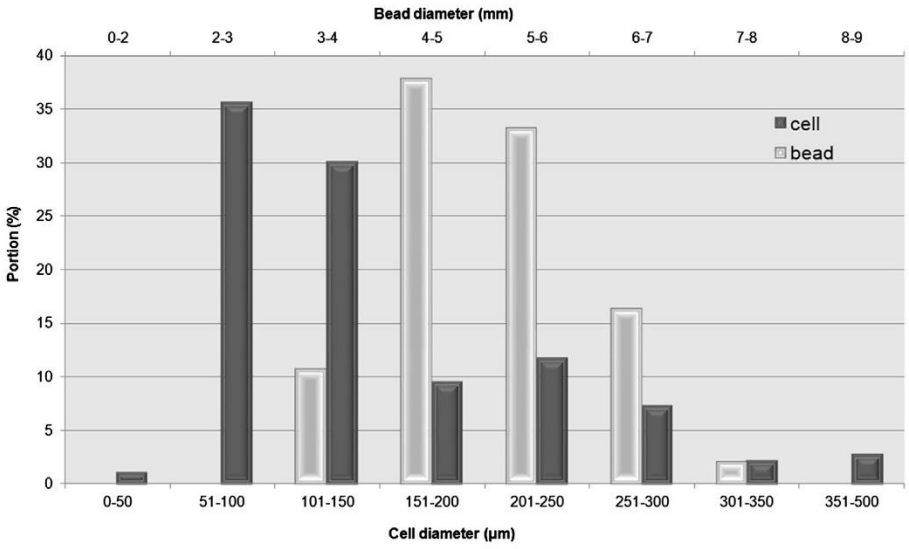


**Fig. 8.** Distribution of beads and cells considering their diameter within the EPS foam slice. Primary horizontal axis presents cell diameter in μm based on SEM imaging whereas secondary horizontal axis presents bead diameter in mm as determined from THz imaging based algorithm.

images. The THz, confocal microscopy and SEM images for EPS and XPS are given in Fig. 6. The macrostructure is visualized by the THz image where one can discriminate between beads in the case of EPS, whereas a microstructure characterized by cell walls and cells is presented with microscopy images. The resolution for THz images was limited down to 100 μm, while confocal microscopy images were recorded using 10× magnification and SEM at a 70× and 75× magnifications for XPS and EPS, respectively.

In addition, the SEM and THz imaging methods in combination with the statistical analysis of the data were used for qualitative evaluation and quantification of cell and bead size distribution through sample slices of the foams. For understanding the bead size and its distribution within the foam, we prepared a special algorithm to extract beads in two dimensions (x-y) using National Instruments (NI) Vision Assistant [34]. The image inspection is performed in steps as schematically shown in flow chart in Fig. 7. The recorded THz image has to be first converted to 8-bit grayscale image. The next step loads the THz image which is additionally processed considering brightness adjustment and geometric matching to convert pixel units to real-world units. This step also includes functions of smoothing pixel intensities of an image, and threshold to emphasis the borders of beads and to fill the holes representing beads. If adequate data are generated, the subsequent particle analysis step removes unwanted particles such as border objects and small objects which are not considered as beads. The last step is related to particle size distribution based on data acquired with the extraction of the maximum Feret diameter of individual beads, i.e. a line connecting the two bead points that are the furthest apart.

For survey of microscopy images, we adopted the same algorithm with some minor changes of image processing and particle analysis. The bead and cell diameter were determined at different smoothing and threshold adjustments. The average values of bead size and cell size were arranged in eight classes with boundary conditions as plotted in Fig. 8. At the macro-scale, the beads with diameter between 4 mm and 6 mm dominate (more than 70%), whereas at the micro-scale the most represented are cells with diameter between 50 μm and 150 μm (more than 65%).

### 3.3. Inclusions and impurity detection

THz inspection has already shown great potential for void and crack detection within the space shuttle insulation foam due to low absorption coefficient and index of refraction in this region [13,23,35]. Voids are pockets of air or gas within the insulating material which distort the shape of the THz pulse if comparing the pulses travelling through non-defective areas and pulses through void areas. Due to the absence of absorbing polymer matrix, an increased total energy at the centre of the defect occurs. Thus, the defects such as voids can be identified and characterized. In the raw grayscale THz image in Fig. 9, voids appear as light shapes, corresponding to the scattering and interference at the edge of the feature and enhanced transmission due to the lack of polymer matrix in the interior. Moreover, the processing of THz images allows determining the dispersion of inhomogeneities such as voids within the polymer foam. Using the similar algorithm developed in NI Vision Assistant and the statistical analysis, the value of voids area per total scanning area can be determined. The results obtained for EPS slice are plotted in Fig. 9 indicating that the investigated foam sample contains

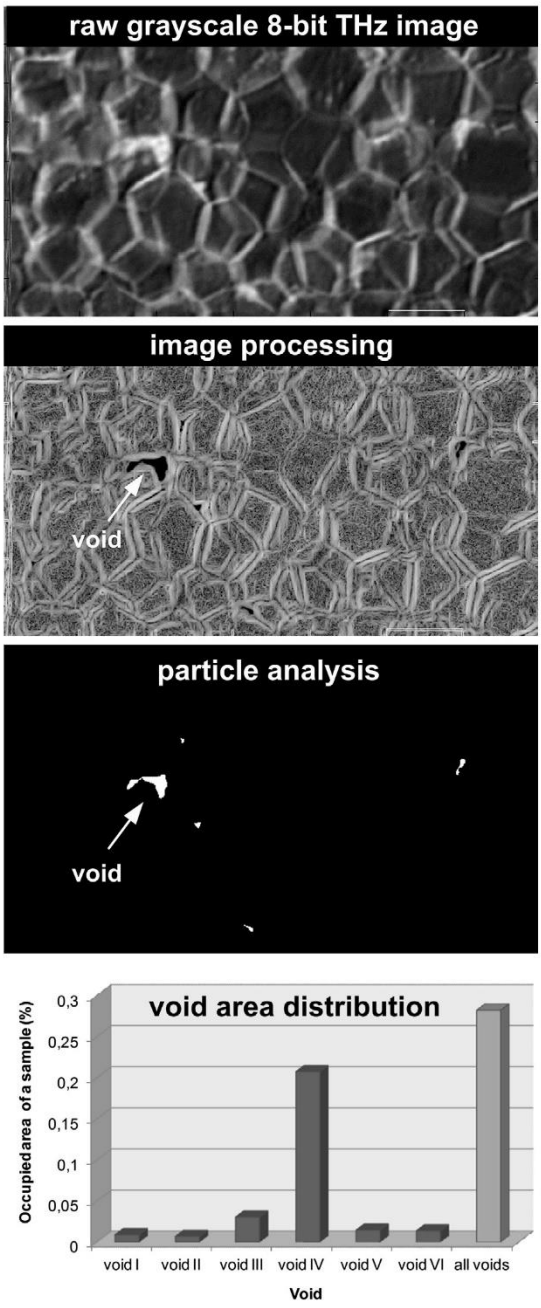


**Fig. 9.** Signal processing and particle analysis of THz image determining the voids dispersion within EPS polymer foam and void area distribution.

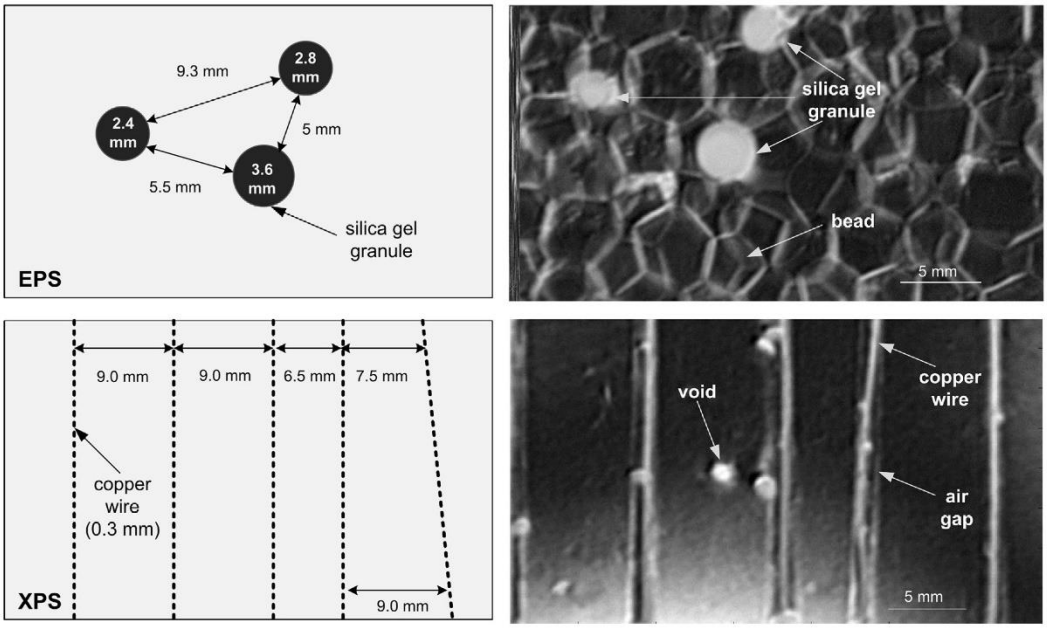


**Fig. 10.** Schematic design of XPS and EPS foam with pre-built inclusions (left) and corresponding THz images of silica gel granules and cooper wires within the polymer foams (right).

less than 0.3% of void area per total scanning area. Determination of this property is crucial for manufacturers since higher volume of voids is not desirable and results in higher transmission as well as conductance.

In addition, THz imaging was used to identify the distribution of pre-built inclusions within the polymer insulation foams, such as incorporated silica gel granules with a diameter from 2.4 mm to 3.6 mm and thin copper wires with a diameter of 0.3 mm. We showed that THz transmission imaging can be used to detect and locate internal inclusions in opaque polymeric insulation materials (Fig. 10). In the case of XPS foam, we can also discriminate between thin copper wires and surrounding air gap. Such results indicate that the TPI is a suitable method for the analysis of inner polymer foam superstructures, especially the degree of orientation and the direction of different fillers (granules, fibers, and agglomerates) embedded in a polymer matrix. Since these properties affect the behavior of insulation materials, information from TPI could contribute to the process of improvement of the thermal insulation properties.

## 4. Conclusions

We demonstrate that several polymer foams feature low absorption in the THz region which makes THz-TDS and TPI viable methods for characterizing macrostructure of various polymer foams with a submillimetre-scale resolution. In addition, THz waves have the ability to image voids, inclusions and bead distribution in these materials. Since the wavelength of THz radiation is comparable to cell size and additives in polymer foams, scattering can distort the propagation of the THz pulses through the material. Hence, we have shown that by measuring the difference between THz waveforms and by calculating the spectroscopic constants one can determine certain material characteristics such as cell density or IR radiation absorption. THz technology is, therefore, a promising method that could also contribute to the production process in order to optimise the structure of porous foams for a given application. It has potential to become an important supplementary or alternative method to SEM and X-ray microtomography for the chemical and structural characterization, as well giving insight into the formation process of these materials. In this way, the THz based structural analysis of foams could enable polymer processing companies and research facilities to optimise their products and production processes in order to improve thermal insulation materials, which would contribute to global efforts for energy conservation.

## Acknowledgements

We thank Prof. Dr. G. Valusis, Dr. I. Kasalynas and their team from the University of Vilnius for assistance in measurements of the THz spectra of insulation polymer foams. The authors would like to acknowledge financial support from the Slovenian Research Agency grants P2-0348-2338 and J2-4266. We would also like to thank the team from Rainbow Photonics AG, Zurich, Switzerland who helped set up the THz system. The authors also acknowledge S. Paskvale (Department of Thin Films and Surfaces of Jozef Stefan Institute) and M. Stefanič (Engineering Ceramics Department of Jozef Stefan Institute) for their support concerning the measurements at confocal microscopy and SEM,

respectively. Special acknowledgement is given to the Saint-Gobain gradbeni izdelki d.o.o., and Fragmat Tim d.d., who provided samples of commercially available insulation materials.

## References

[1] Z. Zhu, C.B. Park, J.H. Zong, Challenges to the formation of nano-cells in foaming processes, International Polymer Processing 23 (2008) 270–276.
[2] C.V. Vo, F. Bunge, J. Duffy, L. Hood, Advances in thermal insulation of extruded polystyrene foams, Cellular Polymers 30 (2011) 137–155.
[3] J. Schellenberg, M. Wallis, Dependence of thermal properties of expandable polystyrene particle foam on cell size and density, Journal of Cellular Plastics 46 (2010) 209–222.
[4] J. Kastner, D. Salaberger, B. Plank, High resolution X-ray computed tomography of fibre and particle filled polymers, in: 12th World Conference on Non-Destructive Testing, WCNDT 2012, Durban, South Africa, 2012.
[5] C. Jordens, S. Wietzke, M. Scheller, M. Koch, Investigation of the water absorption in polyamide and wood plastic composite by terahertz time-domain spectroscopy, Polymer Testing 29 (2010) 209–215.
[6] N. Nagai, T. Imai, R. Fukasawa, K. Kato, K. Yamauchi, Analysis of the intermolecular interaction of nanocomposites by THz spectroscopy, Applied Physics Letters 85 (2004) 4010–4012.
[7] J.L. Willett, R.L. Shogren, Processing and properties of extruded starch/polymer foams, Polymer 43 (2002) 5935–5947.
[8] H.P. Azikri de Deus, M.K. Alves, An application for polymeric foams, in: 2th International Symposium on Solid Mechanics, Brazilian Society of Mechanical Sciences and Engineering, Rio de Janeiro, 2009.
[9] C. Torres-Sanchez, J.R. Corney, Effects of ultrasound on polymeric foam porosity, Ultrasonics Sonochemistry 15 (2008) 408–415.
[10] A. Elmoutaouakkil, G. Fuchs, P. Bergounhon, R. Peres, F. Peyrin, Three-dimensional quantitative analysis of polymer foams from synchrotron radiation x-ray microtomography, Journal of Physics D – Applied Physics 36 (2003) A37–A43.
[11] M. Saadatfar, C.H. Arns, M.A. Knackstedt, T. Senden, Mechanical and transport properties of polymeric foams derived from 3D images, Colloids and Surfaces A: Physicochemical and Engineering Aspects 263 (2005) 284–289.
[12] J.G.F. Wismans, J.A.W. van Dommelen, L.E. Govaert, H.E.H. Meijer, X-ray computed tomography based modelling of polymeric foams, Materials Science Forum 638-642 (2010) 2761–2765.
[13] W.P. Winfree, E.I. Madaras, Detection and characterization of flaws in sprayed on foam insulation with pulsed terahertz frequency electromagnetic waves, in: Proceedings of the 41st AIAA/ASME/SAE/ASEE Joint Propulsion Conference & Exhibit, American Institute of Aeronautics and Astronautics, Inc., Reston, VA, 2005.
[14] M. Naftaly, R.E. Miles, Terahertz time-domain spectroscopy for material characterization, Proceedings of the IEEE 95 (2007) 1658–1665.
[15] N. Nagai, R. Fukasawa, Abnormal dispersion of polymer films in the THz frequency region, Chemical Physics Letters 388 (2004) 479–482.
[16] S. Wietzke, F. Rutz, C. Jördens, N. Krumbholz, N. Vieweg, C. Jansen, R. Wilk, M. Koch, Applications of terahertz spectroscopy in the plastics industry, Terahertz Photonics, Proceedings of SPIE 6840 (2007) V1–V9.
[17] G. Pastorelli, T. Trafela, P. Taday, A. Portieri, D. Lowe, K. Fukunaga, M. Strli&ccaron, Characterisation of historic plastics using terahertz time-domain spectroscopy and pulsed imaging, Analytical and Bioanalytical Chemistry 403 (2012) 1405–1414.
[18] G.Z. Zhao, M. ter Mors, T. Wenckebach, P.C.M. Planken, Terahertz dielectric properties of polystyrene foam, Journal of the Optical Society of America B – Optical Physics 19 (2002) 1476–1479.
[19] Y. Oyama, L. Zhen, T. Tanabe, M. Kagaya, Sub-terahertz imaging of defects in building blocks, NDT & E International 42 (2009) 28–33.
[20] C. Jansen, S. Wietzke, H.Y. Wang, M. Koch, G.Z. Zhao, Terahertz spectroscopy on adhesive bonds, Polymer Testing 30 (2011) 150–154.
[21] E.K. Rahani, T. Kundu, Z.R. Wu, H. Xin, Heat induced damage detection by terahertz (THz) radiation, Journal of Infrared Millimeter and Terahertz Waves 32 (2011) 848–856.
[22] A. Brahm, D. Schmidt, S. Riehemann, G. Notni, F.J. Wostmann, A. Tunnermann, Non-destructive determination of the density distribution of polymer foam models with THz-pulses, in: Infrared Millimeter and Terahertz Waves (IRMMW-THz), 2010 35th International Conference on, 2010, pp. 1–2.
[23] N. Karpowicz, H. Zhong, J.Z. Xu, K.I. Lin, J.S. Hwang, X.C. Zhang, Comparison between pulsed terahertz time-domain imaging and continuous wave terahertz imaging, Semiconductor Science and Technology 20 (2005) S293–S299.
[24] F. Rutz, M. Koch, S. Khare, M. Moneke, H. Richter, U. Ewert, Terahertz quality control of polymeric products, International Journal of Infrared and Millimeter Waves 27 (2006) 547–556.
[25] K.H. Jin, Y.-G. Kim, S.H. Cho, J.C. Ye, D.-S. Yee, High-speed terahertz reflection three-dimensional imaging for nondestructive evaluation, Optics Express 20 (2012) 25432–25440.
[26] E.K. Rahani, T. Kundu, Z.R. Wu, H. Xin, Mechanical damage detection in polymer tiles by THz radiation, IEEE Sensors Journal 11 (2011) 1720–1725.
[27] H. Zhong, J.Z. Xu, X. Xie, T. Yuan, R. Reightler, E. Madaras, X.C. Zhang, Nondestructive defect identification with terahertz time-of-flight tomography, IEEE Sensors Journal 5 (2005) 203–208.
[28] S. Wietzke, C. Jordens, N. Krumbholz, B. Baudrit, M. Bastian, M. Koch, Terahertz imaging: a new non-destructive technique for the quality control of plastic weld joints, Journal of the European Optical Society – Rapid Publications 2 (2007).
[29] N. Krumbholz, T. Hochrein, N. Vieweg, T. Hasek, K. Kretschmer, M. Bastian, M. Mikulics, M. Koch, Monitoring polymeric compounding processes inline with THz time-domain spectroscopy, Polymer Testing 28 (2009) 30–35.
[30] TeraIMAGE, The Flexible Solution for THz Spectroscopy and Imaging, Rainbow Photonics AG, November 20, 2012. http://www.rainbowphotonics.com/pdf/teraimage.pdf.
[31] L. Mutter, F.D.J. Brunner, Z. Yang, M. Jazbinsek, P. Gunter, Linear and nonlinear optical properties of the organic crystal DSTMS, Journal of the Optical Society of America B – Optical Physics 24 (2007) 2556–2561.
[32] E. Nguema, V. Vigneras, J.L. Miane, P. Mounaix, Dielectric properties of conducting polyaniline films by THz time-domain spectroscopy, European Polymer Journal 44 (2008) 124–129.
[33] Y.C. Shen, P.F. Taday, D.A. Newnham, M. Pepper, Chemical mapping using reflection terahertz pulsed imaging, Semiconductor Science and Technology 20 (2005) S254–S257.
[34] NI Vision Assistant, National Instruments, 2010.
[35] D.J. Roth, S. Reyes-Rodriguez, D.A. Zimdars, R.W. Rauser, W.W. Ussery, Terahertz computed tomography of NASA thermal protection system foam materials, Materials Evaluation 69 (2011) 1090–1098.

## 4.3 Scientific article 3: Qualitative and quantitative analysis of calcium-based microfillers using terahertz spectroscopy and imaging

***Authors:*** Andreja Abina, Uroš Puc, Anton Jeglič, Jana Prah, Rimvydas Venckevičius, Irmantas Kašalynas, Gintaras Valušis, and Aleksander Zidanšek
***Publication:*** Talanta
***DOI:*** 10.1016/j.talanta.2015.05.027
***Year:*** ***Volume:***
***Issue:*** ***Pages:***
***Impact factor 2013:*** 3.511 ***Received date:*** 27 February 2015
***Accepted date:*** 12 May 2015 ***Published online:***
***Ranking:***

| Category name | Journal rank in category | Quartile in category |
|---|---|---|
| chemistry, analytical | 12/76 | 1 |

In this chapter, the paper entitled: "Qualitative and quantitative analysis of calcium-based microfillers using terahertz spectroscopy and imaging" by Andreja Abina, Uroš Puc, Anton Jeglič, Jana Prah, Rimvydas Venckevičius, Irmantas Kašalynas, Gintaras Valušis, and Aleksander Zidanšek is presented. The paper is accepted for publication in Talanta.

The paper presented the use of THz spectroscopy and imaging for qualitative and quantitative analysis of calcium-based microfillers. Since the spectroscopic techniques are preferred over microscopy and thermogravimetry, particularly due to its non-destructive nature and short analysis time, we applied THz spectroscopy to analyse calcium-based microfillers concentration in polymer matrix, its granulation and chemical treatment.

It is expected that the growth in various industries, including building and construction, paper industry, plastic industry, pharmaceutical industry, and agriculture, will increase the demand for calcium carbonate ($CaCO_3$) over the next decade, especially on account of technologically developed products with enhanced physical and mechanical properties. In construction industry, $CaCO_3$ is used as a building material, limestone aggregate and as an ingredient in different end products. As it seems that $CaCO_3$ acts as a key material in construction industry, we selected it as a test material in this thesis.

First we studied the optical properties of calcium carbonate powder samples with various particles size and surface modification. The transmission through calcite powder which has sharp absorption peak at around 3.2 THz was studied. The absorption of $CaCO_3$ crystal sample depends on crystal direction, crystal structure, crystal shape, and impurities [101]. In powder samples, there is no angle dependence of spectra because crystal directions in powder are random. In the frequency range between 0.5 THz and 4 THz the scattering effect of the powder sample is small but the granulation of particles showed some differences in THz spectra although the samples had the same chemical composition. The reason for this is the Mie scattering that is strengthened when the particle size is comparable to the wavelength of the EM radiation. Furthermore, the results showed that for the particles of the same granulation but different chemical treatment, the higher concentration of additives increases the absorption peak frequency position. Based on the analysis of peak absorbance amplitude, peak frequency position, and the appearance of additional spectral features, quantitative and qualitative analysis was successfully achieved.

For building-related products especially important is quantitative determination of $CaCO_3$ in mixtures that exist during the production process from lime or in reactions where $CaCO_3$ is used as one of reagents in end product production. Thus, we performed analysis

of the binary mixtures of calcium carbonate mixed with calcium oxide (CaO) and calcium hydroxide ($Ca(OH)_2$). We selected these two substances to show if it is possible to follow the chemistry of calcium carbonate, i.e. the reaction of conversion of limestone to lime and further to calcium hydroxide or vice versa. The THz spectroscopic characterization was carried out to get the knowledge of lime cycle $CaCO_3 \rightarrow CaO \rightarrow Ca(OH)_2 \rightarrow CaCO_3$ based on changes in the crystalline structures of each compound. By comparing the THz spectra of all three chemical compounds, differences in spectral features were clearly observed, which indicates that THz spectroscopy is capable to discriminate between various calcium-based microfillers. The same differences were also confirmed with the multispectral THz imaging. THz imaging was also applied for qualitative analysis of calcium-based microfillers. By using spatial distribution map, the inhomogeneity in concentration of calcium carbonate in polymer matrix was characterized.

In this paper, we demonstrated that the THz spectroscopic technique offers valuable results and can be, in combination with other spectroscopic and microscopic techniques, converted to a powerful rapid analytical tool.

*Covering the objectives of this thesis:* This chapter addresses hypothesis 1, 2 and 4.

*Revised Manuscript (clean copy)
Click here to view linked References

# Qualitative and quantitative analysis of calcium-based microfillers using terahertz spectroscopy and imaging

Andreja Abina [a]*, Uroš Puc [a,b], Anton Jeglič [a,b], Jana Prah[c], Rimvydas Venckevičius,[d] Irmantas Kašalynas,[d] Gintaras Valušis,[d] Aleksander Zidanšek [a,e,f]

[a] Jožef Stefan International Postgraduate School, Jamova 39, SI-1000 Ljubljana, Slovenia, andreja.abina@mps.si, Tel: +386 1 477 36 02; fax: +386 1 477 31 10
[b] Faculty of Electrical Engineering, University of Ljubljana, Tržaška cesta 25, SI-1000 Ljubljana, Slovenia
[c] Calcit d.o.o, Stahovica 15, SI-1242 Stahovica, Slovenia
[d] Optoelectronics Department, Center for Physical Sciences and Technology, LT-01108 Vilnius, Lithuania
[e] Department of Condensed Matter Physics, Jožef Stefan Institute, Jamova 39, SI-1000 Ljubljana, Slovenia, aleksander.zidansek@ijs.si
[f] Faculty of Natural Sciences and Mathematics, University of Maribor, Koroška cesta 160, SI-2000, Maribor, Slovenia

## Abstract

In different industrial applications, several strictly defined parameters of calcium-based microfillers such as average particle size, particle size distribution, morphology, specific surface area, polymorphism and chemical purity, play a key role in the determination of its usefulness and effectiveness. Therefore, an analytical tool is required for rapid and non-destructive characterization of calcium-based microfillers during the synthesis process or before its use in a further manufacturing process. Since spectroscopic techniques are preferred over microscopy and thermogravimetry, particularly due to its non-destructive nature and short analysis time, we applied terahertz (THz) spectroscopy to analyse calcite microfillers concentration in polymer matrix, its granulation and chemical treatment. Based on the analysis of peak absorbance amplitude, peak frequency position, and the appearance of additional spectral features, quantitative and qualitative analysis was successfully achieved. In addition, THz imaging was also applied for both quantitative and qualitative analysis of calcium-based microfillers. By using spatial distribution map, the inhomogeneity in concentration of calcium carbonate in polymer matrix was characterized. Moreover, by THz spectroscopy and imaging different calcium compounds were detected in binary mixtures. Finally, we demonstrated that the applied spectroscopic technique offers valuable results and can be, in combination with other spectroscopic and microscopic techniques, converted to a powerful rapid analytical tool.

## Keywords

Calcium-based microfillers, Granulation, Surface treatment, Terahertz pulsed imaging, Terahertz time-domain spectroscopy.

## 1. Introduction

Calcium carbonate, i.e. $CaCO_3$, is one of the most abundant raw materials that normally naturally occurs as a white mineral with a stable crystal polymorphic arrangement of calcite. Due to unique properties the calcium carbonate has become an important commercial product that is used as a filler, pigment or functional additive [1] in various industrial applications ranging from construction products, paints, glass, ceramics, adhesives, composites, paper, and plastics to animal feeds, food, pharmaceuticals, cosmetics, etc. The manufacturing of different products demands specific grades of calcium carbonate that depend on its physicochemical properties like colour, hardness, chemical purity, average particle size, and particle size distribution which are all determined by controlling the temperature, pressure, concentration, and time during the production process [2, 3]. Since the new applications of calcium carbonate constantly are being developed it is expected that its use will continue to grow in the next decade especially on account of technologically developed products with enhanced

physical and mechanical properties. For this reason an analytical tool is required for rapid and non-destructive characterization of calcium carbonate during the precipitation process or before its use in a further manufacturing process.

For qualitative analysis of calcium-based microfillers several techniques showed a potential such as Fourier transform infrared (FTIR) spectroscopy [4], electron microscopy [5, 6], powder X-ray diffraction [7], and Raman spectroscopy [7, 8]. The spectroscopic methods are preferred over microscopy and thermogravimetry particularly due to its non-destructive nature and short analysis time. The infrared (IR) spectroscopy has already been used to discriminate between calcium carbonate polymorphic forms of calcite, aragonite, and vaterite within binary and ternary mixtures in frequency range from 700 $cm^{-1}$ to 1800 $cm^{-1}$ [9] and from 680 $cm^{-1}$ to 800 $cm^{-1}$ [4], respectively. Moreover, the temperature dependence of absorption for calcite of different grain shapes in frequency range between 83 $cm^{-1}$ and 5000 $cm^{-1}$ measured by FTIR is also reported [10]. Lately, novel analytical techniques have been applied to confirm the polymorphic forms of calcium carbonate such as terahertz (THz) spectroscopy [11-13] and surface analysis techniques, containing X-ray photoelectron spectroscopy and time-of-flight secondary ion mass spectroscopy [14]. Besides qualitative analysis, FTIR spectroscopy has been also used as a quantitative analysis method for the determination of ratios of calcium carbonate against other compounds in mixtures [15, 16] as well as for the detection of different calcium carbonate crystal concentrations in powder mixtures [23]. Hence it follows that spectroscopic techniques can meet the industrial requirements for rapid and non-destructive qualitative characterization of calcite and its quantitative determination in mixtures.

The spectroscopic technique which uses electromagnetic radiation between microwave and near-infrared (IR) frequencies to study the properties of materials [17] is known as THz spectroscopy. The applications where this spectroscopy has shown a potential are increasing over the last two decades mainly due to more accessible instruments which typically operate within the frequency range 0.1–3.0 THz. Currently, the major research is devoted to applications in pharmaceutical industry [18], security [19], medicine [20], and materials characterization [21]. However, some studies reported that calcium carbonate exhibits strong absorption at around 3 THz due to the vibration of calcite molecules [11, 22]. The absorption of a single crystal depends on the crystal direction, crystal size, and crystal shape due to the large birefringence [11]. For powder samples the angle dependence disappears due to the random directions of the crystals. By calculating optical properties the volumetric additive content for various concentrations of calcium carbonate in polymer matrix can be determined [23]. Furthermore, the THz spectra of natural calcium carbonate also show the presence of impurities in powder samples [11] and can differentiate between calcite and aragonite polymorphic forms [13]. In addition, the spectroscopic THz imaging system with the performance optimized for fingerprint-frequencies measurement can be applied for samples imaging in the transmission and reflection geometry. The results obtained by employing the continuous wave spectroscopic THz imaging with InGaAs bow-tie diodes [24], semiconductor-based THz pulsed technology [25], THz antenna coupled field-effect transistors [26], and microbolometers [27] were in good agreement with the FTIR spectroscopy data and provided the spatial distribution of the components in the samples using principal component analysis (PCA). The reported results pointed out that the THz spectroscopy and imaging have a potential to be used for both qualitative and quantitative research in room environment and real time.

The aim of this study was to undertake the analysis of calcium-based microfillers using THz spectroscopy and imaging in order to demonstrate that the applied technology has a potential to quantitatively and qualitatively characterize pure and modified microsized particles in a

powder form. The method is applied for the discrimination between various concentrations of microfillers in polyethylene matrix and various granulations of calcite samples as well as for the detection of additives and surface-modifying agents within calcite microfillers which are present in numerous application cases. In addition, we show that THz spectroscopy is capable to follow the reactions of decarbonation/carbonation route through the detection of formation of chemical reaction products including calcium carbonate, calcium oxide and calcium hydroxide, or the presence of reactants in an incomplete chemical reaction. According to this study, THz spectroscopy can be used as an analytical method for rapid calcium-based microfillers characterization before they are used in a process what is especially desired for quality control aspects in industry.

## 2. Material and methods

### 2.1 Materials and its physicochemical properties

Calcite samples were obtained from Slovenian supplier Calcit d.o.o. which produces calcium carbonate fillers from naturally high-quality white marbled limestone deposit in Slovenia. The particle size distribution was determined by laser granulometer RODOS for samples C-5, C-15, C-40, C-5T and by Micromeritics Sedigraph 5120 for samples C-EX, C-1, C-EXT and C1T. Last method uses the sedimentation technique which measures the gravity-induced settling rates of different size particles in a liquid with known properties. Both data are given for additive-treated samples, i.e. first five samples in Table 1, and surface-modified samples, i.e. last three samples in Table 1 marked with additional letter *T*. The Mohs hardness for all samples has value of 3. In Table 1 also data from chemical analysis are given which are the same for all samples. We selected two series of calcite samples, the additive-treated one and the second where the samples are additionally surface-modified, what makes them hydrophobic. Moreover, we measure the additional natural calcite sample obtained from manufacturer that was not treated in any way, labelled as C-5L.

Apart from calcite powder samples gained from manufacturer, three additional calcium compounds in powder form obtained from Sigma-Aldrich were analysed: calcium carbonate (ACS reagent, ≥99.0%), calcium oxide (meets analytical specification of FCC, ≥96.0%), and calcium hydroxide (ACS reagent, ≥95.0%). As a reference material we selected polyethylene (PE) powder with 53-75 μm particle size obtained from Sigma Aldrich.

### 2.2 Sample preparation

Polyethylene was selected as a reference material because of its high transmission to THz waves and the absence of large absorption peaks in THz spectrum. Calcium compounds powders and PE powder were dried for 24 hours at 65°C in an oven and were stored in a desiccator containing silica gel. For FTIR and THz spectroscopic measurements we prepared pellets with diluting the sample powder in a reference PE powder. All the calcite samples were weighed to 7-8 mg and mixed with 294-296 mg of a reference powder to obtain the mixtures with 2.3-2.6 wt% of each compound. The sample-reference mixture for pellet compression was mixed and grinded by pestle in a mortar. A weighed portion of each sample mixture equivalent to 100 mg was used for the pellet making with a manual hydraulic press. The pellets with a diameter of 12 mm and thickness below 1 mm were compressed at the approximate pressure of 1500 kg/cm$^2$ for 2 min. We use the same procedure for the preparation of pellets containing 7 wt% of the binary mixture of calcium carbonate, calcium oxide or calcium hydroxide, where the ratio between $CaCO_3$ against other two calcium compounds and the ration between calcium hydroxide against calcium oxide were 1:2. In case of quantitative measurements we mixed the calcium carbonate powder with the PE powder of 1 wt%, 2 wt%, 3 wt% and 4 wt%, and the calcium oxide powder with the PE powder with 3

wt%, 5 wt% and 7 wt%. For optical microscopy we used the obtained calcite powders without special sample preparation, whereas for SEM microscopy the calcium carbonate powder were sputtered with gold to ensure better morphological investigation.

### 2.3 THz spectrometer and imager

The experiments were performed by a TeraIMAGE system by Rainbow Photonics AG [28] which enables THz spectroscopic and imaging measurements. A detailed description and schematic drawing of the THz system based on electrooptic organic crystals in transmission is explained elsewhere [29]. The spectra are given for the spectral range from 1.35 THz to 4.20 THz with a spectral resolution of 38.5 GHz at room temperature in a compartment with nitrogen atmosphere to eliminate undesired water absorption effect. For THz spectroscopy the recorded signals were averaged over 10.000 acquisitions in one measurement point and the THz spectra were obtained by averaging at least three measurements in different points on the pellet in order to reduce the effect of the measurement error and to obtain enhanced signal-to-noise ratio. The recorded signals were pre-processed by using the baseline correction, zero-padding and Blackman-Harris apodization prior to Fourier transform of the signal. After the Fourier transform the absorbance $A$ of the sample is calculated by equation $A = -\log_{10} I_S/I_{REF}$, where $I_s$ is the intensity of the THz radiation transmitted through the sample and $I_{REF}$ is the intensity of the THz radiation that passed through the reference. Thus, the method requires two measurements. First, a reference waveform without the sample is measured, followed by the measurement of a sample waveform. All spectral analysis was completed using MATLAB (MathWorks). The error in the spectral features location is presented as an envelope of mean spectrum representing the standard deviation of the uncertainty in the measurement of absorption. For THz imaging the pellet was placed in a sample holder on a translational stage. The spectroscopic images with a spatial resolution of about 1.5 mm were taken by raster scanning over the 48 mm by 18 mm scanning area. The entire frequency spectrum was recorded in every single point of the sample what gives a 3D data set where two axes describe vertical and horizontal spatial dimensions and the third axis represents the spectral frequency dimension.

### 2.4 FTIR spectrometer

For FTIR spectroscopy we used the same reference and sample pellets as for THz measurements. The measurements were performed in a spectral range of 20-500 $cm^{-1}$ (0.6-15 THz) at temperature of 300 K and vacuum environment using the resolution of 5 $cm^{-1}$. In some cases, the transmittance was measured in different sample area applying a 5 mm diameter pinhole. The calculated spectra are presented in frequency range from 1.35-6.0 THz due to the scattering limitation of a reference PE material at higher frequencies. In addition, the obtained spectra are smoothed with the Savitzky-Golay method.

### 2.5 Optical and SEM microscope

For particle size and shape verification we used optical microscopy (Nikon Eclipse E600) at 200x and 1000x magnification. In addition, to verify the crystal shape of pure calcium carbonate crystals, we used scanning electron microscope (JEOL JSM-7600F). The optical micrographs of calcite samples with various granulation and modification are given in Supplementary Fig. 1.

## 3. Results and discussion

### 3.1 Qualitative and quantitative analysis of calcium-based microfillers in polymer matrix

Calcium compounds are widely used as additives in natural or synthetic polymeric compounds to enhance their final chemical and physical properties and to make them suitable for particular applications [30, 31]. As both, the type of additive used as well as its concentration in the polymer matrix are of key importance for the quality and performance of the product, qualitative and quantitative analysis of additives in plastic materials is an important issue. The analysis of additives is difficult, especially due to the low concentrations in a host material, thus a sensitive detection methods are needed. Herein we demonstrated that THz spectroscopy is capable of identification and quantification of calcium compounds in low concentrations in a polyethylene powder.

Most of the fillers and additives differ in their optical properties in the THz frequency range from the host polymer material such as synthetic plastics [23], so that the THz properties of the calcium compounds are expected to carry a measure for the additive concentration determination. In Fig. 1a it is clearly observed that THz spectrum of calcium carbonate (ACS grade, further marked as C-SA) exhibits one characteristic peak at around 3.25 THz that was already reported [11]. By increasing the additive concentration from 1 wt% to 3 wt% the amplitude of the characteristic peak increased due to the large absorption on additive particles in PE. In Fig. 1b this increase in absorbance amplitude is presented over various concentrations of $CaCO_3$ in PE where it is noticeable that the absorbance changes linearly with increasing concentration. However, it is expected that the peak absorbance vs. concentration should pass through the origin, but the data used for linear fitting are highly related with the signal-to-noise-ratio (SNR) of the selected THz system. As can be observed in Fig. 1a the concentration of 1.0 wt% of $CaCO_3$ is almost reached the limit of SNR, thus this data is less reliable, what is also expressed in Fig. 1b where at lower concentrations the absorbance goes toward negative values. Therefore, the region below 1 wt% concentration does not exhibit the real behaviour of the PE-$CaCO_3$ mixture. Due to the high sensitivity of $CaCO_3$ to THz radiation, at the concentration above 3 wt% the absorption reached the signal-to-noise ratio (SNR) of the applied THz system, thus the distortion in characteristic peak occurs and those spectra were excluded from the research. Therefore, for the rest of experimental work, the concentration of 2 wt% of calcite samples were selected. The SNR of selected THz system is frequency dependent as shown in Supplementary Fig. 2.

Based on THz absorption spectrum we performed the spectroscopic THz imaging of the reference pellet and the pellet with 2 wt% of $CaCO_3$. By using PCA the spatial distribution of individual chemical substance, i.e. $CaCO_3$, in the sample were extracted from the multispectral THz images. For this method a 3D data set is needed, where two axes present vertical and horizontal spatial dimensions, and the third axis describes the spectral frequency dimension. The image $I(x,y,\omega)$ observed at each of the frequency $\omega$ is expressed as a linear combination of absorbance spectra $S(\omega)$ and spatial pattern $P(x,y)$ that gives a matrix equation [25]:

$$[I]=[S][P] \quad (1)$$

First 3D data set is compressed to a 2D matrix $I_{N\times L}$, which has $N$ recorded images whose row vectors represent each $L$-pixel image taken at an individual frequency. Assuming that the sample has $M$ substances, each having known absorption spectrum with $N$ frequency components, then a matrix of $S_{N\times M}$ can be created. Since $[I]$ and $[S]$ from Eq. 1 are measured directly, the spatial distribution of individual substance in the sample can be resolved by using a least-squares method which as a result gives the matrix $[P]$ expressed as [25]:

$$[P_{MxL}] = ([S_{NxM}]^t [S_{NxM}])^{-1} [S_{NxM}]^t [I_{NxL}] \quad (2)$$

where $P_{ij}$ is the probability of the occurrence of the $i^{th}$ substance at the $j^{th}$ pixel given in a matrix form and $t$ is the matrix transpose operation. The matrix $[P]$ is also called the spatial

distribution of the samples. The matrix [*S*] is formed by extraction of the measured absorption spectra of each substance *M* at *N* frequencies, whereas [*I*] is a matrix of the observed image generated by a transmission scanning of the sample, where row vectors represent the spatial pattern of each drug with *L* pixels. Since the pellet is not totally homogenous, regions with differences in concentration are identified in the spatial distribution map (Fig. 1c) because there are differences in the amplitude of the absorption through the THz frequency range in different measured points of the pellet. The regions with lower concentration within the pellet of $CaCO_3$ are coloured with bright (yellow) colour and indicated by arrows. The bright (yellow) coloured edges of the pellet and the dark red regions are the contributions of the scattering effect.

The mixture of calcium oxide, CaO, and PE is more transparent in THz frequency range in comparison to calcium carbonate. In this case there is no characteristic peak observed and the absorption increased with the increased frequency through the whole spectral range. However, the CaO sample has a unique spectral response as is shown in Supplementary Fig. 3 with some spectral features marked with red circles that occur for all three tested concentrations, with minimal deviations in frequency location of each spectral feature in the spectral range between 1.35 THz and 4.20 THz. For two CaO concentrations, i.e. 5 wt% and 7 wt% of CaO, the spectra are almost identical, measured in different pellet points, whereas at lower concentration the spectral features are modified due to the limit of SNR. Additionally, it is noticed that the whole spectrum of CaO is shifted at higher absorbance amplitude due to the higher concentration of CaO in PE matrix. From results, we can conclude that the absorbance peak intensity is proportional to the concentration of calcium-based microfiller, what shows that quantitative analysis is possible but the concentration dependence from the SNR of the THz system should be considered. By comparing the THz spectra of $CaCO_3$ and CaO, differences in spectral features are clearly observed, what indicates that THz spectroscopy is capable to discriminate between various calcium-based microfillers.

### 3.2 Analysis of treated and untreated calcium carbonate microfillers

Calcium carbonate fillers obtained by crashing and grinding of natural calcite are often treated with different additives and surface modifying agents such as fatty acids (e.g. stearic acid), silanes, phosphates, titanates, polyacrylates or zirconates [32-34] to improve the filler's characteristics appropriate for a specific application. The analysis of the properties of additive-treated and surface-modified fillers is an important factor during the synthesis and in their final use. Since the THz spectral pattern depends on the crystal structure and the presence of impurities or additives it is expected that small spectral features may occur in the THz spectrum of additive-treated and surface-modified calcite samples [35]. The particles of C-SA powder are in a form of rhombohedra what was also confirmed by SEM (Fig. 1d), whereas the surface of natural calcite particles is changed due to the presence of additives and surface-modifying agents. The smallest particles of calcite are present in C-EX powder, which are comparable to the size of C-SA particles.

In Fig. 2 it is noticeable that the C-SA sample gives narrower spectral peak at around 3.2 THz in comparison to additive-treated and surface-modified calcite samples. The reason is not only the presence of other substances in the natural calcite samples but also the particle size of C-SA which is well below $\lambda/10$ at the frequency where the characteristic peak of $CaCO_3$ occurs, i.e. 3.2 THz, and thus the scattering effect is in the case of C-SA less expressed. Depending on the presence of additives the characteristic absorption peak of additive-treated calcite is slightly shifted to higher frequency compared to the C-SA. The same trend can be observed in the case of surface-modified calcite where additional surface modifying agents are present, thus the absorption peak is slightly shifted to even higher frequency. The position of the absorption peaks for each type of sample with various granulations is depicted in Fig. 2. The

slightly shift of the main absorption peak to higher frequency is observed for all three granulations, at d98 is 3.5 μm, 6.0 μm, and 17.5 μm, for both additive-treated and surface-modified samples. The results in Fig. 2 also show the differences between the spectrum of natural calcite sample without any additive (C-5L) and calcite sample treated with surface modifying agents. In case of C-5L the location of absorption peak is very close to the peak of C-SA. For all calcite samples no distinctive absorption features at frequencies around 2.1 THz and 2.2 THz were observed what is in accordance with the findings from [11] that there is no angle dependence of spectrum for powders because the crystal directions are random. Furthermore, the measurements showed additional small spectral feature that occurs at around 3.7 THz in both samples, natural calcite from manufacturer and ACS grade of $CaCO_3$ due to the scattering on particles of reference material which size is comparable to that frequency.

In Fig. 3 the peak frequency position is given over sample series, including C-SA, laboratory grade, additive-treated, and surface-modified samples. The different size of particles is presented by circles of varying diameter. For surface-modified samples the peak frequency position is inversely proportioned with the particle size. This proportion is not valid for additive-treated samples, most probably due to the differences in additives use for different samples. Among all natural calcite samples the lowest peak position is observed for C-5L where no additives were used, but it is still higher than C-SA due to the presence of natural impurities or the presence of reactants in an incomplete chemical reaction of precipitation. Furthermore, the results show that for the particles of the same granulation but different chemical treatment, higher concentration of additives increases the absorption peak frequency position.

### 3.3 Influence of microfiller granulation on terahertz spectrum

THz spectroscopy utilizes much longer wavelengths than other optical spectroscopic techniques. Therefore, the scattering by microsized particles is less noticeable on THz spectrum, but it is anyway important to consider scattering effects and minimize such effects by using finely milled powders compressed into the pellets or to calculate the THz spectrum by averaging multiple measurements over a large sample area [36]. Hence, it is expected that in the frequency range between 1.35 THz and 2.0 THz the scattering effect of the selected calcite powders is small. Therefore, this part of THz spectrum is excluded from Figs. 4a and 4b. The particle scattering becomes significant with increasing frequency due to the particle size that becomes comparable to the wavelength of THz radiation. [35].

In this study the spectral range between 1.35 THz and 4.0 THz corresponds to the wavelengths between 222 μm and 75 μm, respectively. Since the THz spectrum acquired in a single point measurement is noisy and contains spectral artefacts because of scattering varying across the sample positions, we used averaging of at least three measurements to ensure more reliable THz spectrum. The particle size of a reference PE powder ranges from 53 μm to 75 μm or 5.65 THz to 4.0 THz, respectively. Fig. 4a shows the THz absorption spectra of additive-treated calcite samples with five size categories according to d98 parameter: 3.5 μm, 6.0 μm, 17.5 μm, 70 μm, and 90-150 μm. A major peak at around 3.25 THz appears in all spectra measured for calcite particle sizes up to 150 μm. In addition, some spectral changes in Fig. 4a are visible below and above this characteristic spectral feature. Therefore, the 1$^{st}$ derivative for all spectra was calculated to make these changes more visible. The THz results were compared with the FTIR spectra, thus also the 1$^{st}$ derivative of FTIR spectra were calculated in frequency range 1.5-6.0 THz (Fig. 4c).

In two frequency ranges in Fig. 4b, between 2.50 THz and 3.15 THz as well as between 3.50 THz and 4.0 THz, some additional spectral features like shoulder and small peaks are expressed. In higher frequency region, indicated by dark grey colour in Fig. 4b, two shoulders

at around 3.7 and 4.0 THz are noticeable which are more expressed for samples with smaller particle sizes (d98 < 6 μm). In lower frequency region, indicated by light grey colour, some additional spectral features are observed for samples with greater particle sizes (d98 >70 μm). The differences in the intensity of these additional spectral features for different granulations of calcite samples can be explained by Rayleigh and Mie scattering. In case when the size of particles is smaller than $\lambda/10$, the particles acts as a point scatter and scattered THz waves are almost identical in both forward and backward direction regarding the incident THz beam. For larger particles two processes are known. In case of particles with the size of approximately $\lambda/4$, particles are considered as large particles and the scattering is concentrated in forward direction. When particles are larger than the wavelength of THz wave the scattering intensity in forward direction is even higher. The spectral features above 3.5 THz appears not only due to the scattering on calcite particles, but also on PE particles whose size is comparable to this end of the THz spectral range. The spectral shoulders are the most expressed for sample C-EX and a slightly less for sample C-1 where the particles are smaller than $\lambda/10$ at frequencies between 3.5 THz and 4.0 THz. Therefore, the shoulders appear on account of both the scattering on large PE particles in forward direction and small calcite particles in backward direction regarding the incident THz beam. The d98 parameter of C5 sample is comparable to $\lambda/4$ at 4.0 THz, i.e. 18 μm, thus the particles are considered as large and the scattering is more concentrated in forward direction. Consequently, shoulders are in that case less visible, since the scattering in backward direction is less expressed. Furthermore, shoulders are once again more distinguished when d98 parameter is comparable to the wavelength of THz wave. One can note that the scattering in forward direction is even higher on account of both large PE particles and large calcite particles. In lower THz region the spectral features occur on the curves of 1$^{st}$ derivative for C-15 and C-40 samples due to the presence of large calcite particles which size is comparable to that frequency range.

### 3.4 Analysis of calcium compounds formation during production process

The formation of calcium carbonate fillers is performed industrially subsequently by three processes: calcination or decarbonation, hydration or slaking, and precipitation or carbonation [2, 37]. The calcination is a thermal decomposition of natural calcite source, e.g. limestone, to produce lime or calcium oxide and carbon dioxide:

$$CaCO_3(s) \xrightarrow{\Delta} CaO(s) + CO_2(g) \quad (3)$$

Adding water to the lime produces calcium hydroxide, i.e. $Ca(OH)_2$, during an exothermic reaction:

$$CaO(s) + H_2O(l) \rightarrow Ca(OH)_2(s) \quad (4)$$

The carbonation is a final exothermic reaction between $CO_2$ and $Ca(OH)_2$ that results in the formation of precipitated calcium carbonate (PCC).

$$Ca(OH)_2(aq) + CO_2(g) \rightarrow CaCO_3(s) + H_2O(l) \quad (5)$$

The conditions and mechanism of production effect on the various shapes and sizes of calcium carbonate particles as well as on the presence of impurities including by-products. For instance, the experiments showed that hydroxyl ions are present in calcium carbonate powders due to the incomplete carbonation [38]. Thus, specific agents, e.g. polybasic acid, are required to neutralize the remaining unreacted $Ca(OH)_2$. The same issue is observed for decarbonation route where it is necessary to separate calcium oxide from the unreacted calcium carbonate. All three calcium compounds are widely used as a raw material in chemical industry for numerous applications, dominating in paper industry and construction and building materials, e.g. cement, mortar, plaster, etc. Therefore, in this study we

demonstrated that THz spectroscopy is capable to detect the unreacted calcium compounds in binary powder mixtures without any special sample preparation. The THz spectra of investigated chemical compounds and mixtures were verified by FTIR spectroscopy (Supplementary Fig. 4) where similarities between the THz and FTIR spectra are clearly noticeable in frequency range between 1.35-4.20 THz. For both $CaCO_3$ binary mixtures some additional spectral features are observed in FTIR spectra above the frequency of 4.20 THz. In case of $CaCO_3$/CaO mixture these spectral features most probably occur due to the scattering of THz radiation by CaO particles.

In Fig. 5a the THz spectra of pure calcium compounds are presented. Among all three compounds only $CaCO_3$ showed a characteristic spectral peak at 3.25 THz. The absorption of CaO increases more in comparison to the absorption of $Ca(OH)_2$ through the THz frequency range. However, for CaO some small spectral features can be observed that occur almost at the same frequency locations for samples with different concentration of CaO in PE (Supplementary Fig. 3). Some of these spectral peaks are also present in the TH spectrum of CaO/$CaCO_3$ mixture at around 3.6 THz and 3.9 THz in Fig. 5b that are absent in case of pure $CaCO_3$ sample in Fig. 5a. The main spectral peak at 3.25 THz is widened and shifted slightly to higher frequency due to the presence of CaO which can be considered as an impurity. The presence of $Ca(OH)_2$ in $CaCO_3$ is hardly detected; only small spectral changes are observed regarding the peak shift and spectral features in comparison to the THz spectrum of pure $CaCO_3$. The absorption of CaO/$Ca(OH)_2$ mixture is almost unchanged through the whole THz frequency range. Even more, at higher frequencies the absorption spectra of mixture is lower than in case of pure substances, probably due to the low concentration of CaO in a mixture which was below the limit of detection by THz spectrometer.

In Fig. 6 spectral data are presented as a 3D data set with two axes describing the horizontal and vertical spatial dimensions, and the third axis representing the spectral information considering the absorption at selected frequencies. The THz imaging allows the analysis of pellets containing different chemical compounds due to its unique spectral signatures in the THz frequency range. In Fig. 6 THz images are presented at four different frequencies, two before the characteristic peak of $CaCO_3$ at 1.50 THz and 2.30 THz, the third at the characteristic peak of 3.25 THz, and the last one after that peak at 3.80 THz. THz images at other frequencies in the spectral range between 1.20 THz and 4.27 THz are given as a video clip in a Supplementary data. The colourbar is adjusted to the current situation at selected frequency and should not be comparable between different THz images. In the left upper corner the reference PE pellet is presented which shows no significant absorption through the whole spectrum, thus this area in THz images is coloured almost the same as the background. At 1.50 THz there is no significant difference between pellets due to the low absorption of all calcium compounds at selected frequency. With increasing frequency the absorption of $CaCO_3$ and CaO increases what is noticeable on the second THz image at 2.30 THz where the second and the third pellets are changing colour on account of greater absorption. At 3.25 THz the absorption of $CaCO_3$ achieves peak and after that frequency the absorption decreases. Therefore, on the third THz image the pellet containing $CaCO_3$ is coloured brighter (yellow), whereas on the fourth image at 3.80 THz the same pellet changes colour back to darker tone (blue). The pellets containing CaO is coloured yellow also on the last THz image due the increased absorption. In case of $Ca(OH)_2$ the absorption slightly increases with frequency what causes that the blue colour of the last pellet is brighter on the third and fourth THz image in comparison to the reference pellet. Hence, the multispectral THz imaging allows discriminating between various calcium compounds.

## 4. Conclusions

Qualitative and quantitative analysis of calcium-based microfillers was performed using THz spectroscopy and imaging with complementary optical and SEM microscopy as well as FTIR spectroscopy. Based on spectral changes in characteristic spectral peak of $CaCO_3$ we demonstrated that THz spectroscopy is capable to distinguish between different concentrations, chemical treatments, and granulations of calcite particles in a powder form according to the analysis of peak absorbance amplitude, peak frequency position, and appearance of additional spectral features such as shoulders and small peaks. In addition, the THz spectra of calcium compounds that enter or leave during the carbonation/decarbonation route were recorded and analysed by THz spectrometer. The results showed that each calcium compound has a unique spectral response in the THz frequency range that can be used for identification of the pure compound in binary mixtures. In addition to spectroscopy measurements, the capabilities of THz imaging were also evaluated for both quantitative and qualitative analysis of calcium-based microfillers. By using spatial distribution map, the inhomogeneity in concentration of $CaCO_3$ in polymer matrix was detected. Moreover, by multispectral imaging different calcium compounds were identified. In combination with other spectroscopic and microscopic techniques the results of this research can be even more valuable. The study demonstrated the considerable potential of the applied technique for rapid and accurate analysis of calcium-based microfillers which will continue to play a significant role in products used in everyday life.

**Acknowledgements**

The authors would like to acknowledge financial support from the Slovenian Research Agency grants P2-0348-2338 and J2-4266. We would also like to thank the Department of Condensed Matter Physics at "Jožef Stefan" Institute for their support concerning the measurements at electron and optical microscopy. Special acknowledgement is given to the Calcit d.d., who provided calcite samples.

**Appendix A. Supplementary data**

Supplementary data associated with this article can be found, in the online version at

**References**

[1] Y. Boyjoo, V.K. Pareek, J. Liu, Journal of Materials Chemistry A, 2 (2014) 14270-14288.
[2] J. Kemperl, J. Maček, International Journal of Mineral Processing, 93 (2009) 84-88.
[3] C. Domingo, E. Loste, J. Gómez-Morales, J. García-Carmona, J. Fraile, The Journal of Supercritical Fluids, 36 (2006) 202-215.
[4] N.V. Vagenas, A. Gatsouli, C.G. Kontoyannis, Talanta, 59 (2003) 831-836.
[5] A. Shafiu Kamba, M. Ismail, T.A. Tengku Ibrahim, Z.A.B. Zakaria, Journal of Nanomaterials, 2013 (2013) 9.
[6] L. Brečević, D. Kralj, Croatica Chemica Acta, 80 (2007) 467-484.
[7] S.R. Dickinson, K.M. McGrath, Analyst, 126 (2001) 1118-1121.
[8] U. Wehrmeister, D.E. Jacob, A.L. Soldati, N. Loges, T. Häger, W. Hofmeister, Journal of Raman Spectroscopy, 42 (2011) 926-935.
[9] A.G. Xyla, P.G. Koutsoukos, Journal of the Chemical Society, Faraday Transactions 1: Physical Chemistry in Condensed Phases, 85 (1989) 3165-3172.
[10] T. Posch, A. Baier, H. Mutschke, T. Henning, Astrophys. J., 668 (2007) 993-1000.
[11] M. Mizuno, K. Fukunaga, S. Saito, I. Hosako, Journal of the European Optical Society - Rapid Publications, 4 (2009) 09044.
[12] M. Mizuno, K. Fukunaga, J Biol Phys, 39 (2013) 123-130.
[13] M. Mizuno, K. Fukunaga, S. Saito, I. Hosako, in: 35th International Conference on Infrared Millimeter and Terahertz Waves (IRMMW-THz), 2010, pp. 1-2.
[14] M. Ni, B.D. Ratner, Surface and Interface Analysis, 40 (2008) 1356-1361.
[15] F.B. Reig, J.V.G. Adelantado, M.C.M. Moya Moreno, Talanta, 58 (2002) 811-821.
[16] E. Sağın, H. Böke, N. Aras, Ş. Yalçın, Mater Struct, 45 (2012) 841-849.

[17] A. Abina, U. Puc, A. Jeglič, A. Zidanšek, Applied Spectroscopy Reviews, 50 (2015) 279-303.
[18] D.C. Hufnagle, A.R. Taulbee-Combs, W.U. Spendel, G.E. Pacey, Talanta, 88 (2012) 61-65.
[19] J.S. Caygill, F. Davis, S.P.J. Higson, Talanta, 88 (2012) 14-29.
[20] F. Wahaia, I. Kasalynas, D. Seliuta, G. Molis, A. Urbanowicz, C.D.C. Silva, F. Carneiro, G. Valusis, P.L. Granja, J. Mol. Struct., 1079 (2015) 448-453.
[21] M. Naftaly, R.E. Miles, Proceedings of the IEEE, 95 (2007) 1658-1665.
[22] K.-E. Peiponen, E.M. Vartiainen, T. Unuma, J. Axel Zeitler, P. Silfsten, T. Venäläinen, H. Kishida, Applied Physics Letters, 102 (2013) 181110.
[23] S. Wietzke, C. Jansen, F. Rutz, D.M. Mittleman, M. Koch, Polym. Test, 26 (2007) 614-618.
[24] I. Kasalynas, R. Venckevicius, G. Valusis, IEEE Sens. J., 13 (2013) 50-54.
[25] Y.C. Shen, P.F. Taday, D.A. Newnham, M. Pepper, Semiconductor Science and Technology, 20 (2005) S254–S257.
[26] M. Bauer, R. Venckevičius, I. Kašalynas, S. Boppel, M. Mundt, L. Minkevičius, A. Lisauskas, G. Valušis, V. Krozer, H.G. Roskos, Opt. Express, 22 (2014) 19235-19241.
[27] J. Trontelj, G. Valušis, R. Venckevičius, I. Kašalynas, A. Sešek, A. Švigelj, in: M. Razeghi, A.N. Baranov, J.M. Zavada, D. Pavlidis (Eds.) Proc. SPIE 9199, Terahertz Emitters, Receivers, and Applications V, 2014, pp. 91990K.
[28] TeraIMAGE, The Flexible Solution for THz Spectroscopy and Imaging, Rainbow Photonics AG. Available at: http://www.rainbowphotonics.com/pdf/teraimage.pdf. Accessed Januar 20, 2015.
[29] A. Abina, U. Puc, A. Jeglič, A. Zidanšek, Polym. Test, 32 (2013) 739-747.
[30] W.C.J. Zuiderduin, C. Westzaan, J. Huetink, R.J. Gaymans, Polymer, 44 (2003) 261-275.
[31] K. Gorna, M. Hund, M. Vučak, F. Gröhn, G. Wegner, Materials Science and Engineering: A, 477 (2008) 217-225.
[32] E. Papirer, J. Schultz, C. Turchi, European Polymer Journal, 20 (1984) 1155-1158.
[33] S. Mihajlović, Ž. Sekulić, A. Daković, D. Vučinić, V. Jovanović, J. Stojanović, Ceramics – Silikáty, 53 (2009) 268-275.
[34] G.A. Tribello, C. Liew, M. Parrinello, The Journal of Physical Chemistry B, 113 (2009) 7081-7085.
[35] T. Hong, K. Choi, T. Ha, B. Park, K. Sim, J. Kim, J. Kim, J. Kwon, S. Lee, D. Kang, H. Lee, Journal of the Korean Physical Society, 64 (2014) 727-731.
[36] Y.C. Shen, P.F. Taday, M. Pepper, Applied Physics Letters, 92 (2008) 051103.
[37] Ö. Cizer, C. Rodriguez-Navarro, E. Ruiz-Agudo, J. Elsen, D. Van Gemert, K. Van Balen, J Mater Sci, 47 (2012) 6151-6165.
[38] S.I. Kuriyavar, R. Vetrivel, S.G. Hegde, A.V. Ramaswamy, D. Chakrabarty, S. Mahapatra, Journal of Materials Chemistry, 10 (2000) 1835-1840.

Table 1: Physicochemical properties, average particle size and particle size distribution of calcite samples from limestone deposit (summarized from the manufacturer specifications). d50 is defined as the average diameter particle size distribution and d98 as a top cut or maximum particle size distribution.

| Sample mark | Particle size distribution | | Physical properties | | | Chemical analysis | | |
|---|---|---|---|---|---|---|---|---|
| | d50 (μm) | d98 (μm) | Specific surface area (m2/g) | Density after tamping (g/ml) | Moisture absorption (g/100 g) | $CaCO_3$ | $Fe_2O_3$ | $SiO_2$ |
| C-EX | 0.75 - 0.9 | 3.5 | 9.69 | 0.6 | 34.0 | 98% | 0.01% | 0.02% |
| C-1 | 1.4 – 1.8 | 6.0 | 6.34 | 0.7 | 31.0 | 98% | 0.01% | 0.02% |
| C-5 | 4.0 - 4.5 | 17.5 | 2.10 | 1.0 | 26.0 | 98% | 0.01% | 0.02% |
| C-15 | 12.0 – 16.0 | 70 | 0.75 | 1.2 | 26.0 | 98% | 0.01% | 0.02% |
| C-40 | 16.0 – 25.0 | 90.0 – 150.0 | 0.67 | 1.4 | 24.0 | 98% | 0.01% | 0.02% |
| C-EXT | 0.75 - 0.9 | 3.5 | 9.69 | 0.6 | hydrophobic | 98% | 0.01% | 0.02% |
| C-1T | 1.4 – 1.8 | 6.0 | 6.34 | 0.9 | hydrophobic | 98% | 0.01% | 0.02% |
| C-5T | 4.0 - 4.5 | 17.5 | 2.10 | 1.1 | hydrophobic | 98% | 0.01% | 0.02% |

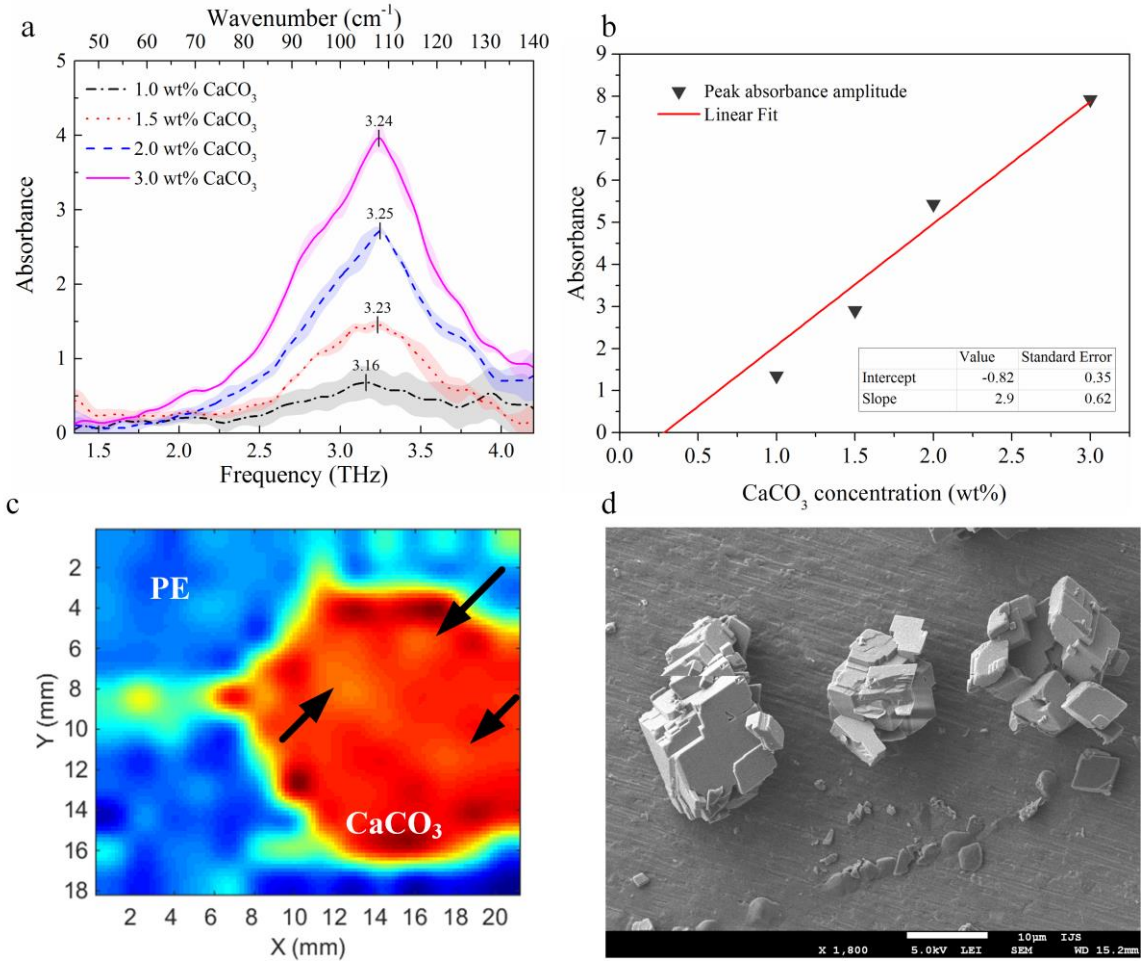


Fig. 1. THz spectra of various concentrations of $CaCO_3$ in PE matrix (a), the dependence of absorbance amplitude over various concentrations of $CaCO_3$ in PE matrix (b), spatial distribution map indicating inhomogeneous regions with different concentrations of $CaCO_3$ in pellet (c), and SEM image of $CaCO_3$ crystals at the 1800x magnification (d).

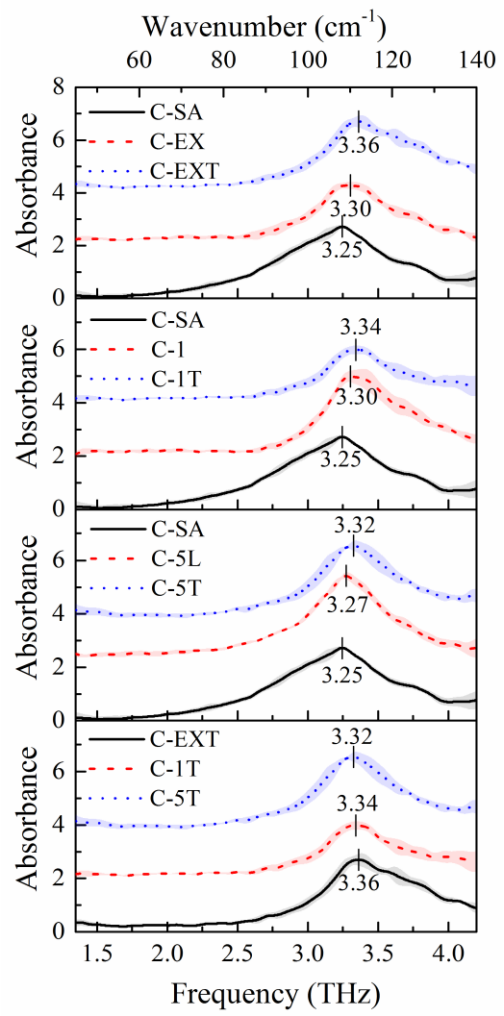


Fig. 2. THz spectra of C-SA against spectra of additive-treated C-EX and surface-modified C-EXT, additive-treated C-1 and surface-modified C-1T, laboratory sample C-5L and surface-modified C-5T, and the comparison of THz spectra for surface-modified calcite samples of different particles size. The spectra are shifted vertically for clarity. The error in the spectral peak location is presented as an envelope of mean spectrum representing the standard deviation of the uncertainty in the measurement of absorption.

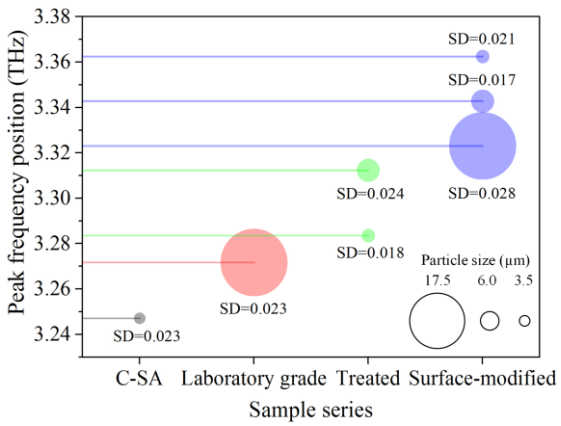


Fig. 3. Comparison between the frequency position of characteristic THz peak for C-SA sample and natural calcite samples of different size treated with additives and surface-modified agents as well as non-treated laboratory calcite sample. Error in the peak position is presented by a value of standard error of the mean spectra next to each circle.

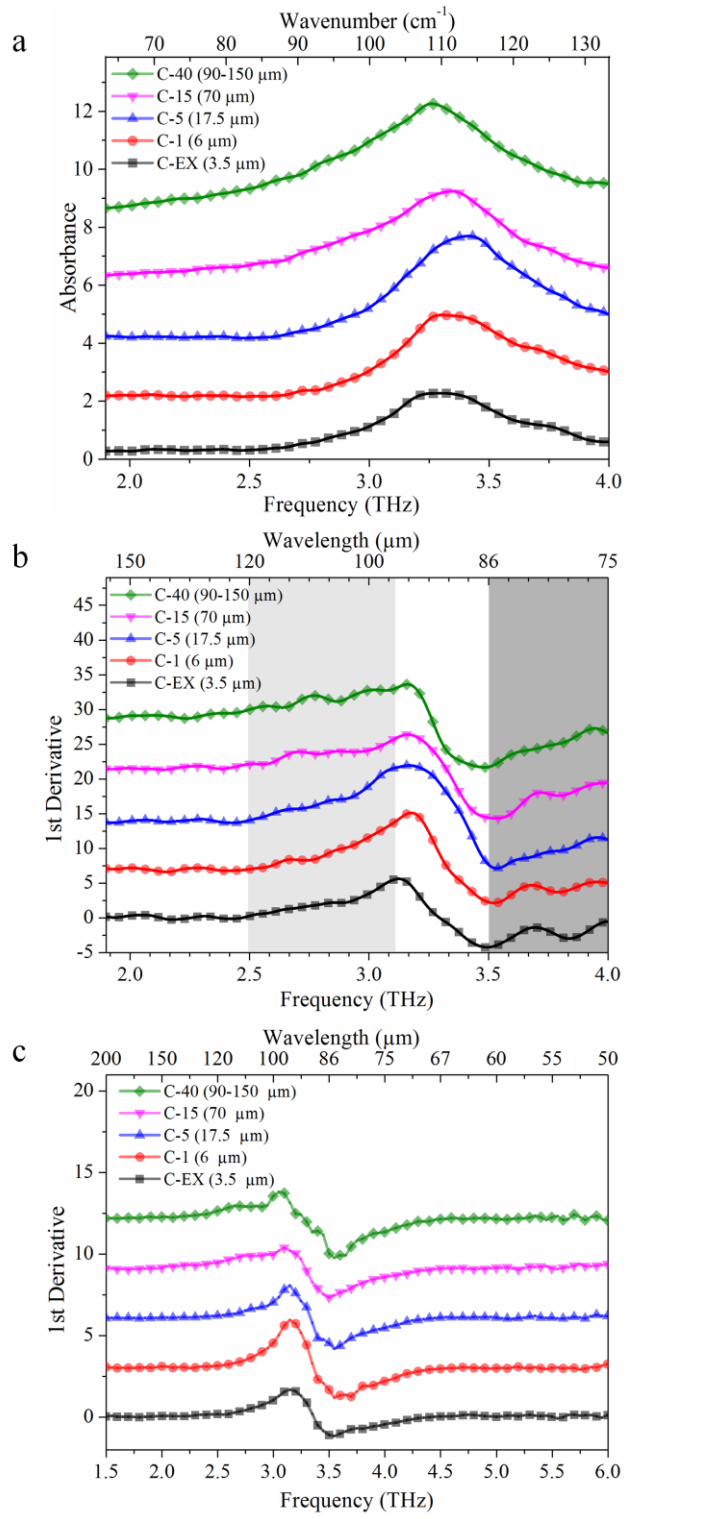


Fig. 4. THz spectra of calcite samples with different particles size according to parameter d98 (a), the 1st derivative of THz absorbance spectra for calcite samples (b), and the 1st derivative of FTIR absorbance spectra for calcite samples of variety of granulations. The spectra and curves are shifted vertically for clarity. The secondary axis of wavelength in graphs (b) and (c) is given as a nonlinear axis.

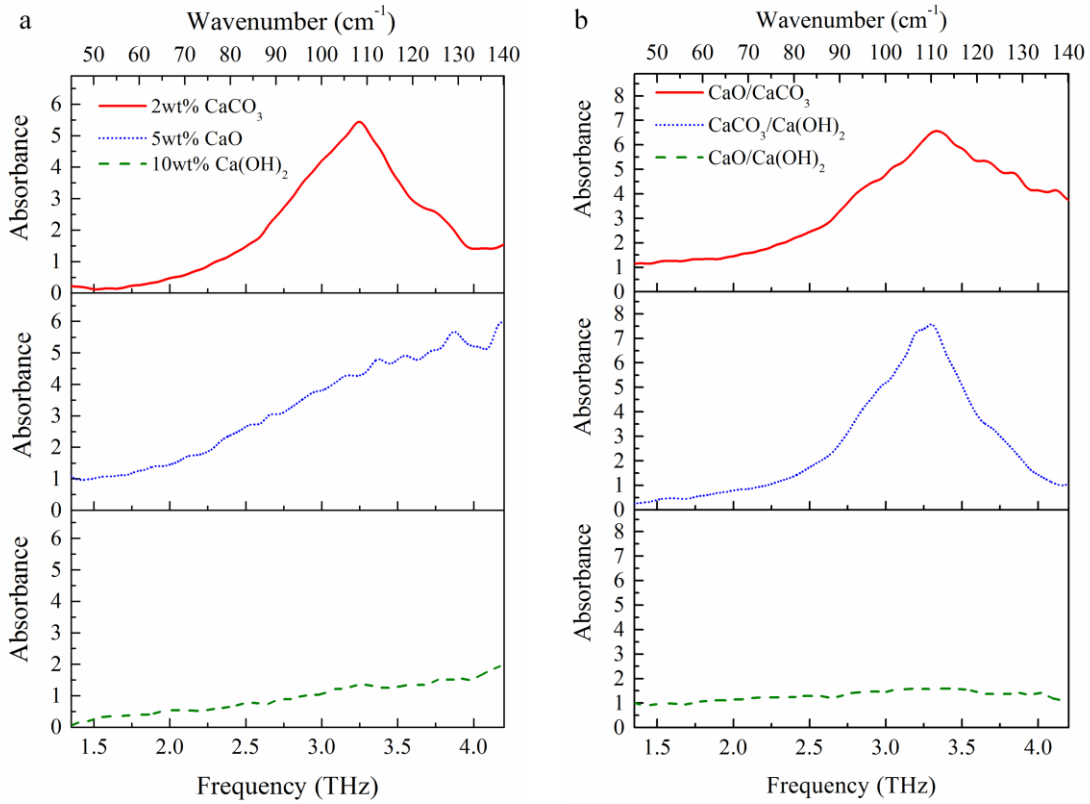


Fig. 5. THz spectra of pure calcium compounds (a) and binary mixtures of calcium compounds (b) in frequency range from 1.35-4.20 THz.

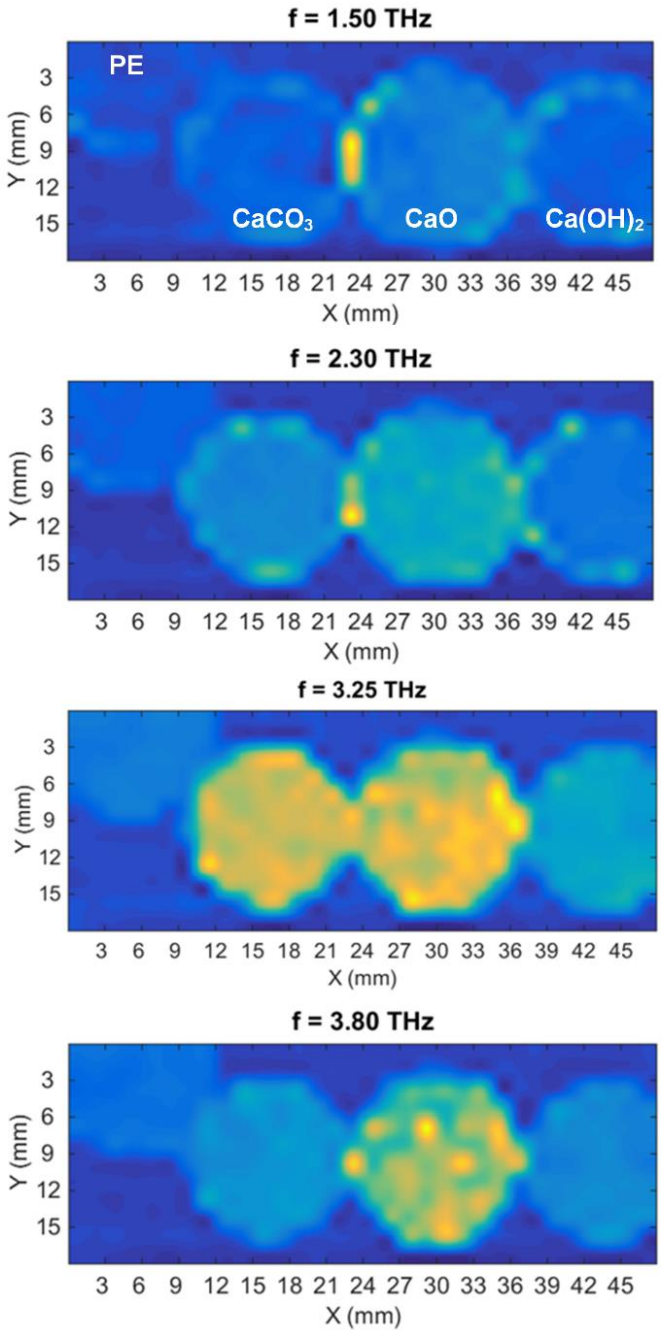


Fig. 6. THz spectral images for pellets containing different chemical compounds (PE reference, calcium carbonate, calcium oxide, and calcium hydroxide) at 1.50 THz, 2.30 THz, 3.25 THz, and 3.80 THz. Yellow (bright) colour presents higher absorption and blue (dark) colour lower absorption at selected THz frequency. Images are taken in characteristic absorption features.

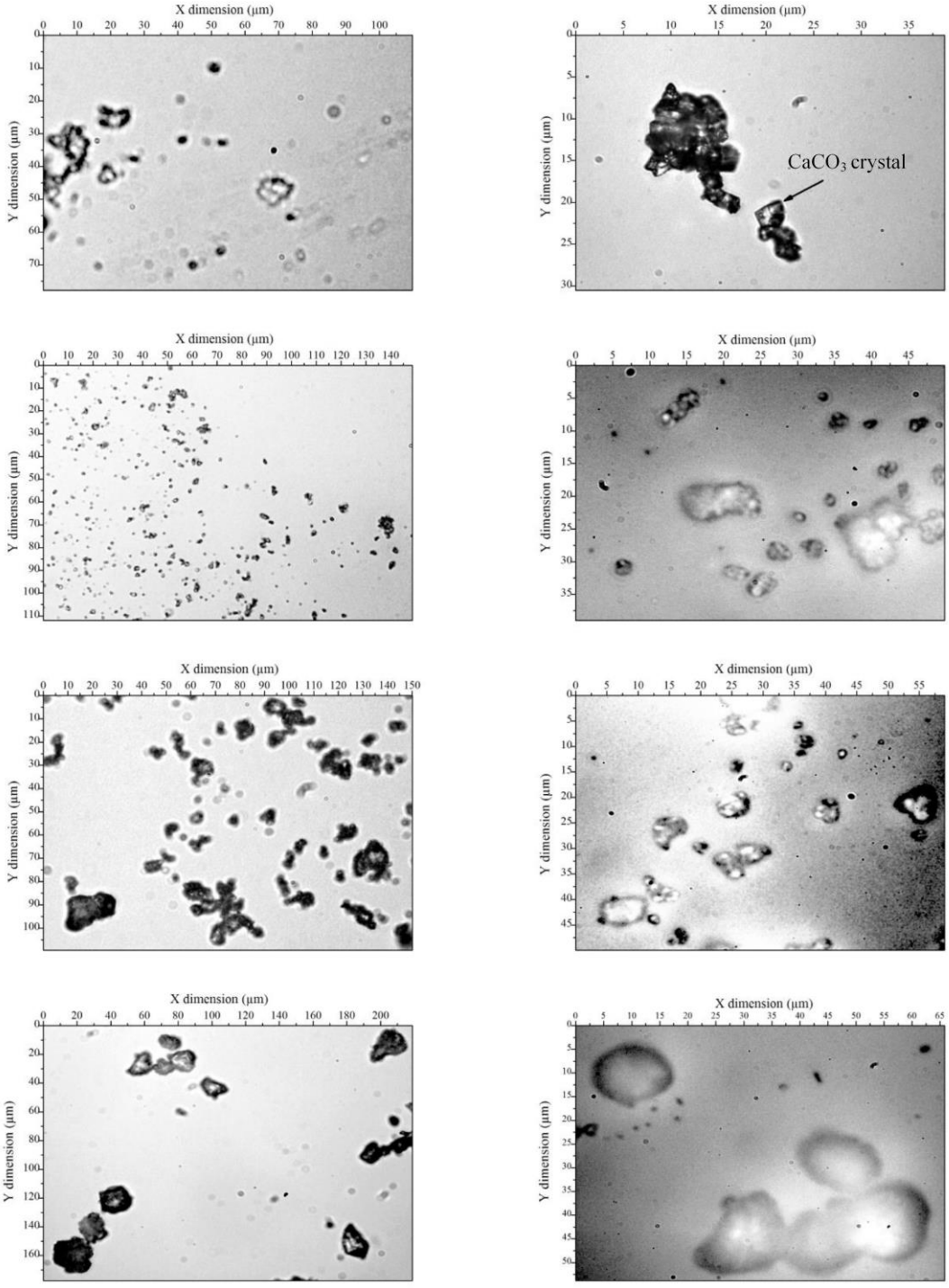


Supplementary Fig. 1. Optical micrographs at a magnification of 200 times (left) and 1000 times (right) for calcite samples with various granulation and modification. The presented micrographs of samples are listed in rows from top as follows: C-SA, C-EX, C-5T, and C-15.

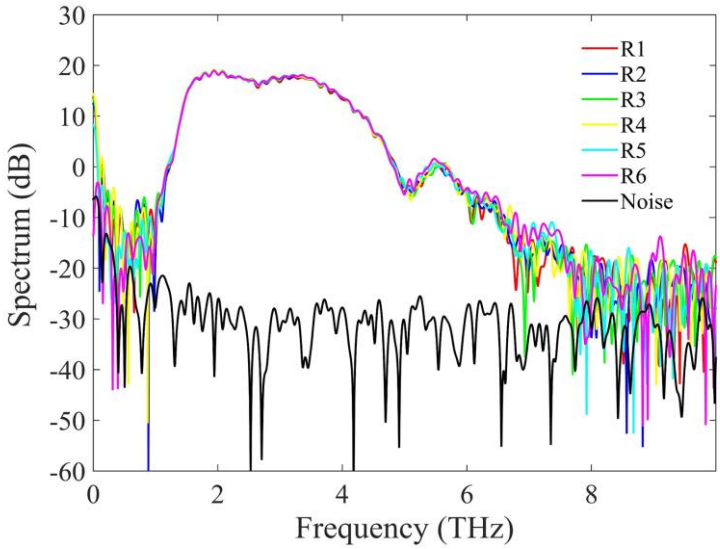


Supplementary Fig. 2. THz power spectrum with a noise floor for six successive measurements in nitrogen atmosphere measured with a THz system based on organic DSTMS electrooptic crystals.

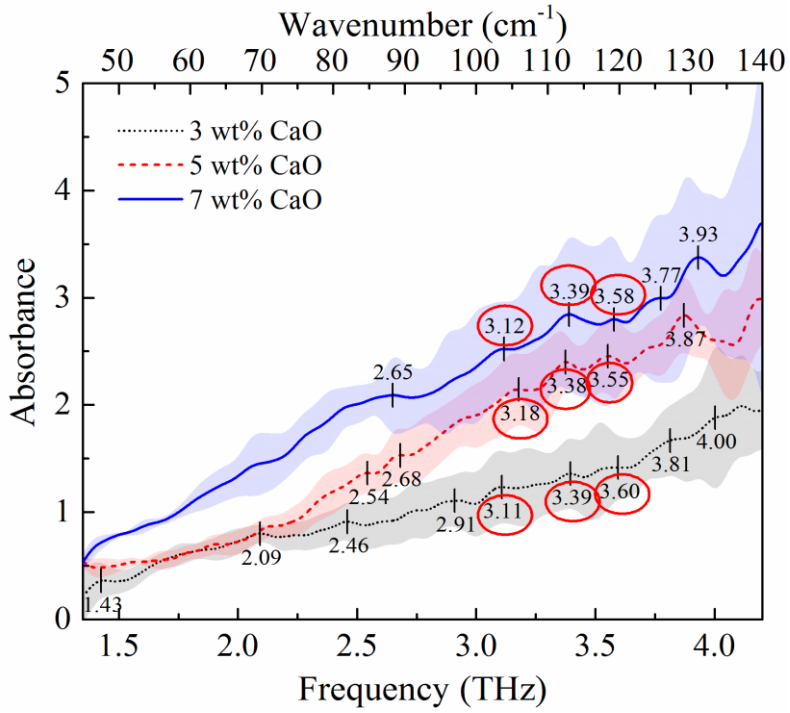


Supplementary Fig. 3. THz spectra for three different concentrations of CaO in PE matrix. The error in the spectral features location is presented as an envelope of mean spectrum representing the standard deviation of the uncertainty in the measurement of absorption.

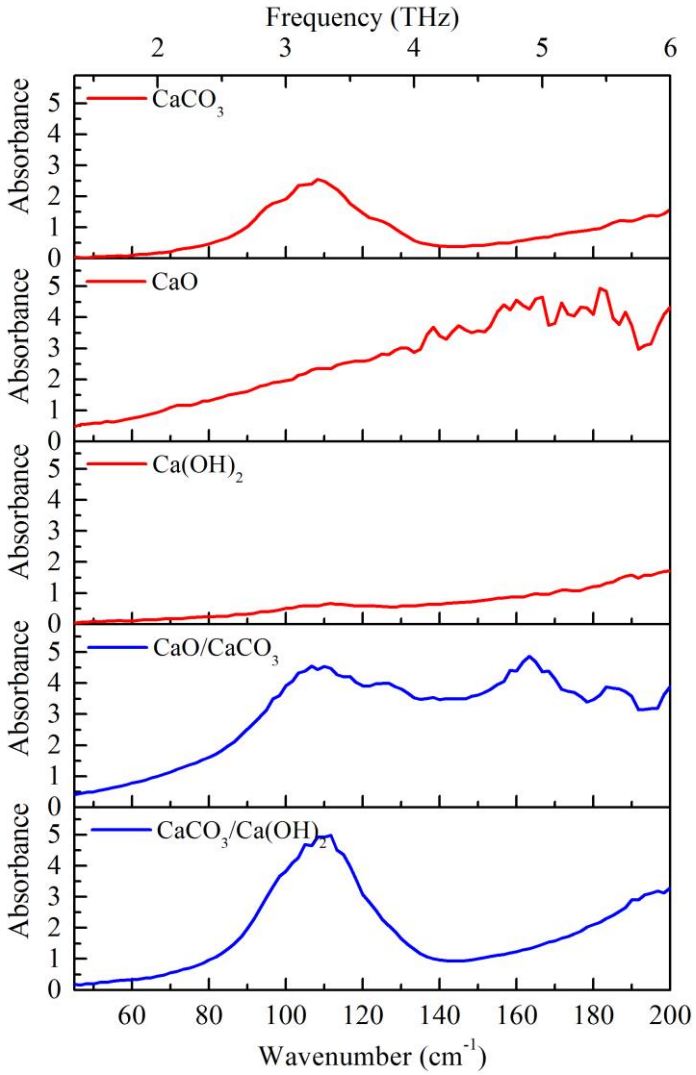


Supplementary Fig. 4. FTIR spectra of pure calcium compounds and $CaCO_3$ binary mixtures with CaO and $Ca(OH)_2$ in PE matrix in frequency range from 1.35-6.0 THz.

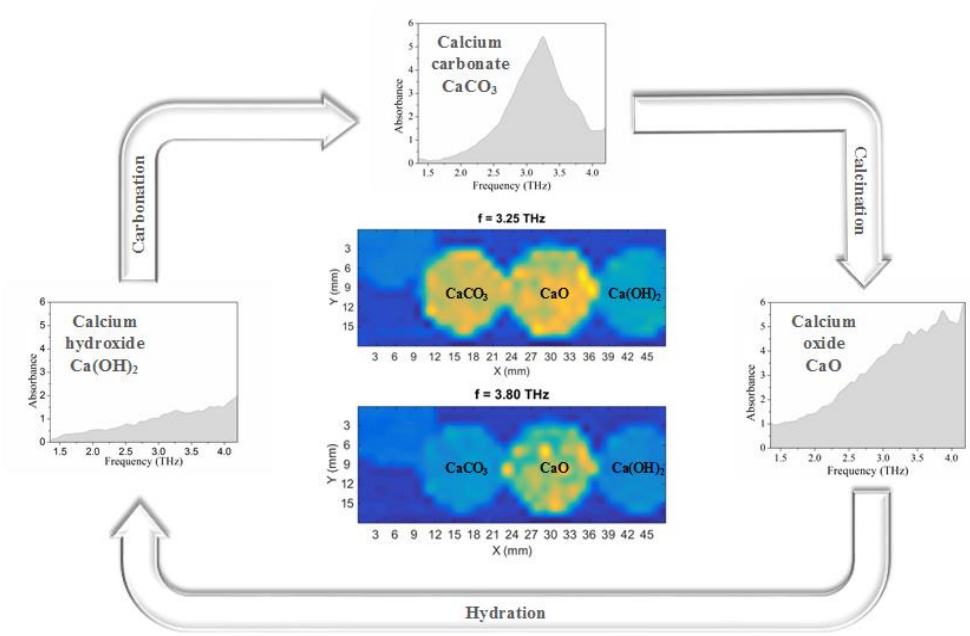


Graphical Abstract

## 4.4 Scientific article 4: Structural characterization of thermal building insulation materials using terahertz spectroscopy and terahertz pulsed imaging

***Authors:*** Andreja Abina, Uroš Puc, Anton Jeglič, and Aleksander Zidanšek
***Publication:*** NDT & E International
***Manuscript number:*** NDTEINT-D-15-00148
***Impact factor 2013:*** 1.717 ***Received date:*** 15 April 2015 (under review)

***Ranking:***

| Category name | Journal rank in category | Quartile in category |
|---|---|---|
| materials science, characterization & testing | 3/33 | 1 |

In this chapter, the paper entitled: "Structural characterization of thermal building insulation materials using terahertz spectroscopy and terahertz pulsed imaging" by Andreja Abina, Uroš Puc, Anton Jeglič, and Aleksander Zidanšek is presented. The paper is under review in NDT & E International.

The structure of insulation materials is often characterized by optical or electron microscopy at the microscale, whereas for macroscopic analysis different NDT methods are currently employed. Although several NDT techniques are available, there is an increasing demand for novel systems with greater reliability, sensibility, in-situ operation as well as simple and fast execution. The utilization of one such method, THz spectroscopy and imaging, was described in this study for the structural characterization of different types of thermal building insulation materials.

In this study, we investigated three types of thermal building insulation materials. First, we expanded our recent results on the structural characterization of insulating polymer foams with the addition of some state-of-the-art polymer foams. For all selected foams the THz absorption coefficients were calculated and THz amplitude imaging was performed to visualize the varying foam structure as well as manufacturing structural defects and internal structures. The calculated absorption coefficients of polymer foams showed an inverse relationship with the thermal conductance. Furthermore, we demonstrated that THz-TDS and TPI can be applied to study the structure of fibre-silica aerogel composite blanket considering the fibre orientation and the organic solvent-induced defect detection. In last case, the temperature induced changes of microencapsulated PCM are determined with the THz spectra analysis. Based on the achieved results, the selected method is promising for a NDT of the thermal insulation material properties and its fibrous, cellular or granular structure.

*Covering the objectives of this thesis:* This chapter addresses hypothesis 1, 2 and 3.

# Structural characterization of thermal building insulation materials using terahertz spectroscopy and terahertz pulsed imaging

Andreja Abina [a,*], Uroš Puc [a,b], Anton Jeglič [a,b], Aleksander Zidanšek [a,c,d]

[a] Jožef Stefan International Postgraduate School, Jamova cesta 39, SI-1000 Ljubljana, Slovenia, andreja.abina@mps.si

[b] Faculty of Electrical Engineering, University of Ljubljana, Tržaška cesta 25, SI-1000 Ljubljana, Slovenia, anton.jeglic@fe.uni-lj.si

[c] Department of Condensed Matter Physics, Jozef Stefan Institute, Jamova cesta 39, SI-1000 Ljubljana, Slovenia, aleksander.zidansek@ijs.si

[d] Faculty of Natural Sciences and Mathematics, University of Maribor, Koroška cesta 160, SI-2000 Maribor, Slovenia

## Abstract

Terahertz (THz) spectroscopy and imaging is used to analyse different types of thermal building insulation materials. First, the absorption coefficients of polymer foams are calculated, showing an inverse relationship with thermal conductance. In addition, manufacturing imperfections and internal structures within the foams are clearly visualized with THz amplitude imaging. Secondly, different fibre orientations within aerogel composite blanket are recognized in THz spectra and amplitude images. Lastly, the phase transition of microencapsulated phase-change material is indicated by occurrence of spectral peaks in THz spectrum. The selected method is promising for a non-destructive testing of the thermal insulation material properties and structure.

**Keywords:** THz spectroscopy, polymer foam, aerogel composite, phase-change material, non-destructive testing.

## 1. Introduction

The effectiveness of thermal insulation materials plays an important role in reducing the heat losses in civil and residential buildings and consequently contributes to lower energy costs [1]. Therefore, the development of high performance thermal insulation materials has become the hot topic of research in both academia and industry. The main function of insulating materials is to ensure low thermal conductivity and thermal transmittance, which are highly dependent on the thickness and structural properties of material (e.g. homogeneity, porosity, humidity, density, inclusions, defects, etc.) as well as the exposed environmental conditions [2]. In comparison to the traditional building envelopes, novel insulation materials have an advantage to become thinner or to be formed in a multilayered structure. These properties of modern insulation, related with high energy efficiency, are usually achieved through nanotechnology research. By incorporating nanosized additives in existing materials and by making pores in the nano range, the enhanced mechanical, thermal, and insulating properties can be reached in addition to the improved material durability and reduced environmental impact [3-5].

The structure of insulation materials is often characterized by optical or electron microscopy at the microscale, whereas for macroscopic analysis different non-destructive testing (NDT) methods are currently employed. Among them the most used are visual methods by means of digital camera and laser scanning [6], ultrasonographic methods using acoustic waves [7], infrared thermography [6] as well as microwave and millimetre

wave imaging [8, 9]. X-ray computed tomography [10] is another method for two- and three-dimensional investigation of the internal structure, however it can be time-consuming and costly. Although several NDT techniques are available, there is an increasing demand for novel systems with greater reliability, sensibility, in-situ operation as well as simple and fast execution. The utilization of one such method, THz spectroscopy, is described in this study.

Construction and building industry lags behind other sectors in applications of THz technology and its innovative practices [11]. For a long time, material properties in a frequency range between 0.3 THz and 10 THz were almost unexplored, mainly due to the lack of powerful and user-friendly THz sources and detectors. However, applications in other fields, including chemistry, pharmacy, physics, medicine, and biology showed great potential for THz spectroscopy to characterize material structure and its composition in a non-destructive and non-contact way [12]. When THz waves pass through material, they produce unique signal and spectral responses which provide information for the analysis of chemical composition, water content, porosity, material thickness, density, material aging, and some other material properties [11, 13]. In addition, supplementary imaging modality can visualize internal and surface defects, artificial inclusions, and manufacturing imperfections [8]. The majority of these approaches can be implemented for the characterization of thermal building insulation materials.

The use of traditional insulation polymer foams is increasing in building industry, particularly due to the material-specific properties such as light weight, high thermal and acoustic insulation properties, and high energy absorption capacity. Since the wavelength of THz waves is comparable to the foam cell size and the size of additives, THz spectroscopy can be used for a foam structure characterization. For instance, in previous study [14] we demonstrated that the polymer foams exhibit high transmission in most of the THz frequency region and by the comparison of transmittance spectra the discrimination of foams without additives and with the addition of small particles is possible. Most recently, there has been a growing interest in imaging of foam materials because understanding their physical and mechanical properties can significantly contribute to the optimization of their structure and composition for a given application. As a THz attenuation through the foam depends on the material density and the dielectric properties of polymer matrix, the selected method showed a potential to be utilized for the visualization of material density distribution [15]. THz imaging has been also used as a non-destructive tool for defects inspection such as voids and delaminations within the lightweight polyurethane sprayed-on foam insulation [16]. From our previously reported results [14], we can conclude that THz imaging can reveal the thermal insulating foam macrostructure like beads and their interconnections as well as artificial inclusions.

Currently, one of the most promising high-performance thermal building insulation material is aerogel [17]. It has a very porous structure, ideal for THz waves to easily penetrate through. Therefore, a THz system can be used to characterize the structure of aerogels concerning the water or other solvent content in pores during and after the drying process, and the distribution of larger pores within the material, which are not desirable for insulation purposes. One study was reported, where THz time-domain spectroscopy (THz-TDS) has been used to study silica aerogels regarding the adsorption process of the molecular vapours of water, ammonia, methyl chloride, and others [18]. Another group of insulation materials that showed great potential in building applications are phase change materials (PCMs) incorporated in the form of microencapsulated particles in a host material, e.g. concrete [19]. Their main function is to change phase from a solid to a

liquid state when heated and vice versa when cooled. For most PCMs this change occurs in the temperature range between 18 and 32 °C [1], which can be detected by THz spectroscopy.

In this study, we investigated three types of thermal building insulation materials. First, we expanded our recent results on the structural characterization of insulating polymer foams with the addition of some state-of-the-art polymer foams. For all selected foams the THz absorption coefficients were calculated and THz pulsed imaging (TPI) was performed to visualize varying foam structure as well as manufacturing structural defects and internal structures. Furthermore, we demonstrate that THz-TDS and TPI can be applied to study the structure of fibre-silica aerogel composite blanket considering fibre orientation and organic solvent-induced defect detection. In last case, the temperature induced changes of microencapsulated PCM are determined with the THz spectra analysis. Based on the achieved results, the selected spectroscopic and imaging method seems to be promising for a qualitative and quantitative NDT of the internal structure and manufacturing characteristics of thermal building insulation materials.

## 2. Experimental

### *2.1 Preparation of material samples*

Several commercially available thermal insulation polymer foams were selected for THz-TDS and TPI measurements. Table 1 summarizes the chemical composition, spatial dimensions, mass, calculated density and thermal conductance (C-value) of selected samples. The C-value is calculated by dividing the thermal conductivity, $k$, available from manufacturer specifications, with the measured thickness of the sample, $d$, expressed with the equation: $C = k/d$. The selected samples were cut with a blade into slices with almost identical planar dimensions according to the THz sample holder size. The slice thickness for each foam sample was measured at ten different positions and its average thickness was calculated. Afterwards, each slice was weighed with the precise balance and its density was calculated per unit volume. The thermal conductivity is given for the first four samples which are actually offered on the market as a thermal insulation material. For the last three samples, the data is not available.

Aerogel thermal insulation blanket (Spacetherm) was purchased from Proctor Group Ltd, whereas microencapsulated phase change material (MPCM24D) was obtained in a form of dry powder from Microtek Laboratories, Inc. For THz-TDS and TPI measurements two slices were cut out of the aerogel blanket considering different fibre orientations (horizontal, vertical). In addition, the horizontally cut slice was impregnated with one drop of paraffin oil. For the PCM measurements, a weighed portion of PCM powder equivalent to 80 mg was gently pressed between two layers of scotch tape with hands into a disk shape within the hole of sample holder with a diameter of 12 mm and thickness below 1 mm.

### *2.2 THz transmission spectroscopy and imaging apparatus*

The experiments were performed by an in-house modified TeraIMAGE system by Rainbow Photonics AG which enables THz-TDS and TPI. A detailed description and schematic drawing of the THz system based on electrooptic organic crystals in transmission geometry is explained in our previous study [14]. The spectra are given for the spectral range from 1.35 THz up to 5.0 THz with a spectral resolution of 38.5 GHz at room temperature in a compartment with nitrogen atmosphere to eliminate undesired water absorption spectral lines. For THz spectroscopy the recorded signals were averaged over 10.000 times per measurement point and the THz spectra were obtained by averaging

ten measurements in different sample points in order to reduce the effect of the measurement error and the structural differences of inhomogeneous materials. The recorded signals were pre-processed by using the following procedure: baseline correction and Blackman-Harris apodization prior to Fourier transform of the signal. After the Fourier transform the absorption coefficient $\alpha$ of the sample is calculated by equation:

$$\alpha \propto -\frac{1}{d}\log_{10}\frac{I_{reference}}{I_{sample}} = \frac{A}{d} \quad (1)$$

where $I_{sample}$ is the intensity of the THz radiation transmitted through the sample, $I_{reference}$ is the intensity of the THz radiation that passed through the reference, $d$ is the sample thickness, and $A$ is the absorbance. As a reference, a nitrogen atmosphere was selected in measurements of polymer foams and a scotch tape in case of aerogel composite and PCM measurements.

For THz imaging measurements, the sample was placed in a sample holder on a translational stage. The amplitude images with a spatial resolution of 0.05 mm or 0.1 mm depending on the sample structure were taken by raster scanning at a fixed temporal delay, in our case at the maximum amplitude of the THz waveform. At each point on the sample, the amplitude of the THz field is recorded in a matrix while scanning the sample across the THz beam. Afterwards, the obtained raw THz amplitude image was enhanced by image processing of brightness and contrast, in addition to mathematical functions (square root, cosine) and median spatial filtering to highlight specific image characteristics.

## 3. Results and discussion

### *3.1 THz spectroscopy and imaging of insulating polymer foams*

Thermal insulating polymer foams are made up of a solid polymer matrix and gas-filled bubbles which give the foam a closed-cell or open-cell structure. Cellular foams are made from small cells separated from each other, e.g. closed-cells in extruded polystyrene (XPS) foam, whereas granular insulation contains small elements with voids, such as beads in expanded polystyrene (EPS) foam. The insulating properties, flexibility and recyclability of foam are determined by micro- and macrostructure, that both are dependent on the size and shape of cells, their number and interconnections (e.g. crosslinking in polyethylene foam). The preferred selection for a good insulator is a large number of smaller pores in the foam which disable the heat transfer with the gas and consequently contributes to the low total thermal conductivity [2]. As the transmission of THz waves through the polymer foam is also related to the foam structure, we presume that there should be a relationship between the thermal conductance and the THz absorption coefficient. Thus, the investigation of THz absorption within the polymer insulating foams can contribute to the understanding of foams physical and mechanical properties as well as its structure and composition.

In previous study, we showed that different polymer foams of the same thickness exhibit different transmittance in the frequency range between 1.0 THz and 6.0 THz due to different structure, i.e. closed-cell and open-cell, the incorporation of graphite particles, chemical composition, and different foam density [14]. Herein, these properties are verified by calculating the absorption coefficients of various polymer foams. Figure 1a shows the absorption coefficients of the most used thermal insulating polymer foams in the frequency range between 1.35 THz and 5.0 THz. The envelope of mean spectra presents the standard deviation of the errors in the measurement of absorption with respect

to the differences in the foam structure across the sample slice. The lowest scattering is observed for XPS foam where the structure of foam is the most homogeneous. In case of EPS foams, the scattering is higher because the wavelength of THz radiation is comparable to the cell size in EPS foam what distorts the propagation of THz pulses through the material. Among all samples, the EPS foam exhibits the lowest absorption coefficient which varies slightly within the frequency range of measurement. The THz absorption coefficient increases with increasing frequency for other three materials, i.e. XPS, Neopor and Bakelite foam. The higher absorbance of Neopor in comparison to EPS is presumable due to the incorporation of carbon particles within the foam which act as an IR absorber and scatter THz waves. The increased density on account of closed-cell structure in case of XPS increases the THz absorbance due to the scattering of THz radiation and absorption effects in compact polymer matrix. The dense polymer foam structure becomes less transparent to IR radiation and the thermal conductivity decreases, which can be clearly seen by comparing the absorption coefficients of open-cell EPS and closed-cell XPS foams with the same chemical composition of polystyrene but different structure. Thus, based on the recorded THz spectra, the one is capable to discriminate between cellular and granular materials. The highest absorption coefficient is observed for Bakelite foam which has the highest density per volume unit. The results on absorption coefficients are in complete agreement with the previously reported transmission spectra in [14].

In Fig. 1b we present the relationship between the thermal conductance and THz absorption coefficient of polymer foams. One can notice that the thermal conductance is inversely proportional to the absorption coefficient given at all three selected THz frequencies. Figure 1b also shows that the THz absorption coefficient varies the most for Bakelite foam which has the highest thermal conductance, whereas for EPS foam the value of $\alpha$ is almost unchanged for all three selected THz frequencies.

Additionally, we examined three insulating foams that are less common in civil building engineering applications. Plastazote is a cross-linked polyethylene foam with a closed-cell structure which is extensively used as an insulation in the aviation and aerospace industry as well as in kitchen appliances. The measurements show that the plastazote foam has a very similar spectral response in the THz frequency range as Neopor, considering the spectrum amplitude level and the increasing absorption coefficient with frequency (Fig. 1c). Moreover, its density per unit volume is also close together. The neoprene foam with closed-cell structure plays an important role in thermal regulation in water environment. The THz spectral response of neoprene foam in Fig. 1c shows characteristic peak at around 3.1 THz. Due to this characteristic THz spectral feature, the neoprene foam can be used for the THz frequency-selective elements, e.g. bandpass filtering. The last tested material was micromass made up from micro-size glass bubbles linked with meniscus-shaped bridges that can be mixed with a polymer-based material and used as a thermal insulation. This material is highly absorbing to THz radiation as presented in Fig. 1c. Because the size of glass spheres is comparable to the wavelength of THz waves, strong scattering is observed in the whole frequency range of the measurement. The results show that both, plastozote and micromass foam absorb nearly as much or more of far IR radiation in comparison to thermal insulting foams that are usually applied as insulator in civil building elements. Therefore, the less common insulating foams in a form of thin panels can be more often applied to reduce heat losses in civil and residential buildings, where usually EPS foam is selected. From the manufacturer specifications and experimental results we found that the increased density

reduces thermal conductivity and increases the THz absorbance. Since the thickness of the foam is presented in both equations, for the calculation of C-value and in equation 1, the thermal conductance, $C$, is in relation with the absorption coefficient, $\alpha$, by the following equation:

$$Ck \propto -\frac{1}{\alpha}\log_{10}\frac{I_{reference}}{I_{sample}} = \frac{A}{\alpha} \quad (2)$$

Hence, THz spectroscopy has a potential to be used as a NDT tool to improve the understanding of the efficiency and behaviour of thermal insulating foam materials.

For the investigation of insulating foam macrostructure, we used TPI which was already applied to reveal the foam structures like beads and their interconnections [14]. The THz amplitude image of EPS in Fig. 2a shows the structure of the open-cell structured foam, considering the beads and their intermediate connections. In the case of plastazote (Fig. 2b), the THz image present the closed-cell structure where the distribution of air bubbles within the foam is clearly visible. In addition, we performed the THz imaging of manufacturing defects and internal structures within the Neopor foam. In Fig. 2c the bead without carbon additive is well observed in THz amplitude image because this part becomes more transparent to IR radiation comparing to the surrounding beads enhanced with IR absorbers. In Fig. 2d the location and size of the hole within the Neopor foam can be identified due to the absence of absorbing polymer matrix in that area. We demonstrated that TPI can be used to detect and locate internal structures and defects in opaque polymer foams.

### *3.2 THz spectroscopy and imaging of aerogel composite blanket*

Silica aerogels are an advanced alternative to traditional insulating polymer foams due to their 2–2.5 times better thermal performance with thermal conductivity from 0.015 W/mK on. However, the high costs of the material still present the main obstacle for its broader use in building industry. The aerogel composite is usually prepared by adding organic or inorganic fibres or a fibrous matrix (e.g. mineral wool, glass, polymer) to a silica gel, following by the supercritical drying of the gel [17]. The mechanical properties of such material strongly depend on the fibre content and the fibre orientation within the sample. Therefore, these parameters determining the fibrous structure of aerogel composite blanket were investigated with THz-TDS and TPI. The selected aerogel composite is made up of several layers composed of small diameter fibres with the mean diameter of around 10 μm. The direction of fibres is usually oriented to the flow direction, thus on micrographs in Fig. 3b in vertical cut the parallel fibres oriented in one direction can be observed, whereas in horizontal cut the fibres are settled more randomly. For this reason, we performed TPI measurement of vertical and horizontal cut slices. TPI images of the two-dimensional surface and internal morphology of the investigated aerogel composite samples are shown in Fig. 3b. As shown in this figure the parallel direction of fibres can be clearly distinguished from randomly oriented fibres from THz amplitude images. In addition, the changes in fibres orientation are presented by THz spectra in Fig. 3a, where the spectral peaks are more expressed in case of parallel orientation of fibres in comparison to perpendicular orientation in the same vertically-cut slice. To summarize, the TPI can reveal the structure of aerogel composite blanket regarding the fibre content as well as the preferential fibre orientation, which determine the physical and mechanical properties of the final material and can be controlled during the technological process.

Fibre-silica aerogel composite blankets are usually water repellent and due to its low surface energy they absorb only liquids with the lower value of surface energy in comparison to aerogel blanket [20]. The absorption mainly depends upon the surface

tension of the liquid and the chemical composition of absorbent, especially on its surface. Therefore, the studies showed that aerogel is an excellent absorber for organic liquids such as oils [20, 21]. In our experiment we selected paraffin oil with quite low surface tension (26 $mNm^{-1}$) allowing to wet the hydrophobic aerogel composite blanket surface. In Fig. 3c, we demonstrate that THz amplitude imaging can visualize that the organic liquid with surface tension below that of the aerogel composite is absorbed and spread within the material.

### *3.3 THz spectroscopy of microencapsulated phase change material*

PCMs incorporated in concrete, gypsum plasterboards, tiles, and insulations, are used to regulate temperature and for heat storage in building materials in order to increase the energy efficiency of buildings. Microencapsulated PCMs are microsized two-component particles, usually in a form of spheres, containing a core PCM material with a melting point in the range from -30 °C to 55 °C and an outer capsule wall frequently made of polymer material. Besides melting temperatures, different PCMs differ in its chemical nature, but during heating/cooling cycles its latent heat retains the same without any changes in physical or chemical properties [19]. Various paraffins are typically used in building materials as PCMs, but its low thermal conductivity in the solid state and a large volume change during phase transition limit their practical building applications [2].

THz-TDS was already applied to characterize the amorphous and crystalline state of inorganic PCM materials used for optical data storage devices [22]. In our experiment, we evaluated an organic PCM material with the paraffin wax as a thermal storage material with a phase change from solid to liquid at a temperature of 24 °C. In Fig. 4a the microscopy image of a selected PCM material is represented, containing spherical particles with an approximate size between 10 μm and 20 μm. First, we placed the PCM powder sample in a refrigerator at -12.5 °C for 2 hours. Afterwards, we recorded THz spectra successively every 3 minutes allowing the sample to warm to room temperature at 21.5 °C. As presented in Fig 4b, the THz spectrum recorded after 4 minutes highly differs from other THz spectra recorded before and after that time. The same trend can be observed in Fig. 4c, where the THz spectra are measured every 3 minutes after the sample was heated with a hair dryer for two minutes. The THz spectrum depicted with circles measured after 3 minutes of heating exhibits different spectral response than the other THz spectra recorded before and after that time. The spectral features that occur in these two spectra depicted with circles in Figs. 4b and 4c are not the consequence of the scattering in PCM particles because its size is not comparable with the wavelength of THz radiation in the selected frequency range. Hence, we assume that these spectral features are the result of phase change of paraffin wax from liquid to solid state and vice versa. The effect is well expressed even at lower frequencies when the sample was heated and left to cool to room temperature. Therefore, the THz spectroscopy can be a suitable method to characterize the influence of PCMs on specific properties (e.g. freeze-thaw durability, the duration of the PCM cooling and heating effect) of matrix material in which PCM can be incorporated, especially polymer matrix which is almost transparent for THz waves.

## 4. Conclusions

In this paper, we showed that THz spectroscopy and imaging has a potential to become a NDT method of choice for evaluation and improvement of the existing thermal insulating materials as well for the development of novel high performance thermal insulation materials. Furthermore, we demonstrated that THz spectroscopy and imaging has the

capabilities to characterize fibrous, cellular and granular types of thermal building insulation materials. The results show that the selected method can be used as a valuable substitute or complement to other non-destructive sensing techniques using ultrasound, microwaves, infrared, or X-ray waves. It is expected that the potential of THz spectroscopy for characterization of thermal building insulation materials will improve significantly when radical progress will be achieved in new high-speed, high-resolution, and high-power sources. Until then, the best accuracy and reliability of results is still achieved with a combination of various NDT methods. However, this study opens some new pathways in the THz based characterization of building and construction materials. Special consideration should be given for the assessment of thermal insulation materials, because the results of this study showed that optical coefficients calculated by THz measurements are in relationship with the material properties providing energy efficient thermal performance.

## Acknowledgements

The authors would like to acknowledge financial support from the Slovenian Research Agency grants P2-0348-2338 and J2-4266. Special acknowledgement is given to the Saint-Gobain gradbeni izdelki, d.o.o. and Microtek laboratories, Inc, who provided samples of commercially available insulation polymer foams and phase change materials, respectively.

## References

[1] Pacheco-Torgal F. Eco-efficient construction and building materials research under the EU Framework Programme Horizon 2020. Constr Build Mater. 2014;51:151-62.

[2] Jelle BP. Traditional, state-of-the-art and future thermal building insulation materials and solutions – Properties, requirements and possibilities. Energy Build. 2011;43:2549-63.

[3] Pacheco-Torgal F, Labrincha JA. The future of construction materials research and the seventh UN Millennium Development Goal: A few insights. Constr Build Mater. 2013;40:729-37.

[4] Sanchez F, Sobolev K. Nanotechnology in concrete – A review. Constr Build Mater. 2010;24:2060-71.

[5] Pacheco-Torgal F, Jalali S. Nanotechnology: Advantages and drawbacks in the field of construction and building materials. Constr Build Mater. 2011;25:582-90.

[6] Costanzo A, Minasi M, Casula G, Musacchio M, Buongiorno MF. Combined Use of Terrestrial Laser Scanning and IR Thermography Applied to a Historical Building. Sensors. 2015;15:194-213.

[7] Torres-Sanchez C, Corney JR. Effects of ultrasound on polymeric foam porosity. Ultrason Sonochem. 2008;15:408-15.

[8] Oyama Y, Zhen L, Tanabe T, Kagaya M. Sub-terahertz imaging of defects in building blocks. NDT and E Int. 2009;42:28-33.

[9] Kim YJ, Jofre L, De Flaviis F, Feng MQ. Microwave subsurface imaging technology for damage detection. J Eng Mech-ASCE. 2004;130:858-66.

[10] Elmoutaouakkil A, Fuchs G, Bergounhon P, Péres R, Peyrin F. Three-dimensional quantitative analysis of polymer foams from synchrotron radiation x-ray microtomography. J Phys D: Appl Phys. 2003;36:A37.

[11] Abina A, Puc U, Jeglič A, Zidanšek A. Applications of Terahertz Spectroscopy in the Field of Construction and Building Materials. Appl Spectrosc Rev. 2014;50:279-303.

[12] Pawar AY, Sonawane DD, Erande KB, Derle DV. Terahertz technology and its applications. Drug Invention Today. 2013;5:157-63.

[13] Jansen C, Wietzke S, Peters O, Scheller M, Vieweg N, Salhi M, et al. Terahertz imaging: applications and perspectives. Appl Opt. 2010;49:E48-E57.

[14] Abina A, Puc U, Jeglič A, Zidanšek A. Structural analysis of insulating polymer foams with terahertz spectroscopy and imaging. Polym Test. 2013;32:739-47.

[15] Brahm A, Schmidt D, Riehemann S, Notni G, Wostmann FJ, Tunnermann A. Non-destructive determination of the density distribution of polymer foam models with THz-pulses. 35th International Conference on Infrared Millimeter and Terahertz Waves (IRMMW-THz). Italy, Rome: IEEE; 2010. p. 1-2.

[16] Zhong H, Xu JZ, Xie X, Yuan T, Reightler R, Madaras E, et al. Nondestructive defect identification with terahertz time-of-flight tomography. IEEE Sens J. 2005;5:203-8.

[17] Baetens R, Jelle BP, Gustavsen A. Aerogel insulation for building applications: A state-of-the-art review. Energy Build. 2011;43:761-9.

[18] Zhang JQ, Grischkowsky D. Terahertz time-domain spectroscopy study of silica aerogels and adsorbed molecular vapors. J Phys Chem B. 2004;108:18590-600.

[19] Ling T-C, Poon C-S. Use of phase change materials for thermal energy storage in concrete: An overview. Constr Build Mater. 2013;46:55-62.

[20] Parale VG, Mahadik DB, Kavale MS, Rao AV, Wagh PB, Gupta SC. Potential Application of Silica Aerogel Granules for Cleanup of Accidental Spillage of Various Organic Liquids. Soft nanosci lett. 2011;1:97-104.

[21] Chandradass J, Kang S, Bae D-s. Synthesis of silica aerogel blanket by ambient drying method using water glass based precursor and glass wool modified by alumina sol. J Non-Cryst Solids. 2008;354:4115-9.

[22] Kadlec F, Kadlec C, Kužel P. Contrast in terahertz conductivity of phase-change materials. Solid State Commun. 2012;152:852-5.

Table 1: Characteristics of insulating polymer foam samples

| Polymer foam | Chemical composition | Slice length (mm) | Slice width (mm) | Slice thickness (mm) | Mass (mg) | Density ($kg/m^3$) | k (W/mK) | C-value ($W/m^2K$) |
|---|---|---|---|---|---|---|---|---|
| EPS | polystyrene | 20 | 20 | 3.25 | 24.6 | 18.92 | 0.040 | 12.31 |
| XPS | polystyrene | 20 | 20 | 2.95 | 34.7 | 29.42 | 0.034 | 11.54 |
| Neopor | polystyrene with nm carbon black | 19 | 20 | 3.03 | 35.3 | 30.72 | 0.032 | 10.57 |
| Phenolic foam | bakelite | 20 | 20 | 2.49 | 33.0 | 33.16 | 0.024 | 9.65 |
| Neoprene | polychloroprene | 21 | 20 | 2.05 | 61.8 | 71.68 | NA | NA |
| Plastazote | polyethylene | 19 | 19 | 2.76 | 31.4 | 31.54 | NA | NA |
| Micromass | glass microspheres | 20 | 20 | 1.60 | 137.5 | 214.84 | NA | NA |

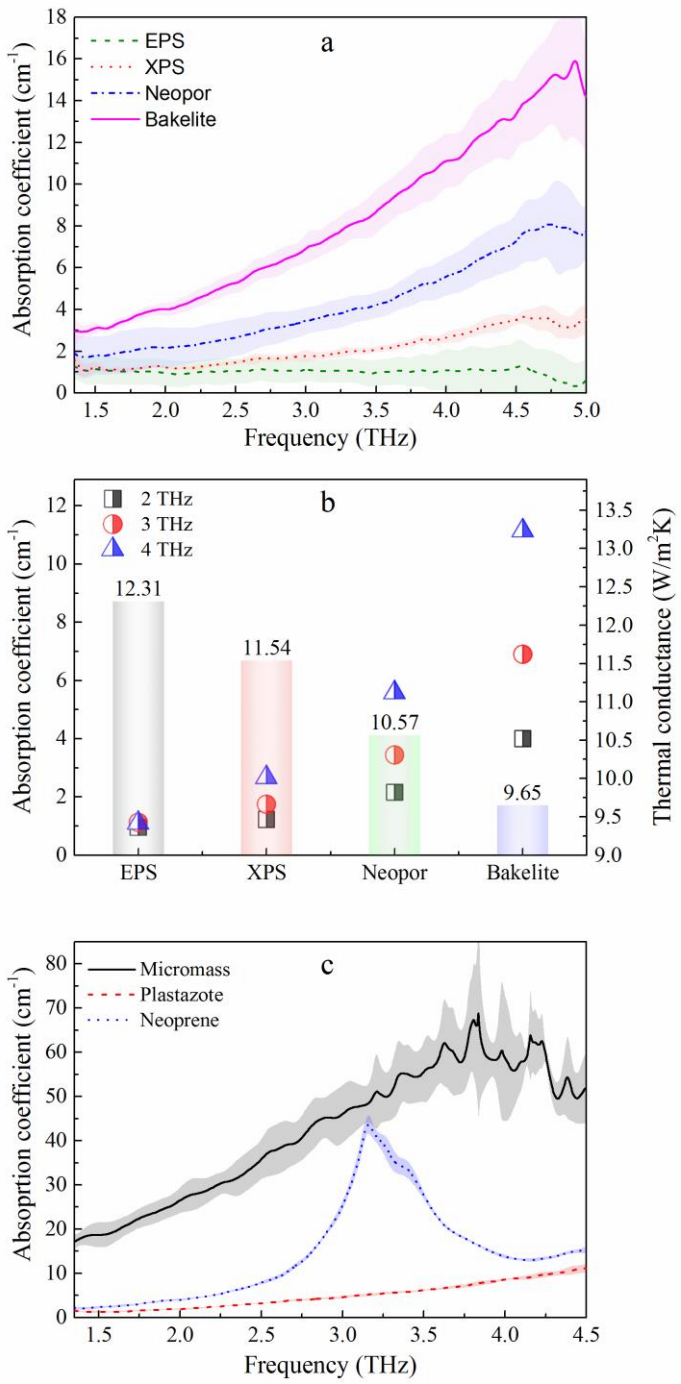


Fig. 1. Absorption coefficient of a variety of thermal insulating polymer foams in the frequency range between 1.35 THz and 5.0 THz (a); relation between absorption coefficient at selected THz frequencies and the thermal conductance of polymer foams (b); absorption coefficients of insulating foams applied for special applications (c).

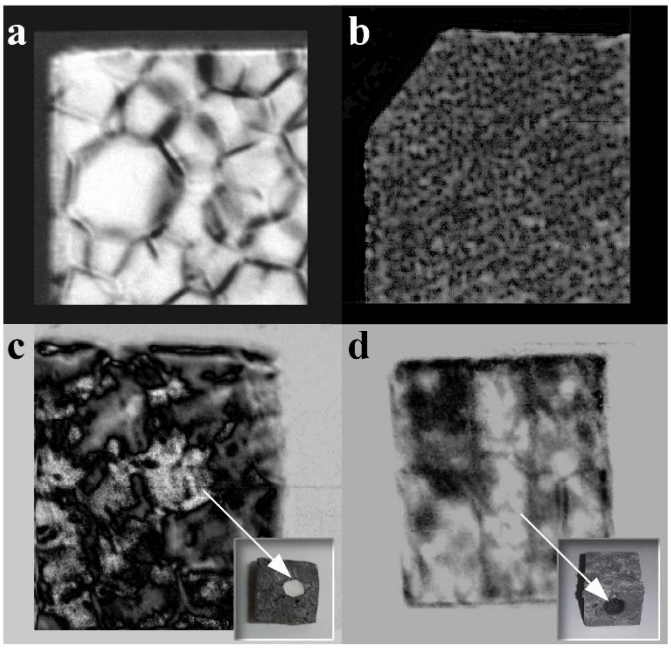


Fig. 2. THz imaging of bead structure in EPS foam (a), closed-cell cross-linked polyethylene foam (b), imperfections (c) and internal structures (d) within the Neopor foam.

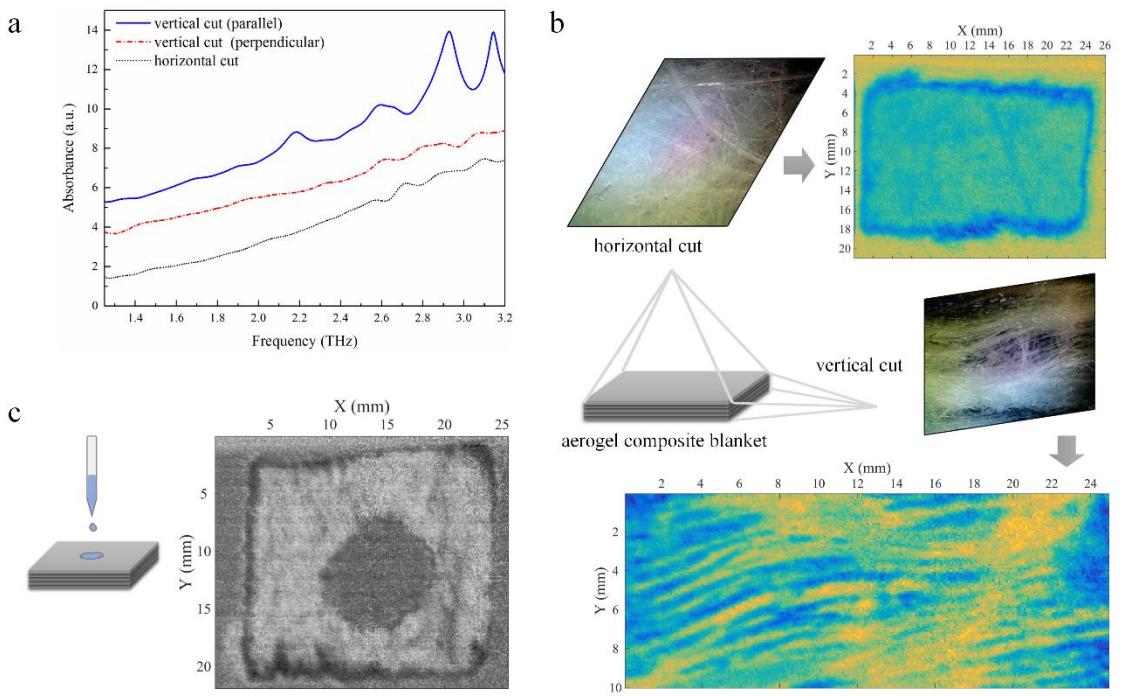


Fig. 3. THz absorbance spectra of aerogel composite blanket for vertical cut in both fibre directions and horizontal cut (a); THz amplitude images and optical microscopy images of horizontal and vertical cut slices of aerogel composite blanket (b); THz amplitude imaging of paraffin drop absorbed within aerogel composite blanket (c).

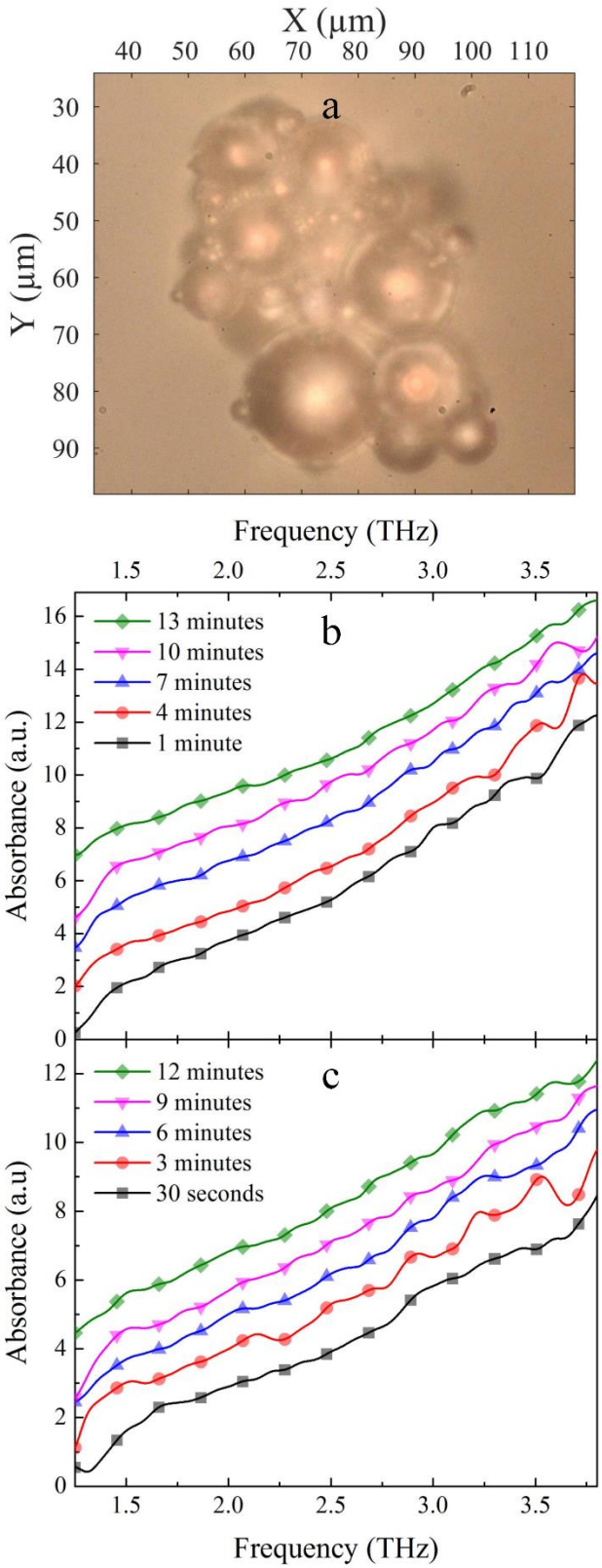


Fig. 4. Microscopy image of microencapsulated PCM at 60x magnification (a). The influence of temperature induced phase change of microencapsulated PCM on THz spectrum during heating from -12.5 °C to room temperature (b) and during cooling from temperature above phase change to room temperature (c).

# 5 Discussion

This chapter draws together and discusses the conclusions from the work presented in this thesis, as well as proposes several directions for further research related to characterization of building and construction materials. The contributions of the thesis and a brief discussion of the results are presented under each stated objective of this thesis:

1. **To make a systematic overview of related work on construction materials and materials used in other fields that can also be applied as construction and building materials;**

NDT methods for assessing the construction materials and building structures have to be extensively developed and tested in accordance to industry that has the need to apply new technologies. After a systematic review of the field, we found that construction and building industry is still behind other sectors in terms of taking advantages of THz technology and its innovative practices. To our knowledge, this dissertation provided the first systematic overview of the current applications of THz technology in that field. During the review we observed that THz waves, when they pass through different materials, produce unique signal and spectral responses that can be applied for the analysis of chemical composition, water content, porosity, material thickness, density, material aging, and others. In addition, the supplementary imaging THz system configuration is capable to visualize hidden internal and surface defects, inclusions, and manufacturing imperfections. These approaches can be partially used also in the construction industry, where THz spectroscopy and imaging can be a valuable substitute or complement to other sensing techniques using ultrasound, microwaves, IR, or X-ray waves. Based on several approaches employed for the characterization of materials similar to those used in construction industry, we can claim that THz technology has a promising potential for both researchers, to understand the structure of construction and building materials, and engineers to manipulate the production processes leading to the enhanced material properties and its durability.

2. **To perform qualitative and quantitative THz spectroscopic and imaging analysis on different types of construction and building materials, including foams, composites, microfillers, and microencapsulated materials;**

Understanding the propagation of THz waves through the selected materials was applied to both, the qualitative and quantitative analysis of the macrostructure of investigated construction materials and its chemical composition. Most of the selected materials (e.g. aerogel composite, microencapsulated PCM, micromass, plastazote, Bakelite foam, calcium oxide, calcium hydroxide) were explored by THz radiation for the first time, thus we contributed to the worldwide databases on THz spectroscopy.

First, we demonstrated that several thermal insulating polymer foams feature low absorption coefficient in the THz region which makes THz-TDS and TPI viable methods for characterizing its macrostructure with a submillimetre-scale resolution. In addition, we showed that THz waves have the ability to image voids, inclusions, manufacturing defects, and bead distribution in these materials. Since the wavelength of THz radiation is

comparable to cell size and additives in polymer foams, we were able to determine certain material characteristics such as cell density or IR radiation absorption by measuring the difference between THz waveforms and by calculating the spectroscopic constants.

Secondly, we applied THz spectroscopy to detect and quantitatively analyse calcite microfillers in polymer matrix, to evaluate the effect of powder granulation on THz spectrum, and to discriminate different chemical treatments. Based on the analysis of peak absorbance amplitude, peak frequency position, and the appearance of additional spectral features, quantitative and qualitative analysis was successfully achieved. In addition, THz imaging was also applied for both quantitative and qualitative analysis of calcium-based microfillers. By using spatial distribution map, the inhomogeneity in concentration of calcium carbonate in polymer matrix was characterized. Moreover, by THz spectroscopy and multispectral imaging different calcium compounds were detected in binary mixtures showing that the selected techniques are capable to follow the reactions of decarbonation/carbonation route or to detect the presence of reactants in an incomplete chemical reaction.

In the third case, the structure of aerogel composite blanket regarding the fibre content as well as the preferential fibre orientation was recognized in THz spectra and THz amplitude images. In case of microencapsulated PCM, its phase transition from solid to liquid and vice versa was indicated by occurrence of spectral features in THz spectrum.

The results of all studies showed the considerable potential of THz spectroscopy and imaging for rapid and accurate qualitative and quantitative analysis of various types of construction and building materials, including powder, granular, fibrous, cellular, and encapsulated materials.

**3. To adapt existing or to develop novel data processing procedures to generate appropriate THz spectra and THz images necessary for construction and building material analysis;**

For spectroscopic data interpretation we used the well-known calculations of spectroscopic constants (transmittance, absorbance, and absorption coefficient). Based on the calculated absorption coefficients and comparison with the manufacturers' specifications, we found that the THz absorption coefficient of polymer foams is inversely proportional to the thermal conductance. The characteristic peak method with a linear regression model was used for estimating the concentration for a particular constituent in mixtures. We proposed a special procedure how to discriminate between various granulations and chemical treatments of particles by using find spectral peak function and by analysing the spectral peak frequency position. This procedure was also used in addition to the calculation of the 1st derivative for explaining the Rayleigh and Mie scattering on particles with different granulation.

The THz imaging was performed in two different ways, as an amplitude imaging where no spectroscopic information is included and by a multispectral imaging where a Fourier transform of the time-domain waveform was calculated to obtain the spectral frequency dimension, allowing imaging at different frequencies. The amplitude images were enhanced by using image processing (brightness, contrast, mathematical functions like square root and cosine, and median spatial filtering) to highlight specific image characteristics. By using a PCA the spatial distribution of map of individual chemical substance in the sample were extracted from the multispectral THz images.

For understanding the bead size and its distribution within the foam, we prepared a special algorithm for image processing and particles analysis to extract beads in 2D using National Instruments Vision Assistant. The same algorithm with some minor changes was applied for survey of microscopy images for the evaluation of cell properties.

4. **To evaluate the THz analytical tool as a testing method for assessment of construction and building materials regarding the key advantages and limitations of the applied technology**

In the thesis, we demonstrated that THz spectroscopy and imaging has the capabilities to characterize powder, fibrous, cellular, granular and microencapsulated types of construction and building materials. The achieved results contribute to a better understanding of the propagation of THz waves through the selected materials that are also widely applied in other research fields. Furthermore, the results indicated that the selected method has several advantages and can be used as a valuable substitute or complement to other non-destructive sensing techniques using ultrasound, microwaves, infrared waves, or X-rays. We showed that THz-TDS and TPI can be used in a combination with other spectroscopic and microscopic techniques to improve the accuracy and reliability of results when evaluating the material structure. After all, the selected method is promising for a non-destructive testing of construction and building materials structure and partially its composition. Due to some system limitations, all measurements in this thesis were performed in a laboratory. Although, the THz techniques can be applied as a testing method for assessment of construction materials during manufacturing process, before that some further research and developments provided in section 4.1 and 5.1 should be executed. It is expected that the potential of THz spectroscopy for characterization of construction materials will improve significantly when radical progress will be achieved in new high-speed, high resolution, and high-power THz systems. Until then, the best accuracy and reliability of results is still achieved with a combination of various NDT methods.

## 5.1 Future challenges

The present status of THz capabilities in construction and building applications is in its early infancy, limited almost only to laboratory testing. Current THz technology will probably remain one of many materials characterization tools, until radical progress will be achieved in the field of new high-speed, high resolution and high-power THz systems. Until then, the research of construction and building materials by using existent THz techniques should be enhanced and brought to such a level that when adequate technology will be at hand it could be easily transferred to a commercial use. There are some research tasks that have to be done in the future:

1. Construction of THz database for construction and building materials that can be a part of a uniform database that is still missing in the field of THz science. Further experiments could also be undertaken to measure the THz spectroscopic parameters of other materials, e.g. core materials of vacuum insulated panels, polyurethane polymer foams, hydrogel, coatings, adhesives, nanofoams, nanoaditives, etc.
2. Since the building materials are not chemically pure and their structure is in most cases inhomogeneous, various statistical analysis methods and computer vision should probably be developed to improve the reliability of THz measurements.
3. Development of novel or adaptation of existing algorithms for signal and image processing to achieve the enhanced interpretation of THz measurement results.
4. Development of tomography THz system and corresponding imaging method that will allow a 3D structure reconstruction similar to the one used in radar or X-ray CT imaging where the principle of voxels is applied.
5. Improved the sensitivity of THz system, thus the detection of small concentrations of additives in construction and building materials should be achieved. By using near-field techniques, higher spatial resolution down to nm could be achieved.
6. Study the influence of temperature and humidity on the analysis of construction and

building materials by THz systems considering existing standards due to the fact that these materials are usually exposed to various environmental conditions.

7. For some advanced construction materials a THz system capable of cryogenic measurements should be developed. Such a system would also contribute to the understanding of thermal properties of building insulation materials.
8. Development of portable battery powered handheld THz systems in reflection mode which can be easily implemented to online monitoring in industry or allow in-site NDT of larger surfaces in various environmental settings, e.g. on historic houses.
9. Development of THz system achieving greater penetration depth necessary for analysis of thicker samples of materials that are usually applied for construction and building purposes.

In our laboratory, we plan to improve the existing THz system with the development of novel mechanical delay line which will speed up the data acquisition and scanning rate necessary to achieve close to real-time spectroscopy and imaging. Furthermore, we are planning to develop a THz imaging system that will operate in reflection mode with a software for 3D image reconstruction similar to the one used for ground penetrating radar. With additional financial support, the THz system will be upgraded to all-fibre setup system for which the current laser source and THz generator/detector would probably be replaced with the photoconductive antennas and high-performance laser. We believe that such a system will give more valid results in laboratory and will be more appropriate for industrial use.

# 6 Conclusions

The work presented in this thesis has been concerned with the structural characterization of construction and building materials by using THz radiation, with the emphasis on thermal insulation materials and microfillers. The experimental work performed in the thesis was initially motivated by searching the possible applications of THz technology in the field of construction and building industry. For realization of THz system application performance, we verified its capabilities in that field and performed some laboratory tests.

Before experimental studies a systematic review was performed in order to explore the capabilities of THz spectroscopy and imaging in the field of materials characterization. In this study we focused on other similar materials and their properties that are also commonly applied in construction and building industry. The existing studies proved that THz technology is a valuable tool in materials inspection. In particular, numerous advantages of THz radiation that enable non-contact, non-ionizing, and room temperature measurements with submillimetre resolution and relatively high accuracy, give THz spectroscopy and imaging an opportunity to be used as a complementary analysis tool to other NDT methods, using ultrasound, microwaves, FIR and NIR radiation, visible light or X-rays. For construction and building materials, the most important knowledge is that when THz waves pass through materials, unique signal and spectral responses are recognized which can be applied for analysis of chemical composition, water content, porosity, material thickness, density, material aging, and other properties potentially interesting for construction industry.

Since the majority of THz studies were dedicated to plastics, glasses, wood, concrete, paints, carbon and glass fibre-based composites, we selected insulating foams, calcium-based microfillers, aerogel composite and microencapsulated PCM, among which some were not yet investigated by THz spectroscopy. With the selection of these materials we covered five different types of materials, including powder, granular, fibrous, cellular, and microencapsulated materials. First, we performed a qualitative and quantitative study on calcium-based microfillers, because chemical substances containing calcium act as a key material in construction industry, especially in a lime cycle. In this study, we applied THz spectroscopy and spectroscopic imaging to analyse microfillers concentration in polymer matrix, its granulation and chemical treatment as well as to identify different calcium-based microfillers based on characteristic spectral responses of each chemical compound that was visualized by THz spectral images. In the second study, we demonstrated that by measuring the difference between THz waveforms and by calculating the spectroscopic constants from THz spectra one can determine certain foam characteristics such as density, IR radiation absorption, thermal conductance, the presence of additives, and cell type. Moreover, the THz imaging was applied to analyse and visualize the beads structure of foams considering bead size and shape, their interconnections and spatial distribution. For foam material, THz imaging turned to be a promising solution to the problems related with identifying and evaluating the presence of air gaps, surface and internal defects, manufacturing imperfections, inclusions and prebuilt internal macrostructures, that all contribute to ensuring safety, durability and efficiency of building constructions. In additional research study, two advanced thermal insulation materials were investigated, including fibre-silica aerogel composite and PCM. The results showed that THz spectroscopy is capable to

resolve the structure of fibrous aerogel composite considering the fibre orientation and to detect the phase change of PCM during freeze-thaw process. The fibrous structure and organic solvent absorption of aerogel composite were also evaluated by THz images.

In discussion, we highlighted some of the future issues that science and engineering will have to consider in order to successfully implement THz applications in construction and building industry. We also emphasized which issue will be addressed in future work from our laboratory. The demonstrations executed in the frame of the thesis are only a start to some of the capabilities which confirm that THz technology has a potential to be applied for characterization of construction and building materials. Future research and progress in THz spectroscopic and imaging development will ensure that the selected method will be more effectively used in that field. For real-world applications the most important factors are high speed, high resolution and high sensitivity of the THz systems. It is hoped that this thesis contributes to current knowledge and understanding about the implementation of THz systems in the selected field and thus, enables some interesting future research and developments.

# 7 Acknowledgements

First, I wish to thank my advisor Prof. Dr. Aleksander Zidanšek for his support and guidance during my doctoral studies. I am also grateful for the support, technical help and advice to my colleague Uroš Puc. I would also like to thank to my research group of collaborators, especially Prof. Dr. Anton Jeglič, Dr. Pavel Cevc and Mr. Vito Eržen, as well as my colleagues from the Jožef Stefan International Postgraduate School (IPS) and the Jožef Stefan Institute (JSI) for many valuable discussions and contributions. I need to express my gratitude to the IPS personnel (Mrs. Margareta, Tadeja, Sergeja and Maša).

The members of my dissertation committee, Prof. Dr. Zvonko Trontelj, Prof. Dr. Anton Jeglič, and Prof. Dr. Gintaras Valusis, have generously given their time and expertise to better my work. I thank them for their contribution and their remarks.

My hopes and dreams to be a small part of the world of research and science would never come true without the meeting with Prof. Dr. Aleksandra Kornhauser-Frazer at my master's degree study, who gave me an opportunity to become a member of Prof. Dr. Blinc research team. At that point, I would like to thank her and also my supervisor at undergraduate study Prof. Dr. Margareta Vrtačnik and her team at the UL, Faculty of Natural Sciences and Engineering, Department of Chemical Education and Informatics, who provided some good recommendations about me to Prof. Dr. Aleksandra Kornhauser-Frazer.

I would like to thank the Department of Condensed Matter Physics at IJS for their support concerning the measurements at electron, confocal and optical microscopy, as well as for the use of other laboratory equipment.

I am grateful to Prof. Dr. Gintaras Valušis and his research team at the Department of Optoelectronics, Center for Physical Sciences and Technology, Vilnius, Lithuania, for their support regarding FTIR and THz measurements, their contribution to the science of paper and sharing a lot of experience.

I must also acknowledge many friends, colleagues, teachers, and other people who assisted, advised, and supported my research and writing efforts over the past few years. Without you, this work would be hardly completed.

Hvala moji in Markovi družini za vso ljubezen, razumevanje in spodbudne besede, ki sem jih bila deležna na poti do uspešno zaključenega študija.

*Last and definitely the most special, I will never forget working with Prof. Dr. Robert Blinc. His words of wisdom will inspire me for life.*

# 8 References


[1] Lewis RA. A review of terahertz sources. *Journal of Physics D: Applied Physics.* 2014;47(37):374001.

[2] Scheller M, Yarborough JM, Moloney JV, Fallahi M, Koch M, Koch SW. Room temperature continuous wave milliwatt terahertz source. *Optics Express.* 2010;18(26):27112-27117.

[3] Walther M, Fischer BM, Ortner A, Bitzer A, Thoman A, Helm H. Chemical sensing and imaging with pulsed terahertz radiation. *Analytical and Bioanalytical Chemistry.* 2010;397(3):1009-1017.

[4] Yu C, Fan S, Sun Y, Pickwell-MacPherson E. The potential of terahertz imaging for cancer diagnosis: A review of investigations to date. *Quantitative Imaging in Medicine and Surgery.* 2012;2(1):33-45.

[5] Naftaly M, Miles RE. Terahertz Time-Domain Spectroscopy for Material Characterization. *Proceedings of the IEEE.* 2007;95(8):1658-1665.

[6] Pawar AY, Sonawane DD, Erande KB, Derle DV. Terahertz technology and its applications. *Drug Invention Today.* 2013;5(2):157-163.

[7] Qin J, Ying Y, Xie L. The Detection of Agricultural Products and Food Using Terahertz Spectroscopy: A Review. *Applied Spectroscopy Reviews.* 2013;48(6):439-457.

[8] Jansen C, Piesiewicz R, Mittleman D, Kurner T, Koch M. The impact of reflections from stratified building materials on the wave propagation in future indoor terahertz communication systems. *Ieee Transactions on Antennas and Propagation.* 2008;56(5):1413-1419.

[9] Oyama Y, Zhen L, Tanabe T, Kagaya M. Sub-terahertz imaging of defects in building blocks. *NDT & E International.* 2009;42(1):28-33.

[10] Piesiewicz R, Jansen C, Wietzke S, Mittleman D, Koch M, Kürner T. Properties of Building and Plastic Materials in the THz Range. *International Journal of Infrared and Millimeter Waves.* 2007;28(5):363-371.

[11] Schwerdtfeger M, Castro-Camus E, Krügener K, Viöl W, Koch M. Beating the wavelength limit: three-dimensional imaging of buried subwavelength fractures in sculpture and construction materials by terahertz time-domain reflection spectroscopy. *Applied Optics.* 2013;52(3):375-380.

[12] Robin T, Bouyé C. THz Technologies Offer Varied Options for Industry. *Industrial Photonics.* 2014;1(4). http://www.photonics.com/Article.aspx?AID=56089.

[13] Brahm A, Schmidt D, Riehemann S, Notni G, Wostmann FJ, Tunnermann A. Non-destructive determination of the density distribution of polymer foam models with THz-pulses. Paper presented at: 35th International Conference on Infrared, Millimeter, and Terahertz Waves (IRMMW-THz); 5-10 September, 2010; Rome, Italy.

[14] Pradarutti B, Riehemann S, Notni G, Tünnermann A. Terahertz imaging for styrofoam inspection. Terahertz Physics, Devices, and Systems II; 11 - 12 September, 2007; Boston, Massachusetts, USA.

[15] Zhao G, Mors Mt, Wenckebach T, Planken PCM. Terahertz dielectric properties of polystyrene foam. *Journal of the Optical Society of America B.* 2002;19(6):1476-

1479.
[16] Pastorelli G, Trafela T, Taday P, et al. Characterisation of historic plastics using terahertz time-domain spectroscopy and pulsed imaging. *Analytical and Bioanalytical Chemistry.* 2012;403(5):1405-1414.
[17] Karpowicz N, Zhong H, Zhang C, et al. Compact continuous-wave subterahertz system for inspection applications. *Applied Physics Letters.* 2005;86(5):054105.
[18] Koch M, Hunsche S, Schumacher P, Nuss MC, Feldmann J, Fromm J. THz-imaging: a new method for density mapping of wood. *Wood Science and Technology.* 1998;32(6):421-427.
[19] Skryl AS, Jackson JB, Bakunov MI, Menu M, Mourou GA. Terahertz time-domain imaging of hidden defects in wooden artworks: application to a Russian icon painting. *Applied Optics.* 2014;53(6):1033-1038.
[20] Yasuda T, Iwata T, Araki T, Yasui T. Improvement of minimum paint film thickness for THz paint meters by multiple-regression analysis. *Applied Optics.* 2007;46(30):7518-7526.
[21] Jördens C, Wietzke S, Scheller M, Koch M. Investigation of the water absorption in polyamide and wood plastic composite by terahertz time-domain spectroscopy. *Polymer Testing.* 2010;29(2):209-215.
[22] Jördens C, Scheller M, Wietzke S, et al. Terahertz spectroscopy to study the orientation of glass fibres in reinforced plastics. *Composites Science and Technology.* 2010;70(3):472-477.
[23] Chady T, Lopato P, Szymanik B. Terahertz and Thermal Testing of Glass-Fiber Reinforced Composites with Impact Damages. *Journal of Sensors.* 2012;2012:14.
[24] Naftaly M, Miles RE. Terahertz time-domain spectroscopy of silicate glasses and the relationship to material properties. *Journal of Applied Physics.* 2007;102(4):043517.
[25] Parrott EPJ, Zeitler JA, Gladden LF, Taraskin SN, Elliott SR. Extracting accurate optical parameters from glasses using terahertz time-domain spectroscopy. *Journal of Non-Crystalline Solids.* 2009;355(37-42):1824-1827.
[26] Dash J, Ray S, Nallappan K, Sasmal S, Pesala B. Non-destructive inspection of internal defects in concrete using continuous wave 2D terahertz imaging system. Paper presented at: 38th International Conference on Infrared, Millimeter, and Terahertz Waves (IRMMW-THz); 1-6 September, 2013; Mainz, Germany.
[27] Dash J, Ray S, Nallappan K, Sasmal S, Pesala B. Terahertz spectroscopy of concrete for evaluating the critical hydration level. Paper presented at: SPIE 8985, Terahertz, RF, Millimeter, and Submillimeter-Wave Technology and Applications VII; 4 February, 2014; San Francicco, US.
[28] Tripathi SR, Ogura H, kawagoe H, et al. Measurement of chloride ion concentration in concrete structures using terahertz time domain spectroscopy (THz-TDS). *Corrosion Science.* 2012;62:5-10.
[29] Verma SK, Bhadauria SS, Akhtar S. Review of Nondestructive Testing Methods for Condition Monitoring of Concrete Structures. *Journal of Construction Engineering.* 2013;2013:11.
[30] Xu G, Zhang X. *Real-Time Identification and Characterization of Asbestos and Concrete Materials with Radioactive Contamination.* Troy, NY, US: Rensselaer Polytechnic Institute;2000.
[31] Labaune J, Jackson JB, Fukunaga K, et al. Investigation of Terra Cotta artefacts with terahertz. *Applied Physics A.* 2011;105(1):5-9.
[32] Ling TC, Poon CS. Use of phase change materials for thermal energy storage in concrete: An overview. *Construction and Building Materials.* 2013;46:55-62.
[33] Jelle BP. Traditional, state-of-the-art and future thermal building insulation

materials and solutions – Properties, requirements and possibilities. *Energy and Buildings.* 2011;43(10):2549-2563.

[34] Pacheco-Torgal F. Eco-efficient construction and building materials research under the EU Framework Programme Horizon 2020. *Construction and Building Materials.* 2014;51:151-162.

[35] Pacheco-Torgal F, Jalali S. Nanotechnology: Advantages and drawbacks in the field of construction and building materials. *Construction and Building Materials.* 2011;25(2):582-590.

[36] Pacheco-Torgal F, Labrincha JA. The future of construction materials research and the seventh UN Millennium Development Goal: A few insights. *Construction and Building Materials.* 2013;40:729-737.

[37] Runkiewicz L. Application of non-destructive testing methods to assess properties of construction materials in building diagnostics. *Architecture Civil Engineering Environment.* 2009;2(2):79-86.

[38] Ikari T, Fukasawa R. Terahertz characterization of construction materials for remote gas sensing. Paper presented at: Infrared, Millimeter, and Terahertz Waves (IRMMW-THz); 21-25 Sept. 2009, 2009.

[39] Elmoutaouakkil A, Fuchs G, Bergounhon P, Péres R, Peyrin F. Three-dimensional quantitative analysis of polymer foams from synchrotron radiation x-ray microtomography. *Journal of Physics D: Applied Physics.* 2003;36(10A):A37.

[40] Van Tittelboom K, Snoeck D, Vontobel P, Wittmann F, De Belie N. Use of neutron radiography and tomography to visualize the autonomous crack sealing efficiency in cementitious materials. *Materials and Structures.* 2013;46(1-2):105-121.

[41] Gómez-Laserna O, Olazabal MÁ, Morillas H, et al. In-situ spectroscopic assessment of the conservation state of building materials from a Palace house affected by infiltration water. *Journal of Raman Spectroscopy.* 2013;44(9):1277-1284.

[42] Fernández-Carrasco L, Torrens-Martín D, Morales LM, Martínez-Ramírez S. Infrared Spectroscopy in the Analysis of Building and Construction Materials. In: Theophanides T, ed. *Infrared Spectroscopy - Materials Science, Engineering and Technology*: InTech; 2012.

[43] Han PY, Tani M, Usami M, Kono S, Kersting R, Zhang X-C. A direct comparison between terahertz time-domain spectroscopy and far-infrared Fourier transform spectroscopy. *Journal of Applied Physics.* 2001;89(4):2357-2359.

[44] Brunner FDJ, Schneider A, Günter P. A terahertz time-domain spectrometer for simultaneous transmission and reflection measurements at normal incidence. *Optics Express.* 2009;17(23):20684-20693.

[45] Trontelj J, Valušis G, Venckevičius R, Kašalynas I, Sešek A, Švigelj A. A high performance room temperature THz sensor. Paper presented at: SPIE 9199, Terahertz Emitters, Receivers, and Applications V; 17 - 18 August, 2014; San Diego, California, United States.

[46] Lu M, Shen J, Li N, et al. Detection and identification of illicit drugs using terahertz imaging. *Journal of Applied Physics.* 2006;100(10):103104.

[47] Fuse N, Takahashi T, Ohki Y, Sato R, Mizuno M, Fukunaga K. Terahertz spectroscopy as a new tool for insulating material analysis and condition monitoring. *Electrical Insulation Magazine, IEEE.* 2011;27(3):26-35.

[48] Wietzke S, Jansen C, Jördens C, et al. Industrial applications of THz systems. Paper presented at: SPIE, International Symposium on Photoelectronic Detection and Imaging 2009: Terahertz and High Energy Radiation Detection Technologies and Applications; 4 August 2009; Beijing, China.

[49] Redo-Sanchez A, Laman N, Schulkin B, Tongue T. Compact, portable Terahertz

systems for on-site inspection applications. Paper presented at: 38th International Conference on Infrared, Millimeter, and Terahertz Waves (IRMMW-THz); 1-6 September, 2013; Mainz, Germany.

[50] Lloyd-Hughes J, Jeon T-I. A Review of the Terahertz Conductivity of Bulk and Nano-Materials. *Journal of Infrared, Millimeter, and Terahertz Waves.* 2012;33(9):871-925.

[51] Zhang X-C, Xu J. *Introduction to THz Wave Photonics.* New York: Springer US; 2010.

[52] Smith PR, Auston DH, Nuss MC. Subpicosecond photoconducting dipole antennas. *IEEE Journal of Quantum Electronics.* 1988;24(2):255-260.

[53] Hu BB, Nuss MC. Imaging with terahertz waves. *Optics Letters.* 1995;20(16):1716-1718.

[54] Siegel PH. Terahertz technology in biology and medicine. *IEEE Transactions on Microwave Theory and Techniques.* 2004;52(10):2438-2447.

[55] Xie L, Yao Y, Ying Y. The Application of Terahertz Spectroscopy to Protein Detection: A Review. *Applied Spectroscopy Reviews.* 2013;49(6):448-461.

[56] Zeitler JA, Taday PF, Newnham DA, Pepper M, Gordon KC, Rades T. Terahertz pulsed spectroscopy and imaging in the pharmaceutical setting - a review. *Journal of Pharmacy and Pharmacology.* 2007;59(2):209-223.

[57] King MD, Buchanan WD, Korter TM. Identification and Quantification of Polymorphism in the Pharmaceutical Compound Diclofenac Acid by Terahertz Spectroscopy and Solid-State Density Functional Theory. *Analytical Chemistry.* 2011;83(10):3786-3792.

[58] Corporation ZT. The Terahertz Wave eBook. 2012: http://dl.z-thz.com/eBook/zomega_ebook_pdf_1206_sr.pdf. Accessed 4.4.2014.

[59] Rahani EK, Kundu T, Wu ZR, Xin H. Mechanical Damage Detection in Polymer Tiles by THz Radiation. *IEEE Sensors Journal.* 2011;11(8):1720-1725.

[60] Davies AG, Burnett AD, Fan W, Linfield EH, Cunningham JE. Terahertz spectroscopy of explosives and drugs. *Materials Today.* 2008;11(3):18-26.

[61] Furuya T, Maeda K, Yamamoto K, et al. Broadband polarization properties of photoconductive spiral antenna. Paper presented at: 34th International Conference on Infrared, Millimeter, and Terahertz Waves (IRMMW-THz); 21-25 September, 2009; Busan, South Korea.

[62] Tani M, Matsuura S, Sakai K, Nakashima S. Emission characteristics of photoconductive antennas based on low-temperature-grown GaAs and semi-insulating GaAs. *Applied Optics.* 1997;36(30):7853-7859.

[63] Tani M, Herrmann M, Sakai K. Generation and detection of terahertz pulsed radiation with photoconductive antennas and its application to imaging. *Measurement Science and Technology.* 2002;13(11):1739.

[64] Moreno E, Pantoja MF, Bretones AR, Ruiz-Cabello M, Garcia SG. A Comparison of the Performance of THz Photoconductive Antennas. *Antennas and Wireless Propagation Letters, IEEE.* 2014;13:682-685.

[65] Saeedkia D. Terahertz photoconductive antennas: Principles and applications. Paper presented at: 5th European Conference on Antennas and Propagation (EUCAP) 11-15 April, 2011; Rome, Italy.

[66] Rostami A, Rasooli H, Baghban H. *Terahertz Technology: Fundamentals and Applications.* Springer-Verlag Berlin Heidelberg; 2011.

[67] Yin X, Ng BW-H, Abbott D. *Terahertz Imaging for Biomedical Applications: Pattern Recognition and Tomographic Reconstruction.* Springer-Verlag New York; 2012.

[68] Ferguson B, Zhang X-C. Materials for terahertz science and technology. *Nature*

*Materials.* 2002;1(1):26-33.
[69] Trzebiatowska-Gusowska M, Plinski EF, Baran J, et al. Terahertz and Raman spectra of non-centrosymmetrical organic molecular crystals. *Optical Materials.* 2014;37:28-35.
[70] Chan WL, Deibel J, Mittleman DM. Imaging with terahertz radiation. *Reports on Progress in Physics.* 2007;70(8):1325-1379.
[71] Shen YC, Taday PF, Newnham DA, Pepper M. Chemical mapping using reflection terahertz pulsed imaging. *Semiconductor Science and Technology.* 2005;20(7):S254.
[72] Shen YC. Terahertz pulsed spectroscopy and imaging for pharmaceutical applications: A review. *International Journal of Pharmaceutics.* 2011;417(1-2):48-60.
[73] Kawase K, Ogawa Y, Watanabe Y, Inoue H. Non-destructive terahertz imaging of illicit drugs using spectral fingerprints. *Optics Express.* 2003;11(20):2549-2554.
[74] Watanabe Y, Kawase K, Ikari T, Ito H, Ishikawa Y, Minamide H. Component analysis of chemical mixtures using terahertz spectroscopic imaging. *Optics Communications.* 2004;234(1–6):125-129.
[75] Sun Y, Sy MY, Wang YX, Ahuja AT, Zhang YT, Pickwell-Macpherson E. A promising diagnostic method: Terahertz pulsed imaging and spectroscopy. *World J Radiol.* 2011;3(3):55-65.
[76] Lee Y-S. Basic Theories of Terahertz Interaction with Matter. *Principles of Terahertz Science and Technology*: Springer US; 2009:1-40.
[77] Theuer M, Harsha SS, Molter D, Torosyan G, Beigang R. Terahertz Time-Domain Spectroscopy of Gases, Liquids, and Solids. *Chemphyschem.* 2011;12(15):2695-2705.
[78] Harde H, Katzenellenbogen N, Grischkowsky D. Terahertz coherent transients from methyl chloride vapor. *Journal of the Optical Society of America B.* 1994;11(6):1018-1030.
[79] Smith RM, Arnold MA. Terahertz Time-Domain Spectroscopy of Solid Samples: Principles, Applications, and Challenges. *Applied Spectroscopy Reviews.* 2011;46(8):636-679.
[80] Bandyopadhyay A, Sengupta A, Barat RB, et al. Effects of scattering on THz spectra of granular solids. *International Journal of Infrared and Millimeter Waves.* 2007;28(11):969-978.
[81] Mittleman DM, Jacobsen RH, Neelamani R, Baraniuk RG, Nuss MC. Gas sensing using terahertz time-domain spectroscopy. *Applied Physics B-Lasers and Optics.* 1998;67(3):379-390.
[82] Hoffmann MC, Brandt NC, Hwang HY, Yeh K-L, Nelson KA. Terahertz Kerr effect. *Applied Physics Letters.* 2009;95(23):231105.
[83] Funkner S, Niehues G, Schmidt DA, Brundermann E. Terahertz Absorption of Chemicals in Water: Ideal and Real Solutions and Mixtures. *Journal of Infrared Millimeter and Terahertz Waves.* 2014;35(1):38-52.
[84] Jepsen PU, Merbold H, Li Z, Xing X, Clark S. Terahertz Time-Domain Spectroscopy of Crystalline and Aqueous Systems. In: Miles RE, Zhang X-C, Eisele H, Krotkus A, eds. *Terahertz Frequency Detection and Identification of Materials and Objects, NATO Science for Peace and Security Series: Physics and Biophysics*. The Netherlands: Springer; 2007.
[85] El Haddad J, Bousquet B, Canioni L, Mounaix P. Review in terahertz spectral analysis. *Trac-Trends in Analytical Chemistry.* 2013;44:98-105.
[86] Zeitler JA, Newnham DA, Taday PF, et al. Temperature dependent terahertz pulsed spectroscopy of carbamazepine. *Thermochimica Acta.* 2005;436(1-2):71-77.

[87] Einfalt T, Planinsek O, Hrovat K. Methods of amorphization and investigation of the amorphous state. *Acta Pharmaceutica.* 2013;63(3):305-334.
[88] Wietzke S, Jansen C, Reuter M, et al. Terahertz spectroscopy on polymers: A review of morphological studies. *Journal of Molecular Structure.* 2011;1006(1-3):41-51.
[89] Wietzke S, Jansen C, Jung T, et al. Terahertz time-domain spectroscopy as a tool to monitor the glass transition in polymers. *Optics Express.* 2009;17(21):19006-19014.
[90] Arik E, Altan H, Esenturk O. Dielectric Properties of Diesel and Gasoline by Terahertz Spectroscopy. *Journal of Infrared, Millimeter, and Terahertz Waves.* 2014;35(9):759-769.
[91] Stephani H, Herrmann M, Wiesauer K, Katletz S, Heise B. Enhancing the interpretability of terahertz data through unsupervised classification. Paper presented at: XIX IMEKO World Congress, Fundamental and Applied Metrology; 6−11 September 2009; Lisbon, Portugal.
[92] Wu H, Heilweil EJ, Hussain AS, Khan MA. Process analytical technology (PAT): Quantification approaches in terahertz spectroscopy for pharmaceutical application. *Journal of Pharmaceutical Sciences.* 2008;97(2):970-984.
[93] Galvão RKH, Hadjiloucas S, Zafiropoulos A, Walker GC, Bowen JW, Dudley R. Optimization of apodization functions in terahertz transient spectrometry. *Optics Letters.* 2007;32(20):3008-3010.
[94] Sankaran S, Ehsani R. Introduction to the Electromagnetic Spectrum. In: Manickavasagan A, Jayasuriya H, eds. *Imaging with Electromagnetic Spectrum, Applications in Food and Agriculture*: Springer; 2014:1-16.
[95] Guillet JP, Recur B, Frederique L, et al. Review of Terahertz Tomography Techniques. *Journal of Infrared, Millimeter, and Terahertz Waves.* 2014;35(4):382-411.
[96] Liu H-B, Zhang X-C. Terahertz Spectroscopy for Explosive, Pharmaceutical, and Biological Sensing Applications. In: Miles RE, Zhang X-C, Eisele H, Krotkus A, eds. *Terahertz Frequency Detection and Identification of Materials and Objects, NATO Science for Peace and Security Series: Physics and Biophysics*. The Netherlands: Springer; 2007.
[97] Fischer B, Hoffmann M, Helm H, Modjesch G, Jepsen PU. Chemical recognition in terahertz time-domain spectroscopy and imaging. *Semiconductor Science and Technology.* 2005;20(7):S246-S253.
[98] Shen Y, Taday PF, Kemp MC. Terahertz spectroscopy of explosive materials. Paper presented at: SPIE 5619, Passive Millimetre-Wave and Terahertz Imaging and Technology; 8 December, 2004; Bellingham, WA, US.
[99] Burnett AD, Fan W, Upadhya PC, et al. Broadband terahertz time-domain spectroscopy of drugs-of-abuse and the use of principal component analysis. *Analyst.* 2009;134(8):1658-1668.
[100] Stillhart M, Schneider A, Günter P. Optical properties of 4-N,N-dimethylamino-4'-N'-methyl-stilbazolium 2,4,6-trimethylbenzenesulfonate crystals at terahertz frequencies. *Journal of the Optical Society of America B.* 2008;25(11):1914-1919.
[101] Mizuno M, Fukunaga K, Saito S, Hosako I. Analysis of calcium carbonate for differentiating between pigments using terahertz spectroscopy. *Journal of the European Optical Society-Rapid Publications.* 2009;4:4.

# Index of Figures

Figure 1.1: *The relationship between three aspects that should be considered when new technology is applied [51].* ..... 4
Figure 2.1: *The THz gap of the electromagnetic spectrum and the interactions between THz waves and molecules that THz technology is able to probe.* ..... 9
Figure 2.2: *Growth of SCI publications for keywords THz spectroscopy and THz imaging for the period 1988-2013 and 1992-2013, respectively*. Adopted from Web of Science Citation, Report made in April 2014. ..... 10
Figure 2.3: *THz generation and detection by PHCA emitter (left) and PHCA detector (right) illuminated by a femtosecond laser pulse.* ..... 13
Figure 2.4: *THz pulse generation through a second order nonlinear process.* ..... 14
Figure 2.5: *Schematic presentation of a typical transmission-mode THz time-domain spectrometer.* Reprinted from [69] and [68]. ..... 15
Figure 2.6: *Schematics of THz spectroscopy in transmission (A) and reflection (B) configuration.* ..... 16
Figure 2.7: *THz imaging methods in time-domain and frequency domain.* ..... 17
Figure 2.8: *Possible interactions between electromagnetic waves and material*..... 18
Figure 2.9: *Measured absorption coefficient for gases (a), water vapour (b), non-polar liquid (c), and solids (d) samples.* Reprinted from [77], [6] and [90]. .. 23
Figure 2.10: *The specific parameters of THz waveform (left) and THz spectrum (right).* Reprinted from [95]. ..... 26
Figure 2.11: *THz waveforms measured after propagation through the plastic layers with various thickness (A) and a linear fit of the measured pulse delay versus plastic sample thickness (B).* Reprinted from [77]. ..... 26
Figure 2.12: *Terahertz spectral image of four samples containing different substances.* The colours in the left image represent a measure for the presence of specific spectral feature, which is characteristic for a certain sample. Reprinted from [3,97]. ..... 29
Figure 2.13: *THz image showing the spatial distributions of two substances, lactose (a), and sucrose (b).* Reprinted from [71]. ..... 30
Figure 3.1: *Schematic illustration of a TeraIMAGE THz spectrometer in transmission mode.* ..... 32
Figure 3.2: *Photograph of a selected THz-TDS system.* ..... 33
Figure 3.3: *Typical THz pulse waveform (a) and THz power spectrum (b) acquired with a TeraIMAGE spectrometer in a nitrogen atmosphere*..... 34
Figure 3.4: *THz reference signals and noise level (a) and THz power spectra with a noise floor (b) for six successive measurements in nitrogen atmosphere*..... 34

# Index of Tables

Table 1. *Characteristics of TeraIMAGE spectroscopic and imaging system.*.....33

# Index of Algorithms

Algorithm 1: *Data pre-processing procedure.* ..... 35
Algorithm 2: *Data post-processing procedure.* ..... 36

# Appendix A: THz measurement flow

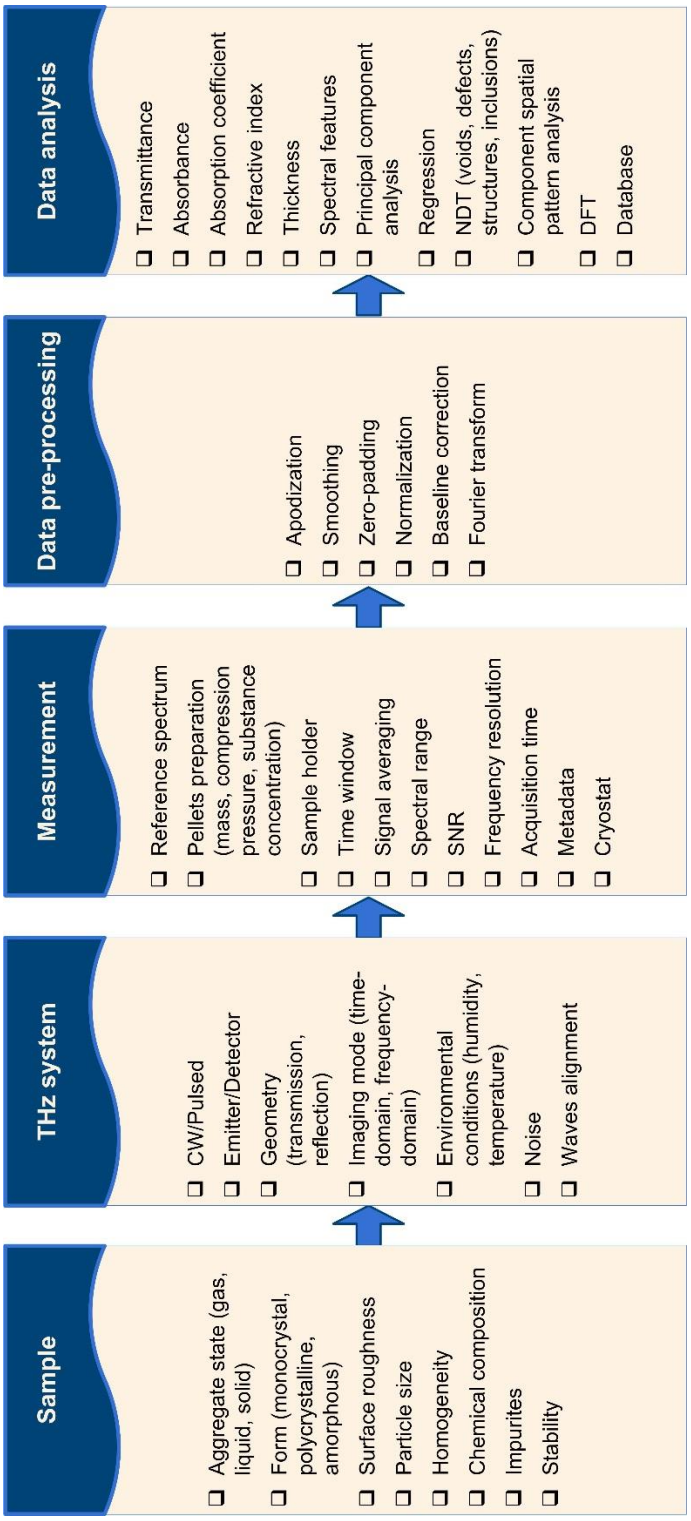

# Appendix B: Matlab functions for data pre-processing

## 1. The Blackman-Harris apodization function

```
% function y = blha(t, tmax, tmax2) where t is the time,
% tmax is the time where the function reaches 0.

function y = blha(t, tmax, tmax2)

if tmax == 0
   p.tmax = max(t);
else
   p.tmax = tmax;
end
if tmax2 == 0
   p.tmax2 = max(t);
else
   p.tmax2 = tmax2;
end

y = 0.42323+0.49755*cos(pi.*t./p.tmax)+0.07922*cos(2.*pi.*t./p.tmax);
y2= 0.42323+0.49755*cos(pi.*t./p.tmax2)+0.07922*cos(2.*pi.*t./p.tmax2);

y = (t>=0).*y+(t<0).*y2-(t>p.tmax).*y-(t<-p.tmax2).*y2;
```

## 2. Calculated spectral amplitude (FFT) from measured time-domain THz amplitude

```
% f is the frequency [THz] and s is the corresponding spectral amplitude
% Set v to 0 to not use zero-passing, and to M>0 to use zero-padding to extend tr to M elements

function [f,s] = ampl2spec2(tr, v)

p.zp = size(tr,1);
if v>0
   p.zp = v;
end

s = fft(tr(:,2),p.zp);                  % Spectrum of signal
N = p.zp;                               % Number of time points
dt = tr(2,1)-tr(1,1);                   % Time step [ps]
f = linspace(0,(N-1)/(N*dt),N);         % Corresponding frequency range
```

# Appendix C: Personal biography

Andreja Abina was born on March 8, 1983 in Brežice, Slovenia. She graduated in 2008 with the work titled "The e-learning object and verification of technical characteristics", at the Faculty of Education, University of Ljubljana, direction Chemistry and Biology. After finishing the undergraduate programme, she started her Scientific Master's Degree Study Programme Chemical Education at the Department of Chemical Education and Informatics, Faculty of Natural Sciences and Engineering, University of Ljubljana. In October 2009, when she successfully concluded the first year of the Master's degree study, she continued her postgraduate study at the Jožef Stefan International Postgraduate School, the PhD program entitled "Nanosciences and Nanotechnologies" under the supervision of Prof. Dr. Aleksander Zidanšek.

In April 2009, she joined the research group at the Jožef Stefan International Postgraduate School, where she started with the research work related to electromagnetic sensing and imaging, based on ground penetrating radar, terahertz spectroscopy and electromagnetic induction. During this period, she collaborated on EU funded project UNCOSS (Underwater coastal sea surveyor), EDA funded projects GUARDED (Generic Urban Area Robotized Detection of CBRNE Devices) and E-STAR (Explosive detection – Spectroscopy, Terahertz technology and Radar), as well as SRA programmes and projects, i.e. New imaging and analytic methods and THz imaging, respectively. She also contributed to several project proposals at national and international levels.

Over the past few years, she has presented her research work at several international journals, conferences and symposiums. Her research interest includes material characterization, terahertz spectroscopy and other electromagnetic sensing methods.

# Appendix D: List of all publications in the period from 2009 in COBISS

**1.01 Original scientific article**

[1] Puc U, Abina A, Rutar M, Zidanšek A, Jeglič A, Valušis G. Terahertz spectroscopic identification of explosive and drug simulants concealed by various hiding techniques. *Applied optics*. 2015;54(14):4495-4502.

[2] Abina A, Puc U, Jeglič A, Zidanšek A. Structural analysis of insulating polymer foams with terahertz spectroscopy and imaging. *Polymer Testing*. 2013;32(4):739-747.

[3] Abina A, Puc U, Cevc P, Jeglič A, Zidanšek A. Terrestrial and underwater pollution-source detection using electromagnetic multisensory robotic system. *Chemical engineering transactions*. 2013;34:61-66.

**1.02 Review article**

[4] Abina A, Puc U, Jeglič A, Zidanšek A. Applications of terahertz spectroscopy in the field of construction and building materials. *Applied Spectroscopy Reviews*. 2015;50(4):279-303.

**1.08 Published scientific conference contribution**

[5] Abina A, Puc U, Jeglič A, Zidanšek A. Terahertz spectroscopy and imaging of foamed polymers. International THz Conference; 9-10 September 2013; Villach, Austria.

[6] Srebotnjak Borsellino M, Abina A, Puc U, Šlaus I, Zidanšek A. Human resources, innovation and sustainable development. 7 th Conference on Sustainable Development of Energy, Water and Environment Systems; 1-7 July, 2012; Ohrid, Republic of Macedonia.

[7] Abina A, Puc U, Jeglič A, Cevc P, Zidanšek A. Terrestrial and underwater pollution monitoring using high-resolution electromagnetic sensors. 7 th Conference on Sustainable Development of Energy, Water and Environment Systems; 1-7 July, 2012; Ohrid, Republic of Macedonia.

[8] Puc U, Abina A, Jeglič A, Cevc P, Zidanšek A. Detection of seabed objects using ground penetrating radar and continuous wave electromagnetic iduction sensor. International Conference on Underwater Remote Sensing, ICoURS'12; 8-11 October, 2012; Brest, France.

[9] Puc U, Abina A, Jeglič A, Cevc P, Zidanšek A. Advanced electromagnetic sensors for sustainable monitoring of industrial processes. International Conference on Efficiency, Cost, Optimization, Simulation and Environmental Impact of Energy Systems, ECOS 2012; 26-29 June, 2012; Perugia, Italy.

[10] Abina A, Puc U, Heath DJ, Puc U, Zidanšek A. Spectroscopic THz imaging using organic DSTMS (4-N,N-dimethylamino-4'-N'-methyl-stilbazolium 2,4,6-

trimethylbenzesulfonate) crystals. 4th Jožef Stefan International Postgraduate School Students Conference; 25 May, 2012; Ljubljana, Slovenia.

[11] Puc U, Abina A, Jeglič A, Cevc P, Zidanšek A. Underwater electromagnetic remote sensing. 4th Jožef Stefan International Postgraduate School Students Conference; 25 May, 2012; Ljubljana, Slovenia.

[12] Puc U, Abina A, Jeglič A, Zidanšek A. Applications of underwater radar. 24th International Conference on Efficiency, Cost, Optimization, Simulation and Environmental Impact of Energy Systems, ECOS 2011; 4-7 July, 2011; Novi Sad, Serbia.

[13] Abina A, Puc U, Milfelner M. Microwave technology for energy transfer from space to Earth. Sustainability and space exploration: report to the Slovenian Association for the Club of Rome. Ljubljana: Slovensko združenje Rimskega kluba; December, 2011; Ljubljana, Slovenia.

[14] Puc U, Abina A, Jeglič A, Milfelner M. Terahertz and optical technology for energy transfer from space to Earth. Sustainability and space exploration: report to the Slovenian Association for the Club of Rome; December, 2011; Ljubljana, Slovenia.

[15] Abina A, Zor M. Detection of discarded household hazardous waste in the ground with ground-penetrating radar method. 5th Dubrovnik Conference on Sustainable Development of Energy, Water and Environment Systems; 29 September - 3 October 2009; Dubrovnik, Croatia.

[16] Abina A, Zor M. Application of ground-penetrating radar to detection of different material objects. 5th Dubrovnik Conference on Sustainable Development of Energy, Water and Environment Systems; 29 September - 3 October, 2009; Dubrovnik, Croatia.

**1.12 Published scientific conference contribution abstract**

[17] Puc U, Abina A, Jeglič A, Heath DJ, Zidanšek A. Tetrahertz and magnetic resonance spectroscopy for the detection of pharmaceutical substances. Paper presented at: MRDE 2013, Magnetic Resonance Detection of Explosives Workshop; 8-12 July, 2013; London, United Kingdom.

[18] Puc U, Abina A, Jeglič A, Zidanšek A. Teraherčna spektralna karakterizacija farmacevtske učinkovine v komercialnih zdravilih = Terahertz spectral characterisation of active substance in commercial pharmaceutical tablets. Paper presented at: 11th Symposia of Physicists at the University of Maribor; 6-8 December, 2012; Maribor, Slovenia.

[19] Abina A, Puc U, Jeglič A, Zidanšek A. Metode pri teraherčnem pulznem slikanju = Methods for terahertz pulse imaging. Paper presented at: 10th Symposia of Physicists at the University of Maribor; 8-10 December, 2011; Maribor, Slovenia.

[20] Puc U, Abina A, Jeglič A, Zidanšek A. Viri in detektorji za spektroskopsko teraherčno slikanje na daljavo = Sources and detectors for stand-off spectroscopic terahertz imaging. Paper presented at: 10th Symposia of Physicists at the University of Maribor; 8-10 December, 2011; Maribor, Slovenia.

[21] Zidanšek A, Abina A, Jeglič A, Cevc P, Polanec J, Puc U. Uporaba georadarja za detekcijo podvodnih objektov. Paper presented at: 14. slovensko srečanje o uporabi fizike; 28 October, 2011; Portorož, Slovenia.

[22] Puc U, Abina A, Zidanšek A, Cevc P. Enodimenzionalni niz anten za georadar = One-dimensional linear array of antennas for georadar. Paper presented at: 9th

Symposia of Physicists at the University of Maribor; 9-11 December, 2010; Maribor, Slovenia.

[23] Abina A, Puc U, Zidanšek A. Izboljšave migracije za raziskave z georadarjem = Improvements of migration for georadar. Paper presented at: 9th Symposia of Physicists at the University of Maribor; 9-11 December, 2010; Maribor, Slovenia.

**2.11 Undergraduate thesis**

[24] Abina A. E-učna enota in preverjanje njenih tehničnih značilnosti = The e-learning object and verification of technical characteristics = graduation thesis. Ljubljana, Slovenia, University of Ljubljana; 2008.

**UNCLASSIFIED**

[25] Zidanšek A, Abina A, Jeglič A, Puc U. Electromagnetic sensing and nature parks. Vol 20. Ljubljana: International Center for Promotion of Enterprises; 2014.